universidad de León

Facultad de Veterinaria

Departamento de Producción Animal

HIGH DENSITY MAPPING TO IDENTIFY GENES ASSOCIATED TO GASTROINTESTINAL NEMATODE INFECTIONS RESISTANCE IN SPANISH CHURRA SHEEP

(MAPEO DE ALTA DENSIDAD PARA LA IDENTIFICACIÓN DE GENES RELACIONADOS CON LA RESISTENCIA A LAS INFECCIONES GASTROINTESTINALES POR NEMATODOS EN EL GANADO OVINO DE RAZA CHURRA)

Marina Atlija

León, Mayo de 2016

Supervisors:

Beatriz Gutiérrez-Gil[1]

María Martínez-Valladares[2, 3]

[1] Departamento de Producción Animal, Facultad de Veterinaria, Universidad de León, Campus de Vegazana s/n, León 24071, Spain.

[2] Instituto de Ganadería de Montaña. CSIC-ULE. 24346. Grulleros. León.

[3] Departamento de Sanidad Animal. Universidad de León. 24071. León.

The research work included in this PhD Thesis memory has been supported by the European funded Initial Training Network (ITN) project NematodeSystemHealth ITN (FP7-PEOPLE-2010-ITN Ref. 264639), a competitive grant from the Castilla and León regional government (Junta de Castilla y León) (Ref. LE245A12-2) and a national project from the Spanish Ministry of Economy and Competitiveness (AGL2012-34437).

Marina Atlija is a grateful grantee of a Marie Curie fellowship funded in the framework of the NematodeSystemHealth ITN (FP7-PEOPLE-2010-ITN Ref. 264639).

“If all the matter in the universe except the nematodes were swept away, our world would still be dimly recognizable, and if, as disembodied spirits, we could then investigate it, we should find its mountains, hills, vales, rivers, lakes, and oceans represented by a film of nematodes. The location of towns would be decipherable, since for every massing of human beings there would be a corresponding massing of certain nematodes. Trees would still stand in ghostly rows representing our streets and highways. The location of the various plants and animals would still be decipherable, and, had we sufficient knowledge, in many cases even their species could be determined by an examination of their erstwhile nematode parasites.”

N. A. Cobb, Yearbook of the United States Department of Agriculture (1914), page 472

Acknowledgements

I would like to acknowledge Prof. Juan Jose Arranz for providing me the opportunity to conduct research in his group and for his advice and support throughout the entire course of my PhD.

I am also grateful for the support and encouragement received from my supervisors, Dr. Beatriz Gutiérrez-Gil and Dr. María Martínez-Valladares, for their knowledge, their critiques, their guidance and their encouragement throughout the course of this study.

I would like to extend my sincere thanks and appreciation to Prof. Francisco Antonio Rojo-Vázquez for his parasitological expertise and a huge amount of literature that helped me to understand these extraordinary organisms.

I would also like to thank to Dr. Johannes Buitkamp to give me a opportunity to work with his group at the Institute for Animal Breeding in Germany, the Bayerische Landesanstalt für Landwirtschaft. Thank you so much for teaching me and introducing me to the complexity of the major histocompatibility complex immune genes.

I had also oportunity to work with Prof. Mike Stear and Dr. Joaquin Prada at the University of Glasgow. I am really thankful for their understanding, disscusion and help which in the end had an impact on my understanding how to approach and deal with my data.

Further, I wouId like to thank all my fellow graduate students and colleagues in the department at University of Leon for their freindship and assistance through these years.

To all my friends, near by to me or far away, thank you so much for your understanding and encouragement in countless moments of crisis. I cannot list all the names here, but you are always on my mind. Your friendship makes my life a wonderful experience.

There are no words to express my gratitude to my Mom, for your constant encouragement, support and for being so strict in terms of getting me to study properly from the very first days of my school.

Finally, I must acknowledge with tremendous and deep thanks my boyfriend, Konrad Burnik. You were always there for me, even we were far away from each other, to give me possitive energy to go beyond my limits with your love, patience, support and unwavering belif in me what help me to complete this dissertation journey. Thank you!

TABLE OF CONTENT

ÍNDICE DE CONTENIDOS

Thesis proposal and objectives

The gastrointestinal nematode (GIN) parasites have proven to be one of the main threats to the outdoor breeding of small ruminants. The cost of this problem for the European sheep livestock industry has been estimated to be approximately 400 million € (Morgan et al., 2013). Current control strategies are mainly based on antihelminthic treatments. However, indiscriminate and frequent use of antihelminthics exerts selection pressure resulting in decline in their efficacy and hence emergence of antihelminthic resistance. From the initial reports of antihelminthic resistance in small ruminants (Waller, 1994), the prevalence of antihelminthic resistances has increased dramatically, with an increase of up to 80% of European flocks showing resistance to benzimidazole (Domke et al., 2012). This scenario shows that current GIN control programs are costly and unsustainable in the long term. Thus, the sustainment of GIN infections is becoming a major problem worldwide and alternative strategies for the control of GIN infections in small ruminants are sought. One of the most promising options for controlling GINs is the exploitation of the host genetic variation by using flocks with more resistant animals, which has been proved to be successful in Australia and New Zealand (Morris et al., 1995; Karlsson and Greeff, 2006; Kemper et al., 2010). However, using classical selection methods based on phenotypes and pedigree information for parasite resistance has important difficulties, as the selection is based on indicator traits, such as faecal egg counts (FEC), or serum levels of Immunoglobulin A (IgA), which are costly and difficult to record routinely and the requirement of the animals to have been exposed to a parasitic challenge. Because of that the detection of genetic markers or genes that directly influence parasite resistance in sheep and the development of appropriate marker- or gene- assisted selection (MAS or GAS) protocols have been suggested as an efficient strategy to improve GIN resistance in sheep.

The research group of Animal Breeding and Genetics of the University of León (also known as ULE MEGA, from *Mejora Genetica Animal*), where this PhD Thesis has been conducted, has a long tradition in the study and the search of genetic solutions for the genetic improvement of Churra sheep, an indigenous sheep breed of the North-West (NW) region of Spain. The Churra sheep has medium size, long wool, and white color with peripheral staining in black affecting the terminal portion of the ears, around the eyes, lips and nose, distal parts of the extremities (Figure 1). This breed is well known for its specialization in milk production and the top quality of its lamb meat. The traditional dairy sheep production in Castilla and León has been closely related to this indigenous sheep breed. Currently, two breeding schemes, one focused in the improvement of milk production traits and one

addressing the interests for lamb production of the non-dairy flocks, are running for this breed under the coordination of the National Association of Churra Breeders (ANCHE). The herd book of this breed was established in 1977 by ANCHE, and the breeding program relies on the production records of selected herds and progeny testing of rams.

Figure 1. Spanish Churra breed, source: http://www.magrama.gob.es/

Since the starting of breeding programme of this breed, the close collaboration stablished between this research group and ANCHE as resulted in a large number of studies focused on the study of the factors and genetic parameters related to traits of economic interest in dairy sheep, such as milk production traits, mammary morphology, functional traits, disease resistance (Baro et al., 1994, Gutiérrez-Gil et al., 2008, 2009a, 2009b, 2010, 2011). Taking advantages of the progress that took place in the field of animal genetics in the last years of the XXth century, with the development of the linkage mapping strategies and the use of microsatellite markers, this group carried out several genome scans with the aim of identifying *Quantitative Trait Loci* (QTL) influencing traits of interest for Churra sheep breeders (Gutiérrez-Gil et al., 2007, 2009a, 2009b). After 2008, with the availability of a medium density SNP-chip genotyping platform, *Illumina* OvineSNP50K BeadChip, the ULE

MEGA research group reported the identification of the first causal mutation or *Quantitative Trait Nucleotide* (QTN) for a dairy QTL in sheep (García-Gámez et al., 2012c) and the causal genetic variants underlying two Mendelian diseases described in Churra sheep (Suarez-Vega et al., 2013, 2015).

Apart the strong effort of this research group to dissect the genetic variation underlying milk production traits, disease resistance traits have also been an important point of interest for this group because of the impact that some diseases such as subclinical mastitis and GIN infections have on the dairy sheep farm´s global economy. In relation to the study of parasite resistance traits, the ULE MEGA research group, through its participation in the European-funded *GeneSheepSafety* project (5^{th} Framework Programme), reported the estimation of genetic parameters for FEC and serum levels of IgA and pepsinogen (Gutiérrez-Gil et al., 2010), and the results of a microsatellite-based genome scan for detection of QTL influencing the mentioned indicator traits in a commercial half-sib population of Spanish Churra sheep (Gutiérrez-Gil et al., 2009b).

Based on the research activity background of the ULE MEGA group, and the availability of the *Illumina* OvineSNP50K BeadChip (referred from now on as 50K-SNP chip), the present PhD Thesis is proposed as a follow-up step of the previously reported microsatellite-based genome scan. Hence, building on the much higher density of genetic marker offered by the 50K-SNP chip, a first objective of this work was the replication of the previously reported QTL for parasite resistance traits and the identification of new QTL using a different subset of half-sib families of the commercial population of Spanish Churra dairy sheep. This first objective was implemented in the framework of the a project funded by the regional government of the Junta of Castilla and León (LE245A12-2), entitled "Detection of genes of resistance to gastrointestinal nematodes in Spanish Churra sheep through the use of genomic tools", and the European funded Initial Training Network (ITN) project entitled "NematodeSystemHealth: a systems biology approach to controlling nematode infections of livestock". Based on the detailed study of the phenotypic data and the DNA samples collected to perform the genome scan based on the 50K-SNP chip, and the scientific training collaborations established within the framework of the ITN-project, two additional objectives were proposed for this PhD project. Hence, in relation to the study of candidate genes for parasite resistance, we performed the study of the genetic variability of two genes of the Major Histocompatibility Complex (MHC) class IIB in the resource Churra sheep population. This study was performed in collaboration with the group led by Johannes Buitkamp at

Bayerische Landesanstalt für Landwirtschaft institute in Grub, Germany. On the other hand, by collaborating with the group led by Professor Michael Stear at the University of Glasgow in United Kingdom, we had the opportunity to develop a mathematical model to deal with FEC data related to the low levels of natural GIN infection shown by the animals included in our study due to the exceptional dry climatic conditions of the sampling period (Spring 2012).

Taking into account all this, the global objective of this Thesis memory is the study of the genetic architecture of GIN resistance in Churra sheep from three different points of view: the use of genomic tools such as the 50K-SNP chip, the study of the genetic variability of candidate genes such as MCH class II genes, and the development of a mathematical model to deal appropriately with the phenotypic data of indicator traits obtained in low infection conditions. The three specific objectives that are followed to build the present work are as follows:

- Detection and replication of QTL underlying resistance to gastrointestinal nematodes in adult sheep using the ovine 50K SNP array by using three different analysis approaches: Linkage Analysis, Combined Linkage Analysis and Linkage Disequilibrium Analysis and Genome-wide Association Analysis.
- Study of the genetic variability of Major Histocompatibility Complex class IIB polymorphism in Spanish Churra sheep through sequencing analysis.
- Development and implementation of an extended Zero-inflated Negative Binomial (ZINB) model in the study of low levels of natural gastrointestinal nematode infections in adult sheep.

Literature review

1. Infection by GINs in sheep

Healthy animals are the most valuable resource for the livestock industry. They provide food (meat and milk), animal products (e.g. wool and leather) and animal manure as a source of organic fertilizer. Worldwide, parasite infections caused by GINs are associated with great economic losses to the livestock industry due to the excessive use of the antihelminthic and/or decreased production performance, such us weight gain, milk and wool production and feed conversion (Stear et al., 2001; Suarez et al., 2009). Moreover, the influence of GINs on body condition might cause a reduced conception rate in the host (Gunn and Irvine, 2003). Thus, infections by GINs are an important problem for sheep breeders and represent one of the most important problems decreasing animal performance in sheep production globally.

Naturally infected sheep are mostly infected with more than one GIN, thus the level of infection and clinical signs can vary greatly between hosts. Many factors are implicated with the severity of disease such as the parasite species, the number of worms present in the gastrointestinal tract, the host condition as health, gender, age and immunity, and the environmental conditions, such as climatic conditions, the pasture type, management, stress and diet. In flocks three major groups of hosts are shown to be susceptible to high intensity infections: (i) young animals, not immunized, (ii), immunocompromised adult animals and (iii) animals exposed to a large number of L3 larvae (Zajac, 2006).

Apart of the number of species in the host, their distribution is of importance as well. In sheep, the nematode populations are aggregated, and this phenomenon is called the overdispersion, in which a majority of sheep cope with low parasite burden and few animals with a high infestation rate (Barger, 1985). There are differences among hosts that have an impact on the overdispersion such as (i) the probability of infection during the grazing (e.g. the infective larvae are not uniformly distributed on the pasture, and if the animal is larger it will consume more food, increasing the likelihood of infection), and (ii) the response of the host during the infection (e.g. an effective immune response of the host leads to less adult worm burden, more inhibited larvae and shorter and less fecund adult female), which can be attributed to a genetic predisposition of the host (Stear et al., 2007).

2. GINs in sheep

2.1. Taxonomy and life cycle of GINs

The Strongylida order includes vast majority of important nematodes found in the gastrointestinal tracts of ruminants, and contains five superfamilies: Ancylostomatoidea, Strongyloidea, Trichostrongyloidea, Metastrongyloidea and Diaphanocephaloidea. This order is characterized by males with a copulatory bursa (Anderson, 2000). In Trichostrongyloidea superfamiliy, the most important parasites that cause infections in grazing sheep include nematodes that affect the abomasum, such as *H. contortus*, *T. circumcincta* and *T. axei* or the intestinal tract such as *T. colubriformis* and *T. vitrinus* (Lee et al., 2011; Papadopoulos et al., 2012). Worms of lesser or occasional importance include *Nematodirus* spp, *Oesophagostomum* spp and *Chabertia ovina*. In the NW of Spain, which is characterized by a Mediterranean climate with continental and Atlantic influences, with cold winters and warm summers, *T. circumcincta* and *Trichostrongylus* spp. remain the dominant species (Diez-Baños et al., 1992; Gutiérrez-Gil et al., 2009b; Martínez-Valladares et al., 2013). The main GIN affecting sheep in the NW of Spain are listed in Table 1.

In relation to the life cycle of the most important and pathogenic GIN in sheep, they have a monoxenous life cycle and live predominantly in the gastrointestinal tract of vertebrate hosts. Their life cycle occurs in two phases: a parasitic stage in the host and a "free-living" stage in the external environment when hosts contaminate the pasture. The parasitic stage involves the ingestion of infective larvae of third stage (L3) during the grazing; then, larvae go through the abomasum or intestine, where they undergo two further moults, to the L4 and L5 stage, and subsequently to the adult stage. Therefore, according to the GIN species, larvae evolution to the next stages takes places in different locations of the gastrointestinal tract: in the abomasum in the case of *T. circumcincta*, *H. contortus* and *T. axei* whereas the rest species of *Trichostrongulus spp* are located in the intestine. Each of these species occupies a different niche of the gastrointestinal track. For example, *T. circumcincta* larvae invade gastric gland where they develop to the L5 and re-emerge into lumen to develop to adult stage, whereas *H. contortus* larvae invade the paramucusal lumen, where they attach themselves and molt to adult stage (Levine, 1968).

Table 1. *List of the most important gastrointestinal nematodes infecting sheep in the NortWest of Spain, including pre-patent periods and localization in the host.*

Family *Genus*	Species	The pre-patent period (days)	Localization in the host
Trichostrongylidae			
Teladorsagia spp.	*T. circumcincta* [a]	18-23	Abomasum
	T. trifurcate [a]	18-23	Abomasum
	T. axei [a]	18-21	Abomasum
	T. vitrinus [a]	18-21	Duodenum
Trichostrongylus spp. [b, c]	*T. colubriformis* [a]	18-21	Small intestine
	T. capricola [a]	-	Abomasum and small intestine
Haemonchus spp.	*H. contortus* [a, b, c]	26-28	Abomasum
Nematodirus spp. [b, c]		21-26	Small intestine
Marshallagia spp.	*M. marshalli* [a]	21-26	Abomasum
	M. occidentalis [a]	21-26	Abomasum
Cooperia spp. [b]		11-14	Small intestine
Ancylostomatidae			
Brunostomum spp. [c]		52-56	Small intestine
Chabertidae			
Oesophagostomum spp [b]		35-42	Large intestine
Chabertia spp.	*C. ovina* [b, c]	42-50	Large intestine

References: [a] Diez-Baños et al., 1992; [b] Pedreira et al., 2006; [c] Martínez-Valladares et al., 2013

When larvae reach the adult stage, they are differentiated in males and females which reproduce sexually. Females produce eggs that are then eliminated and excreted with faeces. In the free-living stage, eggs are present on pasture within the faeces. Inside the eggs, L1 is developed and when eggs hatch, the L1 goes outside and moults into L2 and consequently to L3. L3 larvae migrate out of the faeces, although most of them are retained within 10 cm of the faeces; exceptionally, some larvae might have horizontally migrated up to 100 cm of the faeces (Sykes, 1987). L3, the infective stage, presents a cuticular sheath around them as a protection from the harsh environment conditions. When the climate conditions are favorable, primarily the temperature and moisture (for example 22ºC for *T. circumcincta*, 27ºC for *T. colubriformis* or 32ºC with high moisture (>70%) for *H. contortus* (O'Connor et al., 2006)), the pre-patent period (the period of

time to complete a life cycle from egg to adult) is usually 3-4 weeks, although it also depends on the species and the host (see Figure 2).

Once inside the host, the parasitic stage can be longer due to the phenomenon of hypobiosis, which is defined as a prolonged but temporarily arrested larval development. Hypobiosis represents one of the most useful adaptations of GIN life cycle to ensure survival as it enables the parasite to synchronize its life cycle to the changing environmental conditions. Therefore, hypobiosis ensures survival of the parasite during periods of environmental adversity when conditions for transmission are poor and survival of free-living forms may be minimal (Gibbs, 1982). This phenomenon is specific for the most economically important sheep nematodes, *H. contortus* and *T. circumcincta* species (Roeber et al., 2013). L4 are arrested in the nodules, producing the focal changes on the mucosal surface of abomasum, and they can stay in this stage for up to several months (Sutherland and Scott, 2010). But the moment of the year or the period of time that the larvae are arrested can vary markedly and it depends on various factors such as the parasite species, the geographic region, the host immunity, the environment and also different management regimes. For example, *H. contortus* larvae will likely become dormant during a hot and dry summer while in the autumn, hypobiosis is specific for the *T. circumcincta*. Further, in studies with sheep infected by *T. circumcincta*, it was shown that the level of IgA is positively associated with the number of inhibited L4 larvae (Stear et al., 1995b; McRae et al., 2014b). L4 remain inactive until they receive a sequence of signals (i.e. immunosuppression due to changes in endocrine status, reduced levels of specific IgA in the gut, poor nutrition of ewes and the season of year) that contribute to resume their life cycle. In temperate climate areas, this moment coincides with the peripartum in pregnant sheep and is usually called the "spring rise". Pregnant ewes are the most affected due to a poor immune response, although (reviewed by Barger, 1993) it is thought that the "spring rise" is influenced by other factors since this phenomenon has also been observed, although at low levels, in barren ewes and in males (Blitz and Gibbs, 1972).

The number of eggs produced by GIN varies according to the nematode species; i.e. from few eggs per day (~10) in *Trichostrongylus* spp. (Gibson and Parfitt, 1975), and 500 eggs per day in *T. cirumcincta* (Silvestre and Humbert, 2002), to few thousands of eggs per day, approximately 5000 per day (Silvestre and Humbert, 2002), in *H. contortus*.

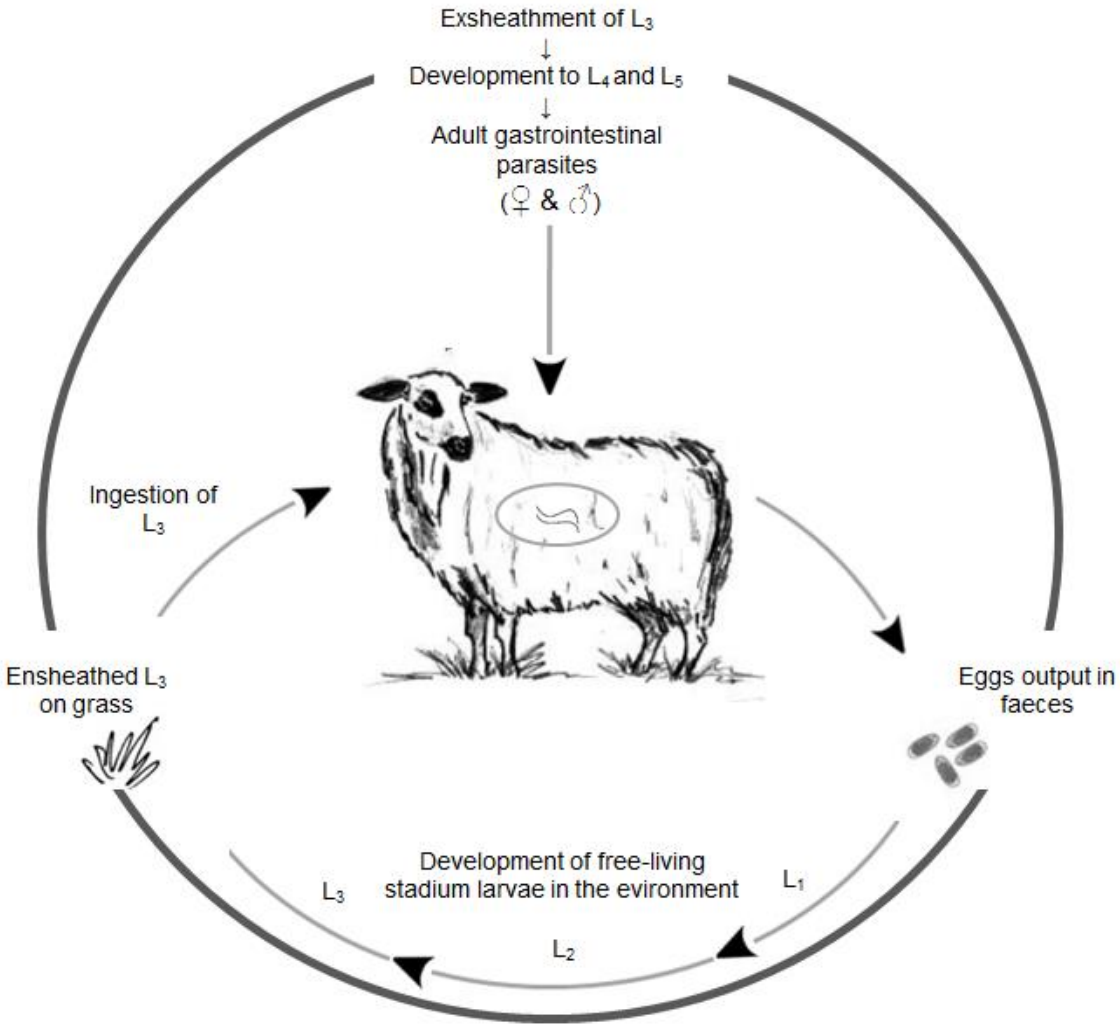

Figure 2. *Life cycle of gastrointestinal nematodes of sheep.*
The parasitic stage includes L4, L5 and adults in the gastrointestinal tract of the host.
The non-parasitic or "free-living" phase includes three different stages of larvae;
L1, L2 and infective L3.

2.2. Most important ovine GINs and their pathogenesis and clinical signs

Grazing sheep are usually infected with more than one species of GIN and therefore the clinical signs can vary according to the number of each infective species (Idris et al., 2012). Moreover, the severity of the infection is influenced by the existence of other concurrent infections, the nutritional state of the host and its ability to develop an immune response (Stear et al., 2003).

2.2.1. Teladorsagia circumcincta

The species *T. circumcincta* is often called brown stomach worm and also known as *Ostertagia circumcincta.* During the infection, it is located in the abomasum of small ruminants (sheep and goats), occasionally in the small intestine, and its principal pathogenic effect is caused by the larvae stage per se. In *T. circumcincta*, the development and emergence of L4 from gastric glands (nodules) cause cellular destruction, which results in loss of parietal cells. Reduction of parietal cells leads to decreased production of hypochlorous acid and consequently the abomasal pH is altered. When pH is over 4.5, pepsinogen is not converted to pepsin, the plasma levels of pepsinogen are increased and the consequence is a reduction in protein digestion. Clinical signs may include diarrhea, dehydration, inappetence, weight loss, edema ("bottle jaw") and, in very severe cases, the death of the host. This infection, known also as ostertagiasis or parasitic gastritis, includes three types of clinical manifestations: (i) Type I, which occurs as a result of recently ingested larvae which evolution to the adult stage, without hypobiosis phase; (ii) Pre-Type II, which occurs when larvae are inhibited, during the hypobiosis and, (iii) Type II, which occurs as a result of the emergence of hypobiotic larvae and usually takes place during the peripartum, in the "spring rise" (Hutchinson, 2009).

2.2.2. Trichostrongylus spp

Trichostrongylus spp are relatively small worms (<1 cm in length) and are mostly located in the small intestine; the exception is *T. axei* which is found in the abomasum where burrows between the epithelial cells and thus occupies a slightly different niche than the other abomasal nematode species (Sutherland and Scott, 2010). These species are present commonly in the warmer parts of temperate regions moving into subtropical areas. Main

species include *T. axei*, *T. colubriformis* and *T. vitrinus*; *T. vitrinus* seems more pathogenic than *T. colubriformis* (Roy et al., 2004).

Larvae of *T. colubriformis* and *T. vitrinus* are established preferentially in the first four meters of the small intestine in sheep. It has been shown that when sheep were infected with both species the establishment of *T. colubriformis* was reduced (Roy et al., 2004). Larvae in the small intestine provoke tunnels above the basal lamina, between enterocytes, mainly at the base of villi, and they are partly embedded in the epithelium through their whole lifetime. Therefore, larvae are the consequence of villus atrophy although it depends on the number of worms implicated (Roy et al., 2004). The clinical signs of this infection disease are very similar to infection by *T. circumcincta*.

2.2.3. Haemonchus contortus

H. contortus is the most pathological parasite in tropical and temperate climates with hot summer. It is one of the most fertile and largest of the GIN species affecting the abomasum of small ruminants. *H. contortus* is also named twisted stomach worm, wire and Barber's pole worm because of the characteristic appearance of females with pale ovaries and uteri twisting for the length of the worm around a red blood-filled intestine. Female worms are up to 3 cm long and male worms are smaller up to 2 cm.

As a hematophagous nematode, L4 and adult worms of *H. contortus* suck blood and damage mucosa. The adult nematode consumes approximately 0.05 ml of blood per day (Clark et al., 1962), and therefore several thousand worms could produce a considerable damage in the host. Hence, in heavy and rapid infections, even animals in good condition may die relatively quickly. The most prominent clinical signals are anemia, ventral edema (bottle jaw), weight loss, and death in the most severe cases (Qamar et al., 2011). In South Africa, the Famacha© system of standard colour charts is used for assessing/scoring the level of anemia by comparison of the colour of the inner lower eyelid; this classification is used for tactical treatment of heavily infected sheep (van Wyk and Bath, 2002).

It has also been shown that in sheep naturally infected with various parasite species, the number of *T. axei* is slightly enhanced (increased) when these sheep are simultaneous infected with *T. circumcincta* and/or *H. contortus* (Diez-Baños et al., 1992).

2.3. Interaction between host and parasite

The most important host defense mechanism for sheep against GINs is the immune system. The immunity of the host reacts through a series of activities that include different components (e.g. dendritic, mast and globule cells, eosinophils, neutrophils, antibodies, lymphocytes), which then detect, attack and eliminate infectious agents. In this scenario, the existence of two defined T helper (Th) cell subsets, which were designated as Th1 and Th2, was shown (Mosmann and Coffman, 1989). These two types of responses are adapted by the host to cope against two types of infectious agents. The microorganisms (viruses and bacteria, protozoa) generally invoke a Th1-type response which predominately is characterized by the secretion of interferon gamma (IFN-γ), interleukin (IL)-2 and tumor necrosis factor (Jankovic et al., 2001). Th2-type response evolved to cope with metazoan and is characterized by the secretion of cytokines such as IL-4, IL-5, IL-10 and IL-13 (Jankovic et al., 2001). The Th2-type response mediates host protection through enhanced tissue repair and reconstruction, the control of inflammation and worm expulsion (Gause et al., 2013). The damage of host tissue is provoked by GINs during its migration in the host to find its niche and/or when it feeds on this host tissue. Thus, the host has to protect itself from the parasites in the most cost-effective approach, either through resistance (which involves mediate the containment, destruction and expulsion of parasites), or through tolerance (which involves wound-healing machinery mechanisms) or through a combination of both (Schneider and Ayers, 2008; Gause et al., 2013).

3. Control of GIN infections

3.1. Antihelminthics

For the last fifty years, the control of the infections by GINs has been managed through the use of commercial antihelminthics (Coop et al., 2002). The first drug in this class, thiabendazole (TBZ), was released in Australia in 1961 (Dunsmore, 1962). Antihelminthics resistance (AR) has emerged as the result of the frequent use of antihelminthics to control GIN infections and management mistakes (Taylor, 2009). This is an important economic problem worldwide.

At present AR is more severe in GINs of small ruminants than in cattle, due to less frequent usage of antihelminthics in cows and prolonged larval survival in cattle dung,

which ensures a large refuge and slower selection for resistance in cattle parasites (Shalaby, 2013). The resistance to TBZ was first described in 1964 in sheep infected with the nematode *H. contortus*, a few years following the introduction of this antihelminthic in Australia. Afterwards it was detected in the other major ovine trichostrongyle nematodes such as *T. circumcincta* and *T. colubriformis*. In the mid 1970s the TBZ antihelminthic resistance was common and was extended to sheep nematodes worldwide. This same event was repeated in 1980, following the introduction of new antihelminthics such as imidazothiazole, tetrahydropyrimidine and macrocyclic lactones. In the early 1980s the first reports of multiple AR in nematodes appeared. Multiple AR, specifically to the three major classes of antihelminthics, benzimidazoles, immidazothiazoles and macrocyclic lactones have been reported in *H. contortus*, *T. circumcincta* and *T. colubriformis*, as reviewed by Kaplan, (2004). Since then, the increasing number of reports on multidrug resistance to these most commonly used antihelminthic families causes concern. In Spain, the latest study in the NW of the country showed the presence of resistance to any drug of these families in 63.6% of the sampled flocks; moreover, multidrug-resistance was also observed in 27.2% of these flocks, being one of them resistant to all antihelminthic families (Martínez-Valladares et al., 2013).

The introduction of two new antihelminthics, like monepantel (Kaminsky et al., 2011) and derquantel (Little et al., 2010), seems to be a temporary solution, although resistant flocks to monepantel have already been described in countries like New Zealand, the Netherlands and Uruguay (Scott et al., 2013; Dobson et al., 2014; Mederos et al., 2014). In order to face this problem different control strategies including selective treatments, grazing management, biological control, nutritional supplementation, vaccination and selection programs, have been proposed. The failure of antihelminthic treatment as a unique sustainable solution to cope with GIN parasites, and its consequences such as high treatment costs, chemical residues in animal products and environment, have pressed the livestock production industry to search for more sustainable strategies. Currently there is a general acceptance that a long-term strategy for sustainable parasite control must be based on the strategy known as "Integrated Parasite Management" (Karlsson and Greef, 2005), which involves as the basis for a strategic and proactive management the following approaches: (i) improving the genetic resistance of the host (at the genetic, non-genetic or nutritional level, through a stress reduction and the improvement of the specific immune response), (ii) controlling parasites in the environment (pasture management, rotational

grazing), (iii) biological control, which includes the use of nematode-natural enemies such us fungi or bacteria, and (iv) monitoring the level of infection such as FEC and/or clinical signs.

3.2. Selection of resistant animals to GIN infection

An alternative control method for GIN infections in sheep is increasing animals' resistance based on genetic selection. For that, given that the resistance to GINs is a complex trait controlled by many genes, we need two simultaneous strategies: getting a deep understanding of the phenotypes that can be considered as indicators of resistance and performing appropriate studies to dissect the complex genetic architecture of the identified indicator traits related with the control of these parasitic diseases in sheep.

The primitive sheep followed a seasonal grazing behavior, which allowed the animals to move freely, depending on the local food supply and climatic conditions. This seasonal grazing favored the parasite control, as the change of pastures made it difficult for the parasites to complete their free-life cycle, reducing their probability of survival. The parasite life-history traits, such us fecundity and survivorship, within a host are critical to the fitness of parasite nematodes (Skorping et al., 1991). Thus, these movements of the host and the inability of the parasites to complete the life cycle favored the selection of parasite populations for increased fecundity to increase their chance of survival. From the host point of view, it is possible that during an early domestication there had been some selection of animals in favor of aversion for high-risk grazing areas, such as those areas close to faeces deposits sites, avoiding the possibility to be infected by GINs (Karlsson and Greeff, 2012). Hence, it has been reviewed in several studies focused on different breeds of sheep, that those animals that avoid a tussock sward (an area with an excess of parasites and nitrogen-rich forage) have lower worm burden (Hutchings et al., 2002, 2003). However this behavior has a disadvantage, which is the reduced productive performance of sheep (Hutchings et al., 2007). This behavior is also proven in natural system, e.g. reindeers avoid pastures where faecal contamination is increased (van der Wal et al., 2000).

Among different alternatives to chemical control, the selection of genetically resistant animals has been suggested to reduce dependence on the use of antihelminthics (Raadsma et al., 1997; Stear et al., 2007). Breed differences in resistance to GINs are well

documented in several breeds such as Florida Native sheep (Radhakrishnan et al., 1972; Bradley et al., 1973), Scottish Blackface (Altaif and Dargie, 1978), St. Croix (Courtney et al., 1985; Gamble and Zajac, 1992), Garole (Nimbkar et al, 2003) and Red Massai breed (Mugambi et al., 1997). In addition, many studies have demonstrated that a significant proportion of the variation in sheep resistance to internal parasites is genetically determined (reviewed by Raadsma et al., 1997). The high level of variability observed within breeds has allowed the development of lines with increased resistance or susceptibility to GIN infections (Andronicos et al., 2010). These selected lines are valuable model to use them to understand the biology of the host response to the parasites infections.

4. Genetic studies about resistance to GIN infections in sheep

As a complex trait, parasite resistance is influenced by many different genes and their interactions, the environment, and the interaction between the genome and the environment. Traditionally, genetic selection of complex traits has been achieved based on phenotypic and pedigree information (Karlsson and Greeff, 2006; Kemper et al., 2010). However, collecting the phenotypes that could be used as indicator traits of parasite resistance, such as FEC, or IgA activity in serum is costly and time-consuming and, in addition, requires the animal to undergo the parasitic challenge at the time of sampling (Riggio et al., 2013). Because of that, and also considering the low to moderate heritabilities reported for parasite resistance indicator traits (reviewed by Stear and Wakelin, 1998 and Bishop and Morris, 2007), the identification of the genes and causal mutations explaining part of the phenotypic variation observed for parasite resistance in sheep populations could be used to select resistant animals only based on molecular information. In the last years, there has been a large progress in the development of sheep genomic resources, such as the whole genome reference sequence of the sheep genome (Oar_v3.1 available at http://www.ensembl.org/Ovis_aries/Info/Index) and the development of genomic tools, especially the medium and high-density SNP genotyping ovine arrays. These resources together with the fast increasing economic availability of genomic technologies (e.g. genotyping-by-sequencing, whole genome sequencing) have already proven to be very useful for the identification of molecular variants underlying monogenic traits (Becker et al., 2010; Suarez-Vega et al., 2013, 2015) and is expected that they will also help accelerate the identification of causal genes explaining phenotypic

variation of traits of complex economic interest in this species (Ron and Weller, 2007), including those related to parasite resistance.

In the last decades there have been many studies focused on improving our understanding about the genetic determinism of parasite resistance in sheep, including studies focused on: (i) the estimation and assessment of genetic parameters of indicator traits (Bishop et al., 2004; Morris et al., 2004; Gutiérrez-Gil et al., 2010), (ii) the genetic variability and the role of some candidate genes (Sayers et al., 2005a; Benavides et al., 2002, 2009), and (iii) the scanning of the genome to identify regions underlying the variation observed in the indicator traits (Beh et al., 2002, Gutiérrez-Gil et al., 2009b; Sallé et al., 2012). We provide below a brief overview of the results and conclusions derived from the three types of studies mentioned.

4.1. Indicator traits of parasite resistance and their heritabilities

The selection for resistance to parasitic diseases has been based traditionally on the use of quantitative measures of phenotypic traits that are associated with the presence of the disease. Ideally, the phenotypic parameter used to monitor the resistance of sheep to GINs, or the ability of the host to response to GINs, should be easy to sample, reliable and repeatable, and its diagnostic method should be fast.

FEC, the number of eggs per gram of faeces, is the most widely trait used as a parameter to measure the degree of resistance to GINs in sheep (Smith et al., 1984; Stear et al., 2004; Davies et al., 2005; Bishop, 2012). In Australia, different studies have shown that selection for parasite resistance can be achieved by selecting animals with low FEC in natural and experimental parasite challenge environments (Karlsson and Greeff, 2006; Kemper et al., 2010). Using FEC as indictor trait of parasite resistance is quite cheap and easy to perform. In addition, this trait also gives access to epidemiological information as the different species of GIN can be identified by the egg size (e.g Nematodirus spp). The reported heritability estimates for the FEC trait range from 0.30 to 0.48 in infections due to *T. circumcincta* (Stear et al., 2009), *T. colubriformis* (Douch et al., 1996; Gruner et al., 2004) and *H. contortus* (Sréter et al., 1994; Gruner et al., 2004). In Soay sheep, a fraction of the genetic component of the FEC variability has been reported to be associated with different genotypes of a region of the MHC (Beraldi et al., 2007).

However, several authors have suggested that FEC alone should not be used to guide treatment or selection related decisions, but the information provided by this trait should be interpreted in conjunction with that derived from additional indicator traits (Bishop, 2012; Roeber et al., 2013). Hence, there are several additional indicator traits that give a differentiated information depending on the state of host, and they can be grouped as follows: (i) measurements of resistance: FEC, worm burden, worm size and fecundity; (ii) measurements related to the immune response: eosinophilia, and levels of different antibodies such as IgA, IgG, IgE and IgM; (iii) measurements of the pathological consequences of infection: anaemia, pepsinogen or fructosamine concentrations; and (iv) measurements related to resilience: growth rate and required treatment frequency (Bishop, 2012).

The parasitic traits, worm count and worm length, are positively correlated with FEC and show heritability values of 0.14 and 0.62 respectively (Stear and Bishop, 1999). Moreover worm count is proposed as a direct method for identifying resistant animals (Sayers and Sweeney, 2005) and it is also correlated with the animal's productivity. However, the measurements of these two traits are difficult to sample as they involve that the host has to be sacrificed.

On the other hand, other studies have reported that the plasma levels of IgA, which has a high heritability (0.56) and repeatability, could be a good trait to consider as an indicator or resistance to GINs (Strain et al., 2002). The serum IgA levels is positively correlated with other immune parameters (eosinophils, mast cell and globule leucocyte), whereas a negative correlation has been observed between IgA and FEC and worm length (Stear et al., 1995b; Martinez-Valladares et al., 2005). A recent study on the validation of the levels of anti-CarLA IgA in saliva performed by ELISA highlighted a number of key practical advantages of this trait over the use of FEC for selection purposes (Shaw et al., 2012). Among these additional advantages these authors underlined that the blood or saliva sample collection is easy and that the use of this immune-assay technique allows a high sample processing throughput. However these authors also mention some disadvantages of the ELISA method such as the need of a huge variety of parasites antigens, the inability to distinguish between current and past infections, since antibodies could sustain for some period (Henderson and Stear, 2006), the fact that in some cases the results do not reflect the intensity of the infection and the poor specificity that this

methodology may show (Doenhoff et al., 2004). Another trait of interest in relation to the immune response is the levels of eosinophils in blood. This trait shows an estimated heritability ranging between 0.43 and 0.48 in lambs of 4-5 months of age, and has been proposed as an indicator trait for genetic selection purposes (Henderson and Stear, 2006).

Plasma pepsinogen is a pathophysiological marker of abomasal lesions mainly caused by the length of the *T. circumcincta* worms (Stear et al., 1999). Pepsinogen is a pro-enzyme produced by chief cells in the abomasum that is converted to its active form, pepsin, by the hydrochloric acid produced by parietal cells. Thus, any cause which leads to increase in the pH of the abomasum prevents the conversion of pepsinogen to pepsin. As it was mentioned earlier, one of the factors is the development and emergence of *T. circumcincta* L4 from gastric glands which results in loss of parietal cells. This leads to decreased production of hypochlorous acid and consequently the abomasal pH is altered.

In naturally exposed adult Spanish Churra sheep, the heritability of FEC, serum levels of pepsinogen and IgA have been shown to range from low to moderate, with values of 0.12, 0.21 and 0.19 respectively (Gutiérrez-Gil et al., 2009b).

4.2. Methods to detect genes influencing GIN resistance in sheep

Gaining knowledge to understand the host-parasite co-evolution is an area in which the discovery of genetic variants underlying trait variation, in both hosts and parasites, is of major interest. The use of molecular markers allows a potentially reliable way to identify genomic regions that are directly related with the resistance to nematodes in sheep. By identifying genetic markers showing association with the quantitative traits under study, which in this involve the phenotypic indicators mentioned earlier, such as FEC, IgA, etc, we will try to identify the mutations that directly influence parasite resistance. In general, there are two different approaches to identify genes underlying the genetic variability observed in complex traits of economic interest: the analysis of candidate genes and the identification of Quantitative Trait Loci, or QTL, through genome-wide scans.

4.2.1. The candidate gene approach

The candidate gene strategy evaluates the relationship between a trait and a specific mutation in functional genes selected for the studied phenotypic trait. In the simplest form of candidate gene studies, the genes to be studied are selected considering their established or putative function and then the genetic variability of that gene is tested for

association with a given trait. In other cases, the study tests whether the expression profile of the candidate gene is upregulated or downregulated in relation to the studied trait (Gossner et al., 2013). In the latter case, we can find the case of the studies based on microarrays or expression arrays (MacKinnon et al., 2009). In some cases the information derived from a genome scan for detection of QTL suggests a positional candidate gene that due to its function becomes a functional candidate. Later studies may directly consider this gene following a candidate gene strategy.

In relation to parasite resistance, it has been shown that resistant animals mount faster immune response than susceptible ones (Terefe et al., 2007). Thus, resistant animals may have more efficient immune mechanisms in which some of the immune genes orchestrate these responses against the pathogens. Therefore, some of the obvious candidate genes to study in candidate gene studies related to parasite resistance in sheep are those related to the immune response.

The host immune system is one of an organism's most complex systems and shows many signs of co-evolution with parasites. The immune system of mammalians can be classically categorized in two parts; “innate” and “adaptive” immunity. Innate immunity, also known as the nonspecific immunity, has two roles to elicit immediate defense as the front line of the host defense and to generate long-lasting adaptive immunity, also known as a specific immunity. Hence, the activation of the innate immune response can be a prerequisite for the triggering of the acquired immunity which is mediated by clonally distributed T and B lymphocytes and is characterized by specificity and memory (Janeway et al., 2001). Based on this, the immune related genes may be distinguished depending on the categorization of the immune response: (i) genes implicated in the innate immunity, a first line of defense, (ii) genes that govern the specificity of adaptive immune response, and (iii) genes affecting the quality of specific immune responses (Axford et al., 1999). In any case, there are many genes that are involved in more than one of these specific mechanisms and a clear frontier between them is not always easy to draw.

In sheep, many studies have used the candidate gene approach to assess the association of functional candidate genes with the ability of the animal to resist the infection by GINs, most of them using FEC as an indicator trait (e.g. Buitkamp et al., 1996; Paterson et al., 1998; Sayers et al., 2005b). Many of these studies were initially focused on the analysis

of genes of the MHC, for which a high level of genetic diversity has been observed (Schwaiger et al., 1995; Buitkamp et al., 1996; Paterson et al., 1998; Sayers et al., 2005b; Keane et al., 2007). Another gene extensively studied in relation to parasite resistance traits in sheep is the *IFN-γ*, which is involved in the Th1 response and is related to chronic infection (Coltman et al., 2001; Sayers et al., 2005a). Other studies implementing the candidate gene approach have assessed the role of the *IgE* gene (Clarke et al., 2001), *IL* (interleukin) *-3*, *-4* and *-5* genes (Benavides et al., 2002), *IL-4* (Benavides et al., 2009), *IL-13* and *ALOX15* (*arachidonate 15-lipoxygenase*) (Wilkie et al., 2015).

In sheep, the MHC class genes are located on chromosome 20 and encode polymorphic glycoproteins composed of nine covalently linked subunits. The association between the MHC and the different degrees of response to the infection has been attributed to polymorphisms in the MHC region based on the known involvement of the MHC gene products in the induction and regulation of the immune response (Cresswell, 1994). The total phenotypic variation explained by the MHC effect in Blackface population is around 11% although this effect accounts for an approximately half proportion of the additive genetic variation (Stear et al., 1997), whereas in the Suffolk population just the Ovar-DRB1 locus accounted for 14% of the phenotypic variation in FEC (Sayers et al., 2005b). Several variants located in the Ovar-D genes of the MHC class II region, including some found in the *Ovar-DRB* (Paterson et al., 1998; Valilou et al., 2015), the *Ovar-DY* (Buitkamp et al., 1996) and the *Ovar-DQA1* genes (Forrest et al., 2010) have demonstrated a significant association with low levels of FEC in different studies conducted with experimentally or naturally infected animals. For example, in a study with Scottish Blackface sheep following natural infection, predominately by *T. circumcincta*, the substitution of the more common alleles by the *Ovar DRB1**1101 allele resulted in a reduction of 22-81 times in the levels of FEC (Schwaiger et al., 1995). In two other studies with the Suffolk breed, the carrier lambs of the *DRB1*1101* allele had a significantly lower worm burden and a higher count of mast cells and lymphocytes in the plasma (Sayers et al., 2005b; Hassan et al., 2011). It has also been shown that the susceptibility to the infection is associated with the *DQA2* MHC class II locus for which increased levels of FEC were reported in lambs carrying the *Ovar DQA2**1201 allele (Hickford et al., 2011).

According to the previously mentioned studies, genes of the MHC class II region arguably provide a promising opportunity for studying how balancing selection operate to maintain genetic variation in sheep populations. Moreover, advancements in our understanding of how to maintain MHC diversity could be exploited in breeding selection to select animals carrying specific haplotypes that provide the best protection against GIN parasites but at the same time sustain in the population other more diverse haplotypes with the aim of improving its general fitness.

As previously mentioned, apart from of the MHC class genes the most studied gene in relation to parasite resistance traits is the *IFN*-γ, which is positioned on OAR3. The IFN-γ protein, which is secreted by Th1 cells, is the main macrophage-activating cytokine. It also activates macrophages, inhibits B cells and is directly cytotoxic for some cells (Janeway et al., 2001). A microsatellite positioned in the intron 1 of *IFN*-γ has been found to be associated with the variation in parasite resistance in feral sheep and several domestic sheep (Crawford and McEwan, 1998; Coltman et al., 2001; Sayers et al., 2005a; Dervishi et al., 2011). Because of its role in the immune response and its association with nematode resistance this gene has received increased attention as a potential candidate gene. However this association was not shown in all studied breeds of sheep, which indicates that the genetic association varies according to the considered breed, as it was also observed for the MHC class genes. These observations would be also compatible with the hypothesis that a different gene located near *IFN-γ*, and showing high linkage disequilibrium with it in certain sheep populations, would be responsible of the identified effects. Other studies have reported that the expression of *IFN-γ* showed no significant difference between resistant and susceptible groups of ewes (Pernthaner et al., 2005; Dervishi et al., 2011).

Interleukins are a group of cytokines that are produced in response to an antigen and function as chemical messengers for regulating the innate and adaptive immune systems (Coondoo, 2011). In humans, it has been shown that genetic variation in interleukins was correlated with parasitic diversity, which indicates that interleukins are subjected to helminth-driven selective pressure (Fumagalli et al., 2009). Therefore they are natural candidates due to their major regulatory role in parasite susceptibility. Moreover several studies have shown the increased expression of interleukins related to helminth Th2 response expression in resistant animals when compared with susceptible individuals

(Pernthaner et al., 2006; Terefe et al., 2007; Shakya et al., 2009). Based on the important role of these genes, Benavides et al. (2002) performed an association analysis between seven microsatellite markers located on OAR5 close to the genes encoding for *IL-3*, *IL-4* and *IL-5* and FEC traits in Corriedale and Polwarth sheep breeds. For the two breeds, marker *CSRD2138* located close to the *IL-4* gene, was consistently associated with a FEC level reduction. A subsequent study testing one SNP per gene located within each of the *IL-3*, *IL-4* and *IL-5* genes has shown that only one SNP included in the *IL-4* gene showed a significant association in one of the breeds (Benavides et al., 2009).

All together the results of the different candidate genes studies for parasite resistance in sheep support the thesis that there is not a single mechanism of parasite resistance and that these mechanisms are controlled by many genes.

The microarray technology allows a rapid, simultaneous screening of many genes for changes in their expression between different cells, and it is used to evaluate the differential expression of specific genes. This methodology has allowed the identification among 100 to 300 patterns of differential gene expression by comparing genetically resistant and susceptible sheep to GINs (Diez-Tascón et al., 2005; Keane et al., 2007).

4.2.2. Detection of QTL based on whole genome scans

The analysis of QTL involves the identification of genomic regions harboring a gene that influences the studied trait or phenotype, by scanning the whole genome and without using previous functional information about possible candidates. Therefore, for QTL detection, known DNA markers or variants distributed throughout the whole genome are used as hallmarks that define each segment of the genome. For the mapping or localization process genetic maps, which provide information about the positions and order of the markers analysed, are used. In the 1990s the most used genetic maps were those based on microsatellite markers, whose density was low compared to the medium/high density of the maps used nowadays, which are based on single nucleotide polymorphisms (SNP) markers whose positions are directly based on the reference genome sequence (Maddox and Cockett, 2007). Considering the higher density offered by the high-throughput platforms available today, known as SNP-chips, the search for QTL can be based on linkage analysis (LA), a combination of linkage and linkage

disequilibrium analysis (LDLA) or by performing a genome-wide association scan (GWAS).

The traditional QTL mapping strategy in livestock species, which has been exploited in many studies published from 1995 to 2011, was to perform LA to assign significant QTL to a specific genome region through the analysis of microsatellite markers. Microsatellites are DNA markers showing variation in the length of short sequences, either a mono-, di-, tri- or tetra- nucleotide, which are repeated between 10 and 50 times. They are single-locus, codominant, spread through the whole genome, relatively easy to find and characterize. Based on their properties they were appointed as marker of choice until high throughput SNP genotyping platforms, or SNP-chips, became available. Microsatellites are not as abundant in the genome as the SNPs are, and the technological limitations for high-throughput genotyping of these markers had determined that the microsatellite-based genome scans were based on 200-300 markers across the whole genome, leading to the conclusion that the estimates of both the location and magnitude of the QTL were approximate (Slate et al., 2009) and required, generally, subsequent fine mapping studies. Many studies based on microsatellite-marker genome scans have searched for QTL associated with resistance to GINs, and reported significant QTL at the genome-wise or chromosome-wise significance level, depending on whether the correction for the multiple number of tests performed in the study took into account the number of tests performed at the genome-wise or chromosome–wise level. For sheep, the information resulting from all these QTL (location, flanking markers, significance level, resource population, etc.) is stored in the publically available database SheepQTLdb (http://www.animalgenome.org/cgi-bin/QTLdb/OA/index).

Considering all these studies, QTL related to resistance to GINs in sheep have been reported in most of the ovine autosomes as well as in the X chromosome (Clarke et al., 2001; Coltman et al., 2001; Beh et al., 2002; Crawford et al., 2006; Davies et al., 2006; Beraldi et al., 2007; Gutiérrez-Gil et al., 2009b; Marshall et al., 2009, 2013; Dominik et al., 2010; Matika et al., 2011; Silva et al., 2012). On chromosome (OAR)3, in the region where the *IFN-γ* gene is located, several QTL have been found to be associated with the expression of IgA and strongyleFEC (Coltman et al., 2001; Beh et al., 2002; Davies et al., 2006; Beraldi et al., 2007; Marshall et al., 2009; Dominik et al., 2010; Matika et al., 2011). In addition, several identified QTL on OAR14 (Gutiérrez-Gil et al., 2009b; Matika

et al., 2011; Silva et al., 2012) and OAR6 (Beh et al., 2002; Beraldi et al., 2007; Davies et al., 2006; Gutiérrez-Gil et al., 2009b; Marshall et al., 2009; Silva et al., 2012) have been reported to be associated with resistance to gastrointestinal parasites in different sheep populations (Figure 3).

Different studies have shown that the resistance to *H. contortus* and *T. circumcincta* is an acquired characteristic (Stear et al., 1999; Beraldi et al., 2008; Singleton et al., 2011) related to the development of a controlled adaptive immune response by differential activation of T cells (Gossner et al., 2012). Different types of immune responses will result in different severity degrees of the disease. On this regard, it is interesting to highlight the QTL located on OAR1 in the Merino breed (Marshall et al., 2009), which includes a gene that encodes for the inhibitory receptor *TIGIT* (*t cell immunoreceptor with ig and itim domains*). This gene is expressed in activated T cells, and its stimulation on T cells has influence on the decreased expression of several transcription factors with a consequent inhibition of proinflammatory (IFN-γ) cytokine production (Thaventhiran et al., 2012). Furthermore, one of the reported QTL influencing GIN resistance is located on OAR20 where the genes belonging to the ovine MHC are located (Davies et al., 2006). Many studies have found associations between the MHC and the resistance to parasites. As we previously mentioned the *Ovar-DRB1* locus, which is included in the MHC class II, has been associated with the resistance to *T. circumcincta* (Schwaiger et al., 1995; Stear et al., 1996; Sayers et al., 2005b). On OAR2 and OAR26, an experimental infection-based study reported by Marshall et al. (2013) detected strong evidence for the presence of a pleiotropic QTL or, alternatively, the presence of two or more linked QTL with effects on multiple resistance indicators for GIN related diseases. In this case, the lack of overlapping with other QTL reported in the same resource population based on field data (Silva et al., 2012) may be attributable to several factors such as age and/or immune status specificity of the QTL, a different level of parasite exposure, or biological differences between field and artificial challenges (Marshall et al., 2013). Generally, most of the published QTL studies have focused on the study of parasite resistance in lambs, as the lambs are more prone to the gastrointestinal infections. One exception to this is the study reported by Gutiérrez-Gil et al. (2009b), where a commercial population of naturally infected Churra adult ewes was analyzed. This study performed a classical LA QTL analysis based on the information provided by 182 microsatellite markers distributed along the 26 ovine autosomes, and reported the identification of five QTL

chromosomal regions. Of these, only one QTL influencing the FEC trait, and located on OAR6, reached the 5% genome-wide significance level. Four other QTL were identified at the 5% chromosome-wise level on chromosomes 1, 10 and 14, wherein three and one of these QTL influenced FEC and the activity of IgA serum levels, respectively (Gutiérrez-Gil et al., 2009b).

In 2009, 50K-SNP chip, which is a genotyping platform that enables to simultaneously interrogation of approximately 50,000 SNP markers became commercially available (Illumina, Inc). Based on this genomic tool many studies had performed later GWAS analyses in relation to GIN resistance traits in sheep. The GWAS approach uses high-throughput genotyping technologies to identify associations between the measurable trait and genetic variants across the entire genome (Pearson and Manolio, 2008). Ideally, the individuals analysed in a GWAS are unrelated. However, if a population structure exists in the analysed populations, e.g. due to family relationship, the analysis can be performed by taking this into account and performing the corresponding correction in the statistical model applied. The first published study reporting a GWAS for parasite resistance in sheep using the 50K-SNP chip revealed several suggestive QTL related to *H. contortus* and *T. colubriformis* resistance for several breeds of sheep (Kemper et al., 2011), although the low power of the experimental design did not allow the detection of any highly significant SNP. In addition to be used to perform GWAS-based analyses, the 50K-SNP chip can be also exploited to perform a medium density LA. Furthermore, based on the marker density offered by this genomic tool, the pedigree information used by LA can be combined with linkage disequilibrium (LD) information obtained at the population level, through a LDLA (Legarra and Fernando, 2009). The advantage of this approach in contrast to a GWAS is expected to suffer less from the multiple testing, and therefore to have more power to detect the existing QTL (Meuwissen, 2010). In a study searching QTL for milk traits in a half-sib population of Churra sheep, the number of QTL detected by LDLA was substantially higher than by the exclusive use of LA or LD (GWAS) (García-Gámez et al., 2012c), supporting the goodness of this methodology for populations where pedigree information can be exploited. In relation to parasite resistance, Sallé et al. (2012) reported many QTL associated with resistance to *H. contortus* using the three mentioned analysis methods (LA, LDLA and GWAS). Based on the information provided by the different analyses, this work identified, among many QTL with moderate or small effects, some critical regions associated to parasite

resistance on OAR5, OAR12, OAR13, and OAR21. Among these QTL, the most important QTL region was positioned on OAR12, where several associations for different indicator traits were confirmed by the different analyses. Based on its role as regulator of insulin-like growth factor (IGF) activity, the *PAPP-A2* (*pappalysin 2*) gene was suggested as a possible candidate gene for that QTL region (Sallé et al., 2012). In a later study, the expression level of *PAPP-A2* was shown to be down-regulated in naïve/challenged sheep, although no differential expression for this gene was detected between challenged resistant and susceptible sheep (Sallé et al., 2014). A remarkable result of the work reported by Sallé et al. (2012) was the identification of a QTL associated with pepsinogen on OAR21, precisely in the region where the gene *PGA5* (*the pepsinogen 5 group 1*) is located (Sallé et al., 2012). The study reported by Riggio et al. (2013) compared two different analysis methods to identify QTL for GIN resistance in a population of Scottish Blackface lambs: the GWAS approach and a regional heritability mapping method (hereafter denoted RHM). Among other identified QTL, this study identified three genome-wise significant QTL: one on OAR14 related to the *Nematodirus*FEC trait, one on OAR6 influencing Strongyles FEC and another one on OAR21 related to body weight. Body weight in lambs is a trait that can be used as indicator trait of parasite resistance due to the significant negative correlation between worm burden and body weight (Bisset et al., 1992; Bishop et al., 1996). The methodological comparison described by Riggio et al. (2013) suggested that the RHM approach is capable of detecting greater variation than GWAS. In a later study where the RHM approach was applied to perform a meta-analysis on three different sheep populations (Scottish Blackface, Sarda × Lacaune and Martinik Black-Belly × Romane) genome-wide significant QTL were detected on OAR4, OAR12, OAR14, OAR19 and OAR20 (Riggio et al., 2014). The QTL on OAR4 and OAR20 were confirmed by different variants of the RHM method, whereas a QTL on OAR20 positioned in the MHC region was identified as the most significant result. In relation to the result on OAR14, it is worth mentioning that a previous study had reported a significant selection sweep in the same region (40.1-55 Mb according to the OAR v2.0) of OAR14 (Fariello et al., 2013) and the QTL region (42-49 Mb and 45-54 Mb according to the Oar_v3.1) reported by Riggio et al. (2014). Based on the multi-locus haplotypes identified in that selection sweep region by Fariello et al. (2013), two possible candidate genes had been identified, the *IRF3* (*interferon regulatory factor 3*) gene and the *TGF-B1* (*transforming growth factor beta-1*) gene. Because these two genes are both related with

the immune response (Jann et al., 2009; Fariello et al., 2013), a possible direct relationship of these results with the QTL reported by Riggio et al. (2014) has been suggested. In another selection sweep mapping study performed in divergent lines of Romney and Perendale sheep, selected bred for high and low faecal nematode egg count (McRae et al., 2014a), the 50K-SNP chip dataset was analysed for selective sweeps specifically related to loci associated with resistance or susceptibility to GIN infection. This study revealed a total of sixteen significant selection signals related to seven candidate genes from a total of 47 genes. The list of candidates included genes involved in chitinase activity and the cytokine response (*CD53*, *CHI3L2*, *CHIA*, *DENND2D*, *RELN*, *NSUN2*, *HRH1*). Only two of the regions were contained within previously identified QTL associated with nematode resistance, which suggests that the selection sweep mapping approach could be an efficient and complementary approach to classical QTL mapping for the identification of QTL related to traits of interest, as shown also in relation to milk production traits in a variety of European dairy and non-dairy sheep breeds (Gutiérrez-Gil et al., 2014). Recently, a GWAS-based study reported in a double backcross population derived from Red Maasai x Dorper backcross population (Benavides et al., 2015) have suggested, among a total of 22 significant QTL regions identified, the presence of several QTL for the FEC trait on OAR6. Interestingly, the target region identified in that chromosome by these authors (55-78 Mb, based on Oar_v3.1 sheep reference genome sequence) is included in the confidence interval of the genome-wise significant QTL reported in Churra sheep through the microsatellite-based genome scan reported by Gutiérrez-Gil et al. (2009b). That region of OAR6 includes numerous annotated genes implicated in cytokine signaling, haemostasis and mucus biosynthesis.

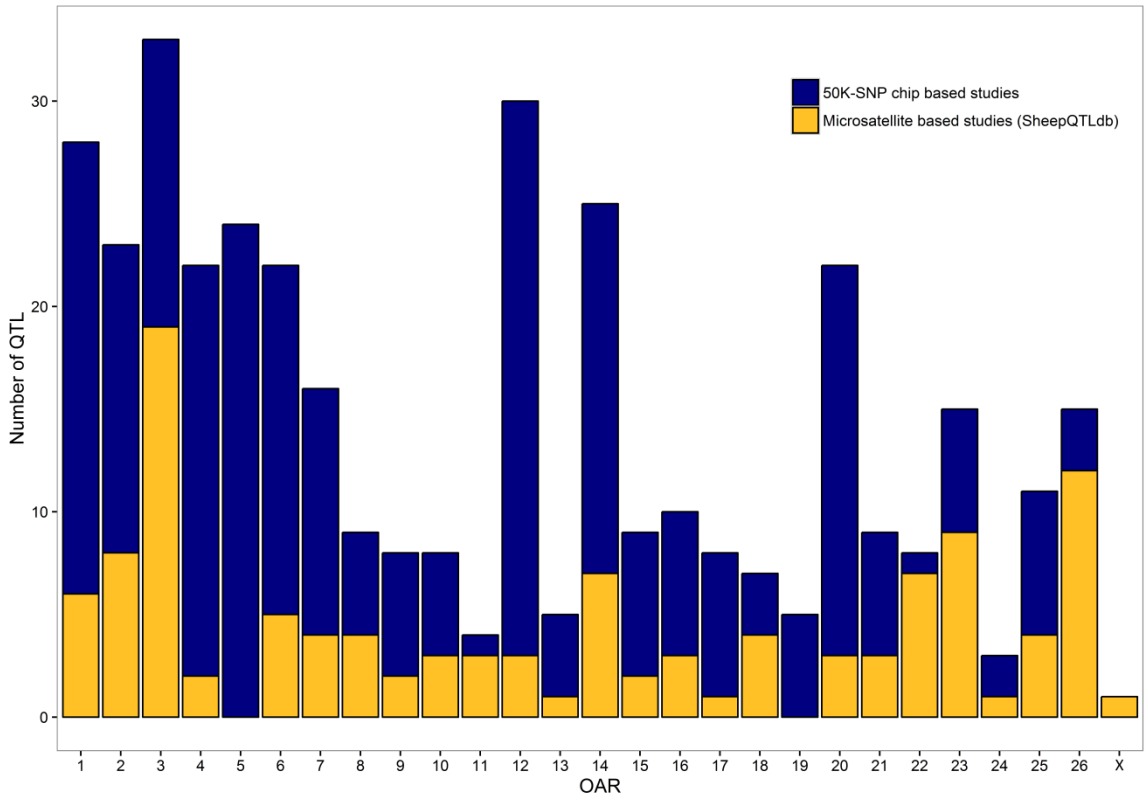

Figure 3. *Distribution of the number of QTL related to parasite resistance traits across the 26 ovine autosomic chromosomes and including X chromosome reported by microsatellite-based genome scan studies (yellow colour; extracted from the SheepQTLdb), and by studies based on the 50K-SNPchip (blue colour).*

All together the global results of sheep QTL studies for GIN resistance involve 116 QTL that are annotated in the SheeQTLdb for parasite resistance traits and immunological traits related to GIN infections based on microsatellite-based genome scans, and 263 QTL reported by more recent studies based on the 50K-SNP chip (Figure 3). These QTL have been detected based on the analysis of specific breeds or in the combination of data from few genetically distant sheep populations. The information derived from these studies can help to increase our understanding on the genetic control of this complex phenotype. As many other complex/quantitative traits of economic interest, these studies support the hypothesis that host resistance to internal nematode parasites is likely to be controlled by a number of loci of small to moderate effects. However, the complexity of the phenotype in question in this case may be considered even higher than traditional production traits because of the complex mechanisms that regulate the host-parasite interactions. Hence, in addition to the differences due to the sheep breed studied and the great variability of experimental designs, or the fact that the studied animals are exposed to a natural or an artificial challenge, several studies suggest that some of the QTL reported in sheep for

parasite resistance are specific of the parasite species (Riggio et al., 2014). This would explain the lack of overlapping between the results of the different studies focused on parasite resistance for different GIN species (e.g. Beh et al., 2002; Gutiérrez-Gil et al., 2009b; Kemper et al., 2011; Silva et al., 2012). In any case, we must also consider that some other QTL identified in relation to the natural parasite infections under different predominant parasite species are coincident (e.g. the OAR6 QTL reported by Gutiérrez-Gil et al., 2009b and Benavides et al., 2015). In addition to these observations, it is worth mentioning the existence of moderate to high genetic correlation between Nematodirus and Strongyles FEC ranging from 0.49 to 0.93 (Bishop et al., 2004). Hence, it is very likely that many other QTL are implicated in common pathways that are underlying resistance to a widely range of different parasite species.

As mentioned earlier, the detection of the genetic variants directly influencing parasite resistance in sheep offers opportunities to substantially improve the health status of sheep populations and, indirectly, reduce the presence of antihelminthics in sheep products, contributing in this way to human health protection. In addition to the ovine 50K-SNP chip, the rapid advances that are taking place in the field of livestock genomics provide additional tools to enhance our understanding of parasite resistance in sheep. Hence, the availability of the ovine high-density SNP-chip since 2013 (the International Sheep Genomics Consortium, Illumina) and the reduced cost of the next generation sequencing technologies, which allow the sequencing of whole genomes (WG-Seq) and transcriptomes (RNA-Seq) (Day-Williams and Zeggini, 2011) may help to reach this objective.

Materials and methods

1. Study area, resource population and sampling

The study was carried out in the region of Castilla y León, in the NW of Spain, and included 17 commercial dairy flocks distributed in seven out of the nine provinces of the region (Burgos, León, Palencia, Segovia, Valladolid, Salamanca and Zamora). In the study area, the flocks are reared under a semi-extensive system in which sheep graze on natural pasture for six hours per day and are kept indoors the rest of the day.

The faecal and blood samples were collected during the 6-months period from December 2011 to June 2012. Prior to sample collection, two conditions had to be met to include a flock in the study: i) the last anthelmintic treatment must have been administered at least two months before collecting the samples, and ii) the sheep had to be grazing at the time of sampling. In addition, the weather data of each farm were collected from the nearest forecast station (www.inforiergo.org). It was collected regarding to the development of larvae on the pasture, which is approximately 30 days, thus we decided to extract the weather data for one month before sampling.

The animals included in this study were ewes obtained by artificial insemination from farms belonging to the Selection Nucleus of the National Association of Churra Breeders (ANCHE). These animals were a subset of those previously genotyped with the 50K-SNP chip by García-Gámez et al. (2012b) which were still alive during the sampling period and for which both phenotypes related to parasite resistance were available.

Faecal samples were collected for each ewe directly from the rectum and blood samples were obtained by venipuncture of the jugular vein. Blood and serum samples were stored at -20 ºC until processing. Therefore this study is based on 529 adult Churra sheep, that belonged to 15 half-sib families, with faecal, blood serum and blood with EDTA samples available, with a mean of 31 animals sampled per flock (range: 11-60 individuals). The age of the sheep included in the study varied between four and 11 years. All of the sheep were undergoing milking at the time of sampling and were experiencing at least their third lactation.

1.1. Faecal samples

1.1.2. Faecal egg count

A modified McMaster technique (MAFF 1986) using zinc sulphate as a flotation solution was used to determine the number of eggs (Neggs) in faeces. The minimum detection limit of this technique was 15 eggs per gram (epg). FEC were determined by multiplying the Neggs observed microscopically by 15.

1.1.3. Larval culture

In each flock, pooled faeces were cultured to recover and identify third-stage larvae (L3) following standard parasitological techniques (MAFF, 1986), where a total of 100 L3 were identified per flock to estimate the percentage of each species.

1.2. Blood samples

1.2.1. Estimation of IgA antibody titre in the serum (or Indirect ELISA for detection of parasite specific IgA)

An indirect ELISA was carried out to determine the optical density (OD) of IgA in the serum. The assay for IgA specific antibody against L4 stage of *T. circumcincta* was performed using a rabbit anti-sheep IgA antibody. The results of ELISA were measured as OD values and were expressed as optical density ratios (ODR) according to the following formula:

$$ODR = \frac{(sampleOD - negativeOD)}{(positiveOD - negativeOD)} \quad (1)$$

1.2.2. DNA extraction

DNA extraction was carried out on ewe's blood samples and ram's frozen semen samples of breed of Spanish Churra sheep and performed using classical phenol-chloroform protocol and ethanol precipitation procedures (Sambrook et al., 1989). The quality and concentration of the obtained DNA was assessed using a spectrophotometer.

2. Analyses related to Objective1

2.1. Resource population

In the present study, several animals were excluded from the initial dataset so phenotypic and genotypic information was analyzed only for 518 Churra ewes. The animals belong to 14 half-sib families, and they were produced using artificial insemination, with an average family size of 37 daughters per sire (range: 12 to 89). Two indicator traits of parasite resistance were used, FEC and IgA.

2.2. Statistical analyses

Prior to further analyses, FEC measurements were log-transformed (LFEC) to reduce over-dispersion, as we did not find any transformation yielding a normalized FEC dataset. However, Box-Cox power transformation was used for the IgA phenotype to obtain a normal distribution of values (IgA_t). We used the R 'car' library to estimate the power parameter λ and carry out the transformation (Fox et al., 2012); the log transformation was also calculated through a command line in R (R Core Team, 2014).

To assess variables influencing the two parasite resistance-related traits under study, an analysis of variance (ANOVA) was performed for LFEC and IgA_t using a general linear model (GLM) through the R command line (R Core Team, 2014), which included the three following fixed effects: Flock, Age and Time point relative to parturition. The Flock effect was classified into 17 groups. Two groups were considered for the Age factor: ewes four to six years old and ewes seven or more years old. Two categories were also considered in relation to the Time point relative to parturition factor: one involving ewes showing a low immune response possibly due to the last stage of pregnancy or the start of lactation (animals sampled two weeks before giving birth or 30 days after birth) and a second including ewes that were outside that specific period (i.e., the 45 days around lambing).

2.3. Genotypes and physical map

In this study we analyzed the 50K-SNP chip genotypes, which were previously obtained from a large population of 1,696 Churra ewes (García-Gámez et al., 2012b). As a previous step, the SNP order and genome positions were updated according to the latest available version of the Ovine Genome Assembly, Oar_v3.1 (www.livestockgenomics.csiro.au/sheep/oar3.1.php), taking into account a 1 cM ~1 Mb conversion rate. Afterwards, quality control (QC) of genotypes was performed for the entire genotyped population following the steps detailed in a previous publication (García-Gámez et al., 2012c). Briefly, QC was performed in seven steps applied to raw genotypes: i) GenCall score for raw genotypes > 0.15; ii) known location of the marker on ovine autosomes; iii) call rate per individual > 0.9; iv) call rate per SNP ≥ 0.95; v) minor allele frequency (MAF) ≥ 0.05; vi) correspondence with Hardy-Weinberg equilibrium (HWE) p-value > 0.00001; vii) analysis of the filtered genotypes using the VerifTyp software to check for Mendelian inconsistencies between parents and offspring (Boichard D and Druet T, personal communication). Afterwards, a total of 43,613 SNPs

located on the 26 ovine autosomes passed the QC process and were subjected to different QTL mapping analyses.

2.4. QTL mapping analyses

Yield deviation (YD)s of transformed data were used as dependent variables for statistical analyses to identify genomic regions influencing resistance to GIN infection. For the two traits under study, YD estimates were calculated following a multivariate animal model using the R command line and the 'lsmeans' library (Lenth, 2013) in which LFEC and IgA_t were corrected for the fixed effect of Flock, which according to the previously described ANOVA analysis, was the only factor significantly influencing the studied traits. Later, the following statistical procedures were used for QTL mapping:

(i) Genome scans based on a classical LA and a combined LDLA procedure were performed at 0.1 cM step intervals using the corresponding analysis options (*calcul = 4*, *calcul = 28*) of the QTLMap software (Filangi et al., 2010). This software also allowed for the calculation of significance thresholds at the chromosome-wise significance level through a total of 1,000 permutations (at 0.1 cM steps) for LA and 1,000 simulations (at 5 cM steps) for LDLA. Genome-wise significance thresholds were based on the chromosome-wise significance threshold by correcting for the total number of chromosomes under analysis. A by-default haplotype size of 4 SNPs was used for LDLA.

For each QTL identified by the across-family LA scan, linkage-based within-family analyses were performed to identify the corresponding segregating families. For significant QTL detected by LA, Likelihood Ratio Test (LRT) values were converted to Logarithm Odds ratio (LOD) values (Beraldi et al., 2007), and confidence intervals (CIs) for the QTL locations were estimated by the widely used 1-LOD drop-off method (Lander and Botstein, 1989). The proportion of the variance explained by the LA QTL was calculated based on the corresponding LOD values using the formula $\sigma_p = 1 - 10^{-\frac{2}{n}LOD}$(Broman and Sen, 2009). In LDLA, the chromosomal regions involving consecutive significant haplotype associations within a chromosome (allowing gaps no greater than 5 cM) were grouped as a significant LDLA interval; other cases were considered isolated significant haplotypes.

For chromosomes showing significant effects identified by both the LA and LDLA genome scans, a linkage disequilibrium analysis (LDA) based on the LDA Decay approach described by Legarra and Fernando (2009) was implemented using the QTLMap software (*calcul = 26*). The aim of this analysis was to distinguish whether the

significant associations identified by LDLA were exclusively due to linkage pedigree-related information or whether an association with the trait could also be identified at the population level. LDA was performed at 0.1 cM step intervals using a by-default 4 SNP haplotype size and 1,000 (at 5 cM steps) simulations for the chromosome-wise threshold calculation. Significant LDA intervals were defined in the same way as for LDLA.

(ii) A GWAS was performed by implementing the following linear mixed model (LMM), which includes the polygenic effect as a random effect and genotypes at single SNP markers as fixed effects:($y = Zu + Xb + e$) where y is defined as the vector of phenotypes (YDs) of the ewes; Z is a matrix associating random additive polygenic effects to individuals; u is a vector containing random polygenic effects; X is a vector with a genotypic indicator (-1, 0, or 1) associating records to the marker effect; b is the allele substitution effect for the particular SNP studied; and e is the random residual. This association analysis was implemented by the Restricted Maximum Likelihood (REML) method using the DMU package (Madsen et al., 2006), and the SNP effect was tested using a Wald test against a null hypothesis of b = 0.

Bonferroni corrections for multiple testing were used for the GWAS-based analyses. However, to account for the existence of linkage disequilibrium between the markers analyzed, rather than performing a conservative Bonferroni correction, we implemented the method proposed by Gao et al. (2010) to calculate the number of independently analyzed markers for each chromosome and for the entire sheep genome. By using a principal component analysis (PCA)-cutoff of 0.975, the total number of independently analyzed markers across the entire genome was 25,881.

We have also performed a search of positional candidates in reference to our results. For that reason, for each significant QTL/association identified, we determined a "target genomic interval" (TGI), which was defined as the corresponding genomic region according to the sheep reference genome assembly Oar_v3.1 to the following: (i) the CI estimated for LA significant QTL and the defined significant LDLA intervals; and (ii) a 250 kb-long interval centered on each of the significant isolated haplotypes detected by LDLA and the significant SNPs identified by GWAS.

Once defined, the TGIs were compared with the Oar_v3.1 span intervals annotated in the Sheep QTL database (SheepQTLdb) (Hu et al., 2013) for previously reported QTL, mainly derived from microsatellite-based genome scans. We also contrasted our TGIs with more recent studies based on the 50K-SNP chip that are not included in this database

(Kemper et al., 2011, Sallé et al., 2012; Riggio et al., 2013, 2014; McRae et al., 2014a; Benavides et al., 2015). For some of these later studies based on the sheep genome assembly Oar_v2.0, when available, the corresponding Oar_v3.1 position of the target marker/interval was considered for the comparison. Only regions mapping within 1 Mb from the defined TGIs were considered to be coincident with our results. For those QTL showing a very long span, the position of the QTL peak was prioritized to determine a possible correspondence.

The extraction of positional candidate genes included in the TGIs according to the sheep genome assembly (Oar_v3.1) was performed using the BioMart web-based tool (Cunningham et al., 2015) (http://www.ensembl.org/biomart/martview/) based on Ensembl release 81. Functional candidate genes related to the QTL identified in this study were identified by comparing the complete list of positional candidate genes extracted with BioMart with a database of 5,029 genes related to immunology. This database was based on the IRIS (1,535 genes; (Kelley et al., 2005)) and ImmPort (4,815 genes) gene lists, both of which are available at (http://www.innatedb.com/redirect.do?go=resourcesGeneLists).

3. Analyses related to Objective 2

3.1. Sequencing analysis of DRB1 exon 2 and study of the DRB1 microsatellite

The microsatellite located immediately downstream of DRB1 exon 2 was amplified using two primers (labelled with FAM). Afterwards, PCR amplicons were verified by 1% agarose gel electrophoresis and were separated and analyzed on an ABI 3130 sequencer. The fragment lengths were determined using the GeneMapper™ software version 4.1. (Applied Biosystems, Foster City, CA, USA).

DRB1 exon 2 was amplified with two primers for direct sequencing. Afterwards, exon 2 was sequenced using three primers, two primers that we used for direct sequencing plus one additional.

3.2. Sequencing analysis of DQB exon 2

PCR and sequencing of ovine DQB exon 2 was done using four different primer pairs: the primers published by van Oorschot and colleagues (1994), termed JM05, combined with

JM06 and JM07 as well as additional primers pairs: LfL#994 combined with JM05 and #1005 combined with #1007. The latter primers were used to obtain sequence information for the complete DQB exon 2 and to simplify assignment of alleles. PCR amplicons of DRB1 and DQB exon 2 were sequenced using the BigDye® terminator v3.1 cycle sequencing kit (Life Technologies). The reactions were run on an ABI 3130 and analyzed with the SeqScape™ software v2.7 (Applied Biosystems, Foster City, CA, USA).

3.3. Description of obtained sequences of MHC class IIB genes

Afterwards, obtained heterozygous sequences were analyzed by using the blast algorithm, either using the IPD-sequence database (DRB1) or an in-house library (DQB). Alignments of nucleotide sequences were done using Clustal W (Thompson et al., 1994) and translation to amino acid sequences was done using BioEdit v7.2.5 (Hall, 1999). Phylogenetic trees were generated using Phylemon 2 (http://phylemon.bioinfo.cipf.es/). Distance matrices were calculated using the ProtDist option of Phylip (v.3.68, Dayhoff PAM matrix), and phylogenetic trees were generated using the Neighbor-Joining Clustering method.

4. Analyses related to Objective 3

4.1. The Zero-Inflated Negative Binomial (ZINB) model

Descriptive statistical analysis for the two traits was conducted for the 529 sampled animals with the 'pastecs' library (Grosjean and Ibanez, 2014) in R (R Core Team, 2014). The Shapiro-Wilk test was carried out to determine if the data for each trait was normally distributed. Due to the large number of zero counts in the FEC data and the fact that the animals graze during short periods of time (semi-extensive rearing system), we decided to use a ZINB model to estimate the zero-inflation parameter and then extended it to discriminate between exposed and unexposed animals. The zero-inflated model with IgA data was compared to a simpler negative binomial model using a likelihood ratio test. Moreover, in this particular study, a zero-inflated model is a biologically meaningful description of the system; the adverse climatic conditions for larval development of the year studied will reduce pasture contamination, and the short grazing periods due to the semi-extensive rearing system will reduce exposure, which means that some animals would not have been infected at the time of sampling, and may not have been infected

since the last antihelminthic treatment. This model also allows for a more natural extension into discriminating between infected and uninfected animals.

4.2. Estimation of zero-inflation

In the zero-inflated model, positive FEC are derived from a negative binominal (NB) distribution, while a zero count can arise from either the NB distribution or the zero distribution (a binary distribution that generates structural zeros). The probability of belonging to the zero distribution is called the zero-inflation parameter. The animals that have zero counts arising from the zero distribution are assumed to have not been infected since the last anthelmintic treatment, so these animals can be excluded from further analysis. A Markov Chain Monte Carlo model similar to the one described in Denwood et al. (2008) using the 'runjags' package (Denwood, 2013) was employed to estimate the zero-inflation parameter.

In this model, the negative binomial distribution arises from a gamma-Poisson mixture distribution. Uninformative priors were used for the parameters of the gamma distribution.

4.3. Extending the ZINB model

A zero-inflation model does not determine which animals are exposed and resistant (as opposed to unexposed). The classical ZINB model was therefore extended to accommodate IgA data as additional information for the animal status, i.e. infected or not recently infected. The animal status is calculated as,

$$Status = \begin{cases} 0; \ not\ recently\ infected & with\ probability\ 1\ \ P, \\ 1; \ infected & with\ probability\ P \end{cases} \quad (2)$$

where status = 0 means that the animal has not been recently infected and status = 1 means that the animal is infected. P is the probability of being recently exposed and is equivalent to one minus the zero-inflation parameter. The raw egg counts (FEC/15) were used and it is assumed that for each animal i, the number of eggs counted arises from the following,

$$Neggs_i = \begin{cases} 0 & if\ Status = 0, \\ Poisson\ (\lambda_i) & if\ Status = 1 \end{cases} \quad (3)$$

where is the number of eggs arising from the gamma distribution (equation 4).

$$\lambda_i \sim gamma\ (shape, rate) \quad (4)$$

with the shape and the rate parameters of the gamma being calculated by the model. Similarly the IgA data can be partitioned in 2 gamma distributions (equation 5) based on the animal status.

$$IgA_i = \begin{cases} gamma\ (sh_1, rt_1) & if\ Status = 0, \\ gamma\ (sh_2, rt_2) & if\ Status = 1 \end{cases} \quad (5)$$

with sh_1, sh_2, rt_1 and rt_2 being the two shapes and two rates respectively that parametrize the two gamma distributions. In the model, samples are drawn for sh_1 and sh_2 as well as for mn_1 and mn_2, which are the two means of the two gamma distributions. The rates are calculated by rate = shape / mean and the mean for the animals not recently infected (mn_1) is always smaller than the mean of the infected (mn_2).

The number of iterations sampled was 50,000, with the first 5,000 being discarded (burn in), and assessed convergence with the Gelman-Rubin statistic from the 'coda' package (Plummer et al., 2006) being under 1.05.

Using the realisations of the animal status across the iterations (unexposed animals have status = 0, exposed and infected have status = 1), it is possible to calculate the probability for each animal to be in one status or the other, P_i^{exp}; animals without zero FEC will always be in the infected status. The animals that were estimated to be unexposed, i.e. the animals with status = 0, in each sample of the Markov Chain were excluded from further analyses, allowing the use of simple statistical tools to analyse the remaining dataset for each sample.

4.4. Correlations between phenotypes

Considering FEC, IgA and the realisations of animal status, P_i^{exp}, the Kendall's rank correlation coefficient was used to estimate the relationships among these three parameters. Correlations were calculated in R, using the 'ltm' package (Rizopoulos, 2006), for each sample of the Markov Chain and the average across the samples.

.

Results

The results of the present PhD Thesis have been compiled in three main research articles, each of them related to each of the proposed specific objectives. In addition, preliminary results of the genome scan performed in the framework of Objective 1 have been presented as conference communications.

LIST OF PUBLICATIONS

Objetive 1.

Marina Atlija, Juan-Jose Arranz, María Martinez-Valladares, Beatriz Gutiérrez-Gil**.** Detection and replication of QTL underlying resistance to gastrointestinal nematodes in adult sheep using the ovine 50K SNP array. *Genetics Selection Evolution* 2016, **48**:4. 20 January 2016.

Marina Atlija, Beatriz Gutiérrez-Gil, María Martinez-Valladares, Luis Fernando de la Fuente Crespo, Juan-Jose Arranz.

Barrido genómico con el SNP-chip ovino 50K para la detección de QTL con influencia sobre la resistencia a nematodos intestinales en el ganado ovino de raza churra: análisis de ligamiento para el recuento de huevos en heces. XV Jornadas sobre producción animal, AIDA (Asociación Interprofesional para el Desarrollo Agrario) 14-15 May 2013.

Marina Atlija, Juan-Jose Arranz, María Martinez-Valladares, Beatriz Gutiérrez-Gil. Search of genomic regions influencing faecal egg count, as an indicator of resistance to gastrointestinal nematode infections, based on the analysis of the OvineSNP50 BeadChip. Proceedings, 10th World Congress of Genetics Applied to Livestock Production (WCGALP). Vancouver, Canada. 17-22 August, 2014.

Objetive 2.

Marina Atlija, Beatriz Gutiérrez-Gil, Juan-Jose Arranz, Jördis Semmer, Michael J Stear, Johannes Buitkamp. Short communication: Major Histocompatibility Complex Class IIB polymorphism in an ancient Spanish breed. *Immunogenetics*; September 2015, Volume 67, Issue 9, pp 531-537.

Objetive 3.

Marina Atlija, Joaquín M Prada Jiménez de Cisneros, Beatriz Gutiérrez-Gil, Francisco Antonio Rojo Vázquez, Michael J Stear, Juan-Jose Arranz, María Martinez-Valladares. Implementation of an extended ZINB model in the study of low levels of natural gastrointestinal nematode infections in adult sheep. *BMC Veterinary Research, submitted*.

Detection and replication of QTL underlying resistance to gastrointestinal nematodes in adult sheep using the ovine 50K SNP array.

Marina Atlija[1], Juan-Jose Arranz[1], María Martinez-Valladares[2,3], Beatriz Gutiérrez-Gil[1]

[1] Departamento de Producción Animal, Facultad de Veterinaria, Universidad de León, Campus de Vegazana s/n, León 24071, Spain.

[2] Instituto de Ganadería de Montaña. CSIC-ULE. 24346. Grulleros. León.

[3] Departamento de Sanidad Animal. Universidad de León. 24071. León.

Genetics Selection Evolution 2016, 48:4. 20 January 2016.

Atlija *et al. Genet Sel Evol (2016) 48:4*
DOI 10.1186/s12711-016-0182-4

GSE Genetics Selection Evolution

RESEARCH ARTICLE Open Access

Detection and replication of QTL underlying resistance to gastrointestinal nematodes in adult sheep using the ovine 50K SNP array

Marina Atlija[1], Juan-Jose Arranz[1], María Martinez-Valladares[2,3] and Beatriz Gutiérrez-Gil[1*]

Abstract

Background: Persistence of gastrointestinal nematode (GIN) infection and the related control methods have major impacts on the sheep industry worldwide. Based on the information generated with the Illumina OvineSNP50 BeadChip (50 K chip), this study aims at confirming quantitative trait loci (QTL) that were previously identified by microsatellite-based genome scans and identifying new QTL and allelic variants that are associated with indicator traits of parasite resistance in adult sheep. We used a commercial half-sib population of 518 Spanish Churra ewes with available data for fecal egg counts (FEC) and serum levels of immunoglobulin A (IgA) to perform different genome scan QTL mapping analyses based on classical linkage analysis (LA), a combined linkage disequilibrium and linkage analysis (LDLA) and a genome-wide association study (GWAS).

Results: For the FEC and IgA traits, we detected a total of three 5 % chromosome-wise significant QTL by LA and 63 significant regions by LDLA, of which 13 reached the 5 % genome-wise significance level. The GWAS also revealed 10 significant SNPs associated with IgA_t, although no significant associations were found for LFEC. Some of the significant QTL for LFEC that were detected by LA and LDLA on OAR6 overlapped with a highly significant QTL that was previously detected in a different half-sib population of Churra sheep. In addition, several new QTL and SNP associations were identified, some of which show correspondence with effects that were reported for different populations of young sheep. Other significant associations that did not coincide with previously reported associations could be related to the specific immune response of adult animals.

Discussion: Our results replicate a FEC-related QTL located on OAR6 that was previously reported in Churra sheep and provide support for future research on the identification of the allelic variant that underlies this QTL. The small proportion of genetic variance explained by the detected QTL and the large number of functional candidate genes identified here are consistent with the hypothesis that GIN resistance/susceptibility is a complex trait that is not determined by individual genes acting alone but rather by complex multi-gene interactions. Future studies that combine genomic variation analysis and functional genomic information may help elucidate the biology of GIN disease resistance in sheep.

Background

Persistence of gastrointestinal nematode (GIN) infection and the related control methods have major impacts on the sheep industry worldwide [1]. The extensive use of anthelmintics has negative consequences, such as the costs of treatments, the emergence of anthelmintic-resistant strains of parasites, and the presence of drug residues in animal products. Among different alternatives to chemical control, the selection of genetically-resistant animals has been suggested to reduce dependence on the

*Correspondence: bgutg@unileon.es
[1] Departamento de Producción Animal, Facultad de Veterinaria, Universidad de León, Campus de Vegazana s/n, León 24071, Spain
Full list of author information is available at the end of the article

use of anthelmintics [2, 3]. Selective breeding for resistance to GIN using fecal egg count (FEC) as an indicator trait has been undertaken for certain sheep breeds [4–6]. However, classical selection for this complex phenotype is hindered by the time-consuming and costly process of recording information for indicator phenotypes (which may also include serum levels of e.g., immunoglobulin A (IgA), IgE and pepsinogen) and by the requirement for animals to be infected by GIN at sampling. These difficulties suggest that selecting animals resistant to GIN infection would be more efficient if it was based on indirect estimates, such as those generated from molecular marker information. In the last few decades, considerable effort has been made to understand the relationship between host and parasite and the mechanisms that underlie host resistance [7]. Moreover, the recent availability of the Illumina OvineSNP50 BeadChip (Illumina Inc., San Diego, CA) (referred to here as the "50 K chip") and a high-quality reference genome assembly [8] may allow for a deeper understanding of the genetic architecture of complex traits in sheep. Effective exploitation of this molecular information will increase our chances of developing protocols that will enable efficient selection of animals with increased resistance to GIN infections.

Because GIN are particularly pathogenic to young naïve animals such as growing lambs, gastrointestinal infections constitute a major cost to the sheep meat industry [9]. Accordingly, most of the quantitative trait locus (QTL) studies on GIN resistance traits [10], including those based on microsatellite markers as well as more recent analyses that exploit the ovine 50 K chip, have been conducted primarily on young animals [11–26]. Conversely, for the Mediterranean dairy sheep industry, a production system that is based on adult ewes and the sale of suckling lambs fed exclusively on maternal milk, replacement ewes and adult sheep are the only animals subjected to the direct effects of helminth infections [27]. In these animals, the breakdown of the acquired immunity to infection that occurs around the time of parturition [28] and the necessity of anthelmintic treatment determine how severe the economic losses will be [29].

Previously, we performed a genome scan using microsatellite markers to identify QTL that influence indicator traits of parasite resistance in adult Churra dairy sheep, an autochthonous dairy breed of the northwest region of Castilla y León in Spain [20]. The lack of strong coincidence between the QTL that we had identified and those previously detected by using lamb data suggested that aside from differences in host-parasite combinations, these QTL could be related to different mechanisms that underlie resistance between adult sheep and lambs.

Within this context, we undertook a new QTL mapping study based on the use of the ovine 50 K chip to genotype a commercial population of Spanish Churra dairy sheep. To follow on the initial linkage analysis-based genome scan reported by Gutiérrez-Gil et al. [20], our study was designed to replicate some of the QTL that were detected by the microsatellite-based scan and to identify new QTL and allelic variants associated with two previously analyzed indicator traits of parasite resistance: FEC and serum levels of IgA. For this purpose, we performed the new analyses using a different set of half-sib families from the same commercial population of Spanish Churra sheep. Taking advantage of the increased marker density offered by the 50 K chip, in addition to classical linkage analysis (LA), we also implemented combined linkage disequilibrium and linkage analysis (LDLA) and genome-wide association study (GWAS) approaches to provide a more complete picture of the QTL that segregate in this ovine population.

Methods

Resource population and sampling

Phenotypic and genotypic information for 518 Churra ewes from the Selection Nucleus of the National Association of Churra Breeders (ANCHE) was analyzed. The animals belonged to 14 half-sib families and were produced by artificial insemination, with an average family size of 37 daughters per sire (ranging from 12 to 89). A single collection of fecal and blood samples was performed for each of the 17 flocks in the Castilla y León region where the animals were raised. The samples were later processed to measure two indicator traits of parasite resistance, FEC and serum IgA levels. The ages of the sheep included in this study ranged from 4 to 11 years. At the time of sampling, all the sheep were undergoing milking and were at least in their third lactation.

Phenotypic records

FEC measurements were determined by floating the feces samples in zinc sulfate (d = 1.33) solution on a McMaster slide and counting the eggs [30]. The detection limit for this technique was 15 eggs per gram (epg). The samples showed a low level of FEC, which was related to the exceptionally small amount of rainfall before and during the sampling period. For each flock, pooled feces were cultured to recover and identify third-stage larvae (L3) using standard parasitological techniques [30]. One hundred L3 were identified per flock to estimate the percentage of each helminth species.

IgA activity in serum was tested against a somatic antigen from the fourth-stage larvae (L4) of *Teladorsagia circumcincta* by indirect ELISA according to a modified protocol that was previously described by Martinez-Valladares et al. [31]. Briefly, ELISA plates (Sigma) were coated overnight with 100 μL of phosphate buffered saline (PBS) solution containing 2.5 μg/mL of *T. circumcincta* L4

somatic antigen. On the following day, the ELISA test was performed in four steps. After each step, the content of the plate was removed, the plate was washed, and each well was filled with a specific reagent; the plates were then incubated for 30 min. The following reagents were used for each step: (1) PT-Milk (4 g powdered milk + 100 mL PBS-Tween 20; PBS-Tween 20: 1 L PBS (pH 7.4) + 1 mL Tween 20 (Sigma)); (2) a sheep serum; (3) a rabbit anti-sheep IgA antibody and (4) a peroxidase substrate and tetramethylbenzidine solution to produce a color reaction that was stopped after 30 min by the addition of 50 µL of 2 M H_2SO_4. The results were measured as optical density (OD) values. Positive and negative controls were included in all the plates; positive controls were obtained from a pool of sera from sheep that were experimentally infected with *T. circumcincta* and negative controls were obtained from non-infected sheep that were maintained indoors. The results are expressed as optical density ratios (ODR) according to the following formula:

$$ODR = \frac{(sampleOD - negativeOD)}{(positiveOD - negativeOD)}$$

Statistical analyses

Prior to further analyses, FEC measurements were log-transformed (LFEC) to reduce over-dispersion, since no transformation yielding a normalized FEC dataset was available. However, Box-Cox power transformation was used for the IgA phenotype to obtain a normal distribution of values (IgA_t). We used the R *'car'* library to estimate the power parameter λ and carry out the transformation [32]; the log-transformation was also calculated through a command line in R [33].

To assess the variables that influence the two parasite resistance-related traits under study, an analysis of variance (ANOVA) was performed for LFEC and IgA_t using a general linear model (GLM) through the R command line [33], which included the three following fixed effects: flock, age and time point relative to parturition. The 'flock' effect was classified into 17 groups. For the 'age' effect, two groups were considered i.e. ewes four to six years old and ewes seven or more years old. For the 'time point relative to parturition' effect, two categories were also considered i.e. one that included ewes that had a low immune response possibly because they were in the last stage of pregnancy or beginning lactation (animals sampled 2 weeks before giving birth or 30 days after birth) and one that included ewes that were outside that specific period.

Genotypes and physical map

We analyzed the genotypes that were obtained with the 50 K chip for a population of 1696 Churra ewes [34], which included animals with available phenotypic measurements for parasite resistance traits. First, SNP order and genome positions were updated according to the latest available version of the ovine Genome Assembly, Oar_v3.1 [35] by considering a 1 cM–1 Mb conversion rate. Then, quality control (QC) of the genotypes was performed for the entire genotyped population according to the protocol described in [34]. Briefly, QC was performed in seven steps that were applied to raw genotypes using the following criteria: (1) a GenCall score for raw genotypes greater than 0.15; (2) known location of the SNPs on the ovine autosomes; (3) a call rate per individual greater than 0.9; (4) a call rate per SNP greater or equal to 0.95; (5) minor allele frequency (MAF) higher than 0.05; (6) a *p* value for Hardy–Weinberg equilibrium (HWE) greater than 0.00001; and (7) analysis of the filtered genotypes using the VerifTyp software to check for Mendelian inconsistencies between parents and offspring (Boichard D and Druet T, personal communication). A total of 43,613 SNPs located on the 26 ovine autosomes passed the QC for the population of 1696 Churra ewes. For these 43,613 SNPs, available genotypes for 518 animals with parasite resistance phenotypes were subjected to different QTL mapping analyses.

QTL mapping analyses

Yield deviations (YD) of transformed data were used as dependent variables for statistical analyses to identify genomic regions that influence resistance to GIN infection. For the two traits under study, YD estimates were calculated following a multivariate animal model using the R command line and the *'lsmeans'* library [36]. LFEC and IgA_t were corrected for the fixed effect of 'flock', which according to the previously described ANOVA analysis, was the only factor that significantly influenced the studied traits. Then, the following statistical procedures were used for QTL mapping:

(1) Genome scans based on a classical LA and a combined LDLA procedure were performed at 0.1 cM step intervals using the corresponding analysis options (*calcul* = 4 and *calcul* = 28) of the QTLMap software [37]. Using this software, we also calculated the significance thresholds at the chromosome-wise significance level through a total of 1000 permutations (at 0.1 cM steps) for LA and 1000 simulations (at 5 cM steps) for LDLA. Genome-wise significance thresholds were based on the chromosome-wise significance threshold by correcting for the total number of chromosomes under analysis. A by-default haplotype size of four SNPs was used for LDLA.

For each QTL identified by the across-family LA scan, linkage-based within-family analyses were performed to identify the corresponding segregating families. For the

significant QTL that were detected by LA, likelihood ratio test (LRT) values were converted to logarithm odds ratio (LOD) values [15], and confidence intervals (CI) for the QTL locations were estimated by the widely used 1-LOD drop-off method [38]. The proportion of phenotypic variance that was explained by the QTL detected by LA was calculated based on the corresponding LOD values using the formula $\sigma_p = 1 - 10^{\frac{-2}{n}LOD}$ [39]. In the LDLA, chromosomal regions that involved consecutive significant haplotype associations within a chromosome (allowing gaps no greater than 5 cM) were grouped as a significant LDLA interval and the remaining ones were considered as isolated significant haplotypes.

For chromosomes with significant effects that were identified by both LA and LDLA genome scans, a linkage disequilibrium analysis (LDA) based on the LDA decay approach of Legarra and Fernando [40] was implemented using the QTLMap software (*calcul* = 26). The aim of this analysis was to determine whether the significant associations identified by LDLA were exclusively due to linkage pedigree-related information or whether an association with the trait could also be identified at the population level. Similar to the previously described LDLA, LDA was performed at 0.1 cM step intervals using a by-default 4-SNP haplotype size and 1000 (at 5 cM steps) simulations for the chromosome-wise threshold calculation. Significant LDA intervals were defined in the same way as for LDLA.

(2) A GWAS was performed by implementing the following linear mixed model (LMM), which includes the polygenic effect as a random effect and genotypes at single SNPs as fixed effects: ($\mathbf{y} = \mathbf{Zu} + \mathbf{X}b + e$) where $\mathbf{y}$ is defined as the vector of phenotypes (YD) of the ewes; $\mathbf{Z}$ is a matrix associating random additive polygenic effects to individuals; $\mathbf{u}$ is a vector containing random polygenic effects; $\mathbf{X}$ is a vector with a genotypic indicator (−1, 0, or 1) that associates records to the marker effect; b is the allele substitution effect for the analyzed SNP; and e is the random residual. This association analysis was implemented by the restricted maximum likelihood (REML) method using the DMU package [41], and the SNP effect was tested using a Wald test against a null hypothesis of $b = 0$.

Bonferroni corrections for multiple-testing were used to estimate the genome-wise and chromosome-wise significant thresholds for the GWAS-based analyses. To account for the existence of linkage disequilibrium (LD) between the analyzed SNPs, rather than performing a conservative Bonferroni correction based on the total number of SNPs analyzed, we implemented the method proposed by Gao et al. [42] to calculate the number of independently analyzed SNPs for each chromosome and for the entire sheep genome. To this end, we used the simpleM test [43], which estimates the actual number of effective tests (Meff) in genome-wide association studies through a principal component analysis (PCA) approach. Using a PCA-cutoff of 0.975, the total number of independently analyzed SNPs across the entire genome was equal to 25,881.

Comparison with previously reported QTL and identification of functional candidate genes

We performed a systematic search for previously reported QTL and associations related to parasite resistance traits in sheep for which a good correspondence was observed with the significant associations that we identified in our study; in addition, we performed a search for positional candidate genes in relation to our results. However, prior to these searches, for each significant QTL and significant SNP association identified, we determined a "target genomic interval" (TGI), which was defined as the genomic region based on the sheep reference genome assembly Oar_v3.1 that corresponded to: (1) the CI that was estimated for the significant QTL detected by LA and for the defined significant LDLA intervals; and (2) a 250 kb-long interval centered on each of the significant isolated haplotypes detected by LDLA and the significant SNPs identified by GWAS.

Once the TGI were defined, they were compared with the Oar_v3.1 intervals that are annotated in the SheepQTL database (SheepQTLdb) [10] for previously reported QTL and that are mainly derived from microsatellite-based genome scans. We also compared these TGI with more recent data from studies based on the 50 K chip that are not included in this database [21–26]. For some of these recent data based on the sheep genome assembly Oar_v2.0, when available, the corresponding Oar_v3.1 position of the target marker/interval was considered for comparison. Only regions that mapped within 1 Mb from the defined TGI were considered to coincide with our results. For the QTL that covered a very long region, the position of the QTL peak was prioritized to determine a possible correspondence.

The extraction of positional candidate genes included in the TGI according to the sheep genome assembly (Oar_v3.1) was performed using the BioMart web-based tool [44] based on the Ensembl release 81. Functional candidate genes related to the QTL identified in this study were identified by comparing the complete list of positional candidate genes extracted with BioMart with a database of 5029 immune-related genes. This database was based on the IRIS (1535 genes [45]) and ImmPort (4815 genes) gene lists, both of which are available at [46].

Results

Phenotypes

The presence of nematodes was confirmed in all the studied flocks with *Trichostrongylus spp.* and *Teladorsagia spp.* being the most prevalent species (49.3 and 48.6 %, respectively) that were identified among the total number of third-stage larvae obtained for the studied population. The prevalence of GIN infection by FEC per flock was 88.2 % (mean = 42.8 epg) and per individual was 45.4 % (mean = 39.4 epg). Faecal egg counts of GIN ranged from 0 to 1290 epg. For individual animals, the mean ODR of the IgA activity was 4.1 and ranged from 0.09 to 32.9.

QTL regions

The LA genome scan identified three 5 % chromosome-wise significant QTL (Table 1); in contrast, the LDLA genome scan identified 63 significant regions at the 5 % chromosome-wise level (Table 2). The LDA, which was performed for the three chromosomes that showed coincident results between the LA and LDLA scans, supported some of the significant signals that were identified previously (See Additional file 1: Table S1, Additional file 2: Figure S1). Although ten significant SNPs associated with IgA_t (Table 3) were identified in the GWAS, no significant associations were detected for LFEC. The significant results are described below and those identified by more than one analysis are highlighted. For ease of comparison, Table 4 provides a summarized representation of the results of the three analyses performed across the entire genome (LA, LDLA and GWAS).

LA results

The across-family regression analysis performed for LFEC and IgA_t across the ovine autosomes identified three chromosome-wide significant QTL. Two of these QTL that are located on OAR6 (OAR for *Ovis aries* chromosome) (peak at 88.1 cM) and OAR8 (peak at 2 cM) had an effect on LFEC (Fig. 1a), whereas the other QTL located on OAR22 (peak at 3.4 cM) had effects on IgA_t (Fig. 1b).

The significant QTL identified by the across-family LA (maximum LRT value and CI estimated by the 1-LOD drop-off method), together with the results of the within-family analyses are in Table 1. The QTL for LFEC on OAR6 and OAR8 segregated in three and two families, respectively, whereas a single family was significant for the QTL for IgA_t on OAR22. The CI that were estimated for the individual segregating families were located in the same region as the corresponding across-family CI, except for the peak for the QTL on OAR8 of Family 4, which was located at a more central position (31.2 cM) compared to the across-family peak at the proximal end of OAR8 (2 cM). However, the statistical profile for this family displayed a second peak reaching the 5 % chromosome-wise significance threshold (LRT = 11.76) at 12 cM, which was closer to the across-family QTL peak. The QTL effects estimated for the individual sires ranged from 0.3 (for the QTL for LFEC on OAR6) to 0.78 (for the QTL for LFEC on OAR8) standard deviations (Table 1). The estimated proportions of phenotypic variance explained by the three QTL identified by the LA were very similar and small (0.075, 0.077 and 0.069 % for the QTL on OAR6, 8 and 22, respectively).

LDLA results

Sixty-three significant QTL were detected at the 5 % chromosome-wise significance level by LDLA (30 for LFEC and 33 for IgA_t). Among these 63 QTL, 13 (six for LFEC and seven for IgA_t) reached the 5 % genome-wise significance level (Table 2; Fig. 1d). For 37 of the significant LDLA associations, nearby significant positions were grouped within a significant LDLA interval (Table 2); the remaining significant QTL identified by LDLA were defined based on isolated significant haplotypes. In addition, the three significant QTL identified by LA (on OAR6, 8 and 22) were supported by the LDLA scan (Table 2) (see Additional file 2: Figure S1). On OAR6, the LDLA results for LFEC revealed two 5 % chromosome-wise significant associations at 36 and 89.9 cM, with the latter being included within the CI of the QTL for LFEC on OAR6 detected by LA (Table 2). This analysis also identified a genome-wise significant association within the interval between 72.3 and 77.2 cM on OAR6.

On OAR8, although the LDLA scan identified a significant association at the proximal end of the chromosome (between 0.3 and 12.8 cM), which corresponded to the across-family CI for the QTL identified by LA, four other significant haplotype associations were identified across the chromosome (Table 2). Coincident with the QTL for IgA_t on OAR22 detected by LA (between 0.3 and 5.8 cM), the LDLA scan revealed a chromosome-wise significant haplotype association (maximum LRT at 6.7 cM) at the proximal end of this chromosome.

LDA results

For the three chromosomes for which the QTLMap LDA approach was implemented, several 5 % chromosome-wise significant associations were identified for the same trait for which significant results were observed in the LA and LDLA (See Additional file 1: Table S1). A correspondence was found between the significant LDA association of the 75.8–85.1 cM region on OAR6 with LFEC and the LA and LDLA results. The other significant associations identified by LDA coincided with QTL detected by LDLA.

Table 1 Significant chromosome-wise QTL detected by linkage analysis (LA)

Trait[a]	OAR[b]	Across-family analysis				Within-family analysis		
		Pos of max LRT (cM)[c]	P_c-value[d]	CI (cM)[e] TGI (Mb)[f]	Positional candidate genes involved in immune response[g]	Segregating family identifier (Pos of max LRT)[h]	CI (cM)[i]	Size effect trait units (SD units)[j]
LFEC	6	88.1	<0.05	80.8–91.4	*AFP, ALB, AMBN, AMTN, AREG, BTC, CXCL1, CXCL10, CXCL11, CXCL9, EREG, GC, IGJ, IL8, MUC7, PF4, PPBP, RASSF6, SCARB2, TMPRSS11D*	Fam. 1 (94.9)	70.0–96.8	0.468 ± 0.015 (0.30)
						Fam. 7 (90.6)	80.4–94.8	−0.499 ± 0.012 (0.32)
						Fam. 11 (86.7)	76.4–96.4	−0.777 ± 0.029 (0.50)
	8	2	<0.05	1–3.4	*CD109, COL12A1, MYO6*	Fam. 4 (31.2)	25.4–35.8	1.218 ± 0.024 (0.78)
						Fam. 11 (1.8)	0–2.9	0.738 ± 0.024 (0.47)
IgA_t	22	3.4	<0.05	0.3–5.8	*PCDH15*	Fam. 8 (6.4)	0.3–9.9	0.527 ± 0.046 (0.68)

[a] Analyzed traits: *LFEC* log-transformed faecal egg count, *IgA*$_t$ Box-Cox-transformed optical density ratio (ODR) values of immunoglobulin A activity

[b] *OAR* ovine chromosome

[c,h] Position of the chromosome (in centiMorgans) at which the maximum likelihood ratio test of the LA is reached in the analysis involving the 14 half-sib families included in this work (across-family analysis) or the individual analysis of the segregating families (those showing a P_c-value <0.05 in the within-family analysis), respectively

[d] *P_c-value* Chromosome-wise significance P-value established through 1000 permutation analysis

[e,i] *CI* Confidence interval (in cM) estimated from the position of the max LRT for the across-family analysis and the within-family analyses, respectively, following the 1-LOD-drop-off method [38]

[f] *TGI* Target genomic interval (Mb) defined as the corresponding genomic region, according to the sheep reference genome assembly Oar_v3.1, to the CI estimated for the LA significant QTL

[g] Positional candidate genes included in the CI of the corresponding QTL that were highlighted by the immune response candidate gene survey performed in the present work as potential functional candidates

[j] Estimated size effect of the QTL identified in the within-family analysis expressed in trait units (Yield Deviations of IgA_t) and in phenotypic SD of the trait (in brackets)

Table 2 Chromosome-wise significant results (P_c-value <0.01) from the combined linkage disequilibrium and linkage analysis (LDLA)

OAR[a]	Trait[b]	Pos of max LRT[c] (cM)	Significant LDLA interval (cM)[d]	P_c-value (P_g-value)[e]	TGI (Mb)[f]	Positional candidate genes involved in immune response[g]
1	LFEC	136.9	136.9–143	<0.05	136.9–143	*CXADR, NRIP1*
	IgA_t	242.4	–	<0.05	242.1–242.5	–
2	LFEC	78.3	–	<0.05	78.17–78.36	–
	IgA_t	188.3	188.01–188.44	<0.05	188.01–188.44	–
3	IgA_t	159.8	–	<0.05	159.67–160.06	–
		177.7	–	<0.05	177.52–177.89	–
4	LFEC	57.9	54–58	<0.05	54–58	*DOCK4, IFRD1, LRRN3*
	IgA_t	8.9	–	<0.0019 (<0.05)	8.66–9.49	–
5	LFEC	5.2	–	<0.0019 (<0.05)	5.02–5.43	*FCHO1, JAK3, MAP1S, UNC13A*
		89.9	–	<0.0019 (<0.05)	89.68–90.14	–
6	LFEC	36	–	<0.05	35.84–36.28	–
		72.5	72.3–77.2	<0.0019 (<0.05)	72.3–77.2	–
		89.9	85–90.2	<0.05	85–90.2	*ALB, AMBN, AMTN, ANKRD17, AREG, BTC, EREG, IGJ, IL8, PF4, PPBP, RASSF6*
7	LFEC	22.8	12.65–25.5	<0.0019 (<0.05)	12.65–25.5	*ACIN1, AJUBA, BBS4, CCNB1IP1, CD276, CDH24, CEBPE, CHD8, CIDEB, CMTM5, DAD1, EFS, EMC4, FEM1B, IL25, IRF9, ITGA11, LRP10, LTB4R, MAP2K1, NEO1, NFATC4, NOX5, NPTN, PIAS1, PSMB5, PSME1, PSME2, RIPK3, RNASE2, RNF31, SMAD3, SMAD6, TRAV16, TRAV21, TRAV24, TRAV27, TRAV36DV7, TRAV39, TRAV4, TRAV41, TRAV5, TRDC, TRDV2, TRDV3, UACA, ZNF219, ZWILCH*
		36.8	36.8–37.3	<0.05	36.8–37.3	–
		53.3	–	<0.05	53.08–53.46	*UNC13C*
8	LFEC	2.3	0.3–12.8	<0.05	0.3–12.8	*CD109, COL12A1, IBTK, IRAK1BP1, MYO6, PHIP, SNAP91, TPBG*
		38.3	37.7–39.2	<0.05	37.7–39.2	–
		49.8	49.59–50.04	<0.05	49.59–50.04	–
		64.1	61.1–64.1	<0.05	61.1–64.1	*BCLAF1, CITED2, IFNGR1, IL20RA, IL22RA2, MAP3K5, PERP, TNFAIP3*
		71.4	71.2–73.8	<0.0019 (<0.05)	71.2–73.8	*PPIL4, STXBP5*
9	LFEC	5.8	–	<0.05	5.64–6.03	*PRKAR1A*
		16.9	–	<0.05	16.75–17.16	–
		24.5	–	<0.05	24.34–24.78	–
		41.7	–	<0.05	41.56–41.96	–
	IgA_t	56.6	55.9–56.6	<0.05	55.9–56.6	*TPD52*
		67.8	63.4–67.8	<0.05	63.4–67.8	*EBAG9*
10	LFEC	71.6	–	<0.05	70.01–71.55	–
	IgA_t	27.2	21.5–27.2	<0.05	21.5–27.2	*CKAP2, FOXO1, FREM2, POSTN, SMAD9*
		52.9	–	<0.05	52.68–53.06	–
		78.6	–	<0.05	78.39–78.8	*SLC10A2*
11	LFEC	4.2	4.1–4.27	<0.05	4.1–4.27	–
	IgA_t	51.1	45.4–51.1	<0.05	45.4–51.1	*ACE, ARHGDIA, B3GNTL1, CD7, CD79B, DDX42, ERN1, FSCN2, GCGR, ICAM2, ITGB3, MAP3K3, MRC2, MYADML2, PSMC5, PSMD12, SMARCD2, SMURF2*
12	LFEC	3.6	–	<0.05	3.34–3.84	*IKBKE, IL10, MAPKAPK2*
12	IgA_t	1.7	–	<0.05	1.52–1.98	*LRRN2, MDM4, NFASC*
		17.7	–	<0.05	17.56–17.96	–

Table 2 continued

OAR[a]	Trait[b]	Pos of max LRT[c] (cM)	Significant LDLA interval (cM)[d]	P_c-value (P_g-value)[e]	TGI (Mb)[f]	Positional candidate genes involved in immune response[g]
		72.3	69.5–75.4	<0.05	69.5–75.4	*CAMK1G, CD34, CD46, CFHR5, IRF6, LAMB3, TRAF5*
13	IgA_t	3.7	3.7–6.3	<0.05	3.7–6.3	–
15	IgA_t	33.6	33.56–33.93	<0.0019 (<0.05)	33.56–33.93	–
		47	47–53.2	<0.05	47–53.2	*ARHGEF17, ARRB1, DNAJB13, FCHSD2, FOLR1, IL18BP, INPPL1, PAAF1, PGAP2, RELT, RPS3, STIM1*
		70.2	70.06–70.47	<0.0019 (<0.05)	70.06–70.47	–
16	IgA_t	10.5	–	<0.05	10.29–10.74	–
		64.8	63.8–64.8	<0.0019 (<0.05)	63.8–64.8	*SEMA5A*
17	IgA_t	18.4	14.6–30.1	<0.0019 (<0.05)	14.6–30.1	*ELMOD2, IL15, PCDH10, PCDH18, PLK4, UCP1*
		36	–	<0.05	35.8–36.22	–
		46	–	<0.05	45.85–46.27	*STX2*
		62.3	62–66.8	<0.0019 (<0.05)	62–66.8	*CMKLR1, CORO1C, HPS4, PIWIL3, PLA2G1B, PXN, RAB35, SART3, SPPL3, TRIAP1, UNG, WSCD2*
20	LFEC	4.8	–	<0.05	4.58–5.04	*BMP5*
21	LFEC	8.1	8.07–8.35	<0.05	8.07–8.35	–
		31.8	31.7–32.24	<0.05	31.7–32.24	–
		43.9	43.7–44.03	<0.05	43.7–44.03	*ACTN3, CTSF, SPTBN2*
21	IgA_t	17.5	16.5–17.5	<0.0019 (<0.05)	16.5–17.5	*GAB2*
		46	45.97–46.25	<0.05	45.97–46.25	*FGF19*
22	IgA_t	6.7	5.3–7.3	<0.05	5.3–7.3	*MBL2, PCDH15*
		19.5	–	<0.05	19.26–19.85	*NKX2-3*
23	IgA_t	8.3	–	<0.05	8.15–8.47	–
		23.3	23.3–28.5	<0.05	23.3–28.5	*DSC1, DSC2, DSC3, DSG1, DSG2, DSG3, DSG4,*
		33.9	32.8–38	<0.05	32.8–38	*ADCYAP1, COLEC12, EMILIN2, GATA6, LAMA3, MIB1, NPC1, ROCK1, THOC1, USP14*
		45.8	41.7–48.5	<0.05	41.7–48.5	*ATP5A1, CIDEA, PIAS2, PSMG2, RALBP1,SIGLEC15, SKOR2, SLC14A1, SMAD2*
		54.9	54.56–55.06	<0.05	54.56–55.06	*TCF4*
24	LFEC	2.2	1.91–2.65	<0.05	1.91–2.65	*CLDN6, CLDN9, HCFC1R1, TNFRSF12A*
		17.9	–	<0.05	17.68–18.12	*UMOD*
25	LFEC	37	36.89–37.21	<0.0019 (<0.05)	36.89–37.21	–

[a] *OAR* ovine chromosome

[b] Analyzed traits: *LFEC* log-transformed faecal egg count, IgA_t Box-Cox-transformed optical density ratio (ODR) values of immunoglobulin A activity

[c] Position of the chromosome (in centiMorgans) at which the maximum likelihood ratio test (LRT) is reached in the LDLA

[d] A significant LDLA interval (in centiMorgans) was defined by clustering consecutive significant 5 % chromosome-wise LDLA associations on a chromosome (allowing gaps no greater than 5 Mb)

[e] P_c-value: chromosome-wise P-value established through 1000 simulations. P_g-value: genome-wise P-value obtained from the P_c-values corrected for the total number of chromosomes analyzed

[f] *TGI* (Mb) Target genomic interval. For each significant LDLA association, target genomic intervals were defined as the genomic region based on the sheep reference genome assembly Oar_v3.1 that corresponded to the defined significant LDLA intervals (for those regions with consecutive significant positions) and a 250-kb long interval centered on each of the significant isolated haplotypes detected by LDLA

[g] Positional candidate genes extracted from the LDLA significant associations (within the significant LDLA interval if identified, or within a ±125 kb interval from the position of maximum LRT-value for the significant QTL based on isolated significant haplotypes) that were identified as potential functional candidate genes in the search for immune-related genes

Table 3 Chromosome-wise SNPs significantly associated with the IgA_t trait as identified by the GWAS

OAR[a]	SNP name	SNP position (Mb)[b]	Allele substitution effect trait units (SD units)[c, d]	Nominal P-value	Corrected P_c-value (P_g-value)[e]	TGI (Mb)[f]
8	OAR8_53084022.1	49,525,147	0.325 ± 0.075 (0.417)	2.04E−05	0.02	49.40–49.65
8	s42819.1	72,402,305	0.190 ± 0.045 (0.243)	3.77E−05	0.037	72.27–72.52
10	s56461.1	17,012,728	0.221 ± 0.050 (0.283)	1.51E−05	0.013	16.88–17.13
10	OAR10_23921485.1	24,187,107	0.203 ± 0.048 (0.260)	2.63E−05	0.022	24.06–24.31
10	s61799.1	30,924,195	0.210 ± 0.051 (0.269)	5.41E−05	0.045	30.79–31.04
11	DU232778_232.1	32,492,623	0.203 ± 0.048 (0.26)	3.74E−05	0.036	32.36–32.61
12	s68938.1	61,866,746	0.233 ± 0.047 (0.299)	1.28E−06	0.001 (0.033)	61.74–61.99
14	OAR14_21336208.1	20,773,096	0.284 ± 0.070 (0.364)	6.75E−05	0.041	20.64–20.89
15	s75729.1	24,870,677	0.266 ± 0.059 (0.341)	8.33E−06	0.007	24.74–24.99
25	s21640.1	13,152,201	0.224 ± 0.056 (0.287)	9.09E−05	0.048	13.02–13.27

[a] *OAR* ovine chromosome

[b] Position of the significant SNP identified by the GWAS analysis based on the Oar_v3.1 version of the Ovine Genome Assembly (http://www.ensembl.org/Ovis_aries/Info/Index)

[c, d] Magnitude of the allele substitution effect, and standard error, in trait units (Yield Deviations of IgA_t) and in phenotypic standard deviations (SD) units (in brackets)

[e] Corrected P-values at the 5 % chromosome-wise level (and 5 % genome-wise level) obtained after applying a Bonferroni correction considering the number of independent markers analyzed for each chromosome and for the whole genome, respectively

[f] *TGI* Target genomic interval defined for the GWAS significant associations as 250 Kb long intervals centered on the significant SNP. The genes within that interval were extracted as positional candidate genes. In this case, none of these genes was identified as functional candidate by the candidate gene survey performed

GWAS results

None of the analyzed SNPs reached significance for LFEC (Table 3; Fig. 2a). For IgA_t, the GWAS identified one 5 % genome-wise significant SNP on OAR12 and nine additional 5 % chromosome-wise significant associations that were distributed on six chromosomes (OAR8, 10, 11, 14, 15 and 25) (Table 3; Fig. 2b). The allelic substitution effect of the significant SNPs identified for IgA_t ranged from 0.243 to 0.417 phenotypic SD units. Although more than one significant SNP was identified on OAR8 and 10, these SNPs were located at relatively large distances on the chromosome (i.e., 22.8 and 13.9 Mb, respectively). Among the ten significant GWAS associations reported here for IgA_t, one located on OAR10 was coincident with a significant QTL identified by LDLA for the same trait (between 21.5 and 27.2 cM), whereas two other associations, located on OAR8, overlapped with QTL for LFEC identified by LDLA.

Correspondence of the detected associations with previously reported QTL for parasite resistance traits

The QTL for parasite resistance traits previously reported in sheep that coincide with the TGI reported here and are associated with the significant QTL and SNP associations identified here are summarized in Additional file 3: Table S2. Overall, we found correspondences with other studies for half of the 76 significant QTL identified by the three genome scans performed in this study.

List of functional candidate genes

A total of 905 unique genes were extracted from the TGI that were defined for the significant QTL detected by LA, LDLA and GWAS (416 and 489 unique genes extracted from FEC- and IgA_t-associated regions, respectively) (see Additional file 4: Table S3). From the list of 5029 known immune-related genes, we performed a survey for positional candidate genes and identified 205 functional candidate genes (indicated in blue font in Additional file 4: Table S3), which were all extracted from TGI related to significant QTL that were detected by LA or LDLA. Gene symbols of these functional candidate genes are in Tables 1 and 2 based on their genomic locations within the corresponding QTL regions.

Discussion

The genetic architecture of resistance to internal parasites is a complex trait that is influenced by many loci with small effects [21]. Using two different approaches to correct for sampling errors associated with single-marker regression, Kemper et al. [21] estimated that the largest effects that influence fecal worm egg count for *Trichostrongylus colubriformis* explained between 0.12 and 0.48 % of the phenotypic variance. These authors suggest that such small effects are shared by many complex traits and are not specific to parasite resistance. The proportions of phenotypic variance explained by the significant LA associations reported here, which were equal to ~0.074 %, are slightly lower than the lower limit of the

Table 4 Summary of the QTL detected by the three analyses performed in this study

OAR[1]	LA[2]	LDLA[3]	GWAS[4]
1		$LFEC_{(a)}$; $IgA_{t(b)}$	
2		$LFEC_{(a)}$; $IgA_{t(b)}$	
3		$IgA_{t(a)}$; $IgA_{t(b)}$	
4		*$IgA_{t(a)}$*; $LFEC_{(b)}$	
5		*$LFEC_{(a)}$; $LFEC_{(b)}$*	
6	$LFEC_{(b)}$	*$LFEC_{(a)}$*; $LFEC_{(b)}$	
7		*$LFEC_{(a)}$*; $LFEC_{(b)}$; $LFEC_{(c)}$	
8	$LFEC_{(a)}$	$LFEC_{(a)}$; $LFEC_{(b)}$; $LFEC_{(c)}$; $LFEC_{(d)}$; *$LFEC_{(e)}$*	$IgA_{t(c)}$; $IgA_{t(e)}$
9		$LFEC_{(a)}$; $IgA_{t(a)}$; $IgA_{t(b)}$; $LFEC_{(b)}$; $LFEC_{(c)}$; $LFEC_{(d)}$	
10		$IgA_{t(b)}$; $IgA_{t(c)}$; $IgA_{t(e)}$; $LFEC_{(f)}$	$IgA_{t(a)}$; $IgA_{t(b)}$; $IgA_{t(d)}$
11		$LFEC_{(a)}$; $IgA_{t(c)}$	$IgA_{t(b)}$
12		$LFEC_{(a)}$; $IgA_{t(a)}$; $IgA_{t\ (b)}$; $IgA_{t(d)}$	*$IgA_{t(c)}$*
13		IgA_t	
14			IgA_t
15		*$IgA_{t(b)}$*; $IgA_{t(c)}$; *$IgA_{t\ (d)}$*	$IgA_{t(a)}$
16		$IgA_{t(a)}$; *$IgA_{t(b)}$*	
17		*$IgA_{t(a)}$*; $IgA_{t(b)}$; $IgA_{t(c)}$; *$IgA_{t(d)}$*	
18			
19			
20		LFEC	
21		$LFEC_{(a)}$; *$IgA_{t(b)}$*; $LFEC_{(c)}$; $LFEC_{(d)}$; $IgA_{t(d)}$;	
22	$IgA_{t(a)}$	$IgA_{t(a)}$; $IgA_{t(b)}$	
23		$IgA_{t(a)}$; $IgA_{t(b)}$; $IgA_{t(c)}$; $IgA_{t(d)}$; $IgA_{t(e)}$	
24		$LFEC_{(a)}$; $LFEC_{(b)}$	
25		*$LFEC_{(b)}$*	$IgA_{t(a)}$
26			

[1] *OAR* ovine chromosome

[2, 3, 4] Significant QTL for the two analyzed traits (*LFEC* log-transformed faecal egg count, *IgA_t* Box-Cox-transformed optical density ratio (ODR) values of immunoglobulin A activity) identified by the three genome scan performed in the present study, using linkage analysis (LA), combined linkage disequilibrium and linkage analysis (LDLA) and genome-wide association study (GWAS)

[a, b, c, d, e, f] Different subscripts letters indicate that the QTL in the same chromosome are located at more than 5 cM/Mb of distance

QTL in normal characters detected at the 5 % chromosome-wise level

QTL in italic characters detected at the 5 % genome-wise level

range reported by Kemper et al. [21], although the estimated effects are within the ranges reported in other related studies [19, 20, 22]. Considering the small size of the targeted genetic effects to be detected, the statistical power of QTL detection for indicators of parasite resistance may be limited in such experiments if the number of sampled individuals is not very large. Based on Weller et al. [47], we estimated that the statistical power of QTL detection for QTL with a substitution effect of 0.2 phenotypic SD units, two alleles with frequencies of 0.25 and 0.75, respectively, and for a trait with a heritability of 0.2 (considering the estimates of Gutiérrez-Gil et al. [48]) was approximately 11 %. This estimate is based on the following assumptions i.e. (1) a type I error rate of 0.05, (2) a 1 % recombination frequency between the QTL and SNP and (3) 37.5 % of the analyzed sires are heterozygous at the QTL.

Our study successfully identified QTL that influence the two indicator traits related to GIN resistance using LA and LDLA, whereas the GWAS analysis only detected significant SNP associations with IgA_t. The different analyses performed in this study can detect significant associations with different features. Hence, because classical LA will only detect QTL in our design if several sires are heterozygous at the same QTL (*Qq*), many marker-trait associations that do not satisfy this assumption but have a genuine association at the population level, will not be detected by LA; however, such associations can be detected by either of the two alternative genome scan analyses performed here i.e. LDLA or GWAS. Therefore, we attempted to present a global picture of the associations that segregate in this commercial sheep population by complementing the limits of classical LA with these alternative LDLA and GWAS approaches, which exploit population information. In our case, the GWAS approach also identified a substantially lower number of associations than LDLA. This may be explained by the fact that modeling both the association (LD) and the transmission (linkage) in a single analysis, LDLA permits to map QTL more accurately than LA while retaining its robustness to spurious associations [40]. In addition, among the different advantages highlighted for the use of LDLA versus GWAS for animal populations, Meuwissen et al. [49] claimed that LDLA is expected to suffer less from multiple-testing, and therefore to have more power to detect the existing QTL.

For the chromosomes that showed coincident significant results identified by LA and LDLA, we performed an exploratory LDA analysis with the QTLMap software (see Additional file 1: Table S1, Additional file 2: Figure S1). This analysis differs from GWAS in that parental haplotypes are pooled in classes that are defined by the identity-by-state (IBS) status of the haplotypes, with each different haplotype class having a specific effect on the quantitative trait [40]. The significant LDA results obtained for OAR6, 8 and 22 supported several of the significant LDLA associations reported for these chromosomes; whereas the LDA result obtained for OAR6 at 85.1 Mb supported the significant QTL that was detected by both LA and LDLA. This observation strengthens the support for the QTL for LFEC identified by LA on OAR6, which suggests that in addition to a family-based linkage information signal, the effect is also due to a genuine association with the trait, although it was not identified in our GWAS (most likely as a consequence of the limited power of the experimental design).

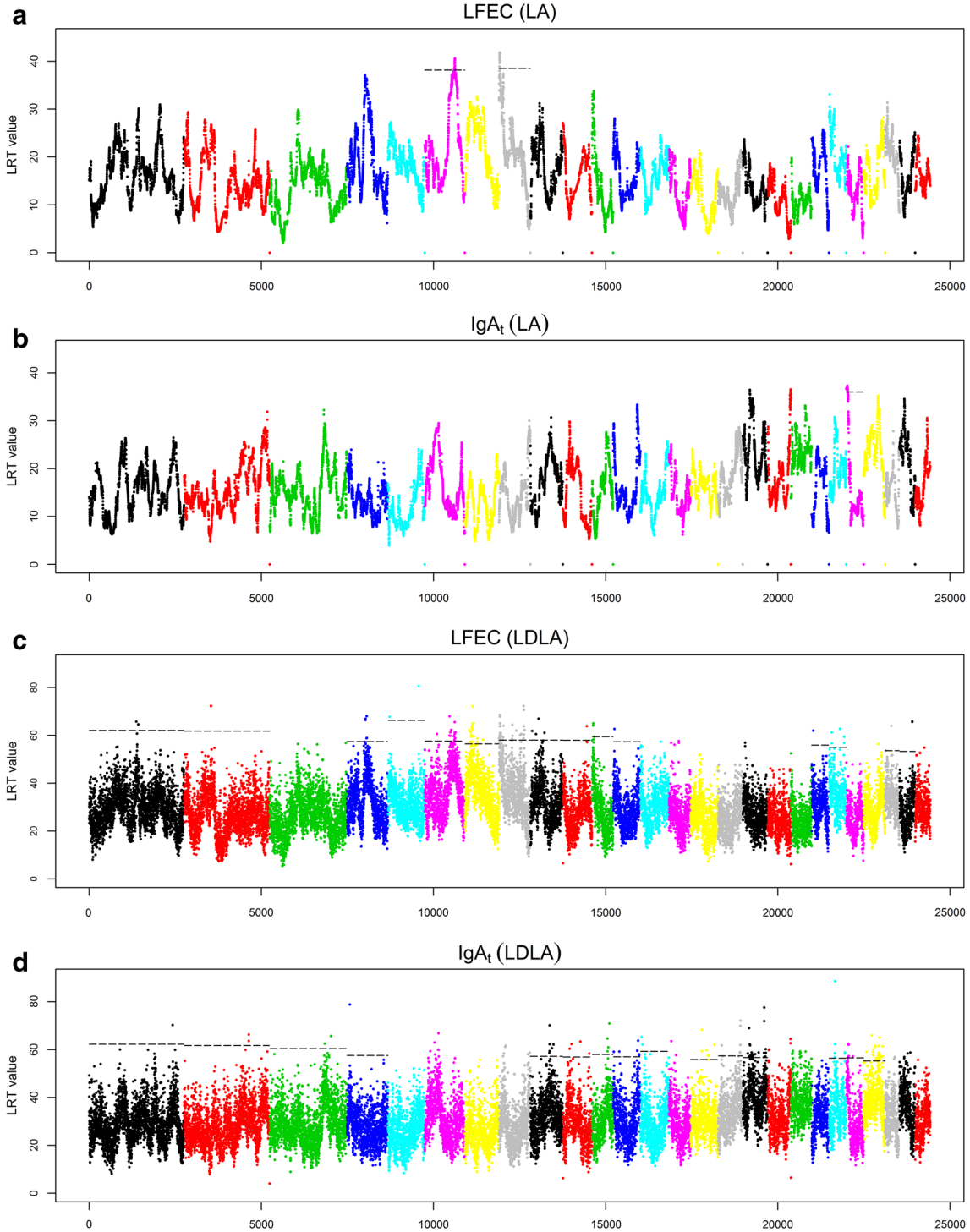

Fig. 1 Results of linkage analysis (LA; **a**, **b**) and combined linkage disequilibrium and linkage analysis (LDLA; **c**, **d**) genome scans performed for the two indicator traits of parasite resistance analyzed. Analyzed traits: *LFEC* Log-transformed faecal egg count, lgA_t Box-Cox-transformed optical density ratio (ODR) values of immunoglobulin A activity. Likelihood ratio test (LRT) values obtained across the 26 ovine autosomes are represented. For those chromosomes that harbor significant QTL, the *horizontal lines* indicate the 5 % chromosome-wise significance threshold for LA (**a**, **b**) and the 5 % chromosome-wise significance threshold for LDLA (**c**, **d**)

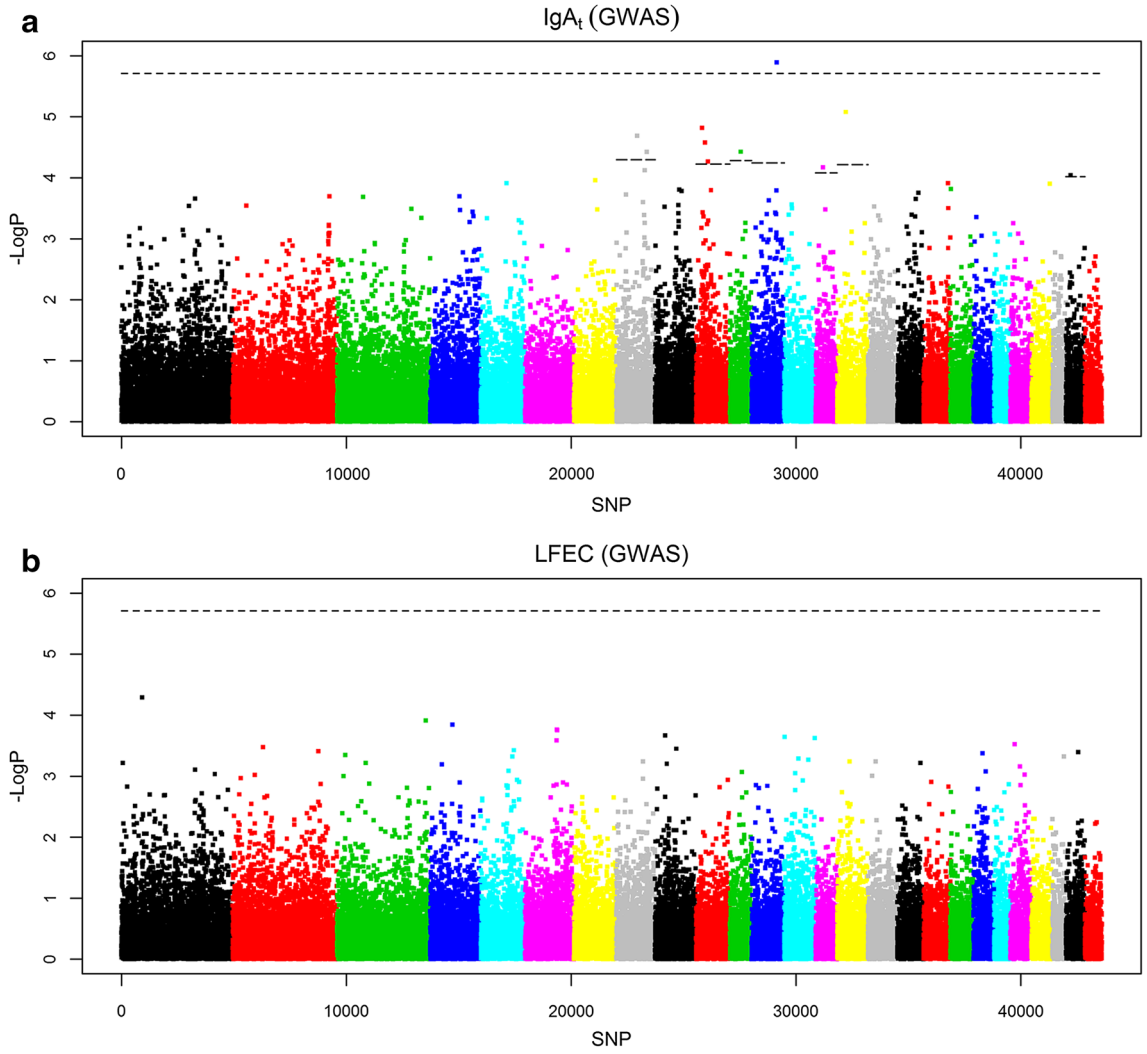

Fig. 2 Results from the genome-wide association study (GWAS) performed for the two indicator traits of parasite resistance analyzed. Analyzed traits: *LFEC* Log-transformed faecal egg count, *IgA$_t$* Box-Cox-transformed optical density ratio (ODR) values of immunoglobulin A activity. The values of the log(1/P-value) are shown for all the 43,613 SNPs that passed the quality control. For the chromosomes that harbor significant SNP associations, the *horizontal lines* indicate the 5 % chromosome-wise significance threshold obtained by applying a Bonferroni correction considering the number of independent SNPs analyzed for each chromosome. The genome-wise significance threshold, considering the number of independent markers analyzed for the entire genome is also represented

Regarding the LFEC-related results for OAR6 that were obtained by LA, LDLA and LDA, in the current study, we replicated the most significant QTL that was previously identified through a microsatellite-based genome scan using a different set of Churra sheep half-sib families [20]. In the latter study, the peak of the genome-wise significant QTL for LFEC was located in the marker interval BM4621-CSN3 on OAR6, which corresponds to a region between 68 and 85.1 Mb in the current sheep genome assembly (Oar_v3.1). The mentioned flanking interval overlaps with the TGI defined here for LFEC on OAR6 by LA (between 80.8 and 91.4 Mb) (Table 1), LDLA (between 72.3 and 77.2 and between 85 and 90.2 Mb) (Table 2) and LDA (between 75.8 and 77.7 and between 85 and 85.1 Mb) (see Additional file 1: Table S1, Additional file 2: Figure S1). This finding provides support for the design and planning of future fine-mapping studies for this chromosomal region. The higher marker density and information provided by the complementary analyses reported here for this region suggest that the OAR6 region ranging from 68 to 91.4 Mb includes several different QTL that directly influence GIN resistance in Churra sheep. Interestingly, a GWAS on a Red Maasai x Dorper backcross sheep population [26] also suggested

the presence of several QTL for FEC in lambs within a region between 55.9 and 78.19 Mb on OAR6. This finding was based on the fact that the most significant SNP association with FEC identified on OAR6 at 74.86 Mb, was proven not to be in LD with nearby clusters of significant markers for the same trait (in intervals between 55.9 and 62.6 Mb, 74.1 and 75.00 Mb, and 78.1 and 78.2 Mb) (see Additional file 3: Table S2). In spite of the remarkable correspondence between these results and our results, the most distal signals that were detected on OAR6 in our study (TGI defined by LA: 80.8 to 91.4 Mb; LDLA: 85 to 90.2 Mb; and LDA: 85 to 85.1 Mb) do not overlap with any previously reported QTL in other populations, but only with those previously reported by Gutiérrez-Gil et al. [20] (see Additional file 3: Table S2) . With the exception of Gutiérrez-Gil et al. [20] work, most studies refer to QTL that are detected for young animals (lambs); thus, the most distal QTL that we identified on OAR6 could be related to specific mechanisms of the immune response that is activated in adult animals. As suggested by Stear et al. [50], the genetic variation in fecal egg counts in lambs is a consequence of genetic variation in worm length and hence worm fecundity; in contrast, mature sheep may be able to regulate both fecundity and worm number. These authors suggested that the lower fecal egg counts observed in adult animals compared to lambs are due to the acquisition of effective immune responses that reduce worm numbers, possibly via immediate hypersensitivity reactions against incoming third-stage larvae [51]. Recent studies have highlighted differences in the pathways involved in innate and acquired resistance [52]. Another correspondence that was observed with the results reported by Gutiérrez-Gil et al. [20] concerned the QTL for LFEC detected by LDLA on OAR10 (TGI: 70.01–71.55 Mb) (see Additional file 3: Table S2). Due to the lack of evidence from the other analyses reported here, this region was not further investigated.

An intriguing finding is that the other two QTL detected by LA in this work did not coincide with QTL that were reported for other sheep populations, whereas three of the ten significant SNP associations identified by GWAS, and 35 of the 63 significant QTL identified by LDLA, overlapped with QTL effects described in other studies (see Additional file 3: Table S2). Indeed, the significant GWAS results coincided with QTL on OAR8 reported by Crawford et al. [13] and Silva et al. [19], on OAR12 by Riggio et al. [24], and on OAR15 by Silva et al. [19] (see Additional file 3: Table S2). In our study, the SNP association on OAR12 at 61.9 Mb was the only one that reached the 5 % genome-wide significance level. Although not mentioned in Additional file 3: Table S2 because there was no complete overlap, Beh et al. [12] used microsatellite markers to identify a QTL in this genomic region (between 63.5 and 71.5 Mb) for FEC-related traits in *T. colubriformis* infection. It should be noted that we did not find a clear correspondence with the classical regions reported to influence parasite resistance traits, such as those that harbor the ovine *IFN-γ* gene (OAR3: 151.53 Mb) [11, 14, 17] or the major histocompatibility complex-related genes (OAR20: 7 Mb; 24–26 Mb; 58–60 Mb) [14].

Among the large number of correspondences between our LDLA results and previously reported studies (see Additional file 3: Table S2), those that are based on data from the 50 K chip are of special relevance because of the proximity between the QTL peaks reported here and in other studies. Apart from the correspondences with the findings of Benavides et al. [26] mentioned above for OAR6, those found for the QTL on OAR5 (TGI: 89.68–90.14 Mb) are particularly relevant. This QTL identified by LDLA is located in a region where several significant effects for a wide range of parasite indicator traits were reported by Sallé et al. [22], which suggests the presence of a QTL with pleiotropic effects.

We identified 205 immune-related genes within the TGI defined by the LA and LDLA (Tables 1, 2) but none of these functional candidate genes were found in the significant GWAS-defined TGI. Some of these immune-related genes are involved in the T helper (Th) 2 cell response, which orchestrates the mechanisms of tissue repair as a primary host defense against helminthes [53], whereas others are linked to the Th1 cell response, which is associated with progression to chronic infection [54].

Due to the large number of significant regions identified and the need for additional fine-mapping results to propose reliable promising causal candidate genes, in the following part, we only discuss below the genes that were identified in relation to the QTL for LFEC identified by LA on OAR6 (TGI: 80.9–91.4 Mb), which include the genes extracted for the LDLA-defined TGI between 85 and 90.2 Mb. The fact that this QTL, previously reported by Gutiérrez-Gil et al. [20], was also identified for the population analyzed here and the support provided by the related signals identified by LDLA/LDA, led us to carry out a preliminary assessment of the 20 positional candidate immune-related genes that map to this region (Table 1). Among these genes, several encode chemokines (IL8, CXCL1, CXCL10, CXCL11, CXCL9, PF4, PPBP), a family of small proteins that play important roles in the immune system through leukocyte recruitment, cell communication and cell activation during infection [55, 56]. In particular, IL8 (or CXCL8) and CXCL1 are involved in the recruitment and activation of neutrophils [55]. IL8 also participates in the recruitment of mast cells, which are frequently associated with the

Th2 cell response [57]. CXCL9, CXCL10 and CXCL11, which are induced by IFN-γ, are involved in promoting the Th1 immune response. In nematode-infected mice, CXCL10 slows down the intestinal epithelial cell turnover rate and thus, increases worm survival [58]. In addition, both PF4 and PPBP have been suggested to play roles in wound healing [59, 60]. Three genes coding for members of the epidermal growth factor family also map to the considered region on OAR6: *AREG* (*amphiregulin*), *BTC* (*betacellulin*) and *EREG* (*epiregulin*). *AREG* is expressed by diverse cell types involved in the immune response, such as activated Th2 cells [61], and is a central mediator of epithelial repair [62]. In mice, lack of *AREG* expression appears to have an effect on the delayed expulsion of GIN [63]. Because wound repair and GIN expulsion are related to the acquired Th2 response [53, 64], genes associated with these mechanisms (e.g., *IL8*, *PF4*, *PPBP* and *AREG*) could be of interest when searching for candidates to explain an adult-specific QTL, such as the QTL detected on OAR6 between 80.8 and 91.4 Mb.

The large number of QTL identified in this study supports the idea that disease susceptibility is not determined by individual genes acting alone but rather by complex multi-gene interactions [65, 66]. Our results are the first steps towards the identification of allelic variants that directly control the phenotypic variation observed for parasite resistance in adult Churra sheep. The identification of causal variants, or SNPs in strong LD with the casual variants, could contribute to the implementation of these results in breeding schemes for the Churra breed population. Future studies that combine genomic variation analysis and functional genomic information may help to elucidate the biology of resistance to GIN diseases in sheep.

Conclusions

In summary, the 50 K chip was used for a medium marker density scan of the sheep genome to identify regions that influence traits related to resistance to GIN infections in adult animals. By exploiting the information obtained at the within-family level and at the population level, three methods of analysis were used (LA, LDLA and GWAS) to provide a global picture of the QTL that segregate in the commercial population of Churra sheep analyzed. Many of the significant associations reported here overlap with previously reported QTL for different populations of young sheep. These results will contribute to identify target regions that control variation of the complex parasite resistance trait in sheep, independently of the age of the animals. Other significant associations that did not coincide with previously reported QTL could be related to the specific immune response of adult animals. This study also replicated a QTL for FEC on OAR6 that was previously reported in a different subset of animals from the commercial population of Churra sheep. Together, the enhanced marker density provided by the 50 K chip and the complementary analyses reported here suggest that several QTL are present in this genomic region. This replication and the re-definition of these genetic effects in the independent population analyzed here provide support for investing future research efforts aimed at identifying the corresponding causal allelic variants. The combination of high-density SNP genotyping (700 K SNP array) and whole-genome sequencing of segregating trios (composed by a segregating sire carrying the *Qq* genotype, and two homozygous daughters for alternative haplotype alleles, *QQ* and *qq*, and showing extreme divergence for the resistance phenotype) could be a powerful strategy to reach this objective.

Additional files

Additional file 1: Table S1. Chromosome-wise significant results (Pc-value < 0.05) identified by the linkage disequilibrium analysis (LDA) performed in the present study for chromosomes (OAR) 6, 8 and 22. Characterization of the chromosome-wise significant results (Pc-value < 0.05) identified by the QTLMap linkage disequilibrium analysis (LDA) that was performed for the three chromosomes showing coincident results in the LA and LDLA genome scans presented here for parasite resistance traits.

Additional file 2: Figure S1. Profiles of the Likelihood Ratio Test (LRT) obtained from the linkage analysis (LA), linkage disequilibrium analysis (LDA) and the combined LDLA performed for chromosomes (OAR) 6 (a; LFEC), 8 (b; LFEC), and 22 (c; lgA_t). For the indicated trait, the LRT results of LA (solid line), LDA (dark gray circle), and LDLA (light gray circle) (y-axis) are plotted against the SNP positions analyzed along chromosomes (OAR) 6, 8 and 22 (x-axis). The 5 % chromosome-wise significance thresholds considered for each of three analyses are represented as horizontal lines.

Additional file 3: Table S2. Summary table of the correspondence between the QTL and SNP associations identified in the present study and other studies previously reported for parasite resistance traits in sheep. This table shows the correspondences found for all the QTL identified in this study (by LA, LDLA and GWAS) (indicated in green cells) with QTL previously reported based on microsatellite-based studies (compiled in the SheepQTLdb; indicated in light orange cells) and SNP chip-based studies (indicated in orange cells).

Additional file 4: Table S3. Total list of annotated genes extracted from the Sheep Genome Assembly v3.1 using the BioMart web-tool for the significant QTL regions and SNP associations identified for the two parasite resistance traits analyzed in the present study. Among the total list of genes extracted, we identified 205 functional candidate genes involved in the immune response, based on our candidate gene survey, which are indicated in blue font colour. The colour of the rows refer to genes extracted based on the results of the Linkage Analysis (LA; green), Combined Linkage Disequilibrium and Linkage Analysis (LDLA; yellow) and Genome-wise Association Study (GWAS; blue).

Authors' contributions

JJA and BGG conceived and designed the study and analyses; MA and MMV carried out the data collection and prepared the phenotype; MA, BGG, and JJA analyzed the data; MA, BGG and JJA drafted the manuscript. All authors read and approved the final manuscript.

Author details

[1] Departamento de Producción Animal, Facultad de Veterinaria, Universidad de León, Campus de Vegazana s/n, León 24071, Spain. [2] Instituto de Ganadería

de Montaña, CSIC-ULE, Grulleros, León 24346, Spain. [3] Departamento de Sanidad Animal, Universidad de León, León 24071, Spain.

Acknowledgements
The authors would like to acknowledge JM Elsen (INRA, France) for providing assistance with interpretation of the QTLMap output. This work was supported by a competitive grant from the Castilla and León regional government (Junta de Castilla y León) (Ref. LE245A12-2) and the AGL2012-34437 project funded by the Spanish Ministry of Economy and Competitiveness (MINECO). M Atlija is a grateful grantee of a Marie Curie fellowship funded by the EC-funded Initial Training Network (ITN) NematodeSystemHealth (FP7-PEOPLE-2010-ITN Ref. 264639). B Gutiérrez-Gil is funded through the Spanish "Ramón y Cajal" Programme (RYC-2012-10230) from the MINECO.

Competing interests
The authors declare that they have no competing interests.

Received: 22 June 2015 Accepted: 5 January 2016
Published online: 20 January 2016

References

1. Kaplan RM, Vidyashankar AN. An inconvenient truth: global worming and anthelmintic resistance. Vet Parasitol. 2012;186:70–8.
2. Raadsma HW, Gray GD, Woolaston RR. Genetics of disease resistance and vaccine response. In: Piper L, Ruvinsky A, editors. The Genetics of Sheep. University Press: Cambridge; 1997. p. 199–224.
3. Stear MJ, Doligalska M, Donskow-Schmelter K. Alternatives to anthelmintics for the control of nematodes in livestock. Parasitology. 2007;134:139–51.
4. Morris CA, Wheeler M, Watson TG, Hosking BC, Leathwick DM. Direct and correlated responses to selection for high or low faecal nematode egg count in Perendale sheep. NZJ Agric Res. 2005;48:1–10.
5. Karlsson LJE, Greeff JC. Selection response in fecal worm egg counts in the Rylington Merino parasite resistant flock. Aust J Exp Agric. 2006;46:809–11.
6. Kemper KE, Elwin RL, Bishop SC, Goddard ME, Woolaston RR. *Haemonchus contortus* and *Trichostrongylus colubriformis* did not adapt to long-term exposure to sheep that were genetically resistant or susceptible to nematode infections. Int J Parasitol. 2009;39:607–14.
7. Grencis RK. Immunity to helminths: resistance, regulation, and susceptibility to gastrointestinal nematodes. Annu Rev Immunol. 2015;33:201–25.
8. Jiang Y, Xie M, Chen W, Talbot R, Maddox JF, Faraut T, et al. The sheep genome illuminates biology of the rumen and lipid metabolism. Science. 2014;344:1168–73.
9. Hein WR, Pernthaner A, Piedrafita D, Meeusen EN. Immune mechanisms of resistance to gastrointestinal nematode infections in sheep. Parasite Immunol. 2010;32:541–8.
10. Hu ZL, Park CA, Wu XL, Reecy JM. Animal QTLdb: an improved database tool for livestock animal QTL/association data dissemination in the post-genome era. Nucleic Acids Res. 2013;41:D871–9.
11. Coltman DW, Wilson K, Pilkington JG, Stear MJ, Pemberton JM. A microsatellite polymorphism in the gamma interferon gene is associated with resistance to gastrointestinal nematodes in a naturally-parasitized population of Soay sheep. Parasitology. 2001;122:571–82.
12. Beh KJ, Hulme DJ, Callaghan MJ, Leish Z, Lenane I, Windon RG, et al. A genome scan for quantitative trait loci affecting resistance to *Trichostrongylus colubriformis* in sheep. Anim Genet. 2002;33:97–106.
13. Crawford AM, Paterson KA, Dodds KG, Diez Tascon C, Williamson PA, Roberts Thomson M, et al. Discovery of quantitative trait loci for resistance to parasitic nematode infection in sheep: I. Analysis of outcross pedigrees. BMC Genomics. 2006;7:178.
14. Davies G, Stear MJ, Benothman M, Abuagob O, Kerr A, Mitchell S, et al. Quantitative trait loci associated with parasitic infection in Scottish blackface sheep. Heredity (Edinb). 2006;96:252–8.
15. Beraldi D, McRae AF, Gratten J, Slate J, Visscher PM, Pemberton JM. Mapping quantitative trait loci underlying fitness-related traits in a free-living sheep population. Evolution. 2007;61:1403–16.
16. Marshall K, Maddox JF, Lee SH, Zhang Y, Kahn L, Graser HU, et al. Genetic mapping of quantitative trait loci for resistance to *Haemonchus contortus* in sheep. Anim Genet. 2009;40:262–72.
17. Dominik S, Hunt PW, McNally J, Murrell A, Hall A, Purvis IW. Detection of quantitative trait loci for internal parasite resistance in sheep. I. Linkage analysis in a Romney × Merino sheep backcross population. Parasitology. 2010;137:1275–82.
18. Matika O, Pong-Wong R, Woolliams JA, Bishop SC. Confirmation of two quantitative trait loci regions for nematode resistance in commercial British terminal sire breeds. Animal. 2011;5:1149–56.
19. Silva MV, Sonstegard TS, Hanotte O, Mugambi JM, Garcia JF, Nagda S, et al. Identification of quantitative trait loci affecting resistance to gastrointestinal parasites in a double backcross population of Red Maasai and Dorper sheep. Anim Genet. 2012;43:63–71.
20. Gutierrez-Gil B, Perez J, Alvarez L, Martinez-Valladares M, de la Fuente LF, Bayon Y, et al. Quantitative trait loci for resistance to trichostrongylid infection in Spanish Churra sheep. Genet Sel Evol. 2009;41:46.
21. Kemper KE, Emery DL, Bishop SC, Oddy H, Hayes BJ, Dominik S, et al. The distribution of SNP marker effects for faecal worm egg count in sheep, and the feasibility of using these markers to predict genetic merit for resistance to worm infections. Genet Res (Camb). 2011;93:203–19.
22. Sallé G, Jacquiet P, Gruner L, Cortet J, Sauvé C, Prévot F, et al. A genome scan for QTL affecting resistance to *Haemonchus contortus* in sheep. J Anim Sci. 2012;90:4690–705.
23. Riggio V, Matika O, Pong-Wong R, Stear MJ, Bishop SC. Genome-wide association and regional heritability mapping to identify loci underlying variation in nematode resistance and body weight in Scottish Blackface lambs. Heredity (Edinb). 2013;110:420–9.
24. Riggio V, Pong-Wong R, Sallé G, Usai MG, Casu S, Moreno CR, et al. A joint analysis to identify loci underlying variation in nematode resistance in three European sheep populations. J Anim Breed Genet. 2014;131:426–36.
25. McRae KM, McEwan JC, Dodds KG, Gemmell NJ. Signatures of selection in sheep bred for resistance or susceptibility to gastrointestinal nematodes. BMC Genomics 2014;15:637.
26. Benavides MV, Sonstegard TS, Kemp S, Mugambi JM, Gibson JP, Baker RL, et al. Identification of novel loci associated with gastrointestinal parasite resistance in a Red Maasai × Dorper backcross population. PLoS One. 2015;10:e0122797.
27. García-Pérez AL, Hurtado A, Oregui LM, Juste RA. Effects of a second annual strategic anthelmintic treatment in dairy sheep in Northern Spain. Small Rumin Res. 2002;43:121–6.
28. Houdijk JGM, Kyriazakis I, Coop RL, Jackson F. The expression of immunity to *Teladorsagia circumcincta* in ewes and its relationship to protein nutrition depend on body protein reserves. Parasitology. 2001;122:661–72.
29. Wolstenholme AJ, Fairweather I, Prichard R, von Samson-Himmelstjerna G, Sangster NC. Drug resistance in veterinary helminths. Trends Parasitol. 2004;20:469–76.
30. Fish and Food Ministry of Agriculture. Manual of veterinary parasitological laboratory techniques. 1986.
31. Martinez-Valladares M. Vara-Del Rio MP, Cruz-Rojo MA, Rojo-Vazquez FA. Effect of a low protein diet on the resistance of Churra sheep to *Teladorsagia circumcincta*. Parasite Immunol. 2005;27:219–25.
32. Fox J, Weisberg S, Bates D, Fox MJ. Package 'car'. Vienna: R Foundation for Statistical Computing; 2012.
33. R Core Team. R: A language and environment for statistical computing. R Foundation for Statistical Computing, Vienna. 2014. http://www.R-project.org/.
34. García-Gámez E, Gutiérrez-Gil B, Sahana G, Sánchez JP, Bayón Y, Arranz JJ. GWA analysis for milk production traits in dairy sheep and genetic support for a QTN influencing milk protein percentage in the *LALBA* gene. PLoS One. 2012;7:e47782.
35. The CSIRO Animal, Food and Health Sciences livestock genomics web site. CSIRO Australia. The *Ovis aries* reference genome assembly (http://www.livestockgenomics.csiro.au/sheep/oar3.1.php). Accessed 21 Jan 2013.
36. Lenth Russell V. lsmeans: least-squares means. R package version 1.06–05. 2013.
37. Filangi O, Moreno C, Gilbert H, Legarra A, Le Roy P, Elsen J. QTLMap, a software for QTL detection in outbred populations. In Proceedings of the 9th World Congress on Genetics Applied to Livestock Production: 1–6 August 2010; Leipzig; 2010.

38. Lander ES, Botstein D. Mapping mendelian factors underlying quantitative traits using RFLP linkage maps. Genetics. 1989;121:185–99.
39. Broman KW, Sen S. A Guide to QTL Mapping with R/qtl (Vol. 46). New York: Springer; 2009.
40. Legarra A, Fernando RL. Linear models for joint association and linkage QTL mapping. Genet Sel Evol. 2009;41:43.
41. Madsen P, Sørensen P, Su G, Damgaard LH, Thomsen H, Labouriau R. DMU-a package for analyzing multivariate mixed models. In Proceedings of the 8th World Congress on Genetics Applied to Livestock Production: 13–18 August 2006; Belo Horizonte. 2006.
42. Gao X, Becker LC, Becker DM, Starmer JD, Province MA. Avoiding the high Bonferroni penalty in genome-wide association studies. Genet Epidemiol. 2010;34:100–5.
43. simpleM. A multiple testing correction program for correlated SNPs. (https://dsgweb.wustl.edu/rgao/). Accessed 15 Nov 2014.
44. Ensembl release 81—August 2015 WTSI/EMBL-EBI (http://www.ensembl.org/biomart/martview/). Accessed 15 Aug 2015.
45. Kelley J, de Bono B, Trowsdale J. IRIS: a database surveying known human immune system genes. Genomics. 2005;85:503–11.
46. Innate Database Gene Lists: (http://www.innatedb.com/redirect.do?go=resourcesGeneLists). Accessed 15 Feb 2015.
47. Weller JI, Kashi Y, Soller M. Power of daughter and granddaughter designs for determining linkage between marker loci and quantitative trait loci in dairy cattle. J Dairy Sci. 1990;73:2525–37.
48. Gutiérrez-Gil B, Pérez J, de la Fuente L, Meana A, Martínez-Valladares M, San Primitivo F, et al. Genetic parameters for resistance to trichostrongylid infection in dairy sheep. Animal. 2010;4:505–12.
49. Meuwissen, T. Use of whole genome sequence data for QTL mapping and genomic selection. In Proceedings of the 9th World Congress on Genetics Applied to Livestock Production: 1–6 August 2010; Leipzig; 2010.
50. Stear MJ, Strain S, Bishop SC. Mechanisms underlying resistance to nematode infection. Int J Parasitol. 1999;29:51–6.
51. Stear MJ, Bishop SC, Doligalska M, Duncan JL, Holmes PH, Irvine J, et al. Regulation of egg production, worm burden, worm length and worm fecundity by host responses in sheep infected with *Ostertagia circumcincta*. Parasite Immunol. 1995;17:643–52.
52. Grencis RK, Humphreys NE, Bancroft AJ. Immunity to gastrointestinal nematodes: mechanisms and myths. Immunol Rev. 2014;260:183–205.
53. Allen JE, Wynn TA. Evolution of Th2 immunity: a rapid repair response to tissue destructive pathogens. PLoS Pathog. 2011;7:e1002003.
54. Else KJ, Finkelman FD, Maliszewski CR, Grencis RK. Cytokine-mediated regulation of chronic intestinal helminth infection. J Exp Med. 1994;179:347–51.
55. Schumacher C, Clark-Lewis I, Baggiolini M, Moser B. High- and low-affinity binding of GRO alpha and neutrophil-activating peptide 2 to interleukin 8 receptors on human neutrophils. Proc Natl Acad Sci USA. 1992;89:10542–6.
56. Trotta T, Costantini S, Colonna G. Modelling of the membrane receptor CXCR3 and its complexes with CXCL9, CXCL10 and CXCL11 chemokines: putative target for new drug design. Mol Immunol. 2009;47:332–9.
57. da Silva EZ, Jamur MC, Oliver C. Mast cell function: a new vision of an old cell. J Histochem Cytochem. 2014;62:698–738.
58. Cliffe LJ, Humphreys NE, Lane TE, Potten CS, Booth C, Grencis RK. Accelerated intestinal epithelial cell turnover: a new mechanism of parasite expulsion. Science. 2005;308:1463–5.
59. Senior RM, Griffin GL, Huang JS, Walz DA, Deuel TF. Chemotactic activity of platelet alpha granule proteins for fibroblasts. J Cell Biol. 1983;96:382–5.
60. Dvonch VM, Murphey RJ, Matsuoka J, Grotendorst GR. Changes in growth factor levels in human wound fluid. Surgery. 1992;112:18–23.
61. Zaiss DM, van Loosdregt J, Gorlani A, Bekker CP, Gröne A, Sibilia M, et al. Amphiregulin enhances regulatory T cell-suppressive function via the epidermal growth factor receptor. Immunity. 2013;38:275–84.
62. Monticelli L, Sonnenberg G, Abt M, Osborne L, Wojno ET, Alenghat T, et al. Innate lymphoid cells promote airway epithelial repair through the amphiregulin-EGFR pathway (P3250). J Immunol. 2013;190:136–7.
63. Zaiss DM, Yang L, Shah PR, Kobie JJ, Urban JF, Mosmann TR. Amphiregulin, a TH2 cytokine enhancing resistance to nematodes. Science. 2006;314:1746.
64. Allen JE, Sutherland TE. Host protective roles of type 2 immunity: parasite killing and tissue repair, flip sides of the same coin. Semin Immunol. 2014;26:329–40.
65. Kadarmideen HN, Watson-Haigh NS, Andronicos NM. Systems biology of ovine intestinal parasite resistance: disease gene modules and biomarkers. Mol BioSyst. 2011;7:235–46.
66. Moore JH. The ubiquitous nature of epistasis in determining susceptibility to common human diseases. Hum Hered. 2003;56:73–82.

Additional file 1 Table S1: Atlija et al. Detection and replication of QTL underlying resistance to gastrointestinal nematodes in adult sheep using an ovine 50K SNP array.

Additional file 1 Table S1. Chromosome-wise significant results (Pc-value < 0.05) identified by the linkage disequilibrium analysis (LDA) performed in the present study for chromosomes (OAR) 6, 8 and 22.

OAR[1]	Trait[2]	Position of maximum LRT[3] (cM)	Significant LDA interval (cM)[4]	P_c-value[5]
6	LFEC	36.0	36-41.8	<0.05
		61.1	-	<0.05
		77.7	75.8-77.7	<0.05
		85.1	85-85.1	<0.05
8	LFEC	37.7	-	<0.0019
		49.8	-	<0.0019
		72.1	64.1-72.1	<0.0019
22	IgA_t	19.5	-	<0.05
		40.5	36-40.6	<0.05

[1]OAR = ovine chromosome
[2]Analyzed traits: *LFEC* Log-transformed faecal egg count; IgA_t Box-Cox-transformed optical density values of immunoglobulin A activity.
[3]Position of the chromosome (in centiMorgans) at which the maximum Likelihood Ration Test (LRT) is reached in the LDA performed in this work.
[4]A significant LDA interval (in centiMorgans) was defined by grouping consecutive significant 5% chromosome-wise LDA associations in a chromosome (allowing gaps no greater than 5 Mb).
[5] P_c-value: Chromosome-wise P-value established through 1,000 simulations.

Additional file 2: Figure S1. Profiles of the Likelihood Ratio Test (LRT) obtained from the linkage analysis (LA), linkage disequilibrium analysis (LDA) and the combined LDLA performed for chromosomes (OAR) 6 (a; LFEC), 8 (b; LFEC), and 22 (c; IgA_t). For the indicated trait, the LRT results of LA (solid line), LDA (dark gray circle), and LDLA (light gray circle) (y-axis) are plotted against the SNP positions analyzed along chromosomes (OAR) 6, 8 and 22 (x-axis). The 5 % chromosome-wise significance thresholds considered for each of three analyses are represented as horizontal lines.

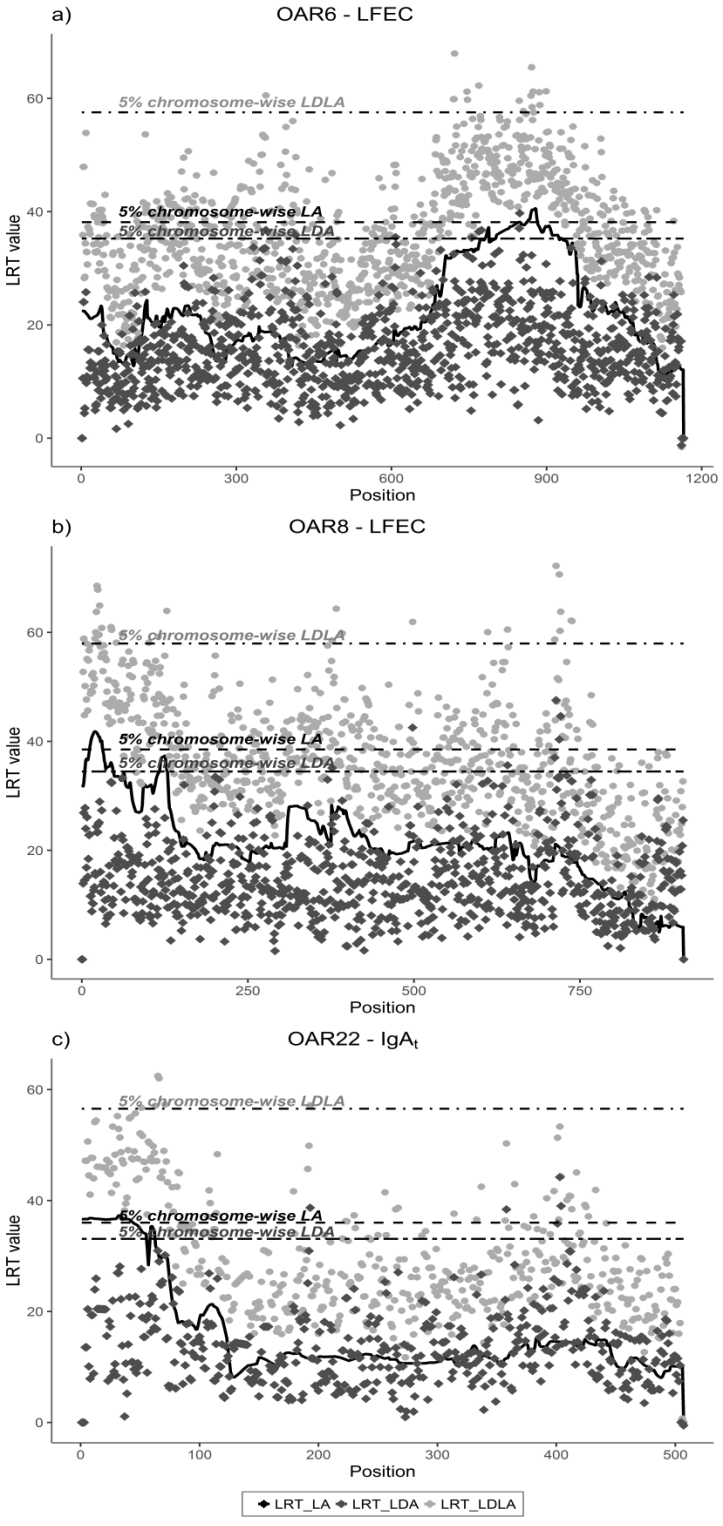

Additional file 3 Table S2: Atlija et al. Detection and replication of QTL underlying resistance to gastrointestinal nematodes in adult sheep using an ovine 50K SNP array
Additional file 3 Table S2. Summary table of the correspondence between the QTL and SNP associations identified in the present study and other studies previously reported for parasite resistance traits in sheep.

QTL identified in the present study[1]						Correspondence with previously reported QTL studies[8]									
Analysis[2]	Trait[3]	OAR[4]	Position of maximum LRT (cM)[5]	Significant interval (cM)[6]	TGI (Mb)[7] (Oar_v3.1)	Trait[9]	SheepQTLdb identifier[10]	Peak[11] (cM)	Span[12] (Mb)	Reference	Trait[9]	SNP marker	Peak (Mb)[13] Oar_v2.0	Span (Mb)[13] Oar_v2.0	Peak or Span (Mb)[14] Oar_v3.1	Reference
LDLA	LFEC	1	136.9	136.9 - 143	136.9 - 143						PCV_a		146.5	21.1–236.6		Sallé et al., 2012
LDLA	IgA_t	1	242.4		242.1-242.5	TFEC_2	12884	305	216.34-273.04	Beh et al., 2002						
LDLA	LFEC	2	78.3		78.17 - 78.36											
LDLA	IgA_t	2	188.3	188.01-188.44	188.01-188.44											
LDLA	IgA_t	3	159.8		159.67 - 160.06											
LDLA	IgA_t	3	177.7		177.52 - 177.89	SFEC_3	12891	223.9	161.95-178.25	Davies et al., 2006						
LDLA	IgA_t	4	8.9		8.66 - 9.49						MFEC	OAR4_3821431.1 - OAR4_11023787.1		3.73-10.23	3.72 - 10.88	Riggio et al., 2014
											MFEC	OAR4_7316477.1 - OAR4_13768293.1		6.89-12.95	7.54 - 13.57	Riggio et al., 2014
LDLA	LFEC	4	57.9	54 - 58	54 - 58											
LDLA	LFEC	5	5.2		5.02 - 5.43											
LDLA	LFEC	5	89.9		89.68 - 90.14						FEC12t		86.7	35.1–94.2		Sallé et al., 2012
											FEC_a		86.7	35.2–94.1		Sallé et al., 2012
											IgGst		87.3	60.5–94.2		Sallé et al., 2012
											PCV2c		87.4	7.6–96.7		Sallé et al., 2012
											PCV2c	OAR5_98137778.1 - OAR5_98330992.1	90.6		89.95 - 90.12	Sallé et al., 2012
											PCVt_a	s36267.1 - OAR5_96703012.1	89.1		88.33 - no info	Sallé et al., 2012
											MFEC	OAR5_92603004.1 - OAR5_98355816.1		84.91-90.70	84.37 - 90.15	Riggio et al., 2014
											MFEC	OAR5_95145531.1 - OAR5_100913555.1		87.58-93.30	87.03 - 92.75	Riggio et al., 2014
LDLA	LFEC	6	36		35.84 - 36.28	FECGEN	16024	45	25.06-62.57	Silva et al., 2012	SFEC16 and SFEC	OAR6_40496376.1	36.33		36.28	Riggio et al., 2013
						FECZ	13843	49.9	16.88-68.02	Duncan et al., 2007						
LDLA	LFEC	6	72.5	72.3 - 77.2	72.3 - 77.2	FECGEN	13988		68.02-85.09	Gutierrez-Gil et al., 2009	AVFEC	OAR6_80892986			74.08	Benavides et al., 2015
											AVFEC	OAR6_80909611			74.09	Benavides et al., 2015
											AVFEC	OAR6_81718546			74.87	Benavides et al., 2015
											AVFEC	OAR6_85263669			78.11	Benavides et al., 2015
											AVFEC	OAR6_85367529			78.19	Benavides et al., 2015
LA	LFEC	6	88.1	80.8-91.4	80.8-91.4	FECGEN	13988		68.02-85.09	Gutierrez-Gil et al., 2009						
LDLA	LFEC	6	89.9	85 - 90.2	85 - 90.2	FECGEN	13988		68.02-85.09	Gutierrez-Gil et al., 2009						
LDLA	LFEC	7	22.8	12.65 - 25.5	12.65 - 25.5						Len		13.8	4.4–21.7		Sallé et al., 2012
											Len	OAR7_15034944.1 - s39389.1	14.9		14.60 - 14.99	Sallé et al., 2012
											Len	s62332.1 - OAR7_17669851.1	16.9		16.81 - 17.08	Sallé et al., 2012
LDLA	LFEC	7	36.8	36.8 - 37.3	36.8 - 37.3						MFEC	OAR7_38845979.1 - OAR7_43867453.1		34.44-39.42	34.63 - 39.60	Riggio et al., 2014
LDLA	LFEC	7	53.3		53.08 - 53.46	HFEC_2	12964	73.9	44.01-56.07	Marshall et al., 2009						
LA	LFEC	8	2	1-3.4	1-3.4											
LDLA	LFEC	8	2.3	0.3 - 12.8	0.3 - 12.8											
LDLA	LFEC	8	38.3	37.7 - 39.2	37.7 - 39.2											
GWAS	IgA_t	8	49.52		49.40 - 49.65											
LDLA	LFEC	8	49.8	49.59 - 50.04	49.59 - 50.04											
LDLA	LFEC	8	64.1	61.1 - 64.1	61.1 - 64.1											
LDLA	LFEC	8	71.4	71.2 - 73.8	71.2 - 73.8	LATRICH_2	12899	113.1	3.05-87.35	Crawford et al., 2006	SFEC24	OAR8_76576205.1	71.68		71.38	Riggio et al., 2013
						LSITRICH_2	12900	113.1	3.05-87.35	Crawford et al., 2006	SFEC24	OAR8_78880291.1	73.73		73.43	Riggio et al., 2013
						FECGEN	16025	127.8	62.54-87.35	Silva et al., 2012						
GWAS	IgA_t	8	72.4		72.27 - 72.52	LATRICH_2	12899	113.1	3.05-87.35	Crawford et al., 2006						
						LSITRICH_2	12900	113.1	3.05-87.35	Crawford et al., 2006						
						FECGEN	16025	127.8	62.54-87.35	Silva et al., 2012						
LDLA	LFEC	9	5.8		5.64 - 6.03											
LDLA	LFEC	9	16.9		16.75 - 17.16	FECGEN	16026	17	0.84-19.04	Silva et al., 2012						
LDLA	LFEC	9	24.5		24.34 - 24.78	SAOS	17194	38	20.71-29.18	Lantier et al., 2012						
LDLA	LFEC	9	41.7		41.56 - 41.96											
LDLA	IgA_t	9	56.6	55.9 - 56.6	55.9 - 56.6						FEC_a		52.3	24.8–94.9		Sallé et al., 2012
LDLA	IgA_t	9	67.8	63.4 - 67.8	63.4 - 67.8						FEC	OAR9_70612779		66.27-67.09	66.62	McRae et al., 2014
GWAS	IgA_t	10	17.01		16.88 - 17.13											
GWAS	IgA_t	10	24.18		24.06 - 24.31											
LDLA	IgA_t	10	27.2	21.5 - 27.2	21.5 - 27.2											
GWAS	IgA_t	10	30.92		30.79 - 31.04											
LDLA	IgA_t	10	52.9		52.68 - 53.06	FECGEN	13989	48	24.22-86.44	Gutierrez-Gil et al., 2009						
LDLA	LFEC	10	71.6		70.01 - 71.55	FECGEN	13989	48	24.22-86.44	Gutierrez-Gil et al., 2009						
LDLA	IgA_t	10	78.6		78.39 - 78.8											

LDLA	LFEC	11	4.2	4.1 - 4.27	4.1 - 4.27										
GWAS	IgA_t	11	32.49		32.36 - 32.61										
LDLA	IgA_t	11	51.1	45.4 - 51.1	45.4 - 51.1										
LDLA	LFEC	12	3.6		3.34 - 3.84										
LDLA	IgA_t	12	1.7		1.52 - 1.98										
LDLA	IgA_t	12	17.7		17.56 - 17.96										
GWAS	IgA_t	12	61.86		61.74 - 61.99						MFEC	OAR12_63132677.1 - OAR12_68810185.1		56.73-62.29	56.69 - 62.22	Riggio et al., 2014
											MFEC	s67454.1 - OAR12_71559303.1		59.51-65.06	59.46 - 64.96	Riggio et al., 2014
LDLA	IgA_t	12	72.3	69.5 - 75.4	69.5 - 75.4	TFEC_2	12889	97	63.53-71.54	Beh et al., 2012						
LDLA	IgA_t	13	3.7	3.7 - 6.3	3.7 - 6.3						IgGmt		0.6	0.2–81.6		Sallé et al., 2012
GWAS	IgA_t	14	20.77		20.64 - 20.89											
GWAS	IgA_t	15	24.87		24.74 - 24.99	FECGEN	16029	40	18.29-30.45	Silva et al., 2012						
LDLA	IgA_t	15	33.6	33.56 - 33.93	33.56 - 33.93	FEC2	13670		30.90-47.52	Phua et al., 2009	AVPCV	OAR15_35337227			33.59	Benavides et al., 2015
LDLA	IgA_t	15	47	47 - 53.2	47 - 53.2						FEC12t		43.5	1.6–52.3		Sallé et al., 2012
LDLA	IgA_t	15	70.2	70.06 - 70.47	70.06 - 70.47											
LDLA	IgA_t	16	10.5													
LDLA	IgA_t	16	64.8	63.8 - 64.8	63.8 - 64.8											
LDLA	IgA_t	17	18.4	14.6-30.1	14.6-30.1	FECGEN	16031	36	5.96-33.12	Silva et al., 2012						
											PCV1c		18.1	12.6–66.7		Sallé et al., 2012
LDLA	IgA_t	17	36		35.8 - 36.22											
LDLA	IgA_t	17	46		45.85 - 46.27											
LDLA	IgA_t	17	62.3	62 - 66.8	62 - 66.8						pHt		63.7	47.5–64.7		Sallé et al., 2012
											PCV_a		65.1	2.8–72.4		Sallé et al., 2012
											Peps2	OAR17_67650184.1 - s10326.1	62.6		62.05 - 62.36	Sallé et al., 2012
LDLA	LFEC	20	4.8		4.58 - 5.04											
LDLA	LFEC	21	8.1	8.07 - 8.35	8.07 - 8.35											
LDLA	IgA_t	21	17.5	16.5 - 17.5	16.5 - 17.5											
LDLA	LFEC	21	31.8	31.7 - 32.24	31.7 - 32.24	SAOS	17195	51	23.63-42.89	Lantier et al., 2012						
						SAOS	17196	58	28.88-42.89	Lantier et al., 2012						
LDLA	LFEC	21	43.9	43.7 - 44.03	43.7 - 44.03		14157		36.56-46.28	Dominik et al., 2010						
LDLA	IgA_t	21	46	45.97 - 46.25	45.97 - 46.25	CEOSIN	14157		36.56-46.28	Dominik et al., 2010						
LA	IgA_t	22	3.4	0.3 - 5.8	0.3 - 5.8											
LDLA	IgA_t	22	6.7	5.3 - 7.3	5.3 - 7.3											
LDLA	IgA_t	22	19.5		19.26 - 19.85						Len	OAR22_23894546.1 - OAR22_24105777.1	20.3		20.02 - 20.24	Sallé et al., 2012
LDLA	IgA_t	23	8.3		8.15 - 8.47											
LDLA	IgA_t	23	23.3	23.3 - 28.5	23.3 - 28.5	TC_IGG_2	12902	30.9	18.60-37.13	Crawford et al., 2006						
						IGE_2	12903	30.9	5.28-23.94	Crawford et al., 2006						
LDLA	IgA_t	23	33.9	32.8 - 38	32.8 - 38	TC_IGG_2	12902	30.9	18.60-37.13	Crawford et al., 2006	FEC_a		32.2	0.3–62.7		Sallé et al., 2012
LDLA	IgA_t	23	45.8	41.7 - 48.5	41.7 - 48.5						WBt		44.1	15–59.8		Sallé et al., 2012
LDLA	IgA_t	23	54.9	54.56 - 55.06	54.56 - 55.06											
LDLA	LFEC	24	2.2	1.91 - 2.65	1.91 - 2.65						SFEC	s72739.1 - s12995.1		0.10-7.65	0.09 - 7.66	Riggio et al., 2014
LDLA	LFEC	24	17.9		17.68 - 18.12											
GWAS	IgA_t	25	13.15		13.02 - 13.27											
LDLA	LFEC	25	37	36.89 - 37.21	36.89 - 37.21											

[1] Significant QTL and SNP-associations reported in the present study based on the results of the genome scans performed using Linkage Analysis (LA; highlighted in green), Combined Linkage Disequilibrium and Linkage Analysis (LDLA; highlighted in yellow) and Genome-wise Association Study (GWAS; highlighted in blue)

[2] Analysis approaches used in the genome scans reported here for parasite resistance traits: LA (Linkage Analysis) and LDLA (Combined linkage disequilibrium and linkage analysis) with the QTLMap software and GWAS (genome-wide association analysis with the DMU software).

[3] OAR = ovine chromosome

[4] Analyzed traits in the present work: LFEC = Log-transformed faecal egg count; IgA_t: Box-Cox-transformed optical density ratio (ODR) values of Immunoglobulin A activity.

[5] Position of the chromosome (in Mega base pairs) at which the the maximum Likelihood Ratio Test was reached for the significant QTL identified by LA or LDLA, or where a significant SNP was identified by GWAS.

[6] Significant interval (in centi Morgans) (only for LDLA): defined by grouping consecutive significant 5% chromosome-wise LDLA associations in a chromosome (allowing gaps no greater than 5 cM).

[7] TGI:Target genomic interval (in Mb) defined as a region of the sheep genome reference assembly Oar_v3.1 that corresponds with (i) the CI estimated for the LA significant QTL and the defined significant LDLA intervals; and (ii) a 250 kb-long interval centered on each of the significant isolated haplotypes detected by LDLA and the significant SNP identified by GWAS.

[8] Previously reported QTL overlapping with the significant QTL reported in the present study; the details provided about these QTL are based on the information provided at the SheepQTL database (SheepQTLdb) for the microsatellite-based studies) or the corresponding reporting article (for the SNP-chip based studies).

[9] Trait for which a significant QTL or marker association has been reported by other studies, as defined in the SheepQTLdb or the corresponding reporting article (See trait description box in sheet 2).

[10] SheepQTLdb identifier: Unique reference number assigned to the QTL/associations storaged at the SheepQTLdb (http://www.animalgenome.org/cgi-bin/QTLdb/OA/index)

[11] Peak location of the significant QTL included in the SheepQTLdb (in cM)

[12] The span of the genomic region of the significant QTL as indicated in the SheepQTLdatabase, based on the sheep genome reference assembly Oar_v3.1.

[13] Peak and span of significant associations identified by a 50K-chip-based study (for those studies referred to the sheep genome assembly Oar_v2.0).

[14] Peak or span of significant associations identified by a 50K-chip-based study (for those studies referred to the sheep genome assembly Oar_v3.1; for the studies originally reported in reference to the assembly Oar_v2.0, the corresponding interval in the Oar_v3.1, if possible, is indicated).

Trait description box (according to SheepQTLdb and SNP-chip based studies)	
FEC	Fecal egg count
AVFEC	average FEC
AVPCV	average packed cell volume
CEOSIN	Change in eosinophil number
FEC_a	animal solution of a mixed model equation with the infection rank added to other fixed effects and animal fitted as a random variable
FEC12t	FEC mean between 25 and 35 d after the 1st challenge
FECGEN	FEC
FECZ	facial eczema susceptibility
HFEC_2	Haemonchus contortus FEC2
IGE_2	Immunoglobulin E nematode
IgGmt	Immunoglobulin G
IgGst	IgG in serum; t fourth root transformation of the variable
LATRICH_2	Abomasal Trichostrongylus sp adults and larvae challenge 2
Len	Female worm length
LSITRICH_2	Small Intestine Trichostrongylus sp adults and larvae challenge2
PCV_a	PCV and the _a stands for as within-animal physiological variation accounted for.
PCV1c	PCVafter 1st challenge; c indicates values corrected with PCV0 fitted as a covariable
PCV2c	PCVafter 2nd challenge; c indicates values corrected with PCV0 fitted as a covariable
PCVt_a	PCV. The t and _a stand for as a fourth root transformation of the variable and within-animal physiological variation accounted for respectively
Peps2	Pepstinogen after 2nd challenge
pHt	Abomasal pH and t stands for as a fourth root transformation of the variable
SAOS	Salmonella abortusovis susceptibility
SFEC_3	Strongyle FEC3
SFEC16	Stronglyle FEC at 16 weeks of age
SFEC24	Stronglyle faecal egg count at 24 weeks of age
TC_IGG_2	Trichostrongylus colubriformis serum Immunoglobulin G challenge 2
TFEC_2	Trichostrongylus colubriformis FEC2
WBt	Worm burden and t stands for as a square root transformation
SAFEC	Strongyles average FEC
MFEC	Mixed FEC
SFEC	Strongyle FEC

Additonal file 4 Table S3: Atlija et al. Detection and replication of QTL underlying resistance to gastrointestinal nematodes in adult sheep using an ovine 50K SNP array.
Additonal file 4 Table S3. Total list of annotated genes extracted from the Sheep Genome Assembly v3.1 using the BioMart web-tool for the significant QTL regions and SNP associations identified for the two parasite resistance traits analyzed in the prese
study.

Trait	Analysis	Number in the list of positional candidate genes per trait	Chromosome Name	Gene Start (bp)	Gene End (bp	Ensembl Gene ID	Ensembl Transcript ID	Gene symbol	Description
IgAt	GWAS	1	8	49477793	49559187	ENSOARG00000013003	ENSOART00000014143	RARS2	arginyl-tRNA synthetase 2, mitochondrial
IgAt	LDLA	2	9	63608850	65007715	ENSOARG00000011267	ENSOART00000012260	CSMD3	CUB and Sushi multiple domains 3
IgAt	LDLA	3	9	67500915	67513034	ENSOARG00000012091	ENSOART00000013150	EBAG9	estrogen receptor binding site associated, antigen, 9
IgAt	LDLA	4	9	67132005	67137894	ENSOARG00000011921	ENSOART00000012967	KCNV1	potassium channel, voltage gated modifier subfamily V, member 1
IgAt	LDLA	5	9	67752028	67841910	ENSOARG00000014426	ENSOART00000015705	NUDCD1	NudC domain containing 1
IgAt	LDLA	6	9	67545553	67751569	ENSOARG00000013110	ENSOART00000014282	PKHD1L1	polycystic kidney and hepatic disease 1 (autosomal recessive)-like 1
IgAt	LDLA	7	9	67362234	67490064	ENSOARG00000012018	ENSOART00000013073	SYBU	syntabulin (syntaxin-interacting)
IgAt	LDLA	8	9	56102648	56149776	ENSOARG00000008295	ENSOART00000009024	TPD52	tumor protein D52
IgAt	LDLA	9	9	56527266	56558510	ENSOARG00000008508	ENSOART00000009259	ZBTB10	zinc finger and BTB domain containing 10
IgAt	LDLA	10	10	21730534	21741216	ENSOARG00000009109	ENSOART00000009917	ALG11	ALG11, alpha-1,2-mannosyltransferase
IgAt	LDLA	11	10	24936260	24960025	ENSOARG00000010275	ENSOART00000011179	ALG5	ALG5, dolichyl-phosphate beta-glucosyltransferase
IgAt	LDLA	12	10	21656704	21730091	ENSOARG00000009056	ENSOART00000009869	ATP7B	copper-transporting ATPase 2
IgAt	LDLA	13	10	21623899	21624597	ENSOARG00000005995	ENSOART00000006512	CCDC70	coiled-coil domain containing 70
IgAt	LDLA	14	10	25350379	25364643	ENSOARG00000010389	ENSOART00000011307	CCNA1	cyclin A1
IgAt	LDLA	15	10	21841539	21861932	ENSOARG00000009289	ENSOART00000010110	CKAP2	cytoskeleton associated protein 2
IgAt	LDLA	16	10	22959747	23019979	ENSOARG00000009574	ENSOART00000010430	COG6	component of oligomeric golgi complex 6
IgAt	LDLA	17	10	25828569	25925624	ENSOARG00000010490	ENSOART00000011423	DCLK1	Uncharacterized protein
IgAt	LDLA	18	10	21515039	21546413	ENSOARG00000008965	ENSOART00000009771	DHRS12	dehydrogenase/reductase (SDR family) member 12
IgAt	LDLA	19	10	24923877	24931650	ENSOARG00000010229	ENSOART00000011130	EXOSC8	exosome component 8
IgAt	LDLA	20	10	22237525	22238862	ENSOARG00000006012	ENSOART00000006530	FOXO1	forkhead box O1
IgAt	LDLA	21	10	23560959	23715430	ENSOARG00000009812	ENSOART00000010687	FREM2	FRAS1 related extracellular matrix protein 2
IgAt	LDLA	22	10	23066861	23125253	ENSOARG00000009621	ENSOART00000010471	LHFP	lipoma HMGIC fusion partner
IgAt	GWAS	23	10	16955899	17063525	ENSOARG00000008014	ENSOART00000008735	LRCH1	leucine-rich repeats and calponin homology (CH) domain containing 1
IgAt	LDLA	24	10	26231353	26232432	ENSOARG00000006073	ENSOART00000006603	MAB21L1	mab-21-like 1 (C. elegans)
IgAt	LDLA	25	10	22088057	22114923	ENSOARG00000009534	ENSOART00000010380	MRPS31	mitochondrial ribosomal protein S31
IgAt	LDLA	26	10	52632844	52906106	ENSOARG00000016305	ENSOART00000017799	MYCBP2	MYC binding protein 2, E3 ubiquitin protein ligase
IgAt	LDLA	27	10	26007917	26592574	ENSOARG00000010627	ENSOART00000011571	NBEA	neurobeachin
IgAt	LDLA	28	10	21807469	21831130	ENSOARG00000009224	ENSOART00000010044	NEK3	NIMA-related kinase 3
IgAt	LDLA	29	10	21746108	21803002	ENSOARG00000009157	ENSOART00000009968	NEK5	NIMA-related kinase 5
IgAt	LDLA	30	10	23478664	23487167	ENSOARG00000009644	ENSOART00000010500	NHLRC3	NHL repeat containing 3
IgAt	LDLA	31	10	24474862	24508794	ENSOARG00000010041	ENSOART00000010931	POSTN	periostin, osteoblast specific factor
IgAt	LDLA	32	10	23488542	23514517	ENSOARG00000009737	ENSOART00000010597	PROSER1	proline and serine rich 1
IgAt	LDLA	33	10	25040237	25049476	ENSOARG00000010378	ENSOART00000011287	RFXAP	regulatory factor X-associated protein
IgAt	LDLA	34	10	25146441	25146761	ENSOARG00000006045	ENSOART00000006573	SERTM1	serine-rich and transmembrane domain containing 1
IgAt	LDLA	35	10	78617440	78638111	ENSOARG00000005368	ENSOART00000005850	SLC10A2	solute carrier family 10 (sodium/bile acid cotransporter), member 2
IgAt	LDLA	36	10	22035177	22064433	ENSOARG00000009523	ENSOART00000010370	SLC25A15	solute carrier family 25 (mitochondrial carrier; ornithine transporter) member 15
IgAt	LDLA	37	10	25005441	25029769	ENSOARG00000010293	ENSOART00000011197	SMAD9	SMAD family member 9
IgAt	LDLA	38	10	25427861	25453683	ENSOARG00000010471	ENSOART00000011399	SPG20	spastic paraplegia 20 (Troyer syndrome)
IgAt	LDLA	39	10	23521617	23548937	ENSOARG00000009746	ENSOART00000010606	STOML3	stomatin (EPB72)-like 3
IgAt	LDLA	40	10	21906715	21935955	ENSOARG00000009388	ENSOART00000010221	THSD1	thrombospondin, type I, domain containing 1
IgAt	GWAS	41	10	24289442	24435384	ENSOARG00000009964	ENSOART00000010848	TRPC4	transient receptor potential cation channel, subfamily C, member 4
IgAt	LDLA	42	10	23949296	23961373	ENSOARG00000009897	ENSOART00000010767	UFM1	ubiquitin-fold modifier 1
IgAt	LDLA	43	10	21876927	21896255	ENSOARG00000009332	ENSOART00000010157	VPS36	vacuolar protein sorting 36 homolog (S. cerevisiae)
IgAt	LDLA	44	10	21328931	21506011	ENSOARG00000008939	ENSOART00000009736	WDFY2	WD repeat and FYVE domain containing 2
IgAt	LDLA	45	11	47222569	47244014	ENSOARG00000012958	ENSOART00000014094	ACE	Uncharacterized protein
IgAt	LDLA	46	11	50420600	50422985	ENSOARG00000018506	ENSOART00000020143	ACTG1	actin gamma 1
IgAt	LDLA	47	11	50164976	50169097	ENSOARG00000017932	ENSOART00000019512	ALYREF	Aly/REF export factor
IgAt	LDLA	48	11	50160594	50165035	ENSOARG00000017916	ENSOART00000019490	ANAPC11	anaphase promoting complex subunit 11
IgAt	LDLA	49	11	50189207	50190485	ENSOARG00000017985	ENSOART00000019572	ARHGDIA	Rho GDP dissociation inhibitor (GDI) alpha
IgAt	LDLA	50	11	50297282	50299639	ENSOARG00000018330	ENSOART00000019943	ARL16	ADP-ribosylation factor-like 16
IgAt	LDLA	51	11	50052768	50086400	ENSOARG00000017643	ENSOART00000019198	ASPSCR1	alveolar soft part sarcoma chromosome region, candidate 1
IgAt	LDLA	52	11	49041879	49146866	ENSOARG00000015890	ENSOART00000017303	B3GNTL1	UDP-GlcNAc:betaGal beta-1,3-N-acetylglucosaminyltransferase-like 1
IgAt	LDLA	53	11	50464135	50499239	ENSOARG00000018651	ENSOART00000020309	BAHCC1	BAH domain and coiled-coil containing 1
IgAt	LDLA	54	11	50728317	50769136	ENSOARG00000000258	ENSOART00000000283	BAIAP2	BAI1-associated protein 2
IgAt	LDLA	55	11	48383457	48474179	ENSOARG00000015595	ENSOART00000016974	BPTF	bromodomain PHD finger transcription factor
IgAt	LDLA	56	11	48377004	48377962	ENSOARG00000015412	ENSOART00000016768	C17orf58	chromosome 17 open reading frame 58
IgAt	LDLA	57	11	49496227	49501084	ENSOARG00000016516	ENSOART00000017987	C17orf62	chromosome 17 open reading frame 62
IgAt	LDLA	58	11	50309566	50313999	ENSOARG00000018332	ENSOART00000019950	CCDC137	coiled-coil domain containing 137
IgAt	LDLA	59	11	47439118	47450900	ENSOARG00000013493	ENSOART00000014676	CCDC47	coiled-coil domain containing 47
IgAt	LDLA	60	11	49837708	49934959	ENSOARG00000016997	ENSOART00000018513	CCDC57	coiled-coil domain containing 57
IgAt	LDLA	61	11	49714298	49717531	ENSOARG00000016754	ENSOART00000018239	CD7	CD7 molecule
IgAt	LDLA	62	11	47554266	47557305	ENSOARG00000014015	ENSOART00000015261	CD79B	CD79b molecule, immunoglobulin-associated beta
IgAt	LDLA	63	11	45629502	45678848	ENSOARG00000011644	ENSOART00000012666	CDC27	cell division cycle 27
IgAt	GWAS	64	11	32482592	32490822	ENSOARG00000016588	ENSOART00000018070	CDRT4	CMT1A duplicated region transcript 4
IgAt	LDLA	65	11	48103026	48141956	ENSOARG00000015133	ENSOART00000016470	CEP95	centrosomal protein 95kDa
IgAt	LDLA	66	11	50811968	50815819	ENSOARG00000000413	ENSOART00000000440	CHMP6	charged multivesicular body protein 6
IgAt	LDLA	67	11	49769083	49798238	ENSOARG00000016829	ENSOART00000018330	CSNK1D	casein kinase 1, delta
IgAt	LDLA	68	11	47293994	47323862	ENSOARG00000013278	ENSOART00000014440	DCAF7	DDB1 and CUL4 associated factor 7
IgAt	LDLA	69	11	50014563	50023438	ENSOARG00000017409	ENSOART00000018949	DCXR	Uncharacterized protein
IgAt	LDLA	70	11	47465640	47490671	ENSOARG00000013540	ENSOART00000014731	DDX42	DEAD (Asp-Glu-Ala-Asp) box helicase 42
IgAt	LDLA	71	11	48096623	48102912	ENSOARG00000015045	ENSOART00000016375	DDX5	DEAD (Asp-Glu-Ala-Asp) box helicase 5
IgAt	LDLA	72	11	49972871	49978551	ENSOARG00000017277	ENSOART00000018806	DUS1L	dihydrouridine synthase 1-like (S. cerevisiae)
IgAt	LDLA	73	11	45819006	45874585	ENSOARG00000012039	ENSOART00000013094	EFCAB13	EF-hand calcium binding domain 13
IgAt	LDLA	74	11	45819006	46286165	ENSOARG00000011927	ENSOART00000012980	EFCAB3	EF-hand calcium binding domain 3
IgAt	LDLA	75	11	50644016	50652441	ENSOARG00000018788	ENSOART00000020467	ENTHD2	ENTH domain containing 2
IgAt	LDLA	76	11	47691468	47769786	ENSOARG00000014398	ENSOART00000015686	ERN1	endoplasmic reticulum to nucleus signaling 1
IgAt	LDLA	77	11	50218977	50220115	ENSOARG00000018108	ENSOART00000019711	FAM195B	family with sequence similarity 195, member B
IgAt	LDLA	78	11	49940273	49955854	ENSOARG00000017168	ENSOART00000018693	FASN	fatty acid synthase
IgAt	LDLA	79	11	49293868	49302299	ENSOARG00000016194	ENSOART00000017634	FN3K	fructosamine 3 kinase
IgAt	LDLA	80	11	49311041	49318361	ENSOARG00000016300	ENSOART00000017749	FN3KRP	fructosamine 3 kinase related protein
IgAt	LDLA	81	11	49408057	49456197	ENSOARG00000016414	ENSOART00000017878	FOXK2	forkhead box K2
IgAt	LDLA	82	11	50397859	50403453	ENSOARG00000018489	ENSOART00000020122	FSCN2	fascin actin-bundling protein 2, retinal
IgAt	LDLA	83	11	47492083	47499382	ENSOARG00000013637	ENSOART00000014843	FTSJ3	FtsJ homolog 3 (E. coli)
IgAt	LDLA	84	11	50226474	50230614	ENSOARG00000018139	ENSOART00000019741	GCGR	glucagon receptor
IgAt	LDLA	85	11	49979394	49983705	ENSOARG00000017353	ENSOART00000018897	GPS1	G protein pathway suppressor 1
IgAt	LDLA	86	11	49503099	49516814	ENSOARG00000016564	ENSOART00000018041	HEXDC	hexosaminidase (glycosyl hydrolase family 20, catalytic domain) containing
IgAt	LDLA	87	11	50284057	50296963	ENSOARG00000018265	ENSOART00000019875	HGS	hepatocyte growth factor-regulated tyrosine kinase substrate
IgAt	LDLA	88	11	47641431	47645553	ENSOARG00000014212	ENSOART00000015481	ICAM2	Uncharacterized protein
IgAt	LDLA	89	11	45762020	45802167	ENSOARG00000011855	ENSOART00000012896	ITGB3	Integrin beta
IgAt	LDLA	90	11	45440771	45606179	ENSOARG00000011438	ENSOART00000012441	KANSL1	KAT8 regulatory NSL complex subunit 1
IgAt	LDLA	91	11	47266979	47290236	ENSOARG00000013121	ENSOART00000014266	KCNH6	potassium channel, voltage gated eag related subfamily H, member 6
IgAt	LDLA	92	11	48337065	48345443	ENSOARG00000015347	ENSOART00000016702	KPNA2	karyopherin alpha 2 (RAG cohort 1, importin alpha 1)
IgAt	LDLA	93	11	47401902	47402623	ENSOARG00000013388	ENSOART00000014558	LIMD2	LIM domain containing 2
IgAt	LDLA	94	11	50040435	50047414	ENSOARG00000017544	ENSOART00000019101	LRRC45	leucine rich repeat containing 45
IgAt	LDLA	95	11	50135356	50141785	ENSOARG00000017782	ENSOART00000019347	MAFG	v-maf avian musculoaponeurotic fibrosarcoma oncogene homolog G

IgAt	LDLA	96	11	47346954	47397045	ENSOARG00000013329	ENSOART00000014499	MAP3K3	mitogen-activated protein kinase kinase kinase 3
IgAt	LDLA	97	11	45315251	45433964	ENSOARG00000011303	ENSOART00000012295	MAPT	microtubule-associated protein tau
IgAt	LDLA	98	11	46538705	46627944	ENSOARG00000012540	ENSOART00000013635	MARCH10	membrane-associated ring finger (C3HC4) 10, E3 ubiquitin protein ligase
IgAt	LDLA	99	11	49004940	49013385	ENSOARG00000015857	ENSOART00000017267	METRNL	meteorin, glial cell differentiation regulator-like
IgAt	LDLA	100	11	46286298	46297443	ENSOARG00000012110	ENSOART00000013171	METTL2A	Uncharacterized protein
IgAt	LDLA	101	11	48040699	48061882	ENSOARG00000014870	ENSOART00000016186	MILR1	mast cell immunoglobulin-like receptor 1
IgAt	LDLA	102	11	46503733	46528230	ENSOARG00000012392	ENSOART00000013476	MRC2	mannose receptor, C type 2
IgAt	LDLA	103	11	50278630	50282028	ENSOARG00000018221	ENSOART00000019825	MRPL12	mitochondrial ribosomal protein L12
IgAt	LDLA	104	11	50119677	50120600	ENSOARG00000000164	ENSOART00000000166	MYADML2	myeloid-associated differentiation marker-like 2
IgAt	LDLA	105	11	45705716	45718546	ENSOARG00000011750	ENSOART00000012780	MYL4	myosin, light chain 4, alkali; atrial, embryonic
IgAt	LDLA	106	11	49475090	49491567	ENSOARG00000016487	ENSOART00000017954	NARF	nuclear prelamin A recognition factor
IgAt	LDLA	107	11	48565854	48584284	ENSOARG00000015771	ENSOART00000017172	NOL11	nucleolar protein 11
IgAt	LDLA	108	11	50102110	50108011	ENSOARG00000017695	ENSOART00000019254	NOTUM	notum pectinacetylesterase homolog (Drosophila)
IgAt	LDLA	109	11	50334386	50381184	ENSOARG00000018408	ENSOART00000020037	NPLOC4	nuclear protein localization 4 homolog (S. cerevisiae)
IgAt	LDLA	110	11	50314135	50315390	ENSOARG00000018364	ENSOART00000019987	OXLD1	oxidoreductase-like domain containing 1
IgAt	LDLA	111	11	50196914	50206198	ENSOARG00000018038	ENSOART00000019634	P4HB	prolyl 4-hydroxylase, beta polypeptide
IgAt	LDLA	112	11	50148105	50155340	ENSOARG00000017906	ENSOART00000019488	PCYT2	phosphate cytidylyltransferase 2, ethanolamine
IgAt	LDLA	113	11	50318674	50319888	ENSOARG00000018382	ENSOART00000020004	PDE6G	phosphodiesterase 6G, cGMP-specific, rod, gamma
IgAt	LDLA	114	11	47943720	48008979	ENSOARG00000014779	ENSOART00000016087	PECAM1	platelet/endothelial cell adhesion molecule 1
IgAt	LDLA	115	11	48609521	48800591	ENSOARG00000015799	ENSOART00000017201	PITPNC1	phosphatidylinositol transfer protein, cytoplasmic 1
IgAt	LDLA	116	11	48078392	48093912	ENSOARG00000014976	ENSOART00000016300	POLG2	polymerase (DNA directed), gamma 2, accessory subunit
IgAt	LDLA	117	11	50211686	50212510	ENSOARG00000018093	ENSOART00000019695	PPP1R27	protein phosphatase 1, regulatory subunit 27
IgAt	LDLA	118	11	47499794	47504262	ENSOARG00000013737	ENSOART00000014948	PSMC5	proteasome (prosome, macropain) 26S subunit, ATPase, 5
IgAt	LDLA	119	11	48879065	48898943	ENSOARG00000015809	ENSOART00000017211	PSMD12	proteasome (prosome, macropain) 26S subunit, non-ATPase, 12
IgAt	LDLA	120	11	50124987	50128563	ENSOARG00000017754	ENSOART00000019321	PYCR1	pyrroline-5-carboxylate reductase 1
IgAt	LDLA	121	11	50037326	50039379	ENSOARG00000017460	ENSOART00000019005	RAC3	ras-related C3 botulinum toxin substrate 3 (rho family, small GTP binding protein Rac3)
IgAt	LDLA	122	11	49984497	49987075	ENSOARG00000017365	ENSOART00000018903	RFNG	RFNG O-fucosylpeptide 3-beta-N-acetylglucosaminyltransferase
IgAt	LDLA	123	11	50830224	51148991	ENSOARG00000000488	ENSOART00000000523	RPTOR	regulatory associated protein of MTOR, complex 1
IgAt	LDLA	124	11	47563592	47595132	ENSOARG00000014087	ENSOART00000015339	SCN4A	sodium channel, voltage gated, type IV alpha subunit
IgAt	LDLA	125	11	50142119	50147468	ENSOARG00000017788	ENSOART00000019356	SIRT7	sirtuin 7
IgAt	LDLA	126	11	49799205	49803627	ENSOARG00000016912	ENSOART00000018418	SLC16A3	solute carrier family 16 (monocarboxylate transporter), member 3
IgAt	LDLA	127	11	50597855	50636930	ENSOARG00000018707	ENSOART00000020367	SLC38A10	solute carrier family 38, member 10
IgAt	LDLA	128	11	47505251	47509171	ENSOARG00000013842	ENSOART00000015067	SMARCD2	SWI/SNF related, actin dependent regulator of chromatin, subfamily d, member 2
IgAt	LDLA	129	11	48151210	48194827	ENSOARG00000015245	ENSOART00000016591	SMURF2	SMAD specific E3 ubiquitin protein ligase 2
IgAt	LDLA	130	11	50050272	50051095	ENSOARG00000017637	ENSOART00000019191	STRA13	stimulated by retinoic acid 13
IgAt	LDLA	131	11	47403627	47425001	ENSOARG00000013434	ENSOART00000014613	STRADA	STE20-related kinase adaptor alpha
IgAt	LDLA	132	11	46811589	47176828	ENSOARG00000012739	ENSOART00000013856	TANC2	tetratricopeptide repeat, ankyrin repeat and coiled-coil containing 2
IgAt	LDLA	133	11	49152968	49292712	ENSOARG00000016006	ENSOART00000017443	TBCD	tubulin folding cofactor D
IgAt	LDLA	134	11	47788873	47856498	ENSOARG00000014649	ENSOART00000015946	TEX2	testis expressed 2
IgAt	LDLA	135	11	46333788	46456079	ENSOARG00000012181	ENSOART00000013258	TLK2	tousled-like kinase 2
IgAt	LDLA	136	11	50321755	50325716	ENSOARG00000018386	ENSOART00000020008	TSPAN10	tetraspanin 10
IgAt	LDLA	137	11	49545105	49546235	ENSOARG00000016694	ENSOART00000018181	UTS2R	urotensin 2 receptor
IgAt	LDLA	138	11	49240308	49242692	ENSOARG00000016190	ENSOART00000017626	ZNF750	zinc finger protein 750
IgAt	LDLA	139	12	74128395	74189805	ENSOARG00000014713	ENSOART00000016018	ASPM	asp (abnormal spindle) homolog, microcephaly associated (Drosophila)
IgAt	LDLA	140	12	71659955	71660764	ENSOARG00000004302	ENSOART00000004684	C1orf74	chromosome 1 open reading frame 74
IgAt	LDLA	141	12	71847530	71871488	ENSOARG00000013305	ENSOART00000014467	CAMK1G	calcium/calmodulin-dependent protein kinase IG
IgAt	LDLA	142	12	73589869	73605431	ENSOARG00000013714	ENSOART00000014923	CD34	CD34 molecule
IgAt	LDLA	143	12	73700588	73737242	ENSOARG00000013891	ENSOART00000015124	CD46	Membrane cofactor protein
IgAt	LDLA	144	12	74087298	74114558	ENSOARG00000014405	ENSOART00000015689	CFHR5	complement factor H-related 5
IgAt	LDLA	145	12	74372414	74515404	ENSOARG00000015257	ENSOART00000016602	CRB1	crumbs family member 1, photoreceptor morphogenesis associated
IgAt	LDLA	146	12	74597237	74860995	ENSOARG00000015345	ENSOART00000016698	DENND1B	DENN/MADD domain containing 1B
IgAt	LDLA	147	12	71583789	71612947	ENSOARG00000012524	ENSOART00000013618	DIEXF	digestive organ expansion factor homolog (zebrafish)
IgAt	LDLA	148	12	69565822	69614212	ENSOARG00000010843	ENSOART00000011795	DTL	denticleless E3 ubiquitin protein ligase homolog (Drosophila)
IgAt	LDLA	149	12	74054568	74071976	ENSOARG00000014258	ENSOART00000015530	F13B	coagulation factor XIII, B polypeptide
IgAt	LDLA	150	12	71772867	71773127	ENSOARG00000004314	ENSOART00000004697	G0S2	G0/G1 switch 2
IgAt	LDLA	151	12	70801226	71071455	ENSOARG00000012227	ENSOART00000013293	HHAT	hedgehog acyltransferase
IgAt	LDLA	152	12	71703835	71763644	ENSOARG00000013020	ENSOART00000014154	HSD11B1	hydroxysteroid (11-beta) dehydrogenase 1
IgAt	LDLA	153	12	69614668	69692390	ENSOARG00000011102	ENSOART00000012082	INTS7	integrator complex subunit 7
IgAt	LDLA	154	12	71642946	71654633	ENSOARG00000012720	ENSOART00000013830	IRF6	Uncharacterized protein
IgAt	LDLA	155	12	70252715	70754047	ENSOARG00000012144	ENSOART00000013209	KCNH1	potassium channel, voltage gated eag related subfamily H, member 1
IgAt	LDLA	156	12	71807820	71847698	ENSOARG00000013143	ENSOART00000014294	LAMB3	laminin, beta 3
IgAt	LDLA	157	12	74963845	74975433	ENSOARG00000015439	ENSOART00000016797	LHX9	LIM homeobox 9
IgAt	LDLA	158	12	69778803	69860630	ENSOARG00000011368	ENSOART00000012361	LPGAT1	lysophosphatidylglycerol acyltransferase 1
IgAt	LDLA	159	12	1647968	1650240	ENSOARG00000002912	ENSOART00000003152	LRRN2	leucine rich repeat neuronal 2
IgAt	LDLA	160	12	1559651	1577436	ENSOARG00000002783	ENSOART00000003016	MDM4	Uncharacterized protein
IgAt	LDLA	161	12	70224382	70225419	ENSOARG00000012084	ENSOART00000013141	NACA	Uncharacterized protein
IgAt	LDLA	162	12	69915816	69927483	ENSOARG00000011466	ENSOART00000012469	NEK2	NIMA-related kinase 2
IgAt	LDLA	163	12	75218230	75298088	ENSOARG00000015482	ENSOART00000016842	NEK7	NIMA-related kinase 7
IgAt	LDLA	164	12	1935014	2090555	ENSOARG00000002978	ENSOART00000003234	NFASC	neurofascin
IgAt	LDLA	165	12	73261010	73466213	ENSOARG00000013487	ENSOART00000014679	PLXNA2	plexin A2
IgAt	LDLA	166	12	70200447	70251222	ENSOARG00000011913	ENSOART00000012960	RCOR3	REST corepressor 3
IgAt	LDLA	167	12	70114121	70117410	ENSOARG00000011679	ENSOART00000012698	RD3	retinal degeneration 3
IgAt	GWAS	168	12	61810410	61835896	ENSOARG00000019017	ENSOART00000020705	RGS8	regulator of G-protein signaling 8
IgAt	LDLA	169	12	71226361	71230852	ENSOARG00000012256	ENSOART00000013324	SERTAD4	SERTA domain containing 4
IgAt	LDLA	170	12	70015802	70019084	ENSOARG00000011554	ENSOART00000012564	SLC30A1	solute carrier family 30 (zinc transporter), member 1
IgAt	LDLA	171	12	71301567	71436787	ENSOARG00000012287	ENSOART00000013359	SYT14	synaptotagmin XIV
IgAt	LDLA	172	12	71661157	71680824	ENSOARG00000012918	ENSOART00000014043	TRAF3IP3	TRAF3 interacting protein 3
IgAt	LDLA	173	12	70142559	70186497	ENSOARG00000011779	ENSOART00000012814	TRAF5	TNF receptor-associated factor 5
IgAt	LDLA	174	12	16999001	17981947	ENSOARG00000010714	ENSOART00000011686	USH2A	Usher syndrome 2A (autosomal recessive, mild)
IgAt	LDLA	175	12	74206553	74247201	ENSOARG00000015070	ENSOART00000016403	ZBTB41	zinc finger and BTB domain containing 41
IgAt	LDLA	176	13	4900219	4905937	ENSOARG00000010789	ENSOART00000011736	BTBD3	BTB (POZ) domain containing 3
IgAt	LDLA	177	13	6086778	6226790	ENSOARG00000010864	ENSOART00000011820	SPTLC3	serine palmitoyltransferase, long chain base subunit 3
IgAt	LDLA	178	15	49946823	49948163	ENSOARG00000004004	ENSOART00000004349	ANAPC15	Uncharacterized protein
IgAt	LDLA	179	15	50442619	50483505	ENSOARG00000005950	ENSOART00000006487	ARAP1	ArfGAP with RhoGAP domain, ankyrin repeat and PH domain 1
IgAt	LDLA	180	15	50996826	51052556	ENSOARG00000007394	ENSOART00000008054	ARHGEF17	Rho guanine nucleotide exchange factor (GEF) 17
IgAt	LDLA	181	15	52667884	52740268	ENSOARG00000011342	ENSOART00000012337	ARRB1	arrestin, beta 1
IgAt	LDLA	182	15	50553684	50569219	ENSOARG00000006493	ENSOART00000007059	ATG16L2	autophagy related 16-like 2 (S. cerevisiae)
IgAt	LDLA	183	15	51636895	51757743	ENSOARG00000009005	ENSOART00000009824	C2CD3	C2 calcium-dependent domain containing 3
IgAt	LDLA	184	15	52188995	52223521	ENSOARG00000010444	ENSOART00000011366	CHRDL2	chordin-like 2
IgAt	LDLA	185	15	49646168	49650973	ENSOARG00000002505	ENSOART00000002710	CHRNA10	cholinergic receptor, nicotinic, alpha 10 (neuronal)
IgAt	LDLA	186	15	50087287	50226656	ENSOARG00000005285	ENSOART00000005764	CLPB	ClpB homolog, mitochondrial AAA ATPase chaperonin
IgAt	LDLA	187	15	51580089	51592425	ENSOARG00000008463	ENSOART00000009209	DNAJB13	DnaJ (Hsp40) homolog, subfamily B, member 13
IgAt	LDLA	188	15	51087487	51151694	ENSOARG00000007784	ENSOART00000008471	FAM168A	family with sequence similarity 168, member A
IgAt	LDLA	189	15	50578436	50817453	ENSOARG00000006995	ENSOART00000007620	FCHSD2	FCH and double SH3 domains 2
IgAt	LDLA	190	15	50010450	50014708	ENSOARG00000004214	ENSOART00000004585	FOLR1	Uncharacterized protein
IgAt	LDLA	191	15	50032806	50034889	ENSOARG00000004298	ENSOART00000004681	FOLR2	Uncharacterized protein
IgAt	LDLA	192	15	49993284	49999169	ENSOARG00000004127	ENSOART00000004489	FOLR3	Uncharacterized protein
IgAt	LDLA	193	15	52799205	52842351	ENSOARG00000011760	ENSOART00000012790	GDPD5	glycerophosphodiester phosphodiesterase domain containing 5
IgAt	LDLA	194	15	33605559	33794217	ENSOARG00000000345	ENSOART00000000365	GRAMD1B	GRAM domain containing 1B
IgAt	LDLA	195	15	49841475	49843715	ENSOARG00000003484	ENSOART00000003786	IL18BP	interleukin 18 binding protein

IgAt	LDLA	196	15	50038039	50052706	ENSOARG00000004577	ENSOART00000004994	INPPL1	inositol polyphosphate phosphatase-like 1
IgAt	LDLA	197	15	51990208	51990507	ENSOARG00000006737	ENSOART00000007319	KCNE3	potassium channel, voltage gated subfamily E regulatory beta subunit 3
IgAt	LDLA	198	15	52790207	52796650	ENSOARG00000011617	ENSOART00000012636	KLHL35	kelch-like family member 35
IgAt	LDLA	199	15	49935033	49940849	ENSOARG00000003896	ENSOART00000004236	LAMTOR1	late endosomal/lysosomal adaptor, MAPK and MTOR activator 1
IgAt	LDLA	200	15	52019118	52020267	ENSOARG00000010038	ENSOART00000010925	LIPT2	lipoyl(octanoyl) transferase 2 (putative)
IgAt	LDLA	201	15	49943475	49948591	ENSOARG00000003996	ENSOART00000004342	LRTOMT	leucine rich transmembrane and O-methyltransferase domain containing
IgAt	LDLA	202	15	52946965	53027884	ENSOARG00000011875	ENSOART00000012914	MAP6	microtubule-associated protein 6
IgAt	LDLA	203	15	51467260	51518202	ENSOARG00000008118	ENSOART00000008838	MRPL48	mitochondrial ribosomal protein L48
IgAt	LDLA	204	15	52451841	52460215	ENSOARG00000010892	ENSOART00000011843	NEU3	sialidase 3 (membrane sialidase)
IgAt	LDLA	205	15	49845465	49883384	ENSOARG00000003626	ENSOART00000003937	NUMA1	nuclear mitotic apparatus protein 1
IgAt	LDLA	206	15	49563016	49637870	ENSOARG00000002200	ENSOART00000002376	NUP98	nucleoporin 98kDa
IgAt	LDLA	207	15	48416675	48417622	ENSOARG00000006344	ENSOART00000006896	OR51A7	olfactory receptor, family 51, subfamily A, member 7
IgAt	LDLA	208	15	47491871	47492806	ENSOARG00000007355	ENSOART00000008001	OR51B4	olfactory receptor, family 51, subfamily B, member 4
IgAt	LDLA	209	15	48804671	48805642	ENSOARG00000006555	ENSOART00000007124	OR51D1	olfactory receptor, family 51, subfamily D, member 1
IgAt	LDLA	210	15	48790046	48790999	ENSOARG00000006540	ENSOART00000007106	OR51E1	olfactory receptor, family 51, subfamily E, member 1
IgAt	LDLA	211	15	48725682	48726644	ENSOARG00000006524	ENSOART00000007089	OR51E2	olfactory receptor, family 51, subfamily E, member 2
IgAt	LDLA	212	15	48411559	48412500	ENSOARG00000006330	ENSOART00000006882	OR51G2	olfactory receptor, family 51, subfamily G, member 2
IgAt	LDLA	213	15	47333753	47334697	ENSOARG00000007265	ENSOART00000007900	OR51I1	olfactory receptor, family 51, subfamily I, member 1
IgAt	LDLA	214	15	47302405	47303343	ENSOARG00000007248	ENSOART00000007885	OR51I2	olfactory receptor, family 51, subfamily I, member 2
IgAt	LDLA	215	15	48342054	48343001	ENSOARG00000006263	ENSOART00000006809	OR51L1	olfactory receptor, family 51, subfamily L, member 1
IgAt	LDLA	216	15	47345482	47346441	ENSOARG00000007279	ENSOART00000007912	OR51Q1	olfactory receptor, family 51, subfamily Q, member 1 (gene/pseudogene)
IgAt	LDLA	217	15	48505514	48506482	ENSOARG00000006403	ENSOART00000006962	OR51S1	olfactory receptor, family 51, subfamily S, member 1
IgAt	LDLA	218	15	48449703	48450686	ENSOARG00000006363	ENSOART00000006918	OR51T1	olfactory receptor, family 51, subfamily T, member 1
IgAt	LDLA	219	15	47619831	47620793	ENSOARG00000007372	ENSOART00000008024	OR51V1	olfactory receptor, family 51, subfamily V, member 1
IgAt	LDLA	220	15	47239828	47240784	ENSOARG00000007204	ENSOART00000007835	OR52D1	olfactory receptor, family 52, subfamily D, member 1
IgAt	LDLA	221	15	48276005	48276964	ENSOARG00000006204	ENSOART00000006743	OR52E2	olfactory receptor, family 52, subfamily E, member 2
IgAt	LDLA	222	15	47176754	47177710	ENSOARG00000007165	ENSOART00000007793	OR52H1	olfactory receptor, family 52, subfamily H, member 1
IgAt	LDLA	223	15	48300654	48301589	ENSOARG00000006217	ENSOART00000006761	OR52J3	olfactory receptor, family 52, subfamily J, member 3
IgAt	LDLA	224	15	48886844	48889584	ENSOARG00000000931	ENSOART00000000996	OR52K2	olfactory receptor, family 52, subfamily K, member 2
IgAt	LDLA	225	15	48961624	48962577	ENSOARG00000006597	ENSOART00000007166	OR52M1	olfactory receptor, family 52, subfamily M, member 1
IgAt	LDLA	226	15	47632476	47633426	ENSOARG00000007386	ENSOART00000008040	OR52Z1	olfactory receptor, family 52, subfamily Z, member 1 (gene/pseudogene)
IgAt	LDLA	227	15	50987484	50988470	ENSOARG00000006714	ENSOART00000007297	P2RY6	pyrimidinergic receptor P2Y, G-protein coupled, 6
IgAt	LDLA	228	15	51819063	51859671	ENSOARG00000009683	ENSOART00000010542	P4HA3	prolyl 4-hydroxylase, alpha polypeptide III
IgAt	LDLA	229	15	51529688	51572161	ENSOARG00000008267	ENSOART00000008993	PAAF1	proteasomal ATPase-associated factor 1
IgAt	LDLA	230	15	50339073	50372682	ENSOARG00000005656	ENSOART00000006165	PDE2A	phosphodiesterase 2A, cGMP-stimulated
IgAt	LDLA	231	15	49530351	49543249	ENSOARG00000001794	ENSOART00000001934	PGAP2	post-GPI attachment to proteins 2
IgAt	LDLA	232	15	51885345	51940213	ENSOARG00000009895	ENSOART00000010773	PGM2L1	phosphoglucomutase 2-like 1
IgAt	LDLA	233	15	51318743	51332717	ENSOARG00000007849	ENSOART00000008545	PLEKHB1	pleckstrin homology domain containing, family B (evectins) member 1
IgAt	LDLA	234	15	52087791	52130016	ENSOARG00000010224	ENSOART00000011126	POLD3	polymerase (DNA-directed), delta 3, accessory subunit
IgAt	LDLA	235	15	51779562	51807897	ENSOARG00000009512	ENSOART00000010361	PPME1	protein phosphatase methylesterase 1
IgAt	LDLA	236	15	51349344	51430404	ENSOARG00000007994	ENSOART00000008700	RAB6A	Uncharacterized protein
IgAt	LDLA	237	15	51071739	51077198	ENSOARG00000007675	ENSOART00000008351	RELT	RELT tumor necrosis factor receptor
IgAt	LDLA	238	15	49756097	49841502	ENSOARG00000003290	ENSOART00000003568	RNF121	ring finger protein 121
IgAt	LDLA	239	15	52279215	52330446	ENSOARG00000010584	ENSOART00000011516	RNF169	ring finger protein 169
IgAt	LDLA	240	15	52780811	52785187	ENSOARG00000011523	ENSOART00000012531	RPS3	ribosomal protein S3
IgAt	LDLA	241	15	49271309	49310125	ENSOARG00000001301	ENSOART00000001400	RRM1	ribonucleotide reductase M1
IgAt	LDLA	242	15	33797432	33823095	ENSOARG00000000681	ENSOART00000000729	SCN3B	sodium channel, voltage gated, type III beta subunit
IgAt	LDLA	243	15	52925655	52931691	ENSOARG00000011824	ENSOART00000012858	SERPINH1	serpin peptidase inhibitor, clade H (heat shock protein 47), member 1, (collagen binding protein 1)
IgAt	LDLA	244	15	52572569	52609330	ENSOARG00000011065	ENSOART00000012037	SLCO2B1	solute carrier organic anion transporter family, member 2B1
IgAt	LDLA	245	15	52404788	52431105	ENSOARG00000010824	ENSOART00000011772	SPCS2	signal peptidase complex subunit 2 homolog (S. cerevisiae)
IgAt	LDLA	246	15	49313828	49506183	ENSOARG00000001632	ENSOART00000001760	STIM1	stromal interaction molecule 1
IgAt	LDLA	247	15	52650458	52651037	ENSOARG00000011251	ENSOART00000012231	TPBGL	trophoblast glycoprotein-like
IgAt	LDLA	248	15	49090555	49100148	ENSOARG00000000944	ENSOART00000001014	TRIM21	tripartite motif containing 21
IgAt	LDLA	249	15	47072080	47086837	ENSOARG00000019099	ENSOART00000020795	TRIM34	Uncharacterized protein
IgAt	LDLA	250	15	48828042	48836776	ENSOARG00000000818	ENSOART00000000876	TRIM68	tripartite motif containing 68
IgAt	LDLA	251	15	47204309	47206468	ENSOARG00000019107	ENSOART00000020804	UBQLN3	ubiquilin 3
IgAt	LDLA	252	15	47197868	47199664	ENSOARG00000007189	ENSOART00000007818	UBQLNL	ubiquilin-like
IgAt	LDLA	253	15	51596036	51598758	ENSOARG00000008561	ENSOART00000009316	UCP2	uncoupling protein 2 (mitochondrial, proton carrier)
IgAt	LDLA	254	15	51622789	51628720	ENSOARG00000008669	ENSOART00000009437	UCP3	uncoupling protein 3 (mitochondrial, proton carrier)
IgAt	LDLA	255	15	52338085	52397903	ENSOARG00000010713	ENSOART00000011662	XRRA1	X-ray radiation resistance associated 1
IgAt	LDLA	256	15	33877224	33882399	ENSOARG00000000770	ENSOART00000000821	ZNF202	zinc finger protein 202
IgAt	LDLA	257	16	10390597	10411746	ENSOARG00000005689	ENSOART00000006197	CCDC125	coiled-coil domain containing 125
IgAt	LDLA	258	16	10486355	10496192	ENSOARG00000005759	ENSOART00000006271	CCNB1	Uncharacterized protein
IgAt	LDLA	259	16	10416374	10438718	ENSOARG00000005719	ENSOART00000006224	CDK7	cyclin-dependent kinase 7
IgAt	LDLA	260	16	10462746	10479624	ENSOARG00000005750	ENSOART00000006259	CENPH	centromere protein H
IgAt	LDLA	261	16	10300925	10319662	ENSOARG00000005589	ENSOART00000006089	MARVELD2	MARVEL domain containing 2
IgAt	LDLA	262	16	10446629	10454736	ENSOARG00000005743	ENSOART00000006253	MRPS36	mitochondrial ribosomal protein S36
IgAt	LDLA	263	16	10325639	10360979	ENSOARG00000005629	ENSOART00000006137	RAD17	RAD17 homolog (S. pombe)
IgAt	LDLA	264	16	63481796	64032598	ENSOARG00000014361	ENSOART00000015644	SEMA5A	sema domain, seven thrombospondin repeats (type 1 and type 1-like), (semaphorin) 5A
IgAt	LDLA	265	16	10511755	10544659	ENSOARG00000005799	ENSOART00000006324	SLC30A5	solute carrier family 30 (zinc transporter), member 5
IgAt	LDLA	266	17	63507291	63604351	ENSOARG00000016430	ENSOART00000017905	ACACB	acetyl-CoA carboxylase beta
IgAt	LDLA	267	17	62600483	62620320	ENSOARG00000013118	ENSOART00000014260	ACADS	acyl-CoA dehydrogenase, C-2 to C-3 short chain
IgAt	LDLA	268	17	65098471	65205105	ENSOARG00000019041	ENSOART00000020733	ADRBK2	adrenergic, beta, receptor kinase 2
IgAt	LDLA	269	17	63655089	63659427	ENSOARG00000016925	ENSOART00000018435	ALKBH2	alkB, alkylation repair homolog 2 (E. coli)
IgAt	LDLA	270	17	62909832	62942889	ENSOARG00000014141	ENSOART00000015401	ANKRD13A	ankyrin repeat domain 13A
IgAt	LDLA	271	17	65805012	65811692	ENSOARG00000000763	ENSOART00000000817	ASPHD2	aspartate beta-hydroxylase domain containing 2
IgAt	LDLA	272	17	62824626	62840416	ENSOARG00000013872	ENSOART00000015097	C12orf43	chromosome 12 open reading frame 43
IgAt	LDLA	273	17	62023701	62101919	ENSOARG00000010904	ENSOART00000011860	CCDC64	coiled-coil domain containing 64
IgAt	LDLA	274	17	18236205	18254301	ENSOARG00000014103	ENSOART00000015357	CCRN4L	CCR4 carbon catabolite repression 4-like (S. cerevisiae)
IgAt	LDLA	275	17	16966513	16999276	ENSOARG00000012717	ENSOART00000013828	CLGN	calmegin
IgAt	LDLA	276	17	64260293	64261387	ENSOARG00000004783	ENSOART00000005209	CMKLR1	chemerin chemokine-like receptor 1
IgAt	LDLA	277	17	62429493	62443897	ENSOARG00000012543	ENSOART00000013636	COQ5	coenzyme Q5 homolog, methyltransferase (S. cerevisiae)
IgAt	LDLA	278	17	63912171	63962877	ENSOARG00000017927	ENSOART00000019511	CORO1C	coronin, actin binding protein, 1C
IgAt	LDLA	279	17	62376933	62378639	ENSOARG00000012290	ENSOART00000013360	COX6A1	cytochrome c oxidase subunit VIa polypeptide 1
IgAt	LDLA	280	17	65972472	65978843	ENSOARG00000001670	ENSOART00000001798	CRYBA4	crystallin, beta A4
IgAt	LDLA	281	17	65956703	65967094	ENSOARG00000001548	ENSOART00000001666	CRYBB1	crystallin, beta B1
IgAt	LDLA	282	17	65012599	65021704	ENSOARG00000019007	ENSOART00000020693	CRYBB2	crystallin, beta B2
IgAt	LDLA	283	17	64996177	65001296	ENSOARG00000018985	ENSOART00000020670	CRYBB3	crystallin, beta B3
IgAt	LDLA	284	17	63767928	63780377	ENSOARG00000017453	ENSOART00000019000	DAO	D-amino-acid oxidase
IgAt	LDLA	285	17	62424499	62426333	ENSOARG00000012429	ENSOART00000013515	DYNLL1	Uncharacterized protein
IgAt	LDLA	286	17	18131831	18226233	ENSOARG00000014035	ENSOART00000015281	ELF2	E74-like factor 2 (ets domain transcription factor)
IgAt	LDLA	287	17	16744037	16884192	ENSOARG00000012281	ENSOART00000013353	ELMOD2	ELMO/CED-12 domain containing 2
IgAt	LDLA	288	17	23881424	23883024	ENSOARG00000014480	ENSOART00000015763	ENO1	enolase 1, (alpha)
IgAt	LDLA	289	17	63105994	63163957	ENSOARG00000014797	ENSOART00000016104	FAM222A	family with sequence similarity 222, member A
IgAt	LDLA	290	17	64084833	64087190	ENSOARG00000018146	ENSOART00000019748	FICD	FIC domain containing
IgAt	LDLA	291	17	63478577	63502074	ENSOARG00000016041	ENSOART00000017471	FOXN4	forkhead box N4
IgAt	LDLA	292	17	35976685	36901504	ENSOARG00000001443	ENSOART00000001546	FSTL5	follistatin-like 5
IgAt	LDLA	293	17	62381913	62389005	ENSOARG00000012338	ENSOART00000013413	GATC	Glutamyl-tRNA(Gln) amidotransferase subunit C, mitochondrial
IgAt	LDLA	294	17	62131393	62180589	ENSOARG00000011301	ENSOART00000012307	GCN1L1	GCN1 general control of amino-acid synthesis 1-like 1 (yeast)
IgAt	LDLA	295	17	62946588	62984945	ENSOARG00000014274	ENSOART00000015549	GIT2	G protein-coupled receptor kinase interacting ArfGAP 2

IgAt	LDLA	296	17	63029293	63041337	ENSOARG00000014443	ENSOART00000015729	GLTP	glycolipid transfer protein
IgAt	LDLA	297	17	62806213	62822635	ENSOARG00000013764	ENSOART00000014999	HNF1A	HNF1 homeobox A
IgAt	LDLA	298	17	65819871	65842502	ENSOARG00000000840	ENSOART00000000903	HPS4	Hermansky-Pudlak syndrome 4
IgAt	LDLA	299	17	29574871	29626707	ENSOARG00000015941	ENSOART00000017363	HSPA4L	heat shock 70kDa protein 4-like
IgAt	LDLA	300	17	15757663	15773243	ENSOARG00000012119	ENSOART00000013183	IL15	interleukin 15
IgAt	LDLA	301	17	15088639	15543935	ENSOARG00000011798	ENSOART00000012835	INPP4B	inositol polyphosphate-4-phosphatase, type II, 105kDa
IgAt	LDLA	302	17	29666962	29744135	ENSOARG00000016297	ENSOART00000017750	INTU	inturned planar cell polarity protein
IgAt	LDLA	303	17	64035323	64040929	ENSOARG00000018011	ENSOART00000019602	ISCU	iron-sulfur cluster assembly enzyme
IgAt	LDLA	304	17	63356340	63376670	ENSOARG00000015859	ENSOART00000017269	KCTD10	potassium channel tetramerization domain containing 10
IgAt	LDLA	305	17	64862406	64986780	ENSOARG00000018865	ENSOART00000020546	KIAA1671	KIAA1671
IgAt	LDLA	306	17	29304822	29427883	ENSOARG00000015300	ENSOART00000016652	LARP1B	La ribonucleoprotein domain family, member 1B
IgAt	LDLA	307	17	17510865	17690533	ENSOARG00000012912	ENSOART00000014033	MAML3	mastermind-like 3 (Drosophila)
IgAt	LDLA	308	17	29495745	29535347	ENSOARG00000015603	ENSOART00000016976	MFSD8	major facilitator superfamily domain containing 8
IgAt	LDLA	309	17	18057614	18082600	ENSOARG00000013893	ENSOART00000015122	MGARP	mitochondria-localized glutamic acid-rich protein
IgAt	LDLA	310	17	17697870	17732659	ENSOARG00000012987	ENSOART00000014117	MGST2	microsomal glutathione S-transferase 2
IgAt	LDLA	311	17	62571900	62575203	ENSOARG00000012941	ENSOART00000014064	MLEC	malectin
IgAt	LDLA	312	17	63274140	63284973	ENSOARG00000014942	ENSOART00000016269	MMAB	methylmalonic aciduria (cobalamin deficiency) cblB type
IgAt	LDLA	313	17	66892378	66937043	ENSOARG00000001775	ENSOART00000001912	MN1	meningioma (disrupted in balanced translocation) 1
IgAt	LDLA	314	17	62296759	62318827	ENSOARG00000012097	ENSOART00000013158	MSI1	musashi RNA-binding protein 1
IgAt	LDLA	315	17	63256007	63274002	ENSOARG00000014824	ENSOART00000016135	MVK	mevalonate kinase
IgAt	LDLA	316	17	65228017	65452813	ENSOARG00000019120	ENSOART00000020825	MYO18B	myosin XVIIIB
IgAt	LDLA	317	17	63380145	63420305	ENSOARG00000015998	ENSOART00000017422	MYO1H	myosin IH
IgAt	LDLA	318	17	17979311	18024296	ENSOARG00000013690	ENSOART00000014901	NAA15	N(alpha)-acetyltransferase 15, NatA auxiliary subunit
IgAt	LDLA	319	17	62841883	62857788	ENSOARG00000013935	ENSOART00000015176	OASL	2-5-oligoadenylate synthetase-like
IgAt	LDLA	320	17	24852357	24866018	ENSOARG00000014523	ENSOART00000015811	PCDH10	protocadherin 10
IgAt	LDLA	321	17	19959248	19972315	ENSOARG00000014358	ENSOART00000015633	PCDH18	protocadherin 18
IgAt	LDLA	322	17	29240707	29257289	ENSOARG00000015225	ENSOART00000016567	PGRMC2	progesterone receptor membrane component 2
IgAt	LDLA	323	17	64675822	64699663	ENSOARG00000018486	ENSOART00000020126	PIWIL3	piwi-like RNA-mediated gene silencing 3
IgAt	LDLA	324	17	62282828	62288877	ENSOARG00000012036	ENSOART00000013090	PLA2G1B	phospholipase A2, group IB (pancreas)
IgAt	LDLA	325	17	29540625	29557094	ENSOARG00000015691	ENSOART00000017078	PLK4	polo-like kinase 4
IgAt	LDLA	326	17	62481545	62485399	ENSOARG00000012764	ENSOART00000013877	POP5	processing of precursor 5, ribonuclease P/MRP subunit (S. cerevisiae)
IgAt	LDLA	327	17	62195843	62212283	ENSOARG00000011850	ENSOART00000012893	PXN	paxillin
IgAt	LDLA	328	17	17920232	17936231	ENSOARG00000013460	ENSOART00000014643	RAB33B	RAB33B, member RAS oncogene family
IgAt	LDLA	329	17	62105682	62115444	ENSOARG00000011008	ENSOART00000011974	RAB35	RAB35, member RAS oncogene family
IgAt	LDLA	330	17	46229193	46308820	ENSOARG00000015746	ENSOART00000017146	RIMBP2	RIMS binding protein 2
IgAt	LDLA	331	17	62447047	62480968	ENSOARG00000012664	ENSOART00000013770	RNF10	ring finger protein 10
IgAt	LDLA	332	17	16327634	16604337	ENSOARG00000012236	ENSOART00000013306	RNF150	ring finger protein 150
IgAt	LDLA	333	17	62187055	62190676	ENSOARG00000011805	ENSOART00000012838	RPLP0	Uncharacterized protein
IgAt	LDLA	334	17	64042329	64081333	ENSOARG00000018082	ENSOART00000019681	SART3	squamous cell carcinoma antigen recognized by T cells 3
IgAt	LDLA	335	17	28468259	28717332	ENSOARG00000014865	ENSOART00000016177	SCLT1	sodium channel and clathrin linker 1
IgAt	LDLA	336	17	17831130	17877926	ENSOARG00000013062	ENSOART00000014199	SETD7	SET domain containing (lysine methyltransferase) 7
IgAt	LDLA	337	17	65698820	65765918	ENSOARG00000000375	ENSOART00000000404	SEZ6L	seizure related 6 homolog (mouse)-like
IgAt	LDLA	338	17	28832970	28833446	ENSOARG00000015149	ENSOART00000016486	SFT2D1	SFT2 domain containing 1
IgAt	LDLA	339	17	64740260	64788309	ENSOARG00000018712	ENSOART00000020369	SGSM1	small G protein signaling modulator 1
IgAt	LDLA	340	17	62257767	62270431	ENSOARG00000011987	ENSOART00000013037	SIRT4	sirtuin 4
IgAt	LDLA	341	17	29631331	29661343	ENSOARG00000016119	ENSOART00000017556	SLC25A31	solute carrier family 25 (mitochondrial carrier; adenine nucleotide translocator), member 31
IgAt	LDLA	342	17	19076299	19158878	ENSOARG00000014253	ENSOART00000015529	SLC7A11	solute carrier family 7 (anionic amino acid transporter light chain, xc- system), member 11
IgAt	LDLA	343	17	62657585	62693241	ENSOARG00000013244	ENSOART00000014399	SPPL3	signal peptide peptidase like 3
IgAt	LDLA	344	17	65844067	65863994	ENSOARG00000001087	ENSOART00000001165	SRRD	SRR1 domain containing
IgAt	LDLA	345	17	62390592	62396924	ENSOARG00000012402	ENSOART00000013479	SRSF9	serine/arginine-rich splicing factor 9
IgAt	LDLA	346	17	63821891	63850180	ENSOARG00000017568	ENSOART00000019280	SSH1	slingshot protein phosphatase 1
IgAt	LDLA	347	17	45920664	45945399	ENSOARG00000015506	ENSOART00000016871	STX2	syntaxin 2
IgAt	LDLA	348	17	63694449	63761537	ENSOARG00000017213	ENSOART00000018734	SVOP	SV2 related protein homolog (rat)
IgAt	LDLA	349	17	16757769	16823818	ENSOARG00000012380	ENSOART00000013459	TBC1D9	TBC1 domain family, member 9 (with GRAM domain)
IgAt	LDLA	350	17	62993132	63004909	ENSOARG00000014399	ENSOART00000015677	TCHP	trichoplein, keratin filament binding
IgAt	LDLA	351	17	65864105	65877487	ENSOARG00000001236	ENSOART00000001326	TFIP11	tuftelin interacting protein 11
IgAt	LDLA	352	17	64011490	64012534	ENSOARG00000017992	ENSOART00000019582	TMEM119	transmembrane protein 119
IgAt	LDLA	353	17	64794593	64800175	ENSOARG00000018818	ENSOART00000020493	TMEM211	transmembrane protein 211
IgAt	LDLA	354	17	65890278	65906516	ENSOARG00000001489	ENSOART00000001596	TPST2	tyrosylprotein sulfotransferase 2
IgAt	LDLA	355	17	62380594	62381944	ENSOARG00000012315	ENSOART00000013387	TRIAP1	TP53 regulated inhibitor of apoptosis 1
IgAt	LDLA	356	17	63068250	63091201	ENSOARG00000014606	ENSOART00000015907	TRPV4	transient receptor potential cation channel, subfamily V, member 4
IgAt	LDLA	357	17	63296464	63339874	ENSOARG00000015640	ENSOART00000017025	UBE3B	ubiquitin protein ligase E3B
IgAt	LDLA	358	17	16847682	16853677	ENSOARG00000012510	ENSOART00000013603	UCP1	mitochondrial uncoupling protein
IgAt	LDLA	359	17	62589771	62594971	ENSOARG00000013039	ENSOART00000014177	UNC119B	unc-119 homolog B (C. elegans)
IgAt	LDLA	360	17	63642936	63652821	ENSOARG00000016873	ENSOART00000018376	UNG	uracil-DNA glycosylase
IgAt	LDLA	361	17	63661804	63683290	ENSOARG00000017038	ENSOART00000018554	USP30	ubiquitin specific peptidase 30
IgAt	LDLA	362	17	64287170	64403969	ENSOARG00000018227	ENSOART00000019834	WSCD2	WSC domain containing 2
IgAt	LDLA	363	17	16219661	16240107	ENSOARG00000012172	ENSOART00000013238	ZNF330	zinc finger protein 330
IgAt	LDLA	364	21	17334948	17360878	ENSOARG00000006601	ENSOART00000007175	ALG8	ALG8, alpha-1,3-glucosyltransferase
IgAt	LDLA	365	21	46224390	46229122	ENSOARG00000017559	ENSOART00000019108	FGF19	fibroblast growth factor 19
IgAt	LDLA	366	21	17151857	17207840	ENSOARG00000006340	ENSOART00000006895	GAB2	Uncharacterized protein
IgAt	LDLA	367	21	17425508	17537448	ENSOARG00000006741	ENSOART00000007331	INTS4	integrator complex subunit 4
IgAt	LDLA	368	21	17410324	17411025	ENSOARG00000015282	ENSOART00000016630	KCTD14	potassium channel tetramerization domain containing 14
IgAt	LDLA	369	21	17274681	17286572	ENSOARG00000006482	ENSOART00000007045	KCTD21	potassium channel tetramerization domain containing 21
IgAt	LDLA	370	21	16876069	17007819	ENSOARG00000006276	ENSOART00000006830	NARS2	asparaginyl-tRNA synthetase 2, mitochondrial (putative)
IgAt	LDLA	371	21	17367736	17375692	ENSOARG00000006694	ENSOART00000007275	NDUFC2	Uncharacterized protein
IgAt	LDLA	372	21	46197149	46203858	ENSOARG00000017515	ENSOART00000019065	ORAOV1	oral cancer overexpressed 1
IgAt	LDLA	373	21	17381192	17381644	ENSOARG00000015271	ENSOART00000016620	THRSP	thyroid hormone responsive
IgAt	LDLA	374	21	17213027	17266909	ENSOARG00000006396	ENSOART00000006955	USP35	ubiquitin specific peptidase 35
IgAt	LA	375	22	337191	347902	ENSOARG00000012940	ENSOART00000014061	CISD1	CDGSH iron sulfur domain 1
IgAt	LDLA	376	22	19523139	19589460	ENSOARG00000012252	ENSOART00000013325	CNNM1	cyclin and CBS domain divalent metal cation transport mediator 1
IgAt	LDLA	377	22	19850565	19864556	ENSOARG00000012685	ENSOART00000013793	COX15	cytochrome c oxidase assembly homolog 15 (yeast)
IgAt	LDLA	378	22	6660975	6667735	ENSOARG00000013619	ENSOART00000014817	DKK1	dickkopf WNT signaling pathway inhibitor 1
IgAt	LDLA	379	22	19807494	19841422	ENSOARG00000012580	ENSOART00000013680	ENTPD7	ectonucleoside triphosphate diphosphohydrolase 7
IgAt	LDLA	380	22	19598844	19759436	ENSOARG00000012426	ENSOART00000013513	GOT1	glutamic-oxaloacetic transaminase 1, soluble
IgAt	LA	381	22	356761	406918	ENSOARG00000012946	ENSOART00000014072	IPMK	inositol polyphosphate multikinase
IgAt	LDLA	382	22	6177045	6182234	ENSOARG00000013530	ENSOART00000014710	MBL2	mannose-binding lectin (protein C) 2, soluble
IgAt	LDLA	383	22	19711068	19713446	ENSOARG00000012498	ENSOART00000013589	NKX2-3	NK2 homeobox 3
IgAt	LDLA	384	22	4372641	5337209	ENSOARG00000013216	ENSOART00000014373	PCDH15	protocadherin-related 15
IgAt	LA	384	22	4372641	5337209	ENSOARG00000013216	ENSOART00000014373	PCDH15	protocadherin-related 15
IgAt	LDLA	385	22	6721273	7267215	ENSOARG00000013625	ENSOART00000014821	PRKG1	protein kinase, cGMP-dependent, type I
IgAt	LDLA	386	22	19775783	19785965	ENSOARG00000012526	ENSOART00000013620	SLC25A28	solute carrier family 25 (mitochondrial iron transporter), member 28
IgAt	LA	387	22	1722301	1722609	ENSOARG00000013042	ENSOART00000014176	SUMO1	small ubiquitin-like modifier 1
IgAt	LDLA	388	22	5810013	5825986	ENSOARG00000013447	ENSOART00000014630	SYCE1	synaptonemal complex central element protein 1
IgAt	LA	389	22	3348127	3348402	ENSOARG00000014747	ENSOART00000016048	UQCRH	cytochrome b-c1 complex subunit 6, mitochondrial
IgAt	LA	390	22	2527743	2531318	ENSOARG00000013084	ENSOART00000014221	ZWINT	ZW10 interacting kinetochore protein
IgAt	LDLA	391	23	34855193	34912259	ENSOARG00000008434	ENSOART00000009182	ABHD3	abhydrolase domain containing 3
IgAt	LDLA	392	23	36069916	36074988	ENSOARG00000009539	ENSOART00000010387	ADCYAP1	adenylate cyclase activating polypeptide 1 (pituitary)
IgAt	LDLA	393	23	43176401	43194125	ENSOARG00000001770	ENSOART00000001908	AFG3L2	AFG3-like AAA ATPase 2
IgAt	LDLA	394	23	41790781	41886203	ENSOARG00000000971	ENSOART00000001042	ANKRD12	ankyrin repeat domain 12

IgAt	LDLA	395	23	33275725	33329932	ENSOARG00000007830	ENSOART00000008530	ANKRD29	ankyrin repeat domain 29
IgAt	LDLA	396	23	42479408	42510105	ENSOARG00000001340	ENSOART00000001442	APCDD1	adenomatosis polyposis coli down-regulated 1
IgAt	LDLA	397	23	23718712	23881329	ENSOARG00000005872	ENSOART00000006391	ASXL3	additional sex combs like transcriptional regulator 3
IgAt	**LDLA**	**398**	**23**	**46071788**	**46080230**	**ENSOARG00000002910**	**ENSOART00000003158**	**ATP5A1**	**ATP synthase, H+ transporting, mitochondrial F1 complex, alpha subunit 1, cardiac muscle**
IgAt	LDLA	399	23	25753012	25820202	ENSOARG00000006302	ENSOART00000006855	B4GALT6	UDP-Gal:betaGlcNAc beta 1,4- galactosyltransferase, polypeptide 6
IgAt	LDLA	400	23	46179200	46222552	ENSOARG00000003069	ENSOART00000003328	C18orf25	chromosome 18 open reading frame 25
IgAt	LDLA	401	23	33388694	33409862	ENSOARG00000007938	ENSOART00000008642	C18orf8	chromosome 18 open reading frame 8
IgAt	LDLA	402	23	33601173	33702730	ENSOARG00000008157	ENSOART00000008876	CABLES1	Cdk5 and Abl enzyme substrate 1
IgAt	LDLA	403	23	43395030	43409914	ENSOARG00000001861	ENSOART00000002000	CEP76	centrosomal protein 76kDa
IgAt	LDLA	404	23	35812588	35813106	ENSOARG00000003899	ENSOART00000004237	CETN1	centrin, EF-hand protein, 1
IgAt	**LDLA**	**405**	**23**	**43145365**	**43155613**	**ENSOARG00000001731**	**ENSOART00000001860**	**CIDEA**	**cell death-inducing DFFA-like effector a**
IgAt	LDLA	406	23	35841446	35870572	ENSOARG00000009352	ENSOART00000010180	CLUL1	clusterin-like 1 (retinal)
IgAt	**LDLA**	**407**	**23**	**35558221**	**35884837**	**ENSOARG00000009301**	**ENSOART00000010122**	**COLEC12**	**collectin sub-family member 12**
IgAt	LDLA	408	23	48396771	48716864	ENSOARG00000003754	ENSOART00000004083	CTIF	CBP80/20-dependent translation initiation factor
IgAt	LDLA	409	23	37913347	38214262	ENSOARG00000010437	ENSOART00000011360	DLGAP1	discs, large (Drosophila) homolog-associated protein 1
IgAt	**LDLA**	**410**	**23**	**26264806**	**26297753**	**ENSOARG00000006732**	**ENSOART00000007324**	**DSC1**	**desmocollin 1**
IgAt	**LDLA**	**411**	**23**	**26317548**	**26353280**	**ENSOARG00000006798**	**ENSOART00000007396**	**DSC2**	**desmocollin 2**
IgAt	**LDLA**	**412**	**23**	**26380250**	**26427620**	**ENSOARG00000006831**	**ENSOART00000007432**	**DSC3**	**desmocollin 3**
IgAt	**LDLA**	**413**	**23**	**26078308**	**26118372**	**ENSOARG00000006551**	**ENSOART00000007125**	**DSG1**	**desmoglein 1**
IgAt	**LDLA**	**414**	**23**	**25896411**	**25927113**	**ENSOARG00000006399**	**ENSOART00000006960**	**DSG2**	**desmoglein 2**
IgAt	**LDLA**	**415**	**23**	**25963537**	**25996637**	**ENSOARG00000006471**	**ENSOART00000007033**	**DSG3**	**desmoglein 3**
IgAt	**LDLA**	**416**	**23**	**26023321**	**26063151**	**ENSOARG00000006534**	**ENSOART00000007103**	**DSG4**	**desmoglein 4**
IgAt	**LDLA**	**417**	**23**	**37418880**	**37475839**	**ENSOARG00000009973**	**ENSOART00000010852**	**EMILIN2**	**elastin microfibril interfacer 2**
IgAt	LDLA	418	23	35889808	35911948	ENSOARG00000009421	ENSOART00000010260	ENOSF1	enolase superfamily member 1
IgAt	LDLA	419	23	45805752	45934686	ENSOARG00000002588	ENSOART00000002826	EPG5	ectopic P-granules autophagy protein 5 homolog (C. elegans)
IgAt	LDLA	420	23	34944301	34972117	ENSOARG00000008455	ENSOART00000009205	ESCO1	establishment of sister chromatid cohesion N-acetyltransferase 1
IgAt	LDLA	421	23	43811482	43818147	ENSOARG00000002183	ENSOART00000002357	FAM210A	family with sequence similarity 210, member A
IgAt	**LDLA**	**422**	**23**	**34474491**	**34503247**	**ENSOARG00000008269**	**ENSOART00000008996**	**GATA6**	**GATA binding protein 6**
IgAt	LDLA	423	23	43042712	43087998	ENSOARG00000001613	ENSOART00000001742	GNAL	guanine nucleotide binding protein (G protein), alpha activating activity polypeptide, olfactory type
IgAt	LDLA	424	23	34979403	35099472	ENSOARG00000008539	ENSOART00000009303	GREB1L	growth regulation by estrogen in breast cancer-like
IgAt	LDLA	425	23	46084041	46095990	ENSOARG00000002975	ENSOART00000003229	HAUS1	HAUS augmin-like complex, subunit 1
IgAt	LDLA	426	23	46984295	47014837	ENSOARG00000003542	ENSOART00000003846	HDHD2	haloacid dehalogenase-like hydrolase domain containing 2
IgAt	LDLA	427	23	43125780	43137181	ENSOARG00000001725	ENSOART00000001854	IMPA2	inositol(myo)-1(or 4)-monophosphatase 2
IgAt	LDLA	428	23	46874987	46976330	ENSOARG00000003483	ENSOART00000003789	KATNAL2	katanin p60 subunit A-like 2
IgAt	LDLA	429	23	24667797	24780463	ENSOARG00000006008	ENSOART00000006529	KLHL14	kelch-like family member 14
IgAt	**LDLA**	**430**	**23**	**32998185**	**33254634**	**ENSOARG00000007694**	**ENSOART00000008393**	**LAMA3**	**laminin, alpha 3**
IgAt	LDLA	431	23	46410617	46609939	ENSOARG00000003204	ENSOART00000003492	LOXHD1	lipoxygenase homology domains 1
IgAt	LDLA	432	23	37477515	37512676	ENSOARG00000010081	ENSOART00000010970	LPIN2	lipin 2
IgAt	LDLA	433	23	43893855	43894748	ENSOARG00000003950	ENSOART00000004291	MC2R	melanocortin 2 receptor (adrenocorticotropic hormone)
IgAt	LDLA	434	23	43867867	43870160	ENSOARG00000002239	ENSOART00000002416	MC5R	melanocortin 5 receptor
IgAt	LDLA	435	23	25268169	25306368	ENSOARG00000006084	ENSOART00000006624	MEP1B	meprin A, beta
IgAt	LDLA	436	23	37178727	37203415	ENSOARG00000009572	ENSOART00000010421	METTL4	methyltransferase like 4
IgAt	**LDLA**	**437**	**23**	**34731944**	**34929704**	**ENSOARG00000008311**	**ENSOART00000009044**	**MIB1**	**mindbomb E3 ubiquitin protein ligase 1**
IgAt	LDLA	438	23	43090283	43103534	ENSOARG00000001718	ENSOART00000001850	MPPE1	metallophosphoesterase 1
IgAt	LDLA	439	23	35051638	35052513	ENSOARG00000008642	ENSOART00000009408	MRTO4	mRNA turnover 4 homolog (S. cerevisiae)
IgAt	LDLA	440	23	37747768	37751509	ENSOARG00000010362	ENSOART00000011272	MYL12A	myosin, light chain 12A, regulatory, non-sarcomeric
IgAt	LDLA	441	23	37767203	37776271	ENSOARG00000010388	ENSOART00000011302	MYL12B	myosin, light chain 12B, regulatory
IgAt	LDLA	442	23	37599839	37713875	ENSOARG00000010213	ENSOART00000011131	MYOM1	myomesin 1
IgAt	LDLA	443	23	42525801	42536308	ENSOARG00000001378	ENSOART00000001480	NAPG	N-ethylmaleimide-sensitive factor attachment protein, gamma
IgAt	LDLA	444	23	37208585	37244969	ENSOARG00000009604	ENSOART00000010464	NDC80	NDC80 kinetochore complex component
IgAt	LDLA	445	23	41731159	41785983	ENSOARG00000000891	ENSOART00000000954	NDUFV2	NADH dehydrogenase (ubiquinone) flavoprotein 2, 24kDa
IgAt	LDLA	446	23	23148484	23611340	ENSOARG00000005828	ENSOART00000006345	NOL4	nucleolar protein 4
IgAt	**LDLA**	**447**	**23**	**33343432**	**33388189**	**ENSOARG00000007905**	**ENSOART00000008614**	**NPC1**	**Niemann-Pick disease, type C1**
IgAt	**LDLA**	**448**	**23**	**46745988**	**46837187**	**ENSOARG00000003371**	**ENSOART00000003661**	**PIAS2**	**protein inhibitor of activated STAT, 2**
IgAt	LDLA	449	23	42545078	42809294	ENSOARG00000001534	ENSOART00000001649	PIEZO2	piezo-type mechanosensitive ion channel component 2
IgAt	LDLA	450	23	42015205	42044225	ENSOARG00000001168	ENSOART00000001248	PPP4R1	protein phosphatase 4, regulatory subunit 1
IgAt	**LDLA**	**451**	**23**	**43413212**	**43501325**	**ENSOARG00000001894**	**ENSOART00000002036**	**PSMG2**	**proteasome (prosome, macropain) assembly chaperone 2**
IgAt	LDLA	452	23	45957490	46061706	ENSOARG00000002845	ENSOART00000003087	PSTPIP2	proline-serine-threonine phosphatase interacting protein 2
IgAt	LDLA	453	23	43434719	43479972	ENSOARG00000001930	ENSOART00000002076	PTPN2	protein tyrosine phosphatase, non-receptor type 2
IgAt	LDLA	454	23	42170178	42217503	ENSOARG00000001243	ENSOART00000001327	RAB31	RAB31, member RAS oncogene family
IgAt	**LDLA**	**455**	**23**	**41973772**	**41997876**	**ENSOARG00000001077**	**ENSOART00000001156**	**RALBP1**	**ralA binding protein 1**
IgAt	LDLA	456	23	33798224	33854696	ENSOARG00000008223	ENSOART00000008961	RBBP8	Uncharacterized protein
IgAt	LDLA	457	23	33444339	33463467	ENSOARG00000008042	ENSOART00000008761	RIOK3	RIO kinase 3
IgAt	LDLA	458	23	25434659	25456840	ENSOARG00000006128	ENSOART00000006662	RNF125	ring finger protein 125, E3 ubiquitin protein ligase
IgAt	LDLA	459	23	25364704	25379553	ENSOARG00000006124	ENSOART00000006655	RNF138	ring finger protein 138, E3 ubiquitin protein ligase
IgAt	LDLA	460	23	46379585	46396292	ENSOARG00000003090	ENSOART00000003348	RNF165	ring finger protein 165
IgAt	LDLA	461	23	43829595	43854463	ENSOARG00000002195	ENSOART00000002370	RNMT	RNA (guanine-7-) methyltransferase
IgAt	**LDLA**	**462**	**23**	**35320769**	**35444675**	**ENSOARG00000008819**	**ENSOART00000009623**	**ROCK1**	**Rho-associated, coiled-coil containing protein kinase 1**
IgAt	LDLA	463	23	43535985	43629299	ENSOARG00000002062	ENSOART00000002231	SEH1L	SEH1-like (S. cerevisiae)
IgAt	LDLA	464	23	44574257	44959623	ENSOARG00000002282	ENSOART00000002467	SETBP1	SET binding protein 1
IgAt	**LDLA**	**465**	**23**	**45776102**	**45791572**	**ENSOARG00000002432**	**ENSOART00000002637**	**SIGLEC15**	**sialic acid binding Ig-like lectin 15**
IgAt	**LDLA**	**466**	**23**	**47077711**	**47118164**	**ENSOARG00000003607**	**ENSOART00000003918**	**SKOR2**	**SKI family transcriptional corepressor 2**
IgAt	**LDLA**	**467**	**23**	**45678576**	**45696614**	**ENSOARG00000002395**	**ENSOART00000002598**	**SLC14A1**	**solute carrier family 14 (urea transporter), member 1 (Kidd blood group)**
IgAt	LDLA	468	23	45567409	45633026	ENSOARG00000002339	ENSOART00000002537	SLC14A2	solute carrier family 14 (urea transporter), member 2
IgAt	LDLA	469	23	43229143	43232905	ENSOARG00000001798	ENSOART00000001933	SLMO1	slowmo homolog 1 (Drosophila)
IgAt	**LDLA**	**470**	**23**	**47676716**	**47729518**	**ENSOARG00000003654**	**ENSOART00000003969**	**SMAD2**	**SMAD family member 2**
IgAt	LDLA	471	23	37272910	37394196	ENSOARG00000009781	ENSOART00000010661	SMCHD1	structural maintenance of chromosomes flexible hinge domain containing 1
IgAt	LDLA	472	23	43245448	43324893	ENSOARG00000001837	ENSOART00000001976	SPIRE1	spire-type actin nucleation factor 1
IgAt	LDLA	473	23	46633893	46700133	ENSOARG00000003330	ENSOART00000003612	ST8SIA5	ST8 alpha-N-acetyl-neuraminide alpha-2,8-sialyltransferase 5
IgAt	**LDLA**	**474**	**23**	**54803976**	**55181403**	**ENSOARG00000005018**	**ENSOART00000005468**	**TCF4**	**transcription factor 4**
IgAt	LDLA	475	23	37866036	37871728	ENSOARG00000010395	ENSOART00000011310	TGIF1	TGFB-induced factor homeobox 1
IgAt	**LDLA**	**476**	**23**	**35493922**	**35529519**	**ENSOARG00000009238**	**ENSOART00000010068**	**THOC1**	**THO complex 1**
IgAt	LDLA	477	23	33467029	33538937	ENSOARG00000008070	ENSOART00000008784	TMEM241	transmembrane protein 241
IgAt	LDLA	478	23	25545403	25629547	ENSOARG00000006219	ENSOART00000006773	TRAPPC8	trafficking protein particle complex 8
IgAt	LDLA	479	23	32856845	32957059	ENSOARG00000007567	ENSOART00000008240	TTC39C	tetratricopeptide repeat domain 39C
IgAt	LDLA	480	23	25838407	25847665	ENSOARG00000006342	ENSOART00000006897	TTR	transthyretin
IgAt	LDLA	481	23	43167420	43174414	ENSOARG00000001739	ENSOART00000001869	TUBB6	tubulin, beta 6 class V
IgAt	LDLA	482	23	41898884	41914904	ENSOARG00000001037	ENSOART00000001108	TWSG1	twisted gastrulation BMP signaling modulator 1
IgAt	LDLA	483	23	42223951	42226256	ENSOARG00000001256	ENSOART00000001340	TXNDC2	thioredoxin domain containing 2 (spermatozoa)
IgAt	LDLA	484	23	35875779	35888637	ENSOARG00000009367	ENSOART00000010195	TYMS	thymidylate synthetase
IgAt	**LDLA**	**485**	**23**	**35461828**	**35491514**	**ENSOARG00000009076**	**ENSOART00000009884**	**USP14**	**ubiquitin specific peptidase 14 (tRNA-guanine transglycosylase)**
IgAt	LDLA	486	23	42246608	42281610	ENSOARG00000001307	ENSOART00000001398	VAPA	VAMP (vesicle-associated membrane protein)-associated protein A, 33kDa
IgAt	LDLA	487	23	35920734	35941754	ENSOARG00000009530	ENSOART00000010381	YES1	YES proto-oncogene 1, Src family tyrosine kinase
IgAt	LDLA	488	23	47876172	48184911	ENSOARG00000003681	ENSOART00000003994	ZBTB7C	zinc finger and BTB domain containing 7C
IgAt	GWAS	489	25	13125601	13155769	ENSOARG00000003900	ENSOART00000004245	BMS1	BMS1 ribosome biogenesis factor
LFEC	LDLA	1	1	137814444	137830717	ENSOARG00000015790	ENSOART00000017191	BTG3	BTG family, member 3
LFEC	LDLA	2	1	137622166	137648808	ENSOARG00000015776	ENSOART00000017175	C21orf91	chromosome 21 open reading frame 91
LFEC	LDLA	3	1	137110839	137133205	ENSOARG00000015708	ENSOART00000017098	CHODL	chondrolectin
LFEC	**LDLA**	**4**	**1**	**137831616**	**137895592**	**ENSOARG00000015844**	**ENSOART00000017255**	**CXADR**	**Uncharacterized protein**
LFEC	LDLA	5	1	141197672	141208257	ENSOARG00000016250	ENSOART00000017697	HSPA13	heat shock protein 70kDa family, member 13

LFEC	LDLA	6	1	141376449	141456365	ENSOARG00000016465	ENSOART00000017932	LIPI	lipase, member I
LFEC	LDLA	7	1	138829036	138829116	ENSOARG00000022207	ENSOART00000024109	MIR99A	oar-mir-99a
LFEC	LDLA	8	1	140597192	140600662	ENSOARG00000001166	ENSOART00000001241	NRIP1	nuclear receptor interacting protein 1
LFEC	LDLA	9	1	141359705	141376292	ENSOARG00000016446	ENSOART00000017910	RBM11	RNA binding motif protein 11
LFEC	LDLA	10	1	141025785	141084949	ENSOARG00000016184	ENSOART00000017622	SAMSN1	SAM domain, SH3 domain and nuclear localization signals 1
LFEC	LDLA	11	1	136961183	137107011	ENSOARG00000015635	ENSOART00000017017	TMPRSS15	transmembrane protease, serine 15
LFEC	LDLA	12	1	139564863	139699601	ENSOARG00000016027	ENSOART00000017466	USP25	ubiquitin specific peptidase 25
LFEC	LDLA	13	4	55507741	55584574	ENSOARG00000002000	ENSOART00000002151	C7orf60	chromosome 7 open reading frame 60
LFEC	LDLA	14	4	56152727	56624017	ENSOARG00000002931	ENSOART00000003200	DOCK4	dedicator of cytokinesis 4
LFEC	LDLA	15	4	55370538	55371650	ENSOARG00000008371	ENSOART00000009104	GPR85	G protein-coupled receptor 85
LFEC	LDLA	16	4	55891561	55921065	ENSOARG00000002410	ENSOART00000002614	IFRD1	interferon-related developmental regulator 1
LFEC	LDLA	17	4	56814519	56853519	ENSOARG00000003322	ENSOART00000003603	IMMP2L	IMP2 inner mitochondrial membrane peptidase-like (S. cerevisiae)
LFEC	LDLA	18	4	57220545	57222916	ENSOARG00000003374	ENSOART00000003663	LRRN3	leucine rich repeat neuronal 3
LFEC	LDLA	19	4	54534231	54573286	ENSOARG00000001892	ENSOART00000002032	PPP1R3A	protein phosphatase 1, regulatory subunit 3A
LFEC	LDLA	20	4	55676429	55677787	ENSOARG00000002280	ENSOART00000002465	STIP1	stress-induced phosphoprotein 1
LFEC	LDLA	21	4	55602198	55647937	ENSOARG00000002128	ENSOART00000002293	TMEM168	transmembrane protein 168
LFEC	LDLA	22	4	56019141	56152140	ENSOARG00000002557	ENSOART00000002774	ZNF277	zinc finger protein 277
LFEC	LDLA	23	5	5072823	5079507	ENSOARG00000015019	ENSOART00000016346	B3GNT3	UDP-GlcNAc:betaGal beta-1,3-N-acetylglucosaminyltransferase 3
LFEC	LDLA	24	5	5303866	5322265	ENSOARG00000016242	ENSOART00000017689	FAM129C	family with sequence similarity 129, member C
LFEC	LDLA	25	5	5098456	5121098	ENSOARG00000015172	ENSOART00000016517	FCHO1	FCH domain only 1
LFEC	LDLA	26	5	5056451	5057662	ENSOARG00000014966	ENSOART00000016289	INSL3	insulin-like 3 (Leydig cell)
LFEC	LDLA	27	5	5040716	5053490	ENSOARG00000014631	ENSOART00000015935	JAK3	Janus kinase 3
LFEC	LDLA	28	5	5138001	5171031	ENSOARG00000015551	ENSOART00000016919	MAP1S	microtubule-associated protein 1S
LFEC	LDLA	29	5	5326356	5333940	ENSOARG00000016351	ENSOART00000017804	PGLS	6-phosphogluconolactonase
LFEC	LDLA	30	5	5340954	5353531	ENSOARG00000016498	ENSOART00000017968	SLC27A1	solute carrier family 27 (fatty acid transporter), member 1
LFEC	LDLA	31	5	5200073	5254985	ENSOARG00000015807	ENSOART00000017217	UNC13A	unc-13 homolog A (C. elegans)
LFEC	LDLA	32	6	87097877	87386270	ENSOARG00000013204	ENSOART00000014359	ADAMTS3	ADAM metallopeptidase with thrombospondin type 1 motif, 3
LFEC	LDLA	33	6	88198267	88224250	ENSOARG00000014129	ENSOART00000015388	AFM	afamin
LFEC	LDLA	34	6	88166794	88190190	ENSOARG00000013966	ENSOART00000015211	AFP	alpha-fetoprotein
LFEC	LDLA	35	6	88136611	88159187	ENSOARG00000013782	ENSOART00000015001	ALB	serum albumin precursor
LFEC	LDLA	36	6	85609383	85620397	ENSOARG00000011393	ENSOART00000012383	AMBN	ameloblastin (enamel matrix protein)
LFEC	LDLA	37	6	85548894	85563111	ENSOARG00000011269	ENSOART00000012251	AMTN	amelotin
LFEC	LDLA	38	6	87848925	88015612	ENSOARG00000013568	ENSOART00000014770	ANKRD17	ankyrin repeat domain 17
LFEC	LDLA	39	6	89053717	89061196	ENSOARG00000015052	ENSOART00000016381	AREG	amphiregulin
LFEC	LDLA	40	6	90517575	90662421	ENSOARG00000016372	ENSOART00000017827	ART3	ADP-ribosyltransferase 3
LFEC	LDLA	41	6	89371412	89414148	ENSOARG00000015138	ENSOART00000016474	BTC	betacellulin
LFEC	LDLA	42	6	85421654	85422814	ENSOARG00000007780	ENSOART00000008469	CABS1	calcium-binding protein, spermatid-specific 1
LFEC	LDLA	43	6	90874665	90952433	ENSOARG00000017181	ENSOART00000018702	CCDC158	coiled-coil domain containing 158
LFEC	LDLA	44	6	90096566	90133537	ENSOARG00000015497	ENSOART00000016865	CDKL2	cyclin-dependent kinase-like 2 (CDC2-related kinase)
LFEC	LDLA	45	6	87832853	87842853	ENSOARG00000013420	ENSOART00000014599	COX18	COX18 cytochrome c oxidase assembly factor
LFEC	LDLA	46	6	85089487	85102981	ENSOARG00000010276	ENSOART00000011186	CSN1S1	casein alpha s1
LFEC	LDLA	47	6	85116827	85122776	ENSOARG00000010477	ENSOART00000011405	CSN2	beta-casein precursor
LFEC	LDLA	48	6	85309552	85316834	ENSOARG00000011084	ENSOART00000012054	CSN3	Kappa-casein
LFEC	LDLA	49	6	90551375	90552865	ENSOARG00000016611	ENSOART00000018092	CXCL10	chemokine (C-X-C motif) ligand 10
LFEC	LDLA	50	6	90569808	90571258	ENSOARG00000016668	ENSOART00000018154	CXCL11	chemokine (C-X-C motif) ligand 11
LFEC	LDLA	51	6	90526788	90531488	ENSOARG00000016543	ENSOART00000018017	CXCL9	chemokine (C-X-C motif) ligand 9
LFEC	LDLA	52	6	85956079	85979964	ENSOARG00000012101	ENSOART00000013163	DCK	deoxycytidine kinase
LFEC	LDLA	53	6	85645805	85663564	ENSOARG00000011508	ENSOART00000012512	ENAM	enamelin
LFEC	LDLA	54	6	88912478	88918744	ENSOARG00000014945	ENSOART00000016265	EPGN	epithelial mitogen
LFEC	LDLA	55	6	80712077	81089105	ENSOARG00000006407	ENSOART00000006970	EPHA5	EPH receptor A5
LFEC	LDLA	56	6	88988358	88994874	ENSOARG00000014953	ENSOART00000016275	EREG	epiregulin
LFEC	LDLA	57	6	90822320	90847927	ENSOARG00000016978	ENSOART00000018493	FAM47E	Uncharacterized protein
LFEC	LDLA	58	6	90870170	90871181	ENSOARG00000017040	ENSOART00000018552	FAM47E-STBD1	FAM47E-STBD1 readthrough
LFEC	LDLA	59	6	85287628	85291459	ENSOARG00000011035	ENSOART00000012004	FDCSP	follicular dendritic cell secreted protein
LFEC	LDLA	60	6	90147948	90162603	ENSOARG00000015652	ENSOART00000017034	G3BP2	GTPase activating protein (SH3 domain) binding protein 2
LFEC	LDLA	61	6	86619919	86657661	ENSOARG00000012835	ENSOART00000013955	GC	group-specific component (vitamin D binding protein)
LFEC	LDLA	62	6	83375633	83391928	ENSOARG00000007526	ENSOART00000008195	GNRHR	gonadotropin-releasing hormone receptor
LFEC	LDLA	63	6	85843020	85852103	ENSOARG00000011898	ENSOART00000012944	GRSF1	G-rich RNA sequence binding factor 1
LFEC	LDLA	64	6	36005466	36125662	ENSOARG00000000117	ENSOART00000000125	HERC3	HECT and RLD domain containing E3 ubiquitin protein ligase 3
LFEC	LDLA	65	6	36197433	36244296	ENSOARG00000000530	ENSOART00000000572	HERC5	HECT and RLD domain containing E3 ubiquitin protein ligase 5
LFEC	LDLA	66	6	36252541	36306670	ENSOARG00000001138	ENSOART00000001229	HERC6	Uncharacterized protein
LFEC	LDLA	67	6	72423581	72437525	ENSOARG00000005761	ENSOART00000006270	IGFBP7	insulin-like growth factor binding protein 7
LFEC	LDLA	68	6	85673288	85682398	ENSOARG00000011599	ENSOART00000012614	IGJ	joining chain of multimeric IgA and IgM
LFEC	LDLA	69	6	88474889	88477180	ENSOARG00000014496	ENSOART00000015785	IL8	interleukin-8
LFEC	LDLA	70	6	85922030	85945597	ENSOARG00000011975	ENSOART00000013027	MOB1B	MOB kinase activator 1B
LFEC	LDLA	71	6	88783856	88905590	ENSOARG00000014880	ENSOART00000016194	MTHFD2L	methylenetetrahydrofolate dehydrogenase (NADP+ dependent) 2-like
LFEC	LDLA	72	6	85510938	85518474	ENSOARG00000011228	ENSOART00000012206	MUC7	mucin 7, secreted
LFEC	LDLA	73	6	90435943	90459828	ENSOARG00000016045	ENSOART00000017475	NAAA	N-acylethanolamine acid amidase
LFEC	LDLA	74	6	36026691	36027272	ENSOARG00000000433	ENSOART00000000465	NAP1L5	nucleosome assembly protein 1-like 5
LFEC	LDLA	75	6	72362608	72373316	ENSOARG00000005082	ENSOART00000005539	NOA1	nitric oxide associated 1
LFEC	LDLA	76	6	90665617	90697165	ENSOARG00000016734	ENSOART00000018226	NUP54	nucleoporin 54kDa
LFEC	LDLA	77	6	85259906	85267164	ENSOARG00000011002	ENSOART00000011971	ODAM	odontogenic, ameloblast asssociated

LFEC	LA	77	6	85259906	85267164	ENSOARG00000011002	ENSOART00000011971	ODAM	odontogenic, ameloblast asssociated
LFEC	LDLA	78	6	89526374	89652510	ENSOARG00000015234	ENSOART00000016575	PARM1	prostate androgen-regulated mucin-like protein 1
LFEC	LA	78	6	89526374	89652510	ENSOARG00000015234	ENSOART00000016575	PARM1	prostate androgen-regulated mucin-like protein 1
LFEC	LDLA	79	6	88584559	88585388	ENSOARG00000014766	ENSOART00000016069	PF4	C-X-C motif chemokine
LFEC	LA	79	6	88584559	88585388	ENSOARG00000014766	ENSOART00000016069	PF4	C-X-C motif chemokine
LFEC	LDLA	80	6	36193017	36193229	ENSOARG00000000447	ENSOART00000000475	PIGY	Uncharacterized protein
LFEC	LDLA	81	6	72374308	72423255	ENSOARG00000005538	ENSOART00000006046	POLR2B	polymerase (RNA) II (DNA directed) polypeptide B, 140kDa
LFEC	LDLA	82	6	88576093	88576890	ENSOARG00000014675	ENSOART00000015973	PPBP	pro-platelet basic protein (chemokine (C-X-C motif) ligand 7)
LFEC	LA	82	6	88576093	88576890	ENSOARG00000014675	ENSOART00000015973	PPBP	pro-platelet basic protein (chemokine (C-X-C motif) ligand 7)
LFEC	LA	83	6	90381690	90414856	ENSOARG00000015945	ENSOART00000017364	PPEF2	protein phosphatase, EF-hand calcium binding domain 2
LFEC	LDLA	84	6	36191044	36192928	ENSOARG00000000388	ENSOART00000000411	PYURF	Uncharacterized protein
LFEC	LDLA	85	6	88284202	88337481	ENSOARG00000014363	ENSOART00000015640	RASSF6	Ras association (RalGDS/AF-6) domain family member 6
LFEC	LA	85	6	88284202	88337481	ENSOARG00000014363	ENSOART00000015640	RASSF6	Ras association (RalGDS/AF-6) domain family member 6
LFEC	LDLA	86	6	90011907	90028803	ENSOARG00000015272	ENSOART00000016621	RCHY1	ring finger and CHY zinc finger domain containing 1, E3 ubiquitin protein ligase
LFEC	LA	86	6	90011907	90028803	ENSOARG00000015272	ENSOART00000016621	RCHY1	ring finger and CHY zinc finger domain containing 1, E3 ubiquitin protein ligase
LFEC	LDLA	87	6	85751041	85822914	ENSOARG00000011735	ENSOART00000012768	RUFY3	RUN and FYVE domain containing 3
LFEC	LA	87	6	85751041	85822914	ENSOARG00000011735	ENSOART00000012768	RUFY3	RUN and FYVE domain containing 3
LFEC	LA	88	6	90704080	90754757	ENSOARG00000016858	ENSOART00000018358	SCARB2	Uncharacterized protein
LFEC	LA	89	6	90476385	90509099	ENSOARG00000016216	ENSOART00000017668	SDAD1	SDA1 domain containing 1
LFEC	LDLA	90	6	86143053	86457688	ENSOARG00000012378	ENSOART00000013467	SLC4A4	solute carrier family 4 (sodium bicarbonate cotransporter), member 4
LFEC	LA	90	6	86143053	86457688	ENSOARG00000012378	ENSOART00000013467	SLC4A4	solute carrier family 4 (sodium bicarbonate cotransporter), member 4
LFEC	LA	91	6	91389433	91392900	ENSOARG00000017421	ENSOART00000018962	SOWAHB	sosondowah ankyrin repeat domain family member B
LFEC	LA	92	6	83218338	83250708	ENSOARG00000007050	ENSOART00000007674	STAP1	signal transducing adaptor family member 1
LFEC	LA	93	6	84886613	84922697	ENSOARG00000009915	ENSOART00000010793	SULT1B1	sulfotransferase family, cytosolic, 1B, member 1
LFEC	LDLA	94	6	84983639	85009405	ENSOARG00000010025	ENSOART00000010910	SULT1E1	sulfotransferase family 1E, estrogen-preferring, member 1
LFEC	LA	94	6	84983639	85009405	ENSOARG00000010025	ENSOART00000010910	SULT1E1	sulfotransferase family 1E, estrogen-preferring, member 1
LFEC	LDLA	95	6	90029942	90043908	ENSOARG00000015330	ENSOART00000016679	THAP6	THAP domain containing 6
LFEC	LA	95	6	90029942	90043908	ENSOARG00000015330	ENSOART00000016679	THAP6	THAP domain containing 6
LFEC	LA	96	6	83559977	83615116	ENSOARG00000007963	ENSOART00000008673	TMPRSS11A	transmembrane protease, serine 11A
LFEC	LA	97	6	83834645	83853787	ENSOARG00000008316	ENSOART00000009048	TMPRSS11B	transmembrane protease, serine 11B
LFEC	LA	98	6	83467399	83534455	ENSOARG00000007770	ENSOART00000008456	TMPRSS11D	transmembrane protease, serine 11D
LFEC	LA	99	6	83893826	83946666	ENSOARG00000008444	ENSOART00000009193	TMPRSS11E	transmembrane protease, serine 11E
LFEC	LA	100	6	83691691	83787544	ENSOARG00000008194	ENSOART00000008918	TMPRSS11F	transmembrane protease, serine 11F
LFEC	LA	101	6	83261448	83354952	ENSOARG00000007255	ENSOART00000007899	UBA6	ubiquitin-like modifier activating enzyme 6
LFEC	LA	102	6	84788460	84812410	ENSOARG00000009742	ENSOART00000010601	UGT2A3	UDP glucuronosyltransferase 2 family, polypeptide A3
LFEC	LA	103	6	84148570	84165137	ENSOARG00000008828	ENSOART00000009610	UGT2B7	UDP-glucuronosyltransferase 2B7 precursor
LFEC	LA	104	6	90232921	90308566	ENSOARG00000015763	ENSOART00000017165	USO1	USO1 vesicle transport factor
LFEC	LDLA	105	6	85710865	85712289	ENSOARG00000007800	ENSOART00000008489	UTP3	UTP3, small subunit (SSU) processome component, homolog (S. cerevisiae)
LFEC	LA	105	6	85710865	85712289	ENSOARG00000007800	ENSOART00000008489	UTP3	UTP3, small subunit (SSU) processome component, homolog (S. cerevisiae)
LFEC	LA	106	6	84034755	84072385	ENSOARG00000008633	ENSOART00000009399	YTHDC1	YTH domain containing 1
LFEC	LDLA	107	7	13809656	13881272	ENSOARG00000018291	ENSOART00000019903	AAGAB	alpha- and gamma-adaptin binding protein
LFEC	LDLA	108	7	21812233	21823012	ENSOARG00000019436	ENSOART00000021168	ABHD4	abhydrolase domain containing 4
LFEC	LDLA	109	7	21383324	21422108	ENSOARG00000019368	ENSOART00000021092	ACIN1	apoptotic chromatin condensation inducer 1
LFEC	LDLA	110	7	20457795	20472266	ENSOARG00000019102	ENSOART00000020803	ADCY4	adenylate cyclase 4
LFEC	LDLA	111	7	19180792	19203994	ENSOARG00000018976	ENSOART00000020660	ADPGK	ADP-dependent glucokinase
LFEC	LDLA	112	7	21485635	21518558	ENSOARG00000019387	ENSOART00000021112	AJUBA	ajuba LIM protein
LFEC	LDLA	113	7	15384728	15392155	ENSOARG00000018551	ENSOART00000020194	ANP32A	Uncharacterized protein
LFEC	LDLA	114	7	20989240	21004806	ENSOARG00000019274	ENSOART00000020990	AP1G2	adaptor-related protein complex 1, gamma 2 subunit
LFEC	LDLA	115	7	23830289	23832121	ENSOARG00000019740	ENSOART00000021496	APEX1	Uncharacterized protein
LFEC	LDLA	116	7	23232512	23251082	ENSOARG00000019687	ENSOART00000021440	ARHGEF40	Rho guanine nucleotide exchange factor (GEF) 40
LFEC	LDLA	117	7	19008549	19107086	ENSOARG00000018958	ENSOART00000020643	ARIH1	ariadne RBR E3 ubiquitin protein ligase 1
LFEC	LDLA	118	7	19146725	19170285	ENSOARG00000018966	ENSOART00000020651	BBS4	Bardet-Biedl syndrome 4
LFEC	LDLA	119	7	21203496	21218824	ENSOARG00000019336	ENSOART00000021059	BCL2L2-PABPN1	BCL2L2-PABPN1 readthrough
LFEC	LDLA	120	7	21381359	21381784	ENSOARG00000011705	ENSOART00000012728	C14orf119	chromosome 14 open reading frame 119
LFEC	LDLA	121	7	21472870	21481572	ENSOARG00000019382	ENSOART00000021108	C14orf93	chromosome 14 open reading frame 93
LFEC	LDLA	122	7	20165317	20178168	ENSOARG00000019036	ENSOART00000020726	C15orf59	chromosome 15 open reading frame 59
LFEC	LDLA	123	7	14132582	14137543	ENSOARG00000018340	ENSOART00000019957	C15orf61	chromosome 15 open reading frame 61
LFEC	LDLA	124	7	14803134	14812332	ENSOARG00000018411	ENSOART00000020035	CALML4	calmodulin-like 4
LFEC	LDLA	125	7	20361121	20363125	ENSOARG00000019063	ENSOART00000020756	CBLN3	cerebellin 3 precursor
LFEC	LDLA	126	7	23946971	23951850	ENSOARG00000019782	ENSOART00000021540	CCNB1IP1	cyclin B1 interacting protein 1, E3 ubiquitin protein ligase
LFEC	LDLA	127	7	20126968	20139147	ENSOARG00000019030	ENSOART00000020717	CD276	CD276 molecule
LFEC	LDLA	128	7	21425499	21433537	ENSOARG00000019374	ENSOART00000021099	CDH24	cadherin 24, type 2
LFEC	LDLA	129	7	21363840	21366310	ENSOARG00000019360	ENSOART00000021084	CEBPE	CCAAT/enhancer binding protein (C/EBP), epsilon
LFEC	LDLA	130	7	22966779	23004178	ENSOARG00000019643	ENSOART00000021394	CHD8	chromodomain helicase DNA binding protein 8
LFEC	LDLA	131	7	20482181	20485060	ENSOARG00000019116	ENSOART00000020815	CIDEB	cell death-inducing DFFA-like effector b
LFEC	LDLA	132	7	14820655	14829797	ENSOARG00000018417	ENSOART00000020044	CLN6	ceroid-lipofuscinosis, neuronal 6, late infantile, variant
LFEC	LDLA	133	7	21159974	21162151	ENSOARG00000019322	ENSOART00000021043	CMTM5	CKLF-like MARVEL transmembrane domain containing 5
LFEC	LDLA	134	7	15187916	15338481	ENSOARG00000018517	ENSOART00000020161	CORO2B	coronin, actin binding protein, 2B
LFEC	LDLA	135	7	20681996	20686678	ENSOARG00000019247	ENSOART00000020961	CPNE6	copine VI (neuronal)
LFEC	LDLA	136	7	21835695	21847699	ENSOARG00000019440	ENSOART00000021171	DAD1	defender against cell death 1
LFEC	LDLA	137	7	20635447	20648453	ENSOARG00000019226	ENSOART00000020937	DCAF11	Uncharacterized protein
LFEC	LDLA	138	7	20491960	20499532	ENSOARG00000019131	ENSOART00000020835	DHRS1	dehydrogenase/reductase (SDR family) member 1
LFEC	LDLA	139	7	12982085	13012004	ENSOARG00000018151	ENSOART00000019759	DIS3L	DIS3 like exosome 3-5 exoribonuclease
LFEC	LDLA	140	7	21173917	21183125	ENSOARG00000019328	ENSOART00000021049	EFS	embryonal Fyn-associated substrate
LFEC	LDLA	141	7	25379333	25382479	ENSOARG00000019895	ENSOART00000021661	EMC4	ER membrane protein complex subunit 4
LFEC	LDLA	142	7	25488301	25504670	ENSOARG00000019905	ENSOART00000021672	EMC7	ER membrane protein complex subunit 7
LFEC	LDLA	143	7	20630230	20635243	ENSOARG00000019216	ENSOART00000020924	EMC9	ER membrane protein complex subunit 9
LFEC	LDLA	144	7	14874519	14885710	ENSOARG00000018433	ENSOART00000020063	FEM1B	fem-1 homolog b (C. elegans)
LFEC	LDLA	145	7	20637495	20638729	ENSOARG00000019230	ENSOART00000020940	FITM1	fat storage-inducing transmembrane protein 1
LFEC	LDLA	146	7	15738043	15934180	ENSOARG00000018604	ENSOART00000020249	GLCE	glucuronic acid epimerase
LFEC	LDLA	147	7	20550490	20556068	ENSOARG00000019160	ENSOART00000020867	GMPR2	guanosine monophosphate reductase 2
LFEC	LDLA	148	7	18748784	18755582	ENSOARG00000018877	ENSOART00000020556	GRAMD2	GRAM domain containing 2
LFEC	LDLA	149	7	19762723	19805163	ENSOARG00000019006	ENSOART00000020692	HCN4	hyperpolarization activated cyclic nucleotide gated potassium channel 4
LFEC	LDLA	150	7	18903379	18935045	ENSOARG00000018930	ENSOART00000020616	HEXA	Beta-hexosaminidase
LFEC	LDLA	151	7	23112936	23156301	ENSOARG00000019672	ENSOART00000021423	HNRNPC	Uncharacterized protein
LFEC	LDLA	152	7	21232828	21239691	ENSOARG00000019342	ENSOART00000021065	HOMEZ	homeobox and leucine zipper encoding
LFEC	LDLA	153	7	21163579	21166254	ENSOARG00000019325	ENSOART00000021045	IL25	interleukin 25
LFEC	LDLA	154	7	20587725	20595992	ENSOARG00000019188	ENSOART00000020895	IPO4	Uncharacterized protein
LFEC	LDLA	155	7	13881328	14108976	ENSOARG00000018328	ENSOART00000019951	IQCH	IQ motif containing H
LFEC	LDLA	156	7	20606992	20610859	ENSOARG00000019201	ENSOART00000020909	IRF9	interferon regulatory factor 9
LFEC	LDLA	157	7	14898977	15033353	ENSOARG00000018483	ENSOART00000020132	ITGA11	integrin, alpha 11
LFEC	LDLA	158	7	20987123	20994794	ENSOARG00000019269	ENSOART00000020983	JPH4	junctophilin 4
LFEC	LDLA	159	7	20353214	20360013	ENSOARG00000019058	ENSOART00000020749	KHNYN	KH and NYN domain containing
LFEC	LDLA	160	7	16078139	16122235	ENSOARG00000018647	ENSOART00000020304	KIF23	kinesin family member 23
LFEC	LDLA	161	7	23857628	23859747	ENSOARG00000019750	ENSOART00000021506	KLHL33	kelch-like family member 33
LFEC	LDLA	162	7	17490057	17496828	ENSOARG00000018750	ENSOART00000020413	LARP6	La ribonucleoprotein domain family, member 6
LFEC	LDLA	163	7	13180064	13195612	ENSOARG00000018240	ENSOART00000019852	LCTL	lactase-like
LFEC	LDLA	164	7	25263546	25270541	ENSOARG00000019872	ENSOART00000021635	LPCAT4	lysophosphatidylcholine acyltransferase 4
LFEC	LDLA	165	7	21570979	21579654	ENSOARG00000019406	ENSOART00000021134	LRP10	low density lipoprotein receptor-related protein 10
LFEC	LDLA	166	7	20690047	20706472	ENSOARG00000019255	ENSOART00000020972	LRRC16B	leucine rich repeat containing 16B

LFEC	LDLA	167	7	17549882	17700850	ENSOARG00000018765	ENSOART00000020437	LRRC49	leucine rich repeat containing 49
LFEC	LDLA	168	7	20473930	20483145	ENSOARG00000019112	ENSOART00000020807	LTB4R	leukotriene B4 receptor
LFEC	LDLA	169	7	13089340	13126170	ENSOARG00000018185	ENSOART00000019790	MAP2K1	mitogen-activated protein kinase kinase 1
LFEC	LDLA	170	7	14159439	14423901	ENSOARG00000018353	ENSOART00000019979	MAP2K5	mitogen-activated protein kinase kinase 5
LFEC	LDLA	171	7	36954401	37310523	ENSOARG00000020597	ENSOART00000022438	MDGA2	MAM domain containing glycosylphosphatidylinositol anchor 2
LFEC	LDLA	172	7	20566246	20567524	ENSOARG00000019172	ENSOART00000020877	MDP1	Uncharacterized protein
LFEC	LDLA	173	7	12553780	12864461	ENSOARG00000018113	ENSOART00000019727	MEGF11	multiple EGF-like-domains 11
LFEC	LDLA	174	7	23334382	23344407	ENSOARG00000019714	ENSOART00000021470	METTL17	methyltransferase like 17
LFEC	LDLA	175	7	22903566	22916131	ENSOARG00000019618	ENSOART00000021365	METTL3	methyltransferase like 3
LFEC	LDLA	176	7	21594251	21603143	ENSOARG00000019414	ENSOART00000021143	MMP14	matrix metalloproteinase-14 precursor
LFEC	LDLA	177	7	21605418	21609783	ENSOARG00000019418	ENSOART00000021148	MRPL52	mitochondrial ribosomal protein L52
LFEC	LDLA	178	7	21105366	21157369	ENSOARG00000019316	ENSOART00000021039	MYH6	myosin, heavy chain 6, cardiac muscle, alpha
LFEC	LDLA	179	7	18469857	18653320	ENSOARG00000018863	ENSOART00000020547	MYO9A	myosin IXA
LFEC	LDLA	180	7	23307594	23313919	ENSOARG00000019706	ENSOART00000021461	NDRG2	NDRG family member 2
LFEC	LDLA	181	7	20084735	20085028	ENSOARG00000011680	ENSOART00000012699	NDUFS6	NADH dehydrogenase (ubiquinone) Fe-S protein 6, 13kDa (NADH-coenzyme Q reductase)
LFEC	LDLA	182	7	20563997	20564961	ENSOARG00000019164	ENSOART00000020870	NEDD8	neural precursor cell expressed, developmentally down-regulated 8
LFEC	LDLA	183	7	19578696	19744979	ENSOARG00000018989	ENSOART00000020682	NEO1	neogenin 1
LFEC	LDLA	184	7	20418413	20426096	ENSOARG00000019084	ENSOART00000020781	NFATC4	nuclear factor of activated T-cells, cytoplasmic, calcineurin-dependent 4
LFEC	LDLA	185	7	21075905	21083199	ENSOARG00000019301	ENSOART00000021019	NGDN	neuroguidin, EIF4E binding protein
LFEC	LDLA	186	7	25283680	25284429	ENSOARG00000019881	ENSOART00000021646	NOP10	NOP10 ribonucleoprotein
LFEC	LDLA	187	7	20485596	20491635	ENSOARG00000019127	ENSOART00000020829	NOP9	NOP9 nucleolar protein
LFEC	LDLA	188	7	15626115	15681874	ENSOARG00000018585	ENSOART00000020230	NOX5	NADPH oxidase, EF-hand calcium binding domain 5
LFEC	LDLA	189	7	19988579	20022706	ENSOARG00000019020	ENSOART00000020707	NPTN	neuroplastin
LFEC	LDLA	190	7	18448836	18454071	ENSOARG00000018808	ENSOART00000020485	NR2E3	nuclear receptor subfamily 2, group E, member 3
LFEC	LDLA	191	7	20676526	20678719	ENSOARG00000019240	ENSOART00000020951	NRL	neural retina leucine zipper
LFEC	LDLA	192	7	20373970	20393188	ENSOARG00000019074	ENSOART00000020769	NYNRIN	NYN domain and retroviral integrase containing
LFEC	LDLA	193	7	22827906	22828859	ENSOARG00000012159	ENSOART00000013224	OR10G2	olfactory receptor, family 10, subfamily G, member 2
LFEC	LDLA	194	7	22842933	22843871	ENSOARG00000012240	ENSOART00000013307	OR10G3	olfactory receptor, family 10, subfamily G, member 3
LFEC	LDLA	195	7	23994539	23995510	ENSOARG00000013184	ENSOART00000014326	OR11H4	olfactory receptor, family 11, subfamily H, member 4
LFEC	LDLA	196	7	24034842	24036234	ENSOARG00000019789	ENSOART00000021548	OR11H6	olfactory receptor, family 11, subfamily H, member 6
LFEC	LDLA	197	7	24029371	24030327	ENSOARG00000013195	ENSOART00000014343	OR11H7	olfactory receptor, family 11, subfamily H, member 7 (gene/pseudogene)
LFEC	LDLA	198	7	22784861	22785802	ENSOARG00000012081	ENSOART00000013137	OR4E2	olfactory receptor, family 4, subfamily E, member 2
LFEC	LDLA	199	7	24971107	24973102	ENSOARG00000019838	ENSOART00000021600	OR4F15	olfactory receptor, family 4, subfamily F, member 15
LFEC	LDLA	200	7	24473979	24476846	ENSOARG00000019812	ENSOART00000021572	OR4K1	olfactory receptor, family 4, subfamily K, member 1
LFEC	LDLA	201	7	24575575	24576888	ENSOARG00000019819	ENSOART00000021579	OR4K13	olfactory receptor, family 4, subfamily K, member 13
LFEC	LDLA	202	7	24552028	24553026	ENSOARG00000014167	ENSOART00000015432	OR4K14	olfactory receptor, family 4, subfamily K, member 14
LFEC	LDLA	203	7	24507711	24508646	ENSOARG00000014050	ENSOART00000015292	OR4K15	olfactory receptor, family 4, subfamily K, member 15
LFEC	LDLA	204	7	24421859	24422791	ENSOARG00000013871	ENSOART00000015094	OR4K2	olfactory receptor, family 4, subfamily K, member 2
LFEC	LDLA	205	7	24465500	24466468	ENSOARG00000013953	ENSOART00000015192	OR4K5	olfactory receptor, family 4, subfamily K, member 5
LFEC	LDLA	206	7	24627333	24649970	ENSOARG00000019827	ENSOART00000021586	OR4L1	olfactory receptor, family 4, subfamily L, member 1
LFEC	LDLA	207	7	24383971	24384891	ENSOARG00000013774	ENSOART00000014982	OR4N2	olfactory receptor, family 4, subfamily N, member 2
LFEC	LDLA	208	7	24542259	24543170	ENSOARG00000014154	ENSOART00000015413	OR4Q2	olfactory receptor, family 4, subfamily Q, member 2 (gene/pseudogene)
LFEC	LDLA	209	7	24315800	24316738	ENSOARG00000013471	ENSOART00000014652	OR4Q3	olfactory receptor, family 4, subfamily Q, member 3
LFEC	LDLA	210	7	24330199	24331128	ENSOARG00000013537	ENSOART00000014723	OR4S1	olfactory receptor, family 4, subfamily S, member 1
LFEC	LDLA	211	7	23180444	23181376	ENSOARG00000012339	ENSOART00000013415	OR5AU1	olfactory receptor, family 5, subfamily AU, member 1
LFEC	LDLA	212	7	23832308	23839289	ENSOARG00000019745	ENSOART00000021501	OSGEP	O-sialoglycoprotein endopeptidase
LFEC	LDLA	213	7	21649804	21664134	ENSOARG00000019429	ENSOART00000021160	OXA1L	oxidase (cytochrome c) assembly 1-like
LFEC	LDLA	214	7	15984367	16058573	ENSOARG00000018618	ENSOART00000020265	PAQR5	progestin and adipoQ receptor family member V
LFEC	LDLA	215	7	23909789	23927859	ENSOARG00000019777	ENSOART00000021535	PARP2	poly (ADP-ribose) polymerase 2
LFEC	LDLA	216	7	18815243	18837049	ENSOARG00000018904	ENSOART00000020588	PARP6	poly (ADP-ribose) polymerase family, member 6
LFEC	LDLA	217	7	20656653	20664937	ENSOARG00000019237	ENSOART00000020948	PCK2	phosphoenolpyruvate carboxykinase 2 (mitochondrial)
LFEC	LDLA	218	7	14709897	14796874	ENSOARG00000018393	ENSOART00000020023	PIAS1	protein inhibitor of activated STAT, 1
LFEC	LDLA	219	7	18780797	18808500	ENSOARG00000018886	ENSOART00000020568	PKM	pyruvate kinase, muscle
LFEC	LDLA	220	7	21222543	21223697	ENSOARG00000019339	ENSOART00000021061	PPP1R3E	protein phosphatase 1, regulatory subunit 3E
LFEC	LDLA	221	7	21538894	21546902	ENSOARG00000019392	ENSOART00000021120	PRMT5	protein arginine methyltransferase 5
LFEC	LDLA	222	7	21444915	21454649	ENSOARG00000019380	ENSOART00000021106	PSMB5	proteasome (prosome, macropain) subunit, beta type, 5
LFEC	LDLA	223	7	20632492	20634912	ENSOARG00000019219	ENSOART00000020930	PSME1	proteasome (prosome, macropain) activator subunit 1 (PA28 alpha)
LFEC	LDLA	224	7	20624296	20630146	ENSOARG00000019212	ENSOART00000020922	PSME2	proteasome (prosome, macropain) activator subunit 2 (PA28 beta)
LFEC	LDLA	225	7	22931663	22944209	ENSOARG00000019625	ENSOART00000021373	RAB2B	RAB2B, member RAS oncogene family
LFEC	LDLA	226	7	20515953	20521527	ENSOARG00000019139	ENSOART00000020844	RABGGTA	Rab geranylgeranyltransferase, alpha subunit
LFEC	LDLA	227	7	21552022	21557344	ENSOARG00000019398	ENSOART00000021125	RBM23	RNA binding motif protein 23
LFEC	LDLA	228	7	20596317	20601666	ENSOARG00000019194	ENSOART00000020906	REC8	REC8 meiotic recombination protein
LFEC	LDLA	229	7	21567500	21571456	ENSOARG00000019403	ENSOART00000021131	REM2	RAS (RAD and GEM)-like GTP binding 2
LFEC	LDLA	230	7	20452478	20456283	ENSOARG00000019090	ENSOART00000020786	RIPK3	receptor-interacting serine-threonine kinase 3
LFEC	LDLA	231	7	23458785	23461851	ENSOARG00000019721	ENSOART00000021477	RNASE1	ribonuclease, RNase A family, 1 (pancreatic)
LFEC	LDLA	232	7	23763858	23767364	ENSOARG00000019732	ENSOART00000021488	RNASE10	ribonuclease, RNase A family, 10 (non-active)
LFEC	LDLA	233	7	23684416	23685590	ENSOARG00000019726	ENSOART00000021482	RNASE12	ribonuclease, RNase A family, 12 (non-active)
LFEC	LDLA	234	7	23296986	23298093	ENSOARG00000019696	ENSOART00000021449	RNASE13	ribonuclease, RNase A family, 13 (non-active)
LFEC	LDLA	235	7	23387783	23390762	ENSOARG00000019719	ENSOART00000021474	RNASE2	Uncharacterized protein
LFEC	LDLA	236	7	23574214	23574657	ENSOARG00000012938	ENSOART00000014060	RNASE4	ribonuclease, RNase A family, 4
LFEC	LDLA	237	7	23705173	23712476	ENSOARG00000019730	ENSOART00000021486	RNASE9	ribonuclease, RNase A family, 9 (non-active)
LFEC	LDLA	238	7	20612233	20623242	ENSOARG00000019207	ENSOART00000020917	RNF31	Uncharacterized protein
LFEC	LDLA	239	7	23041563	23092580	ENSOARG00000019665	ENSOART00000021417	RPGRIP1	retinitis pigmentosa GTPase regulator interacting protein 1
LFEC	LDLA	240	7	13131998	13136564	ENSOARG00000018207	ENSOART00000019815	RPL4	Uncharacterized protein
LFEC	LDLA	241	7	16134652	16136798	ENSOARG00000018666	ENSOART00000020321	RPLP1	Uncharacterized protein
LFEC	LDLA	242	7	22882530	22895039	ENSOARG00000019612	ENSOART00000021355	SALL2	spalt-like transcription factor 2
LFEC	LDLA	243	7	20347783	20350698	ENSOARG00000019051	ENSOART00000020743	SDR39U1	short chain dehydrogenase/reductase family 39U, member 1
LFEC	LDLA	244	7	18728768	18729436	ENSOARG00000011664	ENSOART00000012683	SENP8	Uncharacterized protein
LFEC	LDLA	245	7	14443717	14451450	ENSOARG00000018375	ENSOART00000019998	SKOR1	SKI family transcriptional corepressor 1
LFEC	LDLA	246	7	25288802	25376206	ENSOARG00000019890	ENSOART00000021658	SLC12A6	solute carrier family 12 (potassium/chloride transporter), member 6
LFEC	LDLA	247	7	21187788	21195391	ENSOARG00000019331	ENSOART00000021054	SLC22A17	solute carrier family 22, member 17
LFEC	LDLA	248	7	23322650	23324939	ENSOARG00000019711	ENSOART00000021467	SLC39A2	solute carrier family 39 (zinc transporter), member 2
LFEC	LDLA	249	7	21622104	21648711	ENSOARG00000019424	ENSOART00000021155	SLC7A7	solute carrier family 7 (amino acid transporter light chain, y+L system), member 7
LFEC	LDLA	250	7	21302166	21353769	ENSOARG00000019354	ENSOART00000021077	SLC7A8	solute carrier family 7 (amino acid transporter light chain, L system), member 8
LFEC	LDLA	251	7	13774171	13797299	ENSOARG00000018276	ENSOART00000019886	SMAD3	SMAD family member 3
LFEC	LDLA	252	7	13318677	13395361	ENSOARG00000018258	ENSOART00000019865	SMAD6	SMAD family member 6
LFEC	LDLA	253	7	13129787	13132087	ENSOARG00000018198	ENSOART00000019800	SNAPC5	small nuclear RNA activating complex, polypeptide 5, 19kDa
LFEC	LDLA	254	7	15546150	15578788	ENSOARG00000018567	ENSOART00000020205	SPESP1	sperm equatorial segment protein 1
LFEC	LDLA	255	7	23005696	23040112	ENSOARG00000019652	ENSOART00000021407	SUPT16H	suppressor of Ty 16 homolog (S. cerevisiae)
LFEC	LDLA	256	7	20307303	20322633	ENSOARG00000019044	ENSOART00000020735	TBC1D21	TBC1 domain family, member 21
LFEC	LDLA	257	7	23874336	23908216	ENSOARG00000019765	ENSOART00000021531	TEP1	telomerase-associated protein 1
LFEC	LDLA	258	7	20524488	20538003	ENSOARG00000019146	ENSOART00000020853	TGM1	transglutaminase 1
LFEC	LDLA	259	7	18308126	18416561	ENSOARG00000018796	ENSOART00000020472	THSD4	thrombospondin, type I, domain containing 4
LFEC	LDLA	260	7	21002919	21008164	ENSOARG00000019278	ENSOART00000020994	THTPA	thiamine triphosphatase
LFEC	LDLA	261	7	20547268	20551055	ENSOARG00000019152	ENSOART00000020857	TINF2	TERF1 (TRF1)-interacting nuclear factor 2
LFEC	LDLA	262	7	13014077	13020952	ENSOARG00000018169	ENSOART00000019773	TIPIN	TIMELESS interacting protein
LFEC	LDLA	263	7	16731799	16784020	ENSOARG00000018695	ENSOART00000020351	TLE3	transducin-like enhancer of split 3
LFEC	LDLA	264	7	20568126	20587098	ENSOARG00000019177	ENSOART00000020883	TM9SF1	Uncharacterized protein
LFEC	LDLA	265	7	18953504	18968516	ENSOARG00000018941	ENSOART00000020623	TMEM202	transmembrane protein 202
LFEC	LDLA	266	7	23826406	23829226	ENSOARG00000019736	ENSOART00000021492	TMEM55B	transmembrane protein 55B

LFEC	LDLA	267	7	22913617	22931269	ENSOARG00000019621	ENSOART00000021368	TOX4	TOX high mobility group box family member 4
LFEC	LDLA	268	7	23295408	23302280	ENSOARG00000019694	ENSOART00000021446	TPPP2	tubulin polymerization-promoting protein family member 2
LFEC	LDLA	269	7	21865716	21878952	ENSOARG00000019445	ENSOART00000021176	TRAC	T cell receptor alpha constant
LFEC	LDLA	270	7	22528654	22529146	ENSOARG00000019541	ENSOART00000021281	TRAV16	T cell receptor alpha variable 16
LFEC	LDLA	271	7	22629199	22629733	ENSOARG00000019569	ENSOART00000021313	TRAV21	T cell receptor alpha variable 21
LFEC	LDLA	272	7	22586032	22586498	ENSOARG00000019553	ENSOART00000021295	TRAV24	T cell receptor alpha variable 24
LFEC	LDLA	273	7	22493564	22496187	ENSOARG00000019533	ENSOART00000021274	TRAV27	T cell receptor alpha variable 27
LFEC	LDLA	274	7	22236461	22239682	ENSOARG00000019473	ENSOART00000021210	TRAV36DV7	T cell receptor alpha variable 36/delta variable 7
LFEC	LDLA	275	7	22190500	22191071	ENSOARG00000019462	ENSOART00000021195	TRAV39	T cell receptor alpha variable 39
LFEC	LDLA	276	7	22753258	22754016	ENSOARG00000019603	ENSOART00000021346	TRAV4	T cell receptor alpha variable 4
LFEC	LDLA	277	7	22172767	22173304	ENSOARG00000019461	ENSOART00000021193	TRAV41	T cell receptor alpha variable 41
LFEC	LDLA	278	7	22731007	22732108	ENSOARG00000019594	ENSOART00000021338	TRAV5	T cell receptor alpha variable 5
LFEC	LDLA	279	7	21959296	21963564	ENSOARG00000019448	ENSOART00000021181	TRDC	T cell receptor delta constant
LFEC	LDLA	280	7	22075028	22075517	ENSOARG00000019449	ENSOART00000021182	TRDV2	T cell receptor delta variable 2
LFEC	LDLA	281	7	21954183	21954533	ENSOARG00000011936	ENSOART00000012982	TRDV3	T cell receptor delta variable 3
LFEC	LDLA	282	7	20572513	20574901	ENSOARG00000019183	ENSOART00000020887	TSSK4	testis-specific serine kinase 4
LFEC	LDLA	283	7	23956098	23972223	ENSOARG00000019785	ENSOART00000021543	TTC5	tetratricopeptide repeat domain 5
LFEC	LDLA	284	7	17344502	17432920	ENSOARG00000018732	ENSOART00000020398	UACA	uveal autoantigen with coiled-coil domains and ankyrin repeats
LFEC	LDLA	285	7	52647577	53312875	ENSOARG00000020918	ENSOART00000022790	UNC13C	unc-13 homolog C (C. elegans)
LFEC	LDLA	286	7	21026117	21038765	ENSOARG00000019296	ENSOART00000021012	ZFHX2	zinc finger homeobox 2
LFEC	LDLA	287	7	23218501	23230871	ENSOARG00000019679	ENSOART00000021430	ZNF219	zinc finger protein 219
LFEC	LDLA	288	7	13138422	13178654	ENSOARG00000018225	ENSOART00000019831	ZWILCH	zwilch kinetochore protein
LFEC	LDLA	289	8	63801650	63810872	ENSOARG00000001146	ENSOART00000001223	ABRACL	ABRA C-terminal like
LFEC	LDLA	290	8	6991692	7259520	ENSOARG00000007187	ENSOART00000007814	BCKDHB	branched chain keto acid dehydrogenase E1, beta polypeptide
LFEC	LDLA	291	8	61293172	61313162	ENSOARG00000000096	ENSOART00000000096	BCLAF1	BCL2-associated transcription factor 1
LFEC	LDLA	292	8	49673671	49690577	ENSOARG00000013104	ENSOART00000014246	C6orf163	chromosome 6 open reading frame 163
LFEC	LDLA	293	8	10883260	10897885	ENSOARG00000007593	ENSOART00000008266	C6orf58	chromosome 6 open reading frame 58
LFEC	LDLA	294	8	63577564	63588210	ENSOARG00000000846	ENSOART00000000902	CCDC28A	coiled-coil domain containing 28A
LFEC	LDLA	295	8	273763	410091	ENSOARG00000006251	ENSOART00000006808	CD109	CD109 molecule
LFEC	LDLA	296	8	12047575	12055213	ENSOARG00000007744	ENSOART00000008429	CENPW	centromere protein W
LFEC	LDLA	297	8	49919904	49921988	ENSOARG00000013153	ENSOART00000014299	CGA	glycoprotein hormones, alpha polypeptide
LFEC	LDLA	298	8	64062392	64063183	ENSOARG00000002608	ENSOART00000002821	CITED2	Cbp/p300-interacting transactivator, with Glu/Asp-rich carboxy-terminal domain, 2
LFEC	LDLA	299	8	1763844	1881188	ENSOARG00000006410	ENSOART00000006978	COL12A1	collagen, type XII, alpha 1
LFEC	LA	299	8	1763844	1881188	ENSOARG00000006410	ENSOART00000006978	COL12A1	collagen, type XII, alpha 1
LFEC	LDLA	300	8	10144467	10231584	ENSOARG00000007379	ENSOART00000008038	DOPEY1	dopey family member 1
LFEC	LDLA	301	8	11087179	11120244	ENSOARG00000007696	ENSOART00000008380	ECHDC1	ethylmalonyl-CoA decarboxylase 1
LFEC	LDLA	302	8	63609664	63674228	ENSOARG00000000928	ENSOART00000001004	ECT2L	epithelial cell transforming 2 like
LFEC	LDLA	303	8	6787811	6798574	ENSOARG00000007109	ENSOART00000007733	ELOVL4	ELOVL fatty acid elongase 4
LFEC	LDLA	304	8	8683987	8686126	ENSOARG00000007199	ENSOART00000007830	FAM46A	family with sequence similarity 46, member A
LFEC	LDLA	305	8	37900554	37974589	ENSOARG00000011946	ENSOART00000012992	FBXL4	F-box and leucine-rich repeat protein 4
LFEC	LDLA	306	8	2033574	2194768	ENSOARG00000006499	ENSOART00000007064	FILIP1	filamin A interacting protein 1
LFEC	LA	306	8	2033574	2194768	ENSOARG00000006499	ENSOART00000007064	FILIP1	filamin A interacting protein 1
LFEC	LDLA	307	8	73648814	73670914	ENSOARG00000002736	ENSOART00000002959	GINM1	glycoprotein integral membrane 1
LFEC	LDLA	308	8	63221036	63231257	ENSOARG00000000791	ENSOART00000000845	HEBP2	heme binding protein 2
LFEC	LDLA	309	8	63897955	63909189	ENSOARG00000001155	ENSOART00000001234	HECA	headcase homolog (Drosophila)
LFEC	LDLA	310	8	12637522	12647466	ENSOARG00000007915	ENSOART00000008617	HEY2	hes-related family bHLH transcription factor with YRPW motif 2
LFEC	LDLA	311	8	12413488	12426746	ENSOARG00000007824	ENSOART00000008519	HINT3	histidine triad nucleotide binding protein 3
LFEC	LDLA	312	8	5957391	5969627	ENSOARG00000006997	ENSOART00000007609	HMGN3	high mobility group nucleosomal binding domain 3
LFEC	LDLA	313	8	4223342	4224508	ENSOARG00000019953	ENSOART00000021722	HTR1B	5-hydroxytryptamine (serotonin) receptor 1B, G protein-coupled
LFEC	LDLA	314	8	49997420	49998517	ENSOARG00000020007	ENSOART00000021781	HTR1E	5-hydroxytryptamine (serotonin) receptor 1E, G protein-coupled
LFEC	LDLA	315	8	9173895	9261065	ENSOARG00000007250	ENSOART00000007892	IBTK	inhibitor of Bruton agammaglobulinemia tyrosine kinase
LFEC	LDLA	316	8	62121227	62144778	ENSOARG00000000510	ENSOART00000000546	IFNGR1	interferon gamma receptor 1
LFEC	LDLA	317	8	62006022	62039859	ENSOARG00000000464	ENSOART00000000492	IL20RA	interleukin 20 receptor, alpha
LFEC	LDLA	318	8	62095580	62112331	ENSOARG00000000475	ENSOART00000000508	IL22RA2	interleukin 22 receptor, alpha 2
LFEC	LDLA	319	8	2667931	2775557	ENSOARG00000006728	ENSOART00000007315	IMPG1	interphotoreceptor matrix proteoglycan 1
LFEC	LA	319	8	2667931	2775557	ENSOARG00000006728	ENSOART00000007315	IMPG1	interphotoreceptor matrix proteoglycan 1
LFEC	LDLA	320	8	5632734	5652582	ENSOARG00000006789	ENSOART00000007379	IRAK1BP1	interleukin-1 receptor-associated kinase 1 binding protein 1
LFEC	LDLA	321	8	73673326	73697740	ENSOARG00000002782	ENSOART00000003014	KATNA1	katanin p60 (ATPase containing) subunit A 1
LFEC	LDLA	322	8	10975073	10997537	ENSOARG00000007660	ENSOART00000008339	KIAA0408	KIAA0408
LFEC	LDLA	323	8	73716242	73736759	ENSOARG00000002830	ENSOART00000003064	LATS1	large tumor suppressor kinase 1
LFEC	LDLA	324	8	6267692	6315875	ENSOARG00000007047	ENSOART00000007668	LCA5	Leber congenital amaurosis 5
LFEC	LDLA	325	8	61577863	61807090	ENSOARG00000000337	ENSOART00000000359	MAP3K5	mitogen-activated protein kinase kinase kinase 5
LFEC	LDLA	326	8	61395891	61454357	ENSOARG00000000249	ENSOART00000000265	MAP7	microtubule-associated protein 7
LFEC	LDLA	327	8	10276893	10461247	ENSOARG00000007496	ENSOART00000008163	ME1	malic enzyme 1, NADP(+)-dependent, cytosolic
LFEC	LDLA	328	8	2543505	2642538	ENSOARG00000006673	ENSOART00000007258	MYO6	myosin VI
LFEC	LA	328	8	2543505	2642538	ENSOARG00000006673	ENSOART00000007258	MYO6	myosin VI
LFEC	LDLA	329	8	12446609	12579375	ENSOARG00000007878	ENSOART00000008586	NCOA7	nuclear receptor coactivator 7
LFEC	LDLA	330	8	63237954	63382353	ENSOARG00000000810	ENSOART00000000869	NHSL1	NHS-like 1
LFEC	LDLA	331	8	73755631	73766567	ENSOARG00000002841	ENSOART00000003080	NUP43	nucleoporin 43kDa
LFEC	LDLA	332	8	62414198	62414857	ENSOARG00000002572	ENSOART00000002785	OLIG3	oligodendrocyte transcription factor 3
LFEC	LDLA	333	8	73781503	73809516	ENSOARG00000002890	ENSOART00000003130	PCMT1	protein-L-isoaspartate (D-aspartate) O-methyltransferase
LFEC	LDLA	334	8	61071786	61228713	ENSOARG00000015035	ENSOART00000016364	PDE7B	phosphodiesterase 7B
LFEC	LDLA	335	8	62931849	62944375	ENSOARG00000000612	ENSOART00000000654	PERP	PERP, TP53 apoptosis effector
LFEC	LDLA	336	8	61807965	61916494	ENSOARG00000000382	ENSOART00000000407	PEX7	peroxisomal biogenesis factor 7
LFEC	LDLA	337	8	10231626	10258911	ENSOARG00000007448	ENSOART00000008111	PGM3	phosphoglucomutase 3
LFEC	LDLA	338	8	5690526	5800596	ENSOARG00000006899	ENSOART00000007518	PHIP	pleckstrin homology domain interacting protein
LFEC	LDLA	339	8	38012100	38012714	ENSOARG00000019980	ENSOART00000021753	POU3F1	POU class 3 homeobox 1
LFEC	LDLA	340	8	73595183	73629522	ENSOARG00000002675	ENSOART00000002900	PPIL4	peptidylprolyl isomerase (cyclophilin)-like 4
LFEC	LDLA	341	8	10600314	10601552	ENSOARG00000019961	ENSOART00000021729	PRSS35	protease, serine, 35
LFEC	LDLA	342	8	63676667	63765556	ENSOARG00000001051	ENSOART00000001139	REPS1	RALBP1 associated Eps domain containing 1
LFEC	LDLA	343	8	11122340	11143754	ENSOARG00000007706	ENSOART00000008388	RNF146	Uncharacterized protein
LFEC	LDLA	344	8	11210668	11265163	ENSOARG00000007731	ENSOART00000008414	RSPO3	R-spondin 3
LFEC	LDLA	345	8	10259529	10262959	ENSOARG00000007481	ENSOART00000008144	RWDD2A	RWD domain containing 2A
LFEC	LDLA	346	8	71689824	71690150	ENSOARG00000002635	ENSOART00000002852	SAMD5	sterile alpha motif domain containing 5
LFEC	LDLA	347	8	72614955	72716424	ENSOARG00000002482	ENSOART00000002695	SASH1	SAM and SH3 domain containing 1
LFEC	LDLA	348	8	2363024	2462058	ENSOARG00000006569	ENSOART00000007143	SENP6	SUMO1/sentrin specific peptidase 6
LFEC	LA	348	8	2363024	2462058	ENSOARG00000006569	ENSOART00000007143	SENP6	SUMO1/sentrin specific peptidase 6
LFEC	LDLA	349	8	6486667	6506925	ENSOARG00000007077	ENSOART00000007696	SH3BGRL2	SH3 domain binding glutamate-rich protein like 2
LFEC	LDLA	350	8	61924643	61926684	ENSOARG00000000425	ENSOART00000000448	SLC35D3	solute carrier family 35, member D3
LFEC	LDLA	351	8	10618226	10724797	ENSOARG00000007561	ENSOART00000008233	SNAP91	synaptosomal-associated protein, 91kDa
LFEC	LDLA	352	8	10918094	10962240	ENSOARG00000007631	ENSOART00000008312	SOGA3	Uncharacterized protein
LFEC	LDLA	353	8	71462635	71627320	ENSOARG00000002348	ENSOART00000002551	STXBP5	syntaxin binding protein 5 (tomosyn)
LFEC	LDLA	354	8	73468896	73508892	ENSOARG00000002578	ENSOART00000002792	TAB2	TGF-beta activated kinase 1/MAP3K7 binding protein 2
LFEC	LDLA	355	8	1956483	1993209	ENSOARG00000006481	ENSOART00000007046	TMEM30A	transmembrane protein 30A
LFEC	LA	355	8	1956483	1993209	ENSOARG00000006481	ENSOART00000007046	TMEM30A	transmembrane protein 30A
LFEC	LDLA	356	8	62766200	62780534	ENSOARG00000000569	ENSOART00000000610	TNFAIP3	tumor necrosis factor, alpha-induced protein 3
LFEC	LDLA	357	8	9372575	9373336	ENSOARG00000019958	ENSOART00000021726	TPBG	trophoblast glycoprotein
LFEC	LDLA	358	8	12289261	12403664	ENSOARG00000007813	ENSOART00000008509	TRMT11	tRNA methyltransferase 11 homolog (S. cerevisiae)
LFEC	LDLA	359	8	6885832	6925302	ENSOARG00000007151	ENSOART00000007781	TTK	TTK protein kinase
LFEC	LDLA	360	8	63935536	63987693	ENSOARG00000001219	ENSOART00000001307	TXLNB	taxilin beta

LFEC	LDLA	361	8	9947372	10112581	ENSOARG00000007302	ENSOART00000007945	UBE3D	ubiquitin protein ligase E3D
LFEC	LDLA	362	8	73072326	73189210	ENSOARG00000002548	ENSOART00000002759	UST	uronyl-2-sulfotransferase
LFEC	LDLA	363	8	73543092	73565983	ENSOARG00000002626	ENSOART00000002842	ZC3H12D	zinc finger CCCH-type containing 12D
LFEC	LDLA	364	8	49750324	49791014	ENSOARG00000013132	ENSOART00000014272	ZNF292	zinc finger protein 292
LFEC	LDLA	365	9	16986810	17191518	ENSOARG00000004606	ENSOART00000005030	COL22A1	collagen, type XXII, alpha 1
LFEC	LDLA	366	9	5951709	5952375	ENSOARG00000012209	ENSOART00000013273	PRKAR1A	protein kinase, cAMP-dependent, regulatory, type I, alpha
LFEC	LDLA	367	12	3693804	3701798	ENSOARG00000006176	ENSOART00000006718	DYRK3	dual-specificity tyrosine-(Y)-phosphorylation regulated kinase 3
LFEC	LDLA	368	12	3634935	3656632	ENSOARG00000005917	ENSOART00000006444	EIF2D	eukaryotic translation initiation factor 2D
LFEC	LDLA	369	12	3528897	3547996	ENSOARG00000005570	ENSOART00000006075	IKBKE	inhibitor of kappa light polypeptide gene enhancer in B-cells, kinase epsilon
LFEC	LDLA	370	12	3820935	3824667	ENSOARG00000006292	ENSOART00000006848	IL10	interleukin 10
LFEC	LDLA	371	12	3779570	3783235	ENSOARG00000006187	ENSOART00000006725	MAPKAPK2	mitogen-activated protein kinase-activated protein kinase 2
LFEC	LDLA	372	12	3599548	3629996	ENSOARG00000005737	ENSOART00000006244	RASSF5	Ras association (RalGDS/AF-6) domain family member 5
LFEC	LDLA	373	12	3266745	3517572	ENSOARG00000005343	ENSOART00000005828	SRGAP2	SLIT-ROBO Rho GTPase activating protein 2
LFEC	LDLA	374	20	4600125	4742115	ENSOARG00000006378	ENSOART00000006934	BMP5	bone morphogenetic protein 5
LFEC	LDLA	375	20	4979745	5104686	ENSOARG00000006418	ENSOART00000006973	HMGCLL1	3-hydroxymethyl-3-methylglutaryl-CoA lyase-like 1
LFEC	LDLA	376	21	43889040	43900655	ENSOARG00000006670	ENSOART00000007257	ACTN3	actinin, alpha 3 (gene/pseudogene)
LFEC	LDLA	377	21	31844391	32046759	ENSOARG00000013548	ENSOART00000014736	BARX2	BARX homeobox 2
LFEC	LDLA	378	21	43856804	43872654	ENSOARG00000005964	ENSOART00000006492	BBS1	Uncharacterized protein
LFEC	LDLA	379	21	43926438	43929011	ENSOARG00000015663	ENSOART00000017045	CCDC87	coiled-coil domain containing 87
LFEC	LDLA	380	21	43928754	43942226	ENSOARG00000007385	ENSOART00000008042	CCS	copper chaperone for superoxide dismutase
LFEC	LDLA	381	21	43901359	43906691	ENSOARG00000007209	ENSOART00000007841	CTSF	cathepsin F
LFEC	LDLA	382	21	43823760	43854938	ENSOARG00000005600	ENSOART00000006104	DPP3	dipeptidyl-peptidase 3
LFEC	LDLA	383	21	32204737	32236309	ENSOARG00000013611	ENSOART00000014809	JAM3	junctional adhesion molecule 3
LFEC	LDLA	384	21	8306989	8531593	ENSOARG00000004257	ENSOART00000004639	ME3	malic enzyme 3, NADP(+)-dependent, mitochondrial
LFEC	LDLA	385	21	43785795	43788896	ENSOARG00000005178	ENSOART00000005637	MRPL11	mitochondrial ribosomal protein L11
LFEC	LDLA	386	21	43768738	43776312	ENSOARG00000005005	ENSOART00000005452	NPAS4	neuronal PAS domain protein 4
LFEC	LDLA	387	21	43811532	43819660	ENSOARG00000005351	ENSOART00000005836	PELI3	pellino E3 ubiquitin protein ligase family member 3
LFEC	LDLA	388	21	8160517	8161644	ENSOARG00000014444	ENSOART00000015725	PRSS23	protease, serine, 23
LFEC	LDLA	389	21	43951242	43959921	ENSOARG00000007565	ENSOART00000008236	RBM14	RNA binding motif protein 14
LFEC	LDLA	390	21	43992971	43999246	ENSOARG00000007759	ENSOART00000008444	RBM4B	RNA binding motif protein 4B
LFEC	LDLA	391	21	32201446	32201838	ENSOARG00000015615	ENSOART00000016989	RPS15A	Uncharacterized protein
LFEC	LDLA	392	21	44008864	44040998	ENSOARG00000007959	ENSOART00000008671	SPTBN2	spectrin, beta, non-erythrocytic 2
LFEC	LDLA	393	21	43881708	43888100	ENSOARG00000006309	ENSOART00000006866	ZDHHC24	zinc finger, DHHC-type containing 24
LFEC	LDLA	394	24	18027363	18058341	ENSOARG00000012681	ENSOART00000013786	ACSM5	acyl-CoA synthetase medium-chain family member 5
LFEC	LDLA	395	24	2422235	2428354	ENSOARG00000001019	ENSOART00000001093	CCDC64B	coiled-coil domain containing 64B
LFEC	LDLA	396	24	2411230	2411880	ENSOARG00000010602	ENSOART00000011533	CLDN6	claudin 6
LFEC	LDLA	397	24	2409319	2409972	ENSOARG00000010593	ENSOART00000011522	CLDN9	claudin 9
LFEC	LDLA	398	24	2326580	2328950	ENSOARG00000000607	ENSOART00000000651	FLYWCH1	FLYWCH-type zinc finger 1
LFEC	LDLA	399	24	2300371	2301982	ENSOARG00000000601	ENSOART00000000647	FLYWCH2	FLYWCH family member 2
LFEC	LDLA	400	24	17926803	17941710	ENSOARG00000012472	ENSOART00000013563	GP2	glycoprotein 2 (zymogen granule membrane)
LFEC	LDLA	401	24	2417720	2418730	ENSOARG00000000865	ENSOART00000000924	HCFC1R1	host cell factor C1 regulator 1 (XPO1 dependent)
LFEC	LDLA	402	24	2085032	2099728	ENSOARG00000018685	ENSOART00000020337	KCTD5	potassium channel tetramerization domain containing 5
LFEC	LDLA	403	24	2354639	2358305	ENSOARG00000000662	ENSOART00000000713	KREMEN2	kringle containing transmembrane protein 2
LFEC	LDLA	404	24	2452784	2462350	ENSOARG00000001161	ENSOART00000001242	MMP25	matrix metallopeptidase 25
LFEC	LDLA	405	24	2360706	2362516	ENSOARG00000000676	ENSOART00000000726	PAQR4	progestin and adipoQ receptor family member IV
LFEC	LDLA	406	24	17968114	18015100	ENSOARG00000012592	ENSOART00000013693	PDILT	protein disulfide isomerase-like, testis expressed
LFEC	LDLA	407	24	2046607	2079956	ENSOARG00000018633	ENSOART00000020280	PDPK1	3-phosphoinositide dependent protein kinase 1
LFEC	LDLA	408	24	2363506	2367547	ENSOARG00000000736	ENSOART00000000792	PKMYT1	protein kinase, membrane associated tyrosine/threonine 1
LFEC	LDLA	409	24	2209586	2214013	ENSOARG00000000309	ENSOART00000000327	PRSS21	protease, serine, 21 (testisin)
LFEC	LDLA	410	24	2153764	2159156	ENSOARG00000000159	ENSOART00000000160	PRSS22	protease, serine, 22
LFEC	LDLA	411	24	2109485	2117255	ENSOARG00000018701	ENSOART00000020355	PRSS27	protease, serine 27
LFEC	LDLA	412	24	2258813	2272750	ENSOARG00000000491	ENSOART00000000529	SRRM2	serine/arginine repetitive matrix 2
LFEC	LDLA	413	24	2254105	2257982	ENSOARG00000000340	ENSOART00000000358	TCEB2	transcription elongation factor B (SIII), polypeptide 2 (18kDa, elongin B)
LFEC	LDLA	414	24	2419135	2421780	ENSOARG00000000909	ENSOART00000000975	THOC6	THO complex 6
LFEC	LDLA	415	24	2415241	2416697	ENSOARG00000000747	ENSOART00000000800	TNFRSF12A	tumor necrosis factor receptor superfamily, member 12A
LFEC	LDLA	416	24	17947831	17963018	ENSOARG00000012556	ENSOART00000013656	UMOD	uromodulin

Barrido genómico con el SNP-chip ovino 50K para la detección de QTL con influencia sobre la resistencia a nematodos intestinales en el ganado ovino de raza churra: análisis de ligamiento para el recuento de huevos en heces

Marina Atlija[1], Beatriz Gutiérrez-Gil[1], María Martinez Valladares[2], Luis Fernando de la Fuente Crespo [1], Juan-Jose Arranz[1].

[1] Departamento de Producción Animal, Facultad de Veterinaria, Universidad de León, Campus de Vegazana s/n, 24071 León.

[2] Instituto de Ganadería de Montaña. CSIC-ULE, 24346 Grulleros, León.

XV Jornadas sobre producción animal, AIDA (asociación interprofesional para el desarrollo agrario). Zaragoza, España. 14-15 May 2013.

BARRIDO GENÓMICO CON EL SNP-CHIP OVINO 50K PARA LA DETECCIÓN DE QTL CON INFLUENCIA SOBRE LA RESISTENCIA A NEMATODOS INTESTINALES EN EL GANADO OVINO DE RAZA CHURRA: ANÁLISIS DE LIGAMIENTO PARA EL RECUENTO DE HUEVOS EN HECES

Atlija[1], M., Gutierrez-Gil[1], B., Martinez Valladares[2], M., de la Fuente[1], L. F., Arranz[1], J. J.
[1] Departamento de Producción Animal, Facultad de Veterinaria, Universidad de León, 24071 León. [2]Instituto de Ganadería de Montaña. CSIC-ULE, 24346 Grulleros, León.
e-mail: matl@unileon.es

INTRODUCCIÓN

Las infecciones por nematodos gastrointestinales (GIN) en el ganado ovino siguen siendo una de las enfermedades parasitarias más prevalentes en el ganado ovino, causando importantes pérdidas económicas debido a sus efectos negativos sobre el crecimiento en corderos y la producción de leche en ovejas adultas. El control de GIN en rumiantes se basa en gran medida en el uso de fármacos antihelmínticos en combinación con estrategias de manejo de las zonas de pastoreo. El incremento en la prevalencia de la resistencia parasitaria a los antihelmínticos ha llevado, en los últimos años, a la búsqueda de métodos de controles alternativos entre los cuales cabe destacar la selección genética hacia una mayor resistencia de los animales a estas infecciones parasitarias. Existen varios fenotipos asociados a la resistencia a las GIN. El recuento de huevos en heces, o FEC *(*de inglés *Faecal egg count)*, es el indicador tradicional usado más comúnmente para valorar el nivel de infección parasitaria en base al número de huevos por gramo de heces. Este carácter también pone de manifiesto el producto de los nematodos adultos establecidos y la fecundidad media de las poblaciones parasitarias residentes (Bishop & Stear, 2000). Otros indicadores del nivel de infección parasitaria son el nivel plasmático de inmunoglobulina A (IgA) y de pepsinógeno (Peps). Estudios previos han identificado QTL en relación a la resistencia ovina a GIN (Crawford et al., 2006; Marshall et al., 2009; Gutiérrez-Gil et al., 2009). Es de señalar el barrido genómico basado en 181 marcadores microsatélites realizado en una población de ganado ovino lechero de raza Churra (Gutiérrez-Gil et al., 2009) en el que se identificó un QTL significativo a nivel de significación genómico en el cromosoma OAR6, y otros cuatro QTL a nivel cromosómico en OAR1, OAR10 y OAR14. En el presente trabajo se presentan los resultados de un análisis de ligamiento para el carácter FEC realizado en otra población ovina de raza Churra genotipada con el SNP-chip ovino de media densidad (*Illumina OvineSNP50 BeadChip*).

MATERIAL Y MÉTODOS

Las medidas fenotípicas para el carácter en estudio se obtuvieron de un total de 596 ovejas adultas de raza Churra repartidas en 21 rebaños, de manejo semiextensivo, distribuidos en 8 de las provincias de Castilla y León. Los animales muestreados están distribuidos en 15 familias de medio-hermanas del núcleo de selección de ANCHE. El tamaño medio por familia fue de 33 hijas por macho. Se realizó un único muestreo por rebaño, en el que se obtuvieron para cada animal muestras de heces y sangre. Las heces se recogieron directamente del recto y fueron procesadas para determinar el número de huevos por gramo de heces utilizando una modificación del método McMaster (MAFF, 1986). Tras la transformación logarítmica de los datos, se obtuvieron los valores fenotípicos, estimados como la desviación de la media poblacional del dato fenotípico bruto de cada animal corregido para el efecto rebaño que, debido al diseño experimental, englobó otros factores ambientales relevantes. Se analizaron 43 784 SNPs que habían pasado el control de calidad de genotipos descrito en un trabajo previo (García-Gámez et al., 2012), donde también se elaboró el mapa genético para la población en estudio con una equivalencia de 1 Mb ~ 1 cM para convertir las distancias físicas en distancias genéticas. Para el análisis de ligamiento realizado en los 26 autosomas ovinos se utilizó el programa *QTLMap* (Filangi et al., 2010). Los umbrales de significación a nivel *chromosome-wise* (p_c-value) se obtuvieron mediante un test de permutaciones y a nivel genómico considerando que se analizaron 26 autosomas independientes (*genome-wise;* p_g-value). Para los QTL significativos identificados se calculó el intervalo de confianza (IC) mediante el método LOD drop-off (Lander & Botstein 1989).

RESULTADOS Y DISCUSIÓN

El análisis de ligamiento realizado para el carácter FEC a lo largo del genoma autosómico ovino identificó tres QTL a nivel de significación del 5% *chromosome-wise* en OAR4, 6 y 25, y un QTL significativo al nivel 1% *chromosome-wise* en OAR8 (Figura 1). La caracterización de los QTL detectados en el análisis de toda la población (*across-family*) se muestra en la Tabla 1, donde también se puede encontrar información relativa a las familias que mostraron evidencias significativas de segregación de los QTL identificados a nivel poblacional. Para el QTL menos significativo, localizado en OAR25, se identificaron dos familias segregantes, mientras que en los otros tres casos fueron tres las familias que en el análisis intrafamiliar mostraron p_c-values < 0.05. La posición del QTL sugerida por los análisis intrafamiliares discrepó en algunos casos de la posición del pico del QTL en el análisis intrafamiliar, lo que puede deberse a diferencia en la informatividad de los marcadores o, alternativamente, de la presencia de diferentes QTL segregantes entre las diferentes familias.

Figura 1. Resultados del análisis de ligamiento realizado en la población ovina analizada en este estudio para el carácter FEC

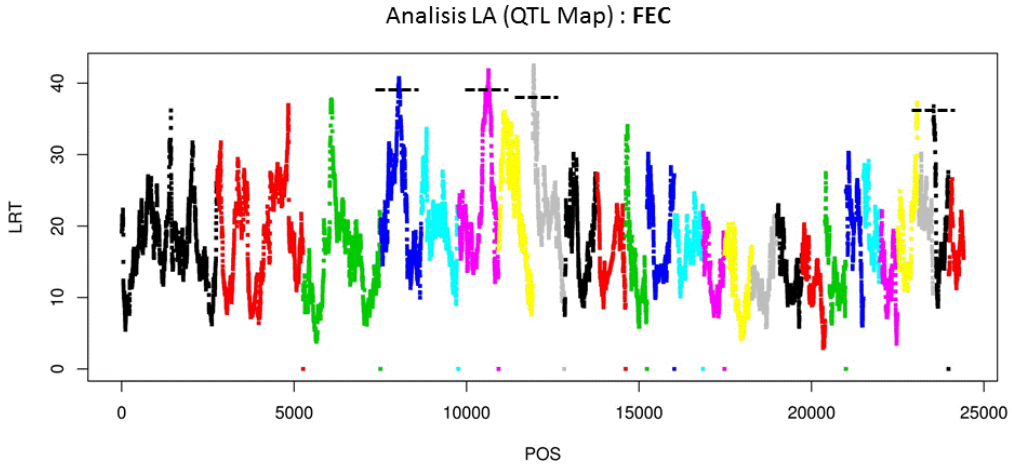

Tabla 1. Caracterización de los QTL identificados a nivel poblacional para el indicador de resistencia a parasitosis gastrointestinales FEC. Se muestran, también los resultados del análisis intrafamiliar para las familias que mostraron evidencia estadística de segregación para alguno de los QTL detectados (p_c-value < 0.05).

OAR	LRT max.	Pos. (cM) LRT max.	Marcadores flanqueantes LRT max.	IC (cM)	Familias segregantes (pc < 0.05)	LRT max.	Pos. (cM) LRT max
4	40.70	54.54	[OAR4_58493210.1 - OAR4_58541568.1]	51.5 - 57.6	fam. 01 fam. 04 fam. 05	11.73 9.70 10.79	54.84 117.94 48.34
6	41.81	87.81	[OAR6_95930760.1 - OAR6_96088929.1]	80.7 – 91.5	fam. 01 fam. 07 fam. 11	10.98 8.73 9.49	95.11 90.21 86.91
8	42.48	2	[OAR8_2125287.1 - OAR8_2209080.1]	1.0 - 3.6	fam. 02 fam. 04 fam. 11	7.77 12.47 9.86	6.40 31.30 1.80
25	36.77	0.88	[OAR25_1031652.1 - s21252.1]	0.1 - 4.1	fam. 05 fam. 16	12.10 13.47	43.28 2.68

El QTL identificado en la parte media de OAR4 se localizó cerca de un QTL previamente descrito para FEC (*Haemonchus contortus*) por Marshall et al. (2009). A este respecto, la coincidencia más destacable fue la identificada en OAR6, ya que el IC aquí estimado para este QTL se solapa con el intervalo flanqueante del QTL más significativo identificado en Churra para la resistencia parasitaria a GIN, y que influía también el recuento de huevos en heces (Gutiérrez-Gil et al., 2009). Los dos QTL identificados en OAR8 y OAR25 se

localizaron en el extremo proximal del correspondiente grupo de ligamiento. Estos cromosomas también contienen QTL previamente descritos en relación a la resistencia a GIN, aunque en ambos casos el máximo estadísticode esos QTL se localiza en una región más distal del cromosoma (Marshall et al., 2009; Crawford et al., 2006) que la identificada como candidata en el presente estudio. Con el objetivo de confirmar los resultados aquí presentados e identificar nuevas regiones de interés, pretendemos realizar análisis adicionales basados en el análisis de ligamiento combinado con análisis de desequilibrio de ligamiento (LDLA) o análisis de asociación a nivel genómico (GWAS). Del mismo modo se planea el estudio de otros fenotipos indicadores de resistencia a GIN, como el nivel plasmático de IgA. La identificación del QTL del cromosoma 6, localizado en la misma región y con efectos sobre el mismo carácter que el descrito anteriormente por Gutiérrez-Gil et al. (2009), sugiere la confirmación de dicho efecto e indicaría la conveniencia de centrar esfuerzos en el mapeo fino de dicha región.

REFERENCIAS BIBLIOGRÁFICAS

• Bishop S.C. & Stear M.J. 2000. Parasitology, 121: 435-440. • Crawford A.M., Paterson K.A., Dodds K.G., Diez Tascon C., Williamson P.A., Roberts Thomson M., et al. 2006. BMC Genomics 18:178. • Filangi O., Moreno C., Gilbert H., Legarra A., Le Roy P., Elsen J.M. 2010. Proceedings of the 9th World Congress on Genetics Applied to Livestock Production: 1-6 August; Leipzig. • García-Gámez E., Sahana G., Gutiérrez-Gil B., Arranz JJ. 2012. BMC Genet.13:43. • Gutiérrez-Gil B., Pérez J., Alvarez L., Martínez-Valladares M., de la Fuente L.F., Bayón Y., Meana A., San Primitivo F., Rojo-Vázquez F.A., Arranz J.J. 2009. Genet Sel Evol. 28;41:46. • Lander E.S., Botstein D. 1989. Genetics 121: 185–99. • MAFF (Ministry of Agriculture, Fisheries and Food). 1986. Manual of Veterinary Parasitological Laboratory Techniques, 3rd edn. London, GB. • Marshall K., Maddox J.F., Lee S.H., Zhang Y., Kahn L., Graser H.U. et al. 2009. Anim Genet. 40: 262-72. • McKellar Q.A., Duncan J.L., Armour J., & McWilliam P. 1986. Res Vet Sci 40, 367-371. • Smith W.D., Jackson F., Jackson E., & Williams J. 1985. Journal of Comparative Pathology 95, 235-245. • Stear M.J., Bishop S.C., Doligalska M., Duncan J.L., Holmes P.H., Irvine J., McCririe L., McKellar Q.A., Sinski E., Murray M. 1995. *Parasite Immunol.* 17: 643–652. • Ziegler I.R., König F.P. 2010. A Statistical Approach to Genetic Epidemiology: Concepts and Applications. 2nd Ed. Wiley-Blackwell.

Agradecimientos: Este trabajo está financiado por los proyectos LE245- A12-2 financiado por la Junta de Castilla y León y *NematodeSystemHealth-Initial Training Network* de la Comisión Europea. M.A. Está financiada por el proyecto *NematodeSystemHealth-Initial Training Network*.

A GENOME SCAN WITH THE OVINE 50K SNP-CHIP FOR THE DETECTION OF QTL INFLUENCING RESISTANCE TO GASTROINTESTINAL NEMATODES IN SPANISH CHURRA SHEEP: LINKAGE ANALYSIS FOR FAECAL EGG COUNT*.*

ABSTRACT: Infections with gastrointestinal nematodes (GIN) remain one of the most prevalent parasitic diseases causing major economic losses in the sheep industries worldwide. In the last years, the increasing prevalence of resistance to anthelmintic has led to the search for alternative control methods such as selective breeding for increased GIN resistance. This study presents a linkage analysis for detection of QTL for faecal egg count (FEC), the traditional indicator trait commonly used to assess the level of GIN by the number of eggs per gram of faeces, in a commercial population of Spanish Churra sheep. The resource population included 596 adult ewes from 21 flocks and 15 half-sib families of the selection nucleus of the Churra sheep breeding programme. Faecal samples were collected from the studied animals for which genotypes for the Illumina OvineSNP50 BeadChip were already available. Chromosome-wise significant QTL were detected on chromosomes 4, 6, 8 and 25. The QTL identified on the first two of these chromosomes showed interesting coincidences with QTL previously reported in sheep for indicators of resistance to GIN. The results reported here suggest that the most significant QTL previously reported for FEC in Churra sheep by a microsatellite-based genome scan, on chromosome 6, is confirmed in the new analysed population.

Keywords: sheep, gastrointestinal nematode infection, resistance, QTL, linkage

Search of genomic regions influencing faecal egg count, as an indicator of resistance to gastrointestinal nematode infections, based on the analysis of the OvineSNP50 BeadChip

Marina Atlija[1], Juan-Jose Arranz[1], María Martinez-Valladares[2], Beatriz Gutiérrez-Gil[1]

[1] Departamento de Producción Animal, Facultad de Veterinaria, Universidad de León, Campus de Vegazana s/n, 24071 León.

[2] Livestock Mountain Institute. The Spanish National Research Council-ULE, 24346 Grulleros, León, Spain.

Proceedings, 10th World Congress of Genetics Applied to Livestock Production (WCGALP). Vancouver, Canada. 17-22 August, 2014.

Search of genomic regions influencing faecal egg count, as an indicator of resistance to gastrointestinal nematode infections, based on the analysis of the OvineSNP50 BeadChip

M. Atlija[1], J.J. Arranz[1], M. Martinez-Valladares[2] and B. Gutierrez-Gil[1]
[1]University of León (ULE), [2]Livestock Mountain Institute. The Spanish National Research Council-ULE, León, Spain.

ABSTRACT: The objective of this study was to perform a preliminary search of genomic regions including Quantitative Trait Loci (QTL) underlying the resistance to gastrointestinal nematode infections (GIN) in a commercial population of Churra sheep by performing linkage (LA) and genome-wide association (GWA) analyses based on SNP-chip data. The studied population included 533 Churra ewes belonging to 15 half-sib families. The ewes and their sires were genotyped with the Illumina 50K BeadChip, whereas measurements of faecal egg count (FEC) were obtained for the ewes using the McMaster method. The LA analysis identified one QTL reaching the 5% chromosome-wise significance level on OAR8, whereas the GWA study found one marker exceeding that significance level on OAR6. A search of candidate genes was performed in the confidence intervals estimated for the QTL detected on these two chromosomes.
Keywords:
Gastrointestinal nematode infection
QTL
GWA analysis
Churra sheep

Introduction

In the last few decades, much effort has been developed to understand the host-parasite relationship. The interest of the sheep industry worldwide on this topic (Taylor (2012)) is driven by the persistent problem with GIN in grazing sheep. In these populations the efficient control of the parasites, which was principally based on anthelmintic treatments, is now limited by the increasing development of nematode resistances to several chemical groups of drugs. Previous studies aiming the detection of QTL associated with nematode resistance were based on low density maps of microsatellite markers (http://www.animalgenome.org/QTLdb/sheep). However, the variety of parasites and sheep breed considered in these studies has resulted in lack of agreement among the results. As a consequence, there is merit in carrying out additional studies based on higher marker density to identify genetic variants with a clear effect on the complex trait of parasite resistance. For now, few GWA studies have been reported in sheep in relation to GIN resistance traits (e.g. Kemper et al. (2011); Riggio et al. (2013)). These GWA studies have been conducted in lambs of breeds specialized for meat and/or wool production, whereas similar analyses in adult dairy sheep populations have not yet been reported. In a previous microsatellite-based genome scan performed in Spanish Churra sheep some regions were found to influence faecal egg count (FEC). In the present study, the genotypes generated with the *Illumina OvineSNP50 BeadChip* were used to identify genomic regions related to this same indicator trait in a different commercial population of Churra sheep by exploiting both LA and GWA analyses.

Materials and Methods

Resource population. Phenotypic and genotypic information for 533 Churra sheep from the Selection Nucleus of the National Association of Churra breeders (ANCHE) was analyzed in the present study. The animals are distributed in 15 half-sib families, with an average family size of 39 daughters per sire (range: 7 to 60). Samples were collected from 17 naturally infected flocks located in the Autonomous Region of Castilla y León. The phenotype trait, FEC, was determined by floating the faeces in zinc sulfate (d=1.33) solution in a McMaster slide and counting the eggs (MAFF (1986)). The samples showed a low level of FEC related to the exceptional scarce precipitation before and during the sampling period. The estimated prevalence of GIN by FEC in flock was 88.2% (mean=42.8 epg) and in sheep was 45.4% (mean= 39.4 epg). Presence of *Trichostrongylus* spp. (49.3%) and *Teladorsagia* spp. (48.6%) was confirmed in all the flocks.

Data analysis. Prior to further analysis, FEC measurements were log-transformed (LFEC) to get an approximation to the normal distribution. For further analyses, the yield deviations (YD) of raw data were used as dependent variables. The YD estimate was calculated following a multivariate animal model in which LFEC was corrected for the fixed flock effect. DNA samples from a larger population of 1,696 individuals (García-Gámez et al. (2012)) that included the animals with FEC measurements analyzed here had been genotyped with the OvineSNP50 BeadChip. In this study, we performed a quality control (QC) of genotypes for the larger population, and following the steps detailed by (García-Gámez et al. (2012)), but after updating the marker order and genome positions according to the most recent version of the Ovine Genome Assembly, v3.1 (www.livestockgenomics.csiro.au/sheep/oar3.1.php). A total of 43,613 SNP located in the ovine autosomes passed the QC in the larger population. From that subset of markers, the genotypes for the smallest population with LFEC available records were subjected to the analyses presented here.

A 1 cM~1 Mb conversion rate was used to obtain the linkage maps used in the classical LA genome scan, which was performed with the QTLMap software (Filangi et al. (2010)). The QTL search was performed every 0.1 cM using the software analysis options corresponding to LA. Significance thresholds at the chromosome-wise level were

determined by 1,000 permutations, and used to obtain the genome-wise significance thresholds by correcting for the total number of chromosomes under analyses. After conversion of LRT values to the LOD values (Beraldi et al. (2007)), confidence intervals (CI) for the significant QTL were estimated using the 1-LOD drop-off method.

The GWA analysis was performed using the DMU software (available at http://dmu.agtsci.dk) based on a linear mixed model (LMM) as previously explained by García-Gamez et al. (2012). The significance levels corresponding to each analyzed marker were corrected with a Bonferroni correction for the total number of markers analyzed across the individual chromosomes and the genome to obtain the corresponding significance thresholds.

Considering the estimated CI from LA, positional candidate genes were extracted from the Ovine Genome Assembly v3.1, available at the Ensembl database (www.ensembl.org/Ovis_aries/Info/Index) and using BioMart (www.ensembl.org/biomart/martview/). From the initial list of positional candidates, the functional candidates were identified based on the physiological known function and literature reports related to the immune response in nematode resistance.

Results and Discussion

The LA analysis for FEC identified one significant QTL at the 5% chromosome-wise level on OAR8, with the peak located at 2 Mb. Six families were significant for this QTL according to the Student-Test provided by the analysis software. The average of the QTL effect in the segregating families was 0.715 in trait units (0.460 SD). For this QTL, the estimated confidence interval (CI) spanned 2.4 Mb (range: 1 to 3.4 Mb). The LA also showed a region on OAR6 was close to the 5% chromosome-wise significance level (maximum located at 88.1 Mb) although did not exceed the threshold. The GWA analysis performed with DMU identified a 5% chromosome-wise significant association for SNP OAR6_83627682.1, located at position 76.601 Mb. The allele substitution effect estimated in trait units for this marker was -0.533 ± 0.113 (0.343 SD). None of the two analyses identified genome-wise significant associations.

Because of the coincident location between the significant result identified by the DMU analysis on OAR6 and the suggestive signal identified on that chromosome by the LA analysis of our resource population, a CI interval was also estimated for the OAR6 QTL based on the LA results. In this case, the CI involved a 12.1 Mb long interval (range 80.5 to 92.6 Mb). Eight families showed a significant Student-Test for this suggestive QTL, whereas the average size of the QTL effect in the segregating families was 0.541 in trait units (0.347 SD). The similar estimated effect for this QTL identified by both, LA and GWA analyses, supports the hypothesis that these two signals are due to the same genetic variation. The search of positional candidate genes yielded a total of 6 and 91 genes for the estimated CI of the OAR8 and OAR6 QTL regions, respectively.

Previous studies have identified significant associations for FEC on OAR8 (Crawford et al. (2006); Marshall et al. (2009); Riggio et al. (2013)), however the corresponding QTL peaks were located at a more distal region of OAR8 than the significant region reported here. Although there is not a clear relationship with parasite resistance for any of the six positional candidates extracted from the OAR6 QTL CI, it is worth mentioning that the product of one of these genes, *COL12A1* (type XII collagen), is found in association with type I collagen (COL I), whose synthesis during parasite infections is suggested to be highly dependent of TH2 cytokines response (Wynn (2004)). Other gene mapping into this CI is *SENP6*, (SUMO1/Sentrin Specific Peptidase 6), an intrinsic attenuator of the inflammation triggered by Toll Like Receptors (Liu et al. (2013)), which are known to be important in maintaining epithelial barrier function in response to enteric pathogens and parasites (Venugopal et al. (2009)).

The suggestive signal identified on OAR6 by QTLMap and the chromosome-wise significant SNP identified by our GWA study overlap with the CI of a genome-wise significant QTL previously reported for the same trait in a different population of Churra sheep, based on a microsatellite–based genome scan (Gutierrez Gill et al. (2009)). Hence, the results presented in the present work for OAR6 may be considered as the replication of the OAR6 QTL previously reported by Gutierrez Gill et al. (2009). However, the limited power of our statistical analysis, due to the large number of zero records for FEC in the analyzed sample may have influenced on the low significant level of the associations identified. Other associations reported on OAR6 for FEC, based on microsatellite markers (http://www.animalgenome.org/QTLdb/sheep) or SNP-chip data (Riggio et al. (2013)) are far away of the QTL reported here in this chromosome.

Among the 91 genes extracted from the estimated CI of the OAR6 QTL, and in addition to the casein coding genes, we have found some interesting functional candidate genes. Four of these six genes, *PF4* (Platelet factor 4), *CXCL1*, *CXCL10* (chemokine ligand 1 and 10) and *IL8* (Interleukin 8), are CXC chemokines and have a known function in relation to immune regulatory mechanisms as they have a role in cellular proliferation and differentiation of epithelial cells and in recruiting of neutrophils, monocyte and fibroblasts to the site of infections (injury) (Gillitzer and Goebeler (2001)). Among them, the coding product of *PF4* stands out due to its role to promote the development of TH2 cytokines and to inhibit the production of TH1 cytokines, the two major mechanisms of the host immune response during parasite infection. On the contrary, the *CXCL10* gene has an opposite effect than *PF4* (Romagani et al. (2005)). IL-8 is involved in cell migration and has a significant role in wound healing (Rennekampff et al. (2000)). It is a potent chemoattractant secreted by the basolateral surface of intestinal epithelial cells (IEC) and

mediates neutophiles recruitment from the lamina propria to the epithelium (Kucharzik et al. (2005)). The two other candidates, *AREG* (Amphiregulin) and *EREG* (Epiregulin), are members of the epidermal growth factor family, and their main functions are related to cellular proliferation, differentiation and survival of epithelial cells (Inatomi et al. (2006)). AREG is produced by T cells and eosinophils and its absence has an influence on delayed expulsion of *T. muris* in mouse model (Zaiss et al. (2006)).

No significant associations were found on OAR1, 10 and 14, where the previous genome-scan reported by Gutierrez-Gil et al. (2009) had identified chromosome-wise significant QTL in Churra sheep.

Conclusion

This preliminary study was based on the analysis of OvineSNP50 Beadchip genotypes in a commercial population of Spanish Churra sheep with available data for FEC, which was used as an indicator of the levels of natural infection by gastrointestinal nematodes. The LA analysis identified one novel significant QTL on 5% chromosome-wise level on OAR8, while the GWA study found one SNP exceeding that significance level on OAR6. As the same region detected by the GWA also showed a suggestive significant QTL in LA, we considered these two signals as a possible replication of a previously reported QTL for FEC in Churra sheep. Functional candidate genes have been identified for the OAR6 and OAR8 QTL reported here. Future work will be focused on the analysis of other indicators of nematode resistance such as the serum levels of immunoglobulin A.

Note: This work was supported by a competitive grant from the Castilla and León regional government (Ref. LE245A12-2). M.Atlija is funded by a MC fellowship of the EC-funded Initial Training Network (ITN) NematodeSystemHealth (Ref. 264639). B. Gutiérrez-Gil is supported by the "Ramón y Cajal" Programme of the Spanish Ministry of Economy and Competitiveness.

Literature Cited

Beraldi, D., McRae, A. F., Gratten, J. et al. (2007). *Int. J. Parasitol*. 37:121–129.

Crawford, A. M., Paterson, K. A., Dodds, K. G. et al. (2006). *BMC Genomics*. 7:178.

Filangi, O., Moreno, C., Gilbert, H. et al. (2010). Proceedings of the 9th World Congress on Genetics Applied to Livestock Production:1-6.

Gao, X., Becker, L. C., Becker, D. M. et al. (2009*). Genet. Epidemiol*. 34:100-105.

García-Gámez, E., Gutiérrez-Gil, B., Sahana, G. et al. (2012). *PLoS ONE* 7(10): e47782.

Gillitzer, R. and Goebeler, M. (2001). *J. Leukoc. Biol.* 69:513-521

Gutiérrez-Gil, B., Pérez, J., Álvarez, L. et al. (2009). *Genet. Sel. Evol*.41:46.

Inatomi, O., Andoh, A., Yagi, Y. (2006). *Int. J. Mol. Med*. 18:497–503.

Kemper, K.. E., Emery, D. L., Bishop, S. C. et al. (2011). *Genet. Res. Camb.* 93:203-219.

Kucharzik, T., Hudson III, J. T., Lügering, A. (2005). *Gut.* 54:1565–1572.

Liu, X., Chen, W., Wang, Q. et al. (2013). *PLoS Pathog*. 9(6):e1003480.

Marshall, K.., Maddox, J. F., Lee, S. H. et al. (2009). *Anim. Genet*. 40:262–272.

Ministry of Agriculture, Fisheries and Food (MAFF), (1986). HMSO, London.1-152.

Rennekampff, H. O., Hansbrough, J. F., Kiessig, V. (2000). *J. Surg. Res.* 93:41-54.

Riggio, V., Matika, O., Pong-Wong, R. et al. (2013). *Heredity*. 110:420-429.

Romagnani, P., Maggi, L., Mazzinghi, B. et al. (2005). *J. Allergy. Clin. Immunol.* 116:1372-1379.

Taylor, M. A. (2012). *Vet. Parasitol.* 189: 2–7

Venugopa, P. G., Nutman, T. B., Semnani, R. T. et al. (2009). *Immunol Res.* 43:252-263.

Wynn, T. A. (2004). 4:583-594.

Zaiss, D. M., van Loosdregt, J., Gorlani, A. et al. (2013). *Immunity*. 38:275-284.

Figure 1: Results obtained for faecal egg count based on the linkage analysis (LA; QTLMap software) presented in this study for the 26 ovine autosomes[§].

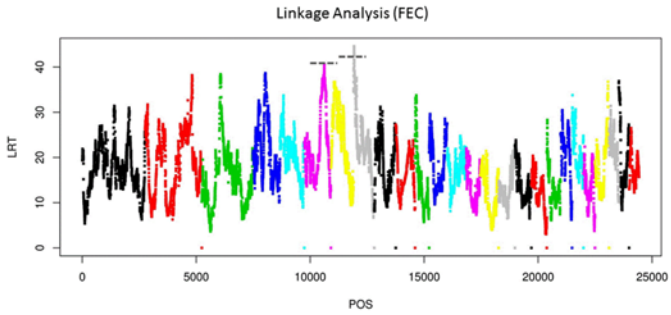

[§] Dotted lines indicate the 5% chromosome-wise significance thresholds estimated by permutation testing for chromosomes 6 and 8.

Figure 2: Result from the Genome-wide Association study (GWAS; DMU software) for faecal egg count across the whole genome (a) and in a detailed view on chromosome 6 (b) [§].

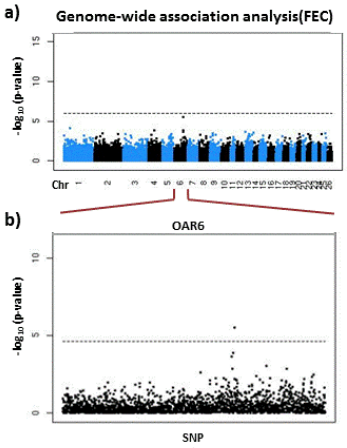

[§] The $\log_{10}$(1/P-value) is depicted here for all the 43,613 SNPs that passed the quality control performed. Dotted lines indicate the 5% genome-wise (a) and 5% chromosome-wise (b) significance thresholds estimated by the corresponding Bonferroni corrections.

Short communication: Major Histocompatibility Complex Class IIB polymorphism in an ancient Spanish breed

Marina Atlija[1], Beatriz Gutiérrez-Gil[1], Juan-Jose Arranz[1], Jördis Semmer[2], Michael J Stear[3], Johannes Buitkamp[2]

[1] Department of Animal Production, Faculty of Veterinary, Campus de Vegazana s/n, University of León, 24071 Leon, Spain

[2] Bavarian State Research Center for Agriculture, Institute of Animal Breeding, 85580 Grub, Germany

[3] University of Glasgow, Biodiversity, Animal Health and Comparative Medicine, Bearsden Road, Glasgow, G61 1QH, United Kingdom

Immunogenetics; Volume 67, Issue 9, pp 531-537. September 2015.

RESULTS

Abstract

Genes from the Major Histocompatibility Complex class II region are involved in the presentation of antigens. Therefore, they have the key role in regulating the immune response and in the resistance to infections. We investigated the Major Histocompatibility Complex class IIB genes, DRB and DQB in Churra sheep, one of the most important indigenous breed of Spain. These genes are among the most polymorphic in the mammalian genome. Furthermore, often different numbers of class IIB genes per haplotype exist, complicating the genotyping and sequencing of these genes. Especially the DQB region is only partially characterized in sheep and the repertoire of DRB and DQB alleles in Churra sheep, an ancient breed is unknown. Here we sequenced the class IIB genes for 15 rams that are the pedigree heads of a selection Nucleus herd. In total we found 12 DRB and 25 DQB alleles. From these 3 and 15 were new, respectively. 14 haplotypes carrying one or two DQB alleles could be deduced and the evolutionary relationship of these was investigated by phylogenetic trees. Based on the sequences of these most common class II alleles a more efficient genotyping system for larger numbers of Churra sheep will be developed.

Keywords

MHC class IIB, DQB, DRB, Churra sheep, genotyping, haplotypes

Introduction

The Major Histocompatibility Complex (MHC) genomic region is gene rich and encodes proteins involved in the innate and adaptive immune system but also other genes with unrelated function (The MHC sequencing consortium 1999). The MHC class I and II sub regions contain some of the most polymorphic genes in the mammalian genome. These classical MHC molecules present antigens to T cell receptors and have the key role in discriminating self from non-self and pathogen recognition by regulating the immune response. Therefore, they are involved *e.g.* in resistance or susceptibility to infectious and autoimmune diseases. A well-studied example in sheep is the association of *DRB1* alleles with resistance to intestinal parasites in sheep, e.g. *Teladorsagia circumcinta* (Buitkamp et al. 1996).

The class II molecules are heterodimers that are encoded by class IIA and class IIB genes. These are highly polymorphic and different numbers of class II genes per haplotype can occur, leading to inter-individual copy number variation. The human and mouse MHC regions are comparatively well characterized and there is a project that aims at sequencing haplotypes in humans. Within this project eight human leukocyte antigen-homozygous cell lines were analysed (Horton et al. 2008) and the longest known MHC sequence has been incorporated into the human genome assembly as a reference. The ovine MHC is located on chromosome 20 and positioned in chromosomal region q15-q23 (Hediger et al. 1991; Mahdy et al. 1989). The genomic variation of the ovine MHC has not been studied systematically for different haplotypes and the actual number of genes per haplotype can only be estimated from cDNA data, some BAC and cosmid sequences, or using direct PCR sequencing.

In Spanish Churra sheep no information about the diversity of MHC genes is available. Since this information is necessary for the development of an effective MHC genotyping system for association studies for disease resistance and will potentially reveal new alleles we sequenced an initial set of MHC class II genes of Spanish Churra rams involved in a selection project.

Ovine DRB genes

For the DRB gene family it is assumed that only one gene per haplotype is functional in sheep (designated *DRB1)* and cattle (designated *DRB3*). It contains a complex, highly

polymorphic microsatellite immediately downstream of exon 2 that is in close linkage disequilibrium with the alleles and seems to coevolve with the upstream region of exon 2 (Schwaiger et al. 1994). Ovine *DRB1* alleles are already included in the Immuno Polymorphism Database (IPD, Robinson et al. 2013) providing a systematic registry and nomenclature. Sequence information is available for many breeds, e.g. Merino, Scottish Blackface, Perendale, Texel, Suffolk, Cheviot, Corriedale, Latxa, Karrantzar, Red Maasai sheep of Kenya, and fat-tailed sheep (Ballingall and Tassi 2010; Jugo and Vicario 2000; Sayers et al. 2005; Schwaiger et al. 1993). The expressed *DRB* is extremely polymorphic with 78 alleles known in sheep and 130 in cattle.

Ovine DQB genes

In contrast, a standard nomenclature is still missing for the ovine *DQB* alleles and these are less well characterized across different breeds. Sequences available in GenBank are mainly derived from the Scottish Blackface and Merino breed (Feichtlbauer-Huber et al. 2000; van Oorschot et al. 1994). It is assumed that single or duplicated DQ haplotypes exist (Schwaiger et al. 1996), but allelic variation and the number of genes are not known for most of the sheep breeds.

Sheep used for sequencing

Spanish Churra is an autochthonous breed from the region of Castilla and León in the north-west of Spain. Churra sheep originated from the Iberian Peninsula. Churra is one of the most important indigenous breeds of Spain, known for its high specialization in milk production and the quality of its lamb. The Churra sheep have medium size, long wool, and white color with peripheral staining in black affecting the terminal portion of the ears, around the eyes, lips and nose, distal parts of the extremities. Two breeding schemes, one focused in the improvement of milk production traits and one addressing the interests for lamb production of the non-dairy flocks, are running for this breed under the coordination of the National Association of Churra Breeders (ANCHE). The herd book was established in 1977 by ANCHE, A total of 172,658 ewes were registered in 2013, of which 92% were reproductive (Ministry of Agriculture, Food and Environment, 2013). The breeding program relies on the production records of selected herds and progeny testing of rams. The Churra selection scheme was described by De la Fuente et al. (1995).

The animals studied in the present work are 15 Spanish Churra rams from the region of Castilla y León. These rams belonged to the Selection Nucleus of ANCHE and were siring 1,681 ewes from a commercial population previously analysed in a genotyping project with the *Illumina* OvineSNP50 BeadChip (Garcia-Gamez et al. 2012). As pedigree heads of this population the 15 rams studied here were selected as an initial set of animals to assess the genetic variability of the MHC class II genomic region through sequencing analysis. DNA extraction was carried out for a total of 15 frozen ram semen samples from Spanish Churra sheep and performed using classical phenol-chloroform protocol and ethanol precipitation procedures (Sambrook et al. 1989). The quality and concentration of the DNA was assessed using a spectrophotometer.

Materials and methods

G*enotyping of the DRB1 microsatellite*

The microsatellite located immediately downstream of *DRB1* exon 2 was amplified with the primers LfL#1008 and #1009 (labelled with FAM, see table 1) from 30 ng of DNA solution with standard buffer conditions (2.0 mM $MgCl_2$, dNTP's, 25 nM each), and 0.35 units of HotStar-taq polymerase (Qiagen, Hilden, Germany) in a final volume of 10 µl on a t gradient 96-well thermocycler (Biometra, Göttingen, Germany). Primer concentrations were 300 nM. Cycling was for 15 min at 95°C, and 32x[30 sec at 94°C, 45 sec at 58°C, 60 sec at 74°C]. Fragments were separated and analyzed on an ABI 3130 sequencer. The fragment lengths were determined using the GeneMapper™ software version 4.1. (Applied Biosystems, Foster City, CA, USA).

Amplification and sequencing of DRB1 *and* DQB

DRB1 exon 2 was amplified with primers LfL#984 and #987 for direct sequencing. Exon 2 was sequenced using primers LfL#984, #987 and, #1012. Cycling was for 15 min at 95°C, and 35x[30 sec at 94°C, 60 sec at 58°C, 60 sec at 74°C].

The ovine *DQB* exon 2 was amplified and sequenced using four different primer pairs: the primers published by van Oorschot and colleagues (1994), termed JM05 (LfL#991), combined with JM06 (LfL#993) and JM07 (LfL#992) as well as two additional primers pairs: LfL#994 combined with LfL#991 and #1005 combined with #1007, subsequently termed system JM06. JM07, #994, and #1007. The latter primers were used to obtain sequence information for the complete DQB exon 2 and to simplify assignment of alleles.

Cycling was done with a drop-down protocol for 15 min at 95°C, and 13x[30 sec at 94°C, 60 sec at 64°C-0.5°C/cycle, 60 sec at 74°C], and 30x[30 sec at 94°C, 45 sec at 60°C, 60 sec at 74°C].
PCR products were sequenced using the BigDye® terminator v3.1 cycle sequencing kit (Life Technologies). The reactions were run on an ABI 3130 and analyzed with the SeqScape™ software v2.7 (Applied Biosystems, Foster City, CA, USA).

Sequence analysis

Heterozygous sequences were analyzed by using the blast algorithm, either using the IPD-sequence database *(DRB1)* or an in-house library *(DQB)*. The designation of known *DRB1* follows the IPD nomenclature, the *DQB* alleles (published and new) were transferred to an internal database and named according to their accession numbers (ESM_1.pdf). We aligned nucleotide sequences with Clustal W (Thompson et al. 1994) and derived amino acid sequences with BioEdit v7.2.5 (Hall 1999). Phylogenetic trees were generated using Phylemon 2 (http://phylemon.bioinfo.cipf.es/). Distance matrices were calculated using the ProtDist option of Phylip (v.3.68, Dayhoff PAM matrix), phylogenetic trees were generated using the Neighbor-Joining Clustering method.

Results and discussion

Churra DRB1 *alleles*

The *DRB1* microsatellite fragment length ranges from 200 to >450 bps, indicating, that the full range of complex microsatellite alleles observed in other breeds (Schwaiger et al. 1993) also occur in the Churra breed. By direct sequencing of the second exon, 12 *DRB1* alleles were observed in 15 rams (Fig. 1), 3 of them being new at the amino acid level. Ovine *DRB1* alleles were deposited in Genbank under accession numbers KR048663 (OvarDRB1*0303N1), KR048664 (OvarDRB1*2001N), KR048665 (OvarDRB1*1604N2) (ESM 1). Five rams were homozygous at the microsatellite marker and *DRB1*. When comparing the amino acids occurring at the positions known to be polymorphic in *DRB* almost all except positions 31 and 76, are polymorphic in the alleles from the limited number of animals. From the 82 different amino acids occurring at the polymorphic positions of the sequences included in the IPD database 66 occur in the 15 Spanish Churra rams (Fig. 2).

Churra DQB *alleles*

The *DQB* genes were amplified with four different downstream primers (table 1). PCR products of the expected size could be obtained for all 15 rams for systems JM06, JM07, and LfL#1005-1007 and for 14 rams using LfL#994. Finally, all *DQB* alleles could unambiguously be determined. Two to four alleles per ram occurred. We obtained a total of 25 *DQB* alleles from the rams investigated (Fig. 3). The 15 new ovine *DQB* sequences were deposited in Genbank under the accession numbers KR048647 (LfL#006), KR048648 (LfL#007), KR048649 (LfL#010), KR048650 (LfL#022), KR048651 (LfL#033), KR048652 (LfL#046), KR048653 (LfL#051), KR048655 (LfL#062), KR048656 (LfL#072), KR048657 (LfL#075), KR048658 (LfL#076), KR048659 (LfL#077), KR048660 (LfL#078), KR048661 (LfL#080), KR048662 (LfL#081) (ESM_1). None of the 15 rams was homozygous at the DQB locus.

Usually, when starting to analyze MHC class II genes in a new population previously unknown alleles will occur. Using direct sequencing it can be hard to resolve all alleles from heterozygous animals due to multiple polymorphic positions. By using the additional primer systems #1007 and #994 all genotypes could be fully solved, mainly because one of the alleles that were coamplified with the systems JM06 or -JM07 could be amplified as a unique sequence with one of the additional primers. Even though only a small number of animals were sequenced, the most common alleles are likely to be included. Adding these new alleles to the database allows more efficient assignment of alleles from direct sequencing of *DQB* and *DRB* since the chance that at least one allele is known increases.

Churra class IIB haplotypes

Starting with the rams homozygous for the *DRB1* locus, 14 haplotypes could be formally deduced (table 2). The microsatellite and *DRB1* alleles are highly correlated, but between *DRB1* and *DQB* recombination seem to occur (for example haplotypes #001 - #046 - DRB1*0801 – 249 and #069 - DRB1*0801 – 249, table 2). On the other hand some haplotypes carry alleles that differ only by one base and may be generated by mutation or microconversion (DQB#079 – DRB1*2002 – 241 and DQB#079 – DRB1*2001N – 241).

Results

We observed one or two DQB genes per haplotype. This supports the findings in previous investigations (Feichtlbauer-Huber et al. 2000; Schwaiger et al. 1996; van Oorschot et al. 1994).

Two groups of DQB alleles are differentially amplified by the primers "JM06" and "JM07" that hybridize to the very 3-prime end of exon 2 (Fig. 3, corresponding to the acid motifs APFTW, JM06, and LITSLQR, JM07). It has been hypothesized that these two groups can reliably be allocated to a *DQB1* and *DQB2* locus. Even though many haplotypes carrying two DQB genes follow this scheme in Churra, two genotypes clearly contradict this hypothesis: animal 10 carries alleles LfL#57, #051, and #006 and animal 15 carries alleles LfL#076, #077, and #078 that all amplify with JM06 (ESM 2).

Therefore, it is more plausible, that, in some cases the genomic organization of haplotypes in sheep resembles the findings in cattle (Russell 2000), that contradicts the hypothesis, that the DQB alleles can be assigned to single loci solely by the 3 prime sequence of exon 2.
Phylogenetic analyses shows, that the alleles amplifying with JM06 and JM07 cluster together (Fig. 4 A). Even when the 3 prime end covered by the JM06 and JM07 primer sequences is skipped from the analysis the structure of the phylogenetic tree stays stable, with the exception of allele DQB_027 and the alleles DQB_058 and _069 (Fig. 4 B).

Concluding statement

We identified 9 known and 3 new *DRB1* as well as 10 known and 15 new *DQB* alleles in Spanish Churra sheep. Furthermore, we were able to identify 14 haplotypes in this limited number of animals. Based on these results an efficient genotyping system can be developed. It relies on the usage of additional primers, a database containing all published and new MHC class IIB alleles, and information on Churra specific haplotypes. In addition, the results contribute to the understanding of class IIB haplotype organization and evolution.

Acknowledgments

This work was supported by an EU Marie Curie ITN (FP7 #264639).

Contribution of authors:

MA: genotyping and sequencing of Spanish Churra ram samples; preparation of the manuscript

BGG, JJA Sampling animals, editing of the manuscript

JS: development of PCR conditions and evaluation of heterozygous sequences

MS: revised the manuscript

JB: development of primer systems; preparation of the manuscript

References

Ballingall KT, Tassi R (2010) Sequence-based genotyping of the sheep MHC class II DRB1 locus. Immunogenetics 62:31-9

Bondinas GP, Moustakas AK, Papadopoulos GK (2007) The spectrum of HLA-DQ and HLA-DR alleles, 2006: a listing correlating sequence and structure with function. Immunogenetics 59:539-53

Buitkamp J, Filmether P, Stear MJ, Epplen JT (1996) Class I and class II *major histocompatibility complex* alleles are associated with faecal egg counts following natural, predominantly *Ostertagia circumcincta* infection. Parasitology Research 82:693-696

De la Fuente LF, Baro JA, San Primitivo F (1995) Breeding programme for the Spanish Churra sheep breed. *In* D. G (ed.) Strategies for sheep and goat breeding. CIHEAM, Cahiers Options Méditerranéennes, Zaragoza

Feichtlbauer-Huber P, Stear MJ, Fries R, Buitkamp J (2000) Reference-strand-mediated conformation analysis of *MHC* alleles: a new method for high-resolution typing of the *Ovar-DQB* genes. Immunogenetics 51:65-68

Garcia-Gamez E, Gutierrez-Gil B, Sahana G, Sanchez JP, Bayon Y, Arranz JJ (2012) GWA analysis for milk production traits in dairy sheep and genetic support for a QTN influencing milk protein percentage in the LALBA gene. PLoS One 7:e47782

Hall TA (1999) BioEdit: a user-friendly biological sequence alignment editor and analysis program for Windows 95/98/NT. Nucl. Acids. Symp. 41:95-98

Hediger R, Ansari HA, Stranzinger GF (1991) Chromosome banding and gene localizations support extensive conservation of chromosome structure between cattle and sheep. Cytogenet Cell Genet 57:127-34

Horton R, Gibson R, Coggill P, Miretti M, Allcock RJ, Almeida J, Forbes S, Gilbert JG, Halls K, Harrow JL, Hart E, Howe K, Jackson DK, Palmer S, Roberts AN, Sims S, Stewart CA, Traherne JA, Trevanion S, Wilming L, Rogers J, de Jong PJ, Elliott JF, Sawcer S, Todd JA, Trowsdale J, Beck S (2008) Variation analysis and gene annotation of eight MHC haplotypes: the MHC Haplotype Project. Immunogenetics 60:1-18

Jugo BM, Vicario A (2000) Single-strand conformational polymorphism and sequence polymorphism of Mhc-DRB in Latxa and Karrantzar sheep: implications for Caprinae phylogeny. Immunogenetics 51:887-97.

Mahdy EA, Makinen A, Chowdhary BP, Andersson L, Gustavsson I (1989) Chromosomal localization of the ovine major histocompatibility complex (OLA) by in situ hybridization. Hereditas 111:87-90

Robinson J, Halliwell JA, McWilliam H, Lopez R, Marsh SG (2013) IPD--the Immuno Polymorphism Database. Nucleic Acids Res 41:D1234-40

Russell GC (2000) Sequence duplication at the 3' end of BoLA-DQB genes suggests multiple allelic lineages. Immunogenetics 52:101-6

Sambrook J, Fritsch EF, Maniatis T (1989) Molecular Cloning: A Laboratory Manual. Cold Spring Harbor Laboratory Press

Sayers G, Good B, Hanrahan JP, Ryan M, Angles JM, Sweeney T (2005) Major histocompatibility complex DRB1 gene: its role in nematode resistance in Suffolk and Texel sheep breeds. Parasitology 131:403-9

Schwaiger F-W, Maddox J, Ballingall K, Buitkamp J, Crawford A, Dutia BM, Epplen JT, Ferguson ED, Groth D, Hopkins J, Rhind SM, Sargan D, Wetherall J, Wright H (1996) The ovine major histocompatibility complex. *In* Schook LB, Lamont SJ (eds.) The major histocompatibility complex region of domestic animal species. CRC PRESS, INC., 2000 Corporate Blvd. N.W., Boca Raton, FL33431, USA

Schwaiger F-W, Weyers E, Buitkamp J, Ede AJ, Crawford A, Epplen JT (1994) Interdependent *MHC-DRB* exon-plus-intron evolution in artiodactyls. Molecular Biology and Evolution 11:239-249

Schwaiger FW, Weyers E, Epplen C, Brun J, Ruff G, Crawford A, Epplen JT (1993) The paradox of MHC-DRB exon/intron evolution: alpha-helix and beta- sheet encoding regions diverge while hypervariable intronic simple repeats coevolve with beta-sheet codons. J Mol Evol 37:260-72

The MHC sequencing consortium (1999) Complete sequence and gene map of a human major histocompatibility complex. Nature 401:921-923

Thompson JD, Higgins DG, Gibson TJ (1994) CLUSTAL W: improving the sensitivity of progressive multiple sequence alignment through sequence weighting, position-specific gap penalties and weight matrix choice. Nucleic Acids Res 22:4673-80

van Oorschot RA, Maddox JF, Adams LJ, Fabb SA (1994) Characterization and evolution of ovine MHC class II DQB sequence polymorphism. Anim Genet 25:417-24

Tables

Table 1: *Oligonucleotide primers used for amplification and sequencing of MHC class II sequences*

Name	Sequence	Location
Amplification of the repeat adjacent to exon 2 of oaDRB1		
LfL#1008	GCAGCGGCGAGGTGAGC	DRB exon 2/F
LfL#1009	FAM-CACTCACAGTCGTACACACTCG	DRB1 intron 2/R
Amplification and sequencing of exon 2 of oaDRB1		
LfL#984	CTCATTAGCCTCTCCCCAG	DRB1 intron 1/F
LfL#986	CACTCACAGTCGTACACACTCG	DRB1 intron 2/R
Additional 3'sequencing primer for oaDRB1		
LfL#987	ACACTGCTCCACACTGGC	DRB1 exon 2/intron 2/R
LfL#1012	ACACTGCTCCACAITGGC	DRB1 exon 2/intron 2/R
Amplification and sequencing of oaDQB		
LfL#991 (~JM05)	CTGACCGAGCGGCTGT	DQB intron 1/F
LfL#993 (~JM06)	CCGCTGCCAGGTGAAGG	DQB exon 2/intron 2/R
LfL#992 (~JM07)	CGCCGCTGCAAGGATGTGATGAG	DQB exon 2/intron 2/R
LfL#994	CGGCTCTCTGTCCCATCC	DQB intron 2/R
LfL#1005	CTGACCGAGCGGCTGTCT	DQB intron 1/F
LfL#1007	CTCGCGCGCTGAGTC	DQB intron 2/R

Table 2: *MHC class II B haplotypes derived from 15 Spanish Churra rams*

Haplotype	DQB		DRB1	DRBMS
1	#046	#001	0801	249
2	#069	-	0801	249
3	#060	#058	0502	237
4	#054	-	0502	237
5	#027	-	0501	237
6	#081	#006	2101	200
7	#054	-	2101	200
8	#079	-	2001N	241
9	#079	-	2001	241
10	#072	-	0401	233
11	#079	-	2002	241
12	#075	-	1604	232
13	#074	-	2101	227
14	#033	#022	0702	> 450

DQB, *DQB* alleles; DRB1, *DRB1* alleles; DRBMS, fragment length of the complex microsatellite located 5-prime of exon 2 of the *DRB1*.

Figures

Figure 1: *Derived amino acid sequences of OvarDRB1 alleles from 15 Spanish Churra rams*

*The derived amino acid sequence from DRB1 exon 2 from Spanish Churra rams aligned to allele OvarDRB1*0101 (that does not occur in these animals). Dots indicate residues that are identical to OvarDRB1*0101. Known alleles were designated according to the IPD nomenclature, new alleles were indicated by the designation of the most similar allele followed by an 'N'. Positions participating in the antigen binding site are indicated in gray; numbers below the sequences give the pocket of the antigen binding site (1, 4, 6, 7, 9); ! indicates residues that form hydrogen bonds with the antigenic peptide; the disulfide-bridge is indicated in orange; @ homodimerization patch (involved in T lymphocyte receptor-induced homodimerization); ~ intra-chain salt bridges , +/- respective charge.*

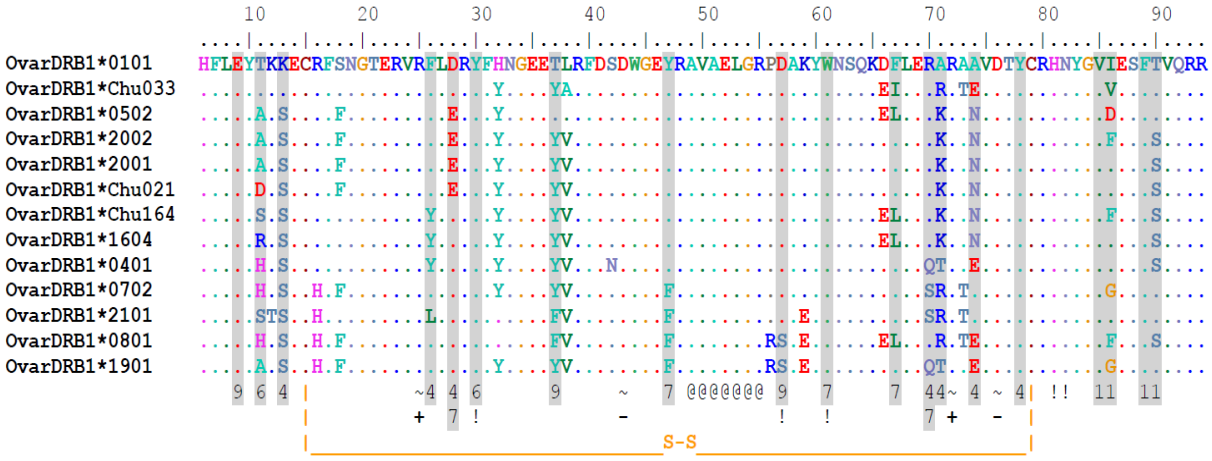

Figure 2: *Amino acid variation in Spanish Churra vs. published DRB1 alleles Numbering of positions according to Bondinas et al. (2007); positions involved in the antigen binding sites are indicated by grey background; amino acids that do not occur in the preliminary set of alleles in the Spanish Churra breed are given in red.*

Churra						AS Position	Published						
T	S	H	A	R	D	11	T	S	H	A	R	D	Y
				K	T	12	K	T	R				
				K	S	13	K	S	R				
				R	H	16	R	H					
				S	F	18	S	F					
			F	Y	L	26	F	Y	L				
				D	E	28	D	E					
					F	31	F	Y					
				H	Y	32	H	Y	T				
			T	Y	F	37	T	Y	F	N			
			L	A	V	38	L	A	V				
				S	N	42	S	N					
				Y	F	47	Y	F					
					A	51	A	T					
				P	R	56	P	R	Q				
				D	S	57	D	S	A	E			
				K	E	59	K	E					
					Y	60	Y	Q	H				
				D	E	66	D	E	N				
			F	I	L	67	F	I	L				
			R	Q	S	70	R	Q	S				
		A	T	R	K	71	A	T	R	K			
				A	T	73	A	T					
			A	E	N	74	A	E	N				
					D	76	D	N					
					Y	78	Y	V					
	I	V	F	D	G	86	I	V	F	D	G		
				T	S	90	T	S	A				

Figure 3: *Derived amino acid sequences of OvarDQB alleles from 15 Spanish Churra rams. New alleles from this publication are indicated with a star (*). Other symbols and numbering see legend to Fig. 1.*

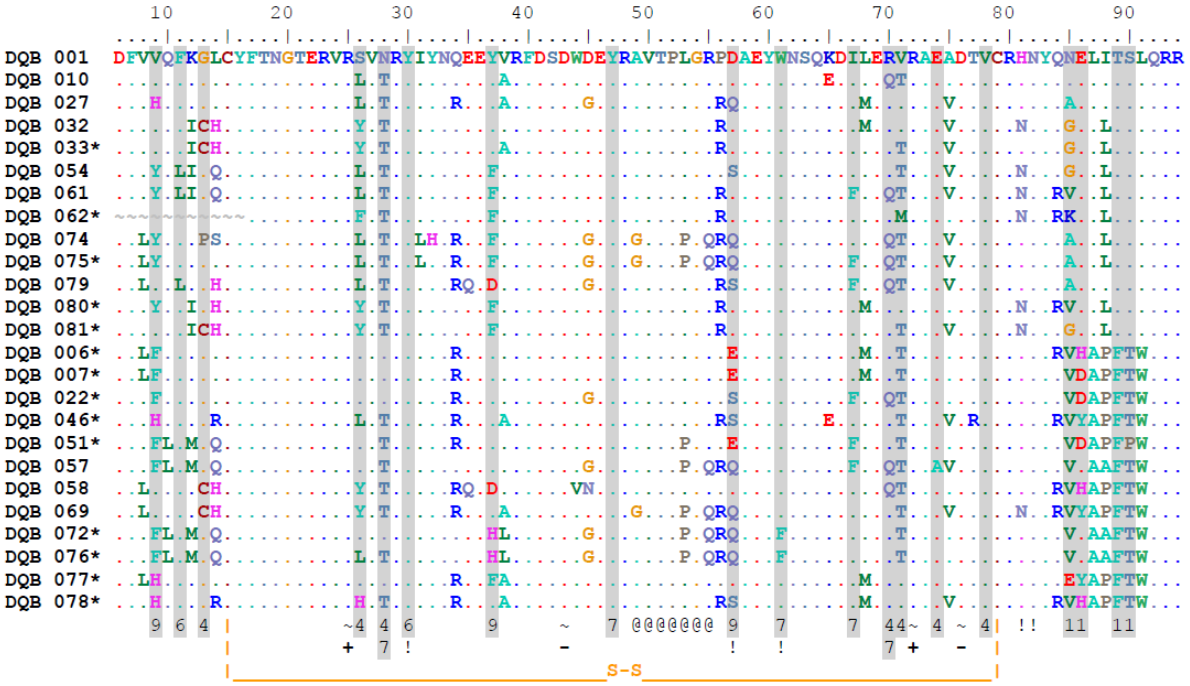

Figure 4: *Phylogenetic trees for DQB alleles from Churra sheep. Neighbor Joining clustering was used to generate phylogenetic trees from the full amino acid sequences (to position 94) from Fig. 3 (A) as well as for the sequences without the 3 prime end (to position 87) (B). Alleles amplifying with primer JM06 are shown in blue, those amplifying with JM07 in red. Numbers at the branches give the distance values between joined neighbors from the neighbor joining matrix.*

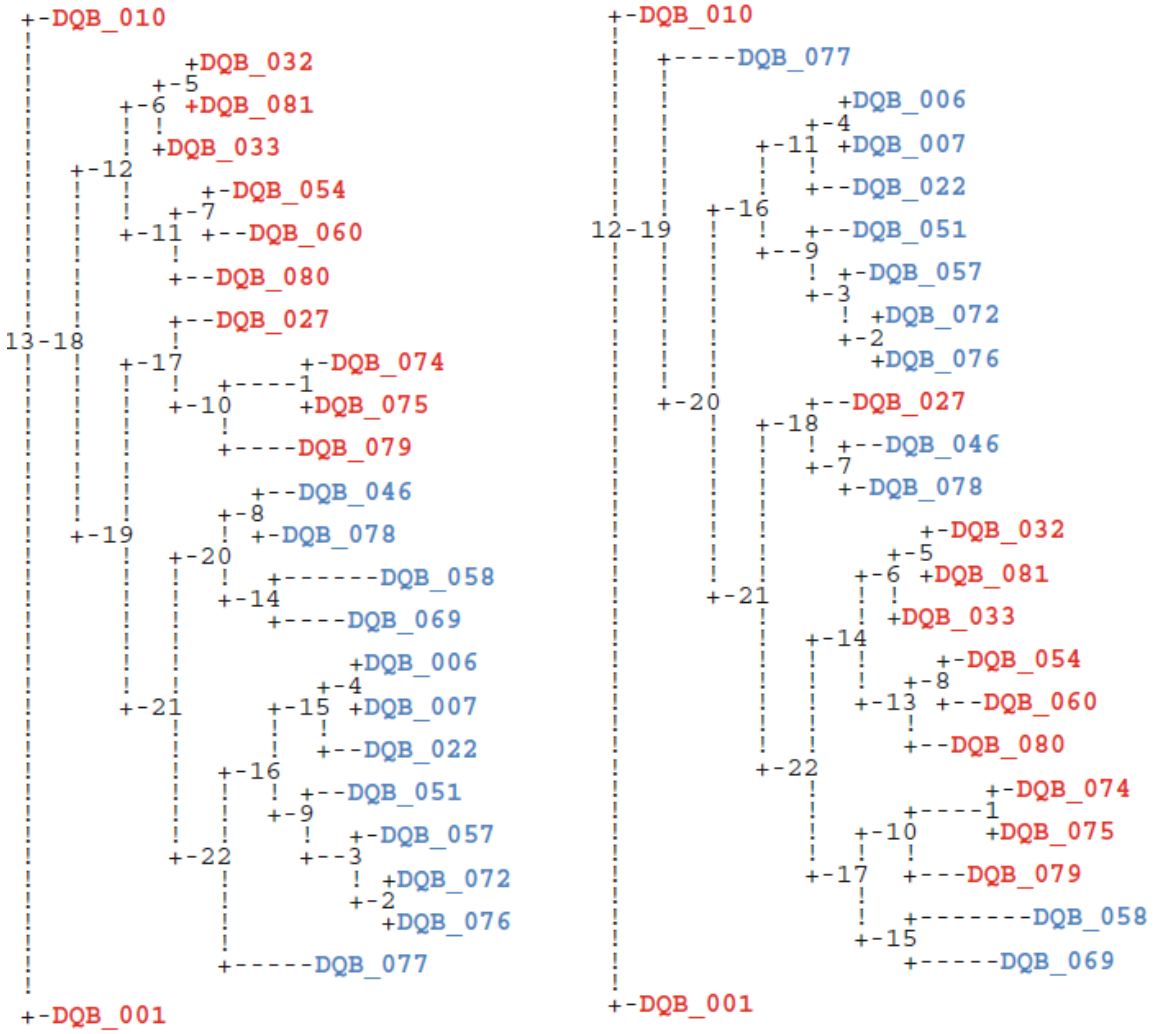

Supplementary information

Table S1: *Alleles used for setting up the local DQB database and allele designation*

Allel Number	AccNumber	Alternative AccNumber or allele name
1	Z28424.1	HQ728696.1
2	HQ728684.1	
3	AJ238931.1	
4	EU176819.1	HQ728666.1
5	AJ238938.1	HQ728672.1
006^{N}	KR048647	DQBG_Neu4
007^{N}	KR048648	DQBG_Neu4_2
8	AJ238938.1	HQ728672.1
9	AJ238933.1	
010^{N}	KR048649	DQB 15_Neu2
11	U07031.1	
12	HQ728670.1	
13	AJ238934.1	
14	HQ728689.1	
15	HQ728693.1	
16	AJ238932.1	
17	HQ728677.1	
18	AH001247.2	
19	HQ728687.1	
20	HQ728694.1	
21	EU176819.1	HQ728667.1
022^{N}	KR048650	DQBB_Neu4
23	HQ728670.1	HM367630.1
24	AJ238935.1	
25	HQ728677.1	
26	HM367629.1	
27	HQ728675.1	JQ824377.1
28	AJ238939.1	
29	AJ238936.1	HQ728694.1
30	AJ238944.1	
31	Z28425.1	
32	HQ728690.1	
033^{N}	KR048651	DQBX_Neu5
34	HQ728687.1	
35	HQ728697.1	
36	AJ238946.1	

37	Z28423.1	HQ728668.1
38	HQ728676.1	
39	L08792.1	
40	HQ728675.1	U07033.1
41	AJ238946.1	HQ728680.1
42	HQ728671.1	GU191453.1
43	AJ238937.1	
44	HQ728678.1	
45	AJ238945.1	
046[N]	KR048652	DQB 27_Neu_3
47	HQ728678.1	
48	HQ728686.1	
49	HQ728686.1	
50	HQ728685.1	
051[N]	KR048653	DQBS_Neu_9
52	Z28523.1	
53	Z28422.1	
54	HQ728692.1	
55	GU191457.1	
56	U07028.1	
57	HQ728683.1	
58	GU191454.1	
59	AJ238942.1	
60	HQ728688.1	
61	Deleted	
062[N]	KR048655	DQBV_Neu9
63	HQ728682.1	
64	GU191456.1	
65	U07032.1	
66	AJ238941.1	
67	HQ728668.1	Z28423.1
68	GU191458.1	
69	HQ728695.1	GU191459.1
70	HQ728669.1	
71	HQ728681.1	GU191455.1
072[N]	KR048656	DQB*Tnew1_4
73	AJ238940.1	
74	HQ728691.1	
075[N]	KR048657	DQBY_Neu_3
076[N]	KR048658	VG10473_2
077[N]	KR048659	VG10473_3
078[N]	KR048660	VG10473_4

79	HQ728679.1	
080[N]	KR048661	IJ10492_1
081[N]	KR048662	DQB*19_Neu_4

[N] This publication

Table S2: *Genotypes of 15 Churra rams for DQB, DRB1 microsatellite and DRB1*

Animal	DQB				DRBMS		DRB1	
1	#054		#006	#081	200		2101	
2	#079		#072		233	241	401	Chu021
3	#079		#033	#022	> 450	241	702	Chu021
4	#079		#006	#081	202	241	2101	2001
5	#079		#006	#081	200	241	2101	2001
6	#074		#006	#081	200	227	2101	2101
7	#075		#006	#081	200	232	2101	1604
8	#027		#060	#058	237		502	
9	#054		#060	#058	237		502	
10	#057	#051	#006	#080	233	327	401	Chu033
11	#010		#007	#062	232	327	Chu164	Chu033
12	#060	#058	#001	#046	237	249	502	801
13	#069		#001	#046		249		801
14	#079		#001	#046	241	249	2002	801
15	#032	#076	#077	#078	249		1901	

Implementation of an extended ZINB model in the study of low levels of natural gastrointestinal nematode infections in adult sheep

Marina Atlija[1], Joaquín M Prada Jiménez de Cisneros[2,3], Beatriz Gutiérrez-Gil[4], Francisco Antonio Rojo-Vázquez[4,5], Michael J Stear[2], Juan-Jose Arranz[1] and María Martínez-Valladares[1,4]

[1] Departamento de Producción Animal, Universidad de León, Campus de Vegazana s/n, 24071, León, Spain

[2] Institute of Biodiversity, Animal Health and Comparative Medicine, University of Glasgow, Bearsden Road, Glasgow G61 1QH, UK

[3] Department of Ecology and Evolutionary Biology, Princeton University, Princeton, NJ 08540, USA

[4] Instituto de Ganadería de Montaña, CSIC-ULE, 24346, Grulleros, León, Spain

[5] Departamento de. Sanidad Animal, Universidad de León, Campus de Vegazana s/n, 24071, León, Spain

(Submitted)

ABSTRACT

In this study, two traits related with resistance to gastrointestinal nematodes (GIN) were measured in 529 adult sheep: faecal egg count (FEC) and activity of immunoglobulin A in plasma (IgA). A zero inflated negative binomial model (ZINB) model was used to calculate the extent of zero inflation for FEC; the model was extended to include information from the IgA responses. In this dataset, 64% of animals had zero FEC while the ZINB model suggested that 38% of sheep had not been recently infected with GIN. The IgA activities were then used to decide which sheep had been exposed and were relatively resistant and which sheep had not been recently exposed. Animals with zero FEC and high IgA activity were considered resistant while animals with zero FEC and low IgA activity were considered as not recently infected. For the animals considered as exposed to the infection, the correlations among the studied traits were estimated, and the influence of these traits on the discrimination between unexposed and infected animals was assessed. These correlations will be useful in the development of a reliable index of GIN resistance that could be of assistance for the study of host resistance in studies based on natural infection, especially in adult sheep, and also the design of breeding programs aimed at increasing resistance to parasites.

Key words: Gastrointestinal nematodes, Sheep, Prevalence, Egg count, IgA, ZINB.

INTRODUCTION

Infection by gastrointestinal nematodes (GIN) is common in ruminants worldwide, causing major economic losses due to decreased growth and milk production [1, 2]. Grazing ruminants are infected by a variety of species of GIN with different pathogenicities and geographical distributions [3].

The control of GIN in ruminants is largely based on the use of anthelmintics, combined with grazing management strategies. However, anthelmintic resistance has appeared worldwide [4–6]. In northwest (NW) Spain, a recent survey showed that GIN in 63.6% of the sampled flocks were resistant to at least one of the most commonly used drugs [7]. The increasing prevalence of anthelmintic resistance has led to the search for alternative control methods, such as selective breeding for resistance to GIN. However, for this purpose, the identification of an appropriate method to measure resistance to infection is necessary, especially in conditions where the worm burden is low. Hence, a sensitive method for detecting infections is needed.

Faecal egg counts (FEC) have been the traditional indicator trait used to assess the level of infection, based on the number of eggs per gram (epg) of faeces, and it is related to both the worm burden and the fecundity of female adults in the host [8, 9, 12]. Faecal egg counts have been used to measure genetic resistance to GIN, although in natural infections they can be quite variable both within and between populations [10]. However, FEC are not particularly sensitive and should be interpreted in conjunction with information about the nutritional status, age and management of sheep flocks [11]. As adult sheep are in general more resistant than naïve young animals, their FECs tend to be lower, adding an additional limitation to the sensitivity problem of the technique.

Other phenotypes related to GIN infections, such as the levels of IgA in serum may be taken into account with the goal of defining resistant animals under natural conditions. IgA is a secreted antibody that plays a major role in gut infections. Animals that display high IgA activity have been shown to present lower FEC and shorter adult female *Teladorsagia circumcincta* among experimentally and naturally infected sheep [9, 13, 14].

The distribution of FEC in naturally infected populations is characteristically over-dispersed within domestic and wild animals [15, 16], as well as in human populations

[17]. The negative binomial (NB) distribution has been widely used to describe parasite eggs distribution. However, when there are more zero FEC values than expected, zero-inflated negative binomial (ZINB) models are more appropriate [15, 18]. A zero-inflated distribution is a mixture of two distributions and can arise if some animals with zero egg counts have been exposed and are resistant to the infection while other animals with zero egg counts have not been exposed or recently infected e.g. no established worms since the last anthelmintic treatment. Resistant animals tend to have few parasite eggs in their faeces. Due to the McMaster measurement technique, small egg numbers are difficult to detect and will be counted as zero, whether the animal has really zero eggs or just a small number of them. We hypothesize that by exploiting additional information, such as that provided by parasite-specific IgA activity, we could improve the ability to discriminate animals with low level of infection with zero egg counts from unexposed / recently uninfected animals. Therefore, the objective of the study was to determine the prevalence of GIN infections in naturally infected adult sheep showing low levels of infection by combining information from the two widely used indicator traits previously mentioned (FEC and IgA). For this purpose, we applied a ZINB model and extended it to include data from IgA responses. For the subset of animals that were considered as exposed to the infection based on the ZINB model, we calculated the correlations among the two indicator traits related to the infection by GIN (FEC, IgA) and the hidden variable of animal status (i.e. the parameter that determines if the animal has been recently infected or not). The aim was to test whether we could improve the value of mixture and enhance the utility of the ZINB model in animals naturally infected with low doses of parasites.

MATERIALS AND METHODS

Study area and animal sampling

The study was carried out in the region of Castilla y León, in the NW of Spain, and included 17 commercial dairy flocks distributed in seven out of the nine provinces of the region (Burgos, León, Palencia, Segovia, Valladolid, Salamanca and Zamora) (Figure 1). In the study area, the flocks are reared under a semi-extensive system in which sheep graze on natural pasture for six hours per day and are kept indoors for the rest of the day. The average size of the sampled flocks was 912, ranging from 302 to 2121 animals per flock.

The survey was conducted from December 2011 to June 2012. This period was extremely dry (additional file 1). Two conditions had to be met to include a flock in the study: first, the last anthelmintic treatment must have been administered at least two months before collecting the samples, and second, the sheep had to be grazing at the time of sampling. The animals included in this study were ewes obtained by artificial insemination from farms belonging to the Selection Nucleus of the National Association of Churra Breeders (ANCHE). Moreover, these animals were a subset of those previously genotyped with the *Illumina* OvineSNP50 BeadChip by [19] which were still alive during the sampling period and for which both phenotypes related to parasite resistance were available. Faecal samples were collected for each ewe directly from the rectum and blood samples were obtained by venipuncture of the jugular vein. Serum samples were stored at -20 ºC until processing. This study is based on 529 adult Churra sheep with faecal and blood serum samples. The mean number of sheep sampled per flock was 31 (range: 11-60 individuals). The age of the sheep included in the study varied between 4 and 11 years. All of the sheep were undergoing milking at the time of sampling and were experiencing at least their third lactation.

Parasitological measures

A modified McMaster technique [20] using zinc sulphate as a flotation solution was used to determine the number of eggs in faeces. The minimum detection limit of this technique was 15 eggs per gram (epg). Faecal egg counts were determined by multiplying the number of eggs observed microscopically (Neggs) by 15.

In each flock, pooled faeces were cultured to recover and identify third-stage larvae (L3) following standard parasitological techniques [20]. A total of 100 L3 were identified per flock to estimate the percentage of each species.

Titre of IgA

An indirect ELISA was carried out to determine the activity of IgA in the serum, results were scored as optical density (OD). The preparation of somatic antigen from fourth-stage larvae (L4) of *T. circumcincta* was conducted as previously described by [21]. Microtitre plates (Sigma) were coated with 100 µl of PBS containing 2.5 µg/ml of *T. circumcincta* L4 somatic antigen, after which the plates were stored overnight at 4 ºC. After discarding their contents, the plates were blocked with 250 µl of PT-Milk (4 g

powdered milk + 100 ml PBS-Tween; PBS-Tween: 1 L PBS pH 7.4 + 1 ml Tween) for 30 min at 37 ºC. Then, the blocking buffer was discarded, and 100 µl of serum was added, followed by incubation for 30 min at 37 ºC. After washing the plates four times with PBS-Tween, 100 µl of a rabbit anti-sheep IgA antibody, conjugated to horseradish peroxidase (Serotec), at a dilution of 1/500 in PT-Milk, was added, followed by incubation for 30 min at 37 ºC. The plates were then washed again four times with PBS-Tween and subsequently incubated in a peroxidase substrate and tetramethylbenzidine solution to produce a colour reaction, which was stopped by the addition of 50 µl of 2 M H_2SO_4. Finally, the absorbance was measured at 450 nm in a microplate reader (Titertek Multiskan). Positive and negative controls were included in every plate. Positive controls were obtained from a pool of serum from experimentally infected sheep with *T. circumcincta* and negative controls from non-infected sheep that were kept indoors. The results were expressed as the optical density ratio (ODR):

$$ODR = \frac{sample\ OD - negative\ OD}{positive\ OD - negative\ OD} \quad (1)$$

Descriptive statistics

Descriptive statistical analysis for the two traits was conducted for the 529 sampled animals with the 'pastecs' package [22] in R [23]. The Shapiro-Wilk test was carried out to determine if the data for each trait was normally distributed. Due to the large number of zero counts in the FEC data and the fact that the animals graze during short periods of time (semi-extensive rearing system), we decided to use a ZINB model to estimate the zero-inflation parameter and then extended it to discriminate between exposed and unexposed animals. The zero inflated model with IgA data was compared to a simpler negative binomial model using a likelihood ratio test. Moreover, in this particular study, a zero inflated model is a biologically meaningful description of the system; the adverse climatic conditions for larval development of the year studied will reduce pasture contamination, and the short grazing periods due to the semi-extensive rearing system will reduce exposure, which means that some animals would not have been infected at the time of sampling, and may not have been infected since the last anthelmintic treatment. The zero inflated model also allows for a more natural extension into discriminating between infected and uninfected animals.

Estimation of zero-inflation

In the zero inflated model, positive FEC are derived from a NB distribution, while a zero count can arise from either the NB distribution or the zero distribution (a binary distribution that generates structural zeros). The probability of belonging to the zero distribution is called the zero-inflation parameter. The animals that have zero counts arising from the zero distribution are assumed to have not been infected since the last anthelmintic treatment, so these animals can be excluded from further analysis. A Markov Chain Monte Carlo model similar to the one described in Denwood *et al.* [15] using the '*runjags*' package [24] was employed to estimate the zero-inflation parameter.

In this model, the negative binomial distribution arises from a gamma-Poisson mixture distribution. Uninformative priors were used for the parameters of the gamma distribution. The posterior distribution of the zero-inflation parameter is shown in Figure 2.

Extending the ZINB model

A zero-inflation model does not determine which animals are exposed and resistant (as opposed to unexposed). The classical ZINB model was therefore extended to accommodate IgA data as additional information for the animal status, i.e. infected or not recently infected. The animal status is calculated as,

$$Status = \begin{cases} 0; not\ recently\ infected & with\ probability\ 1 - P, \\ 1; infected & with\ probability\ P \end{cases} \quad (2)$$

where status = 0 means that the animal has not been recently infected and status = 1 means that the animal is infected. P is the probability of being recently exposed and is equivalent to one minus the zero-inflation parameter. The raw egg counts (FEC/15) were used and it is assumed that for each animal *i*, the number of eggs counted arises from the following,

$$Neggs_i \sim \begin{cases} 0 & if\ Status = 0, \\ Poisson\ (\lambda_i) & if\ Status = 1 \end{cases} \quad (3)$$

where λ_i is the number of eggs arising from the gamma distribution (equation 4).

$$\lambda_i \sim gamma\ (shape, rate) \quad (4)$$

with the shape and the rate parameters of the gamma being calculated by the model. Similarly the IgA data can be partitioned in 2 gamma distributions (equation 5) based on the animal status.

$$IgA_i = \begin{cases} gamma(sh_1, rt_1) & if\ Status = 0, \\ gamma(sh_2, rt_2) & if\ Status = 1 \end{cases} \quad (5)$$

with sh_1, sh_2, rt_1 and rt_2 being the two shapes and two rates respectively that parametrize the two gamma distributions. In the model, samples are drawn for sh_1 and sh_2 as well as for mn_1 and mn_2, which are the two means of the two gamma distributions. The rates are calculated by rate = shape / mean and the mean for the animals not recently infected (mn_1) is always smaller than the mean of the infected (mn_2). The fully annotated R code of the model is given in the additional file 3.

The number of iterations sampled was 50,000, with the first 5,000 being discarded (burn in), and assessed convergence with the Gelman-Rubin statistic from the '*coda*' package [25] being under 1.05.

Using the realisations of the animal status across the iterations (unexposed animals have status = 0, exposed and infected have status = 1), it is possible to calculate the probability for each animal to be in one status or the other, $P^{\exp}{}_i$; animals without zero FEC will always be in the infected status. The animals that were estimated to be unexposed, i.e. the animals with status = 0, in each sample of the Markov Chain were excluded from further analyses, allowing the use of simple statistical tools to analyse the remaining dataset for each sample.

Correlations between phenotypes

Considering FEC, IgA and the realisations of animal status, $P^{\exp}{}_i$, the Kendall's rank correlation coefficient was used to estimate the relationships among these three parameters. We used Kendall's rank because it is an appropriate non-parametric hypothesis test. Correlations were calculated in R, using the '*ltm*' package [26], for each sample of the Markov Chain and the average across the samples is reported below.

RESULTS

Descriptive statistics of the phenotypic data

Faecal egg counts and larval identification: Faecal egg counts of GIN ranged from 0 to 1,290 epg. In 64% of the faecal samples no eggs were detected. The FEC mean and total variance were 38.2 (±105.9) and 11,218.9 respectively. The FEC distribution was heavily skewed to the right and showed a high level of over-dispersion (Figure 3a). The Shapiro-

Wilk test for the FEC data indicated a clear deviation from normality (p-value < 2.2 x10^{-16}). Most of the eggs detected in positive samples were strongyle-type.

Apart from the GIN eggs, other parasite eggs were detected in faeces: 13.3% of the sheep sampled had *D. dendriticum* eggs, with a range of 0-1,035 epg; 2.9% had *Trichuris* spp. eggs (0-30 epg), two animals (0.9%), had *Moniezia* spp. eggs (0-1,035 epg) and one ewe had *Capillaria* spp eggs at a concentration of 15 eggs per gram.

After collecting L3 from coprocultures, we identified the following genera of GIN: *Trichostrongylus* spp. (49.3%), *T. circumcincta* (48.6%), *Nematodirus* spp. (1.4%) and *Cooperia* spp. (0.7%). In all flocks, we confirmed the presence of *T. circumcincta*. We also observed a number of lungworm larvae, though they were not identified to the species level.

IgA activity in the serum samples: For individual animals, the mean ODR was 4.1 (± 4.3), showing a range between 0.09 and 32.9; the ODR variance was 18.4. The distribution of IgA activities was positively skewed (Figure 3b) with most of the sheep displaying relatively low IgA values, and only a few sheep presenting particularly high levels of IgA.

The Shapiro-Wilk test indicated a clear deviation from the normality (p-value < 2.2 x10^{-16}). The Kolmogorov-Smirnov test indicated that the IgA was not gamma distributed (p-value = 0.0088), however this is due to the long tail of high IgA values. If the analysis is done with 10 animals less (effectively cutting the max IgA values to 20), the test indicates that the data is indeed gamma distributed (p-value = 0.21).

Zero-inflation parameter and extension of the ZINB model for FEC data

To verify that the data is zero inflated, a likelihood ratio test was performed comparing the ZINB model to a simpler NB model, with a p-value of the likelihood ratio test = 6.62 x10^{-5}, which indicates that the zero-inflated model provides a better fit to the data. The mean of the zero-inflation parameter was 0.38, this indicates that on average, 38% of all the animals were not exposed and infected since the last anthelmintic treatment (two months before the samples were taken), therefore it was estimated that 328 ewes were infected at sampling, even though only 190 had non-zero FEC. The zero-inflation parameter credible interval was much narrower when using the extended ZINB model as opposed to the ZINB model using FEC data only (from 0.013-0.46 to 0.25-0.49). The distribution of the probability of being exposed across all the animals in the data is shown in Figure 4.

RESULTS

Associations between phenotypes

The associations between phenotypes was calculated for the subset of animals that were considered exposed to the infection based on the implementation of the extended ZINB model (status = 1) in each sample of the Markov Chain. The correlations between Neggs, IgA and the estimated probability of being exposed to infection ($P^{\exp}{}_i$) are shown in Table 1. The phenotypic correlation between plasma IgA and number of eggs was close to zero and not statistically significant, while animal status was positively correlated to the number of eggs and IgA.

DISCUSSION

Adult female sheep play a key role in the epidemiology of GIN infection because eggs deposited during the periparturient period influence the severity of the infection during the grazing season. However, outside the periparturient period, egg counts in adult sheep are typically low [27]. In general, GIN populations in naturally infected sheep are usually over-dispersed, with the majority of sheep showing low epg values and only a few sheep presenting a high level of infection [28]. In addition, some infected sheep will have low egg counts [8]. Therefore, supplementary information is needed as well as egg counts to determine which sheep are infected in adult sheep flocks.

In this study, the mean FEC per flock was quite low (38.2 epg) compared with other studies carried out in the same area (NW of Spain). Gutiérrez-Gil *et al.* [29] reported that the mean FEC was 260 epg between the years 1999 and 2003. Similar records were described by Martínez-Valladares *et al.* [30], who showed that the prevalence of GIN, based solely on the presence or absence of FEC, in sheep flocks was 100%, and the mean epg was 237.2 (± 375.9) between the years 2006 and 2011. In the current study, the low levels of infection are likely a consequence of the exceptional climatic conditions during this study since the longevity of infective trichostrongylid L3 nematodes is related to temperature and humidity [30, 31]. The table in additional file 1 displays the mean temperature and precipitation for the period between December-June of the last five years (2007/2008 – 2011/2012) in the region of Castilla y León, highlighting the fact that the year 2011/2012 was extremely dry. According to Martínez-Valladares *et al.* [30], there is a direct relationship between GIN infection levels and the humidity of ambient air.

Faecal egg count, which has been for many years the traditional diagnostic tool for assessing GIN infection, has a low sensitivity [32], especially for very low counts as is the case in this study. Therefore, when the excretion of eggs in faeces is low, it is necessary to use other, more sensitive, diagnostic methods that might provide a more reliable indicator of infection.

IgA activity in the current study is moderately high, and this is presumed to be due to the fact that the antibodies persist for some time after GIN infection. The experimental studies of different breeds of sheep infected with GIN showed IgA activity for prolonged periods of time post infection. In an experiment carried out by Henderson and Stear [33], the peak of IgA was at 6-10 days after a deliberate infection with *T. circumcincta* in sheep although detectable IgA was evident six weeks later. Furthermore in an experiment with Churra sheep, Martínez-Valladares *et al*. [34] also showed that the elevated level of IgA in blood and nasal secretions was maintained four weeks post infection with this same parasite species. In the study by MacKinnon *et al*. [35] IgA activity was also evident four weeks post infection with *Haemonchus contortus* in Caribbean hair sheep.

In this study, a ZINB model was used to calculate the extent of zero inflation. This approach has been applied to several parasitic infections [15, 17, 18]. This model was then extended to identify the animals that are likely to be uninfected. This was done by adding the IgA information to the model. In a ZINB model using only FEC data, the model would not be able to assign animals with zero FEC as infected or uninfected (Additional file 2).

There is heterogeneity among animals in the intensity of infection. Some infected animals will be exposed to more parasites than others. Both genetic variation in resistance and variation in exposure will contribute to the observed variation in IgA activity and FEC in exposed animals. Among animals that have not been exposed to parasites, FEC will be zero and parasite-specific IgA will be very low or zero. Animals with zero FEC and zero or low IgA activity are therefore more likely to be unexposed but it is possible that some of these animals have been exposed to low intensities of infection. Therefore the extension of the ZINB model to include additional data does not guarantee that every animal will be correctly assigned. It does however improve the discrimination between exposed and unexposed animals and make subsequent analyses based on exposed animals more reliable (Figure 4, Supplementary Material 2).

To our knowledge, this is the first description of a ZINB model for the analysis of multiple traits with the aim of discerning which animals are infected and which have not been recently exposed or exposed to a very low infection level. This procedure is relatively straightforward and allows the study of nematode infections in adult animals and in flocks with low prevalence of infection, such as in Mediterranean dairy farms where animals are under a semi-extensive management system. The approach improves our ability to identify animals that have been infected with GIN, even at low FEC, which is needed for the study of host resistance in naturally infected individuals and the breeding of resistant sheep.

Because the over-dispersion pattern of GIN (number of eggs and adult worms found in the host) is also observed in other hosts such as cattle, free-range pigs, chickens, humans and wild animals [36–38], the approach described here could also be useful in other systems.

The correlations between the number of eggs and IgA and animal status were calculated using the non-parametric Kendall's test. Although the number of eggs has been found negatively correlated with IgA in young lambs [39, 40], in the case of adult sheep, this correlation is not as clear and both Coltman *et al.* [39] and Gutiérrez-Gil *et al.* [29] reported non-significant correlations in naturally infected adult sheep after comparing logFEC and IgA against somatic antigen from *T. circumcincta* L4. Our results are similar, and suggest that this correlation is indeed close to zero in adult sheep. In experimentally infected adult sheep, Martinez-Valladares *et al*. [9] showed negative correlations between IgA in gastric mucus and FEC whereas the correlation between FEC and the serum IgA levels (which are lower than in the gastric mucus) were not significant. The absence of a clear correlation between plasma IgA and FEC may be a consequence of the fact that plasma IgA shows a complex relationship with mucosal IgA [41]. Alternatively, adult sheep may show greater IgE activity; reduced numbers of established parasites would decrease IgA responses and the relative importance of IgA on egg output would be lowered [43].

The extension of the ZINB model has allowed us to combine the information from two different traits that can indicate resistance or susceptibility to GIN. The IgA response was added to the model to help discriminate between unexposed and infected animals with zero FEC. Recent research has produced an index of the intensity of nematode infection

in young lambs [42] and the observed correlations among the parasitological variable are necessary for this process. As mentioned previously, the use of a reliable indicator trait may be of interest not only for the management of parasite infections but also for the design of breeding programs aimed at achieving resistance to parasites.

In summary, in the current study, two different phenotypes related to GIN infection (FEC and IgA against somatic antigen from L4 of *T. circumcincta*) were analysed. There was a high percentage of sheep without eggs in faeces (64%) and a zero inflated model was used to detect the amount of zero inflation in the data. The ZINB model suggested that 38% of sampled sheep had not been exposed to nematode infection in the previous two months, since the last anthelmintic treatment. Therefore, in addition to FEC data, the evaluation of IgA in serum may help to distinguish adult animals with low level of infection from resistant animals assist selective breeding for resistance to GIN.

COMPETING INTERESTS

The authors declare that they have no competing interests.

AUTHORS CONTRIBUTION

M. A. analyzed the samples in the wetlab and helped in the statistical analysis. J. M. P. created the mathematical model and performed the statistical analysis. M. S. and J. M. P. conceived the mathematical study. B. G. G., J. J. A. and M. M. V. designed the data sourcing and sample collection. M. A., J. M. P. B. G. G. and M. M. V. drafted the manuscript. M. J. S., J. J. A. and F. A. R. V. coordinated the study and critically corrected the manuscript. All authors read and approved the final manuscript.

ACKNOWLEDGEMENTS

This work was supported by a competitive grant from the Castilla and León regional government (Junta de Castilla y León) (Ref. LE245A12-2); the EC-funded Initial Training Network (ITN) NematodeSystemHealth (M. A. and J. M. P., P7-KBBE-2009-3-245140); the BBSRC grant BB/L004004070/1; the Spanish “Ramón y Cajal” Programme from the Spanish Ministry of Economy and Competitiveness (B. G. G., RYC-2012-10230) and a postdoctoral Jae-Doc contract from the Consejo Superior de Investigaciones Científicas (CSIC) and co-funded by the European Social Fund (M. M. V.).

REFERENCES

1. Stear MJ, Bishop SC, Mallard BA, Raadsma H: **The sustainability, feasibility and desirability of breeding livestock for disease resistance.** *Res Vet Sci* 2001, **71**:1–7.

2. Suarez VH, Cristel SL, Busetti MR: **Epidemiology and effects of gastrointestinal nematode infection on milk productions of dairy ewes**. *Parasite* 2009, **16**:7.

3. Dobson RJ, LeJambre L, Gill JH: **Management of anthelmintic resistance: inheritance of resistance and selection with persistent drugs**. *Int J Parasitol* 1996.

4. Papadopoulos E, Gallidis E, Ptochos S: **Anthelmintic resistance in sheep in Europe: A selected review**. *Vet Parasitol* 2012, **189**:85–88. [*Special Issue: Update on Parasitic Diseases of Sheep*]

5. Torres-Acosta JFJ, Mendoza-de-Gives P, Aguilar-Caballero AJ, Cuéllar-Ordaz JA: **Anthelmintic resistance in sheep farms: Update of the situation in the American continent**. *Vet Parasitol* 2012, **189**:89–96. [*Special Issue: Update on Parasitic Diseases of Sheep*]

6. Roeber F, Jex AR, Gasser RB: **Impact of gastrointestinal parasitic nematodes of sheep, and the role of advanced molecular tools for exploring epidemiology and drug resistance - an Australian perspective**. *Parasit Vectors* 2013, **6**:153.

7. Martinez-Valladares M, Martinez-Perez JM, Robles-Perez D, Cordero-Perez C, Famularo MR, Fernandez-Pato N, Castanon-Ordonez L, Rojo-Vazquez FA: **The present status of anthelmintic resistance in gastrointestinal nematode infections of sheep in the northwest of Spain by in vivo and in vitro techniques**. *Vet Parasitol* 2013.

8. Bishop SC, Stear MJ: **The use of a gamma-type function to assess the relationship between the number of adult Teladorsagia circumcincta and total egg output.** *Parasitology* 2000, **121 (Pt 4**:435–40.

9. Martínez-Valladares M, Vara-Del Río MP, Cruz-Rojo MA, Rojo-Vázquez FA: **Genetic resistance to Teladorsagia circumcincta: IgA and parameters at slaughter in Churra sheep.** *Parasite Immunol* 2005, **27**:213–8.

10. Stear MJ, Bairden K, Duncan JL, Gettinby G, McKellar QA, Murray M, Wallace DS: **The distribution of faecal nematode egg counts in Scottish Blackface lambs following**

natural, predominantly Ostertagia circumcincta infection. *Parasitology* 1995, **110**:573–581.

11. McKenna PB: **Faecal egg counts as a guide for drench use**. *N Z Vet J* 2002, **50**:123–124.

12. Villanua D, Perez-Rodrigues L, Gortazar C, Hofle U, Vimuela J: **Avoiding bias in parasite excretion estimates: the effect of sampling time and type of faeces**. *Parasitology* 2006, **133**:251–259.

13. Stear MJ, Bishop SC, Doligalska M, Duncan JL, Holmes PH, Irvine J, McCririe L, McKellar QA, Sinski E, Murray M: **Regulation of egg production , worm burden , worm length and worm fecundity by host responses in sheep infected with Ostertagia circumcincta**. *Regulation* 1995:643–652.

14. Strain S, Bishop SC, Henderson NG, Kerr A, McKellar QA, Mitchell S, Stear MJ: **The genetic control of IgA activity against Teladorsagia circumcincta and its association with parasite resistance in naturally infected sheep.** *Parasitology* 2002, **124**(Pt 5):545–52.

15. Denwood MJ, Stear MJ, Matthews L, Reid SWJ, Toft N, Innocent GT: **The distribution of the pathogenic nematode Nematodirus battus in lambs is zero-inflated.** *Parasitology* 2008, **135**:1225–35.

16. Ziadinow I, Deplazes P, Mathis A, Mutunova B, Abdykerimov K, Nurgaziev R, Torgerson P: **Frequency distribution of Echinococcus multilocularis and other helminths of foxes in Kyrgyzstan**. *Vet Parasitol* 2010, **171**:286–292.

17. Walker M, Hall A, Anderson RM, Basanez M: **Density-dependent effects on the weight of female Ascaris lumbricoides infections of humans and its impact on patterns of egg production**. *Parasite Vectors* 2009, **2**.

18. Nodtvedt A, Dohoo I, Sanchez J, Conboy G, DesCjteaux L, Keefe G, Leslie K, Campbell J: **The use of negative binomial modelling in a longitudinal study of gastrointestinal parasite burdens in Canadian dairy cows**. *Can J Vet Res* 2002, **66**:249–257.

19. García-Gámez E, Gutiérrez-Gil B, Sahana G, Sánchez J-P, Bayón Y, Arranz J-J: **GWA analysis for milk production traits in dairy sheep and genetic support for a QTN influencing milk protein percentage in the LALBA gene**. *PloS One* 2012, **7**:e47782.

20. Ministry of Agriculture F, (MAFF) F: *Manual of Veterinary Parasitological Laboratory Techniques*. HMSO; 1986.

21. Strain SAJ, Stear MJ: **The recognition of molecules from fourth-stage larvae of Ostertagia circumcincta by IgA from infected sheep**. *Parasite Immunol* 1999, **21**:163–168.

22. Grosjean P, Ibanez F: **pastecs: Package for Analysis of Space-Time Ecological Series**. *R Package Version 13-18* 2014.

23. Team RDC: **R: A Language and Environment for Statistical Computing**. *R Found Stat Comput Vienna Austria* 2011.

24. Denwood MJ: **runjags: Interface utilities, parallel computing methods and additional distributions for MCMC models in JAGS**. *Httpcranr-Proj* 2014.

25. Plummer M, Best N, Cowles K, Vines K: **CODA: Convergence Diagnosis and Output Analysis for MCMC**. *R News* 2006, **6**:7–11.

26. Rizopoulos D: **ltm: An R package for latent variable modeling and item response theory analyses**. *J Stat Softw* 2006, **17**:1–25.

27. Stear MJ, Fitton L, Innocent GT, Murphy L, Rennie K, Matthews L: **The dynamic influence of genetic variation on the susceptibility of sheep to gastrointestinal nematode infection.** *J R Soc Interface R Soc* 2007, **4**:767–76.

28. Barger IA: **The statistical distribution of trichostrongylid nematodes in grazing lambs**. *Int J Parasitol* 1985.

29. Gutiérrez-Gil B, Pérez J, de la Fuente LF, Meana A, Martínez-Valladares M, San Primitivo F, Rojo-Vázquez FA, Arranz JJ: **Genetic parameters for resistance to trichostrongylid infection in dairy sheep.** *Anim Int J Anim Biosci* 2010, **4**:505–12.

30. Martinez-Valladares M, Robles-Perez D, Martinez-Perez JM, Cordero-Perez C, Famularo MR, Fernandez-Pato N, Gonzalez-Lanza C, Castanon-Ordonez L, Rojo-Vazquez FA: **Prevalence of gastrointestinal nematodes and Fasciola hepatica in sheep in the northwest of Spain: relation to climatic conditions and/or man-made environmental modifications**. *Parasite Vector* 2013.

31. O'Connor LJ, Walkden-Brown SW, Kahn LP: **Ecology of the free-living stages of major trichostrongylid parasites of sheep**. *Vet Parasitol* 2006, **142**:1–15.

32. Raadsma H, Gray GD, Woolaston RR: **Breeding for disease resistance in Merino sheep in Australia.** *Rev Sci Tech Int Off Epizoot* 1998, **17**:315–328.

33. Henderson NG, Stear MJ: **Eosinophil and IgA responses in sheep infected with Teladorsagia circumcincta.** *Vet Immunol Immunopathol* 2006, **112**:62–6.

34. Martínez-Valladares M, Vara-Del Río MP, Cruz-Rojo MA, Rojo-Vázquez FA: **Effect of a low protein diet on the resistance of Churra sheep to Teladorsagia circumcincta.** *Parasite Immunol* 2005, **27**:219–25.

35. MacKinnon KM, Zajac AM, Kooyman FNJ, Notter DR: **Differences in immune parameters are associated with resistance to Haemonchus contortus in Caribbean hair sheep**. *Parasite Immunol* 2010, **32**:484–493.

36. Boes J, Coates S, Medley GF, Varady M, Eriksen L, Roepstorff A, Nansen P: **Exposure of sows to Ascaris suum influences worm burden distributions in experimentally infected suckling piglets.** *Parasitology* 1999, **119 (Pt 5**:509–20.

37. Vercruysse J, Dorny P: **Integrated control of nematode infections in cattle: a reality? A need? A future?**. *Int J Parasitol* 1999, **29**:165–75; discussion 183–4.

38. Weyher AH, Ross C, Semple S: **Gastrointestinal Parasites in Crop Raiding and Wild Foraging Papio anubis in Nigeria**. *Int J Primatol* 2006, **27**:1519–1534.

39. Coltman DW, Wilson K, Pilkington JG, Stear MJ, Pemberton JM: **A microsatellite polymorphism in the gamma interferon gene is associated with resistance to gastrointestinal nematodes in a naturally-parasitized population of Soay sheep.** *Parasitology* 2001, **122**(Pt 5):571–82.

40. Davies G, Stear MJ, Bishop SC, Road B, Glasgow G: **Genetic relationships between indicator traits and nematode parasite infection levels in 6-month-old lambs**. *Vet Parasitol* 2005:143–150.

41. Prada Jiménez de Cisneros J, Matthews L, Mair C, Stefan T, Stear MJ: **The transfer of IgA from mucus to plasma and the implications for diagnosis and control of nematode infections.** *Parasitology* 2014, **141**:875–9.

42. Mair C, Matthews L, De Cisneros JPJ, Stefan T, Stear MJ: **Multitrait indices to predict worm length and number in sheep with natural, mixed predominantly Teladorsagia circumcincta infection**. *Parasitology* 2015, **FirstView**:1–10.

43. Stear MJ, Strain SAJ, Bishop SC. **How lambs control infection with *Ostertagia circumcincta***. Vet Immunol Immunopathol. 1999;72:213-8.

Figures

Figure 1. *Map of the region of Castilla y Leon (Spain). The map shows the location of the farms where the flocks were sampled.*

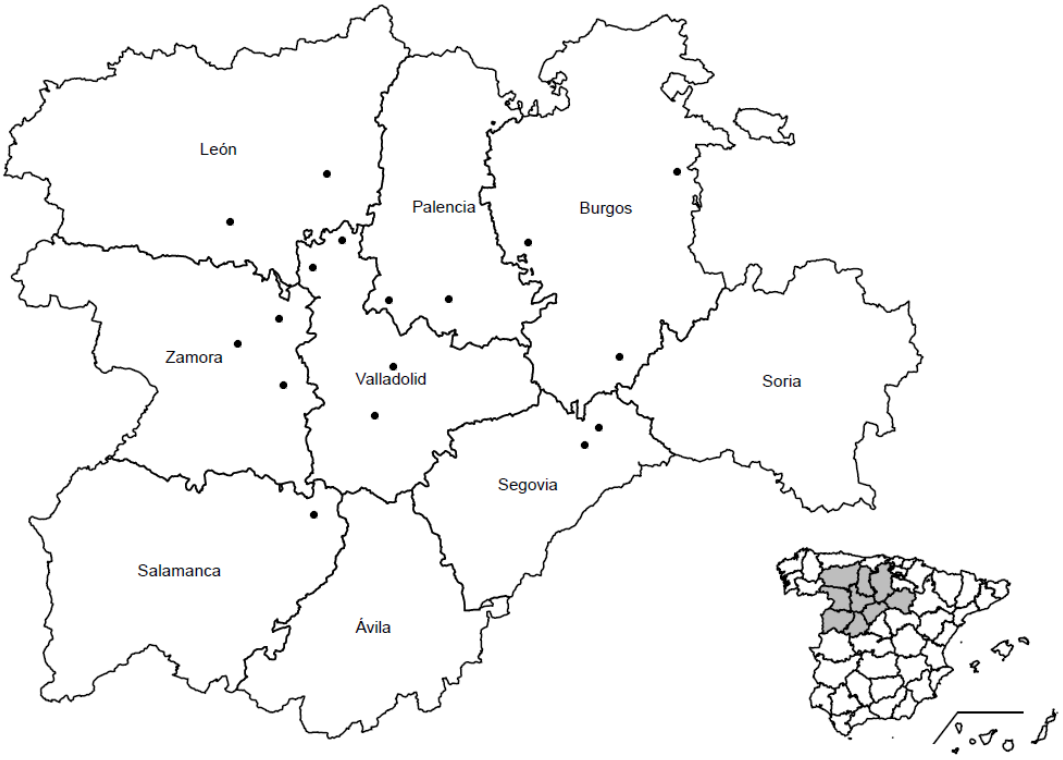

Figure 2. *Posterior distribution of the zero-inflation parameter. Posterior distribution obtained from the extended ZINB model. Each colour represents a different chain. Both chains have a mean around 0.38 and no sample was recovered from either of the chains with a zero-inflation parameter equal to zero (minimum value recovered = 0.12).*

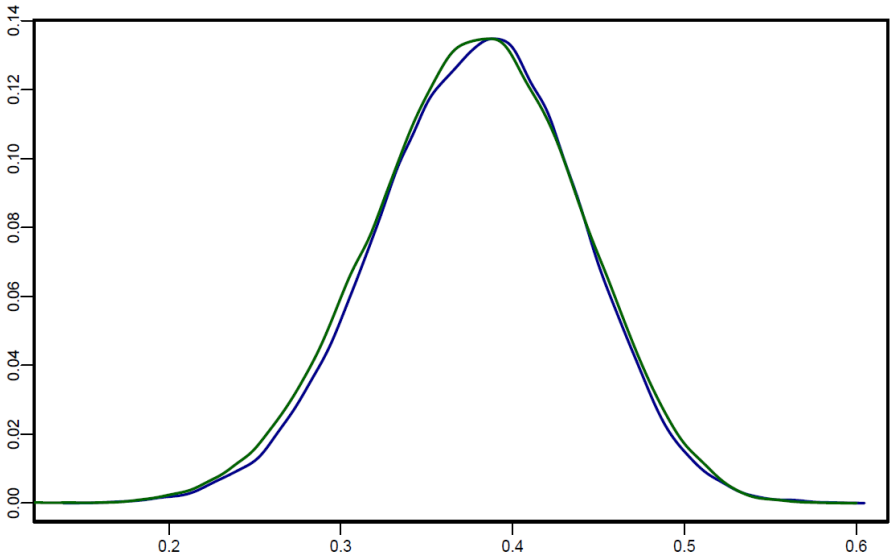

Figure 3. *Distribution of the raw data. Distribution of (a) faecal egg counts and (b) plasma IgA across the 529 Spanish adult Churra ewes.*

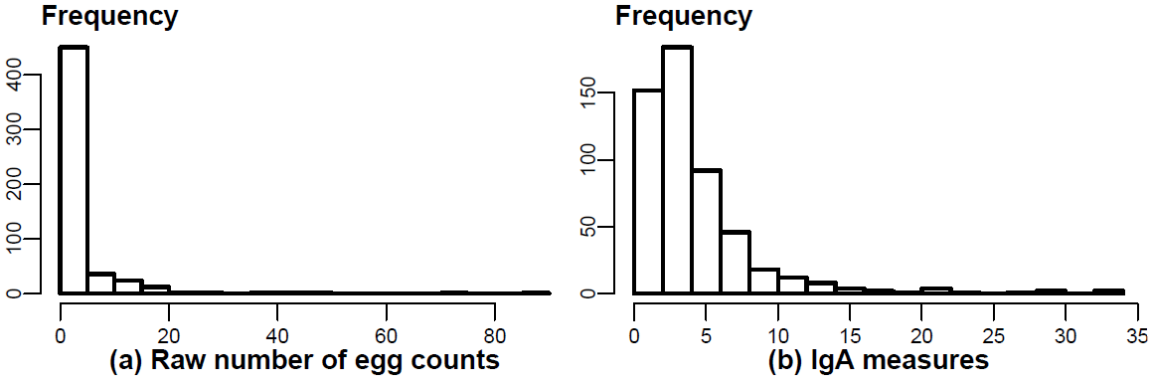

Figure 4. *Histogram of the probability of being exposed. Probability of being exposed and infected,* $P^{\exp}{}_i$ *, for the 529 animals sampled, which is calculated from the realisations of animal status (unexposed vs exposed) across the samples of the MCMC chain.*

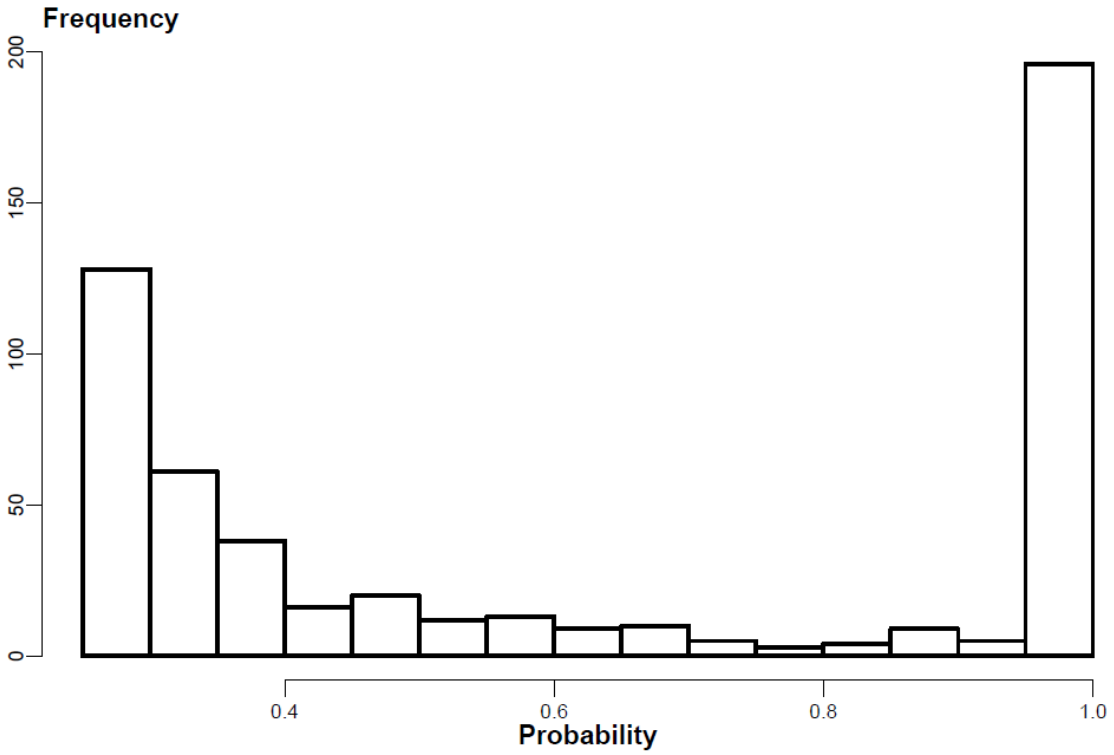

Tables

Table 1. *Estimated correlations in the Churra sheep population. Neggs is the number of eggs counted, IgA is the activity of IgA in serum (Optical density ratio) and* $P^{\exp}{}_i$ *is the probability of being exposed.*

	Neggs	IgA	$P^{exp}i$
Neggs	1	0.012	0.67**
IgA		1	0.18**
$P^{exp}i$			1

** P < 0.001; *P < 0:015

Supplementary material

Additional File 1: *Mean temperatures (ºC) and precipitation (mm) from December to June during the sampling period (highlighted in gray), and during the four previous years.*

Month	2007/2008		2008/2009		2009/2010		2010/2011		2011/2012	
	^{0}C	mm	^{0}C	Mm	^{0}C	Mm	^{0}C	mm	^{0}C	mm
December	1.9	11.4	2.9	50.3	3.7	110.4	3.1	92.5	3.8	14.0
January	4.5	33.2	2.7	38.1	3.4	62.1	3.9	42.4	2.4	12.2
February	6.3	32.5	4.3	21.2	3.6	59.3	4.5	28.5	1.9	5.8
March	6.5	16.6	7.5	12.5	6.2	55.3	7.3	41.1	8.0	9.8
April	9.5	68.4	8.6	28.4	11.0	37.6	12.2	43.2	7.7	72.7
May	12.2	100.3	14.9	22.6	12.3	36.0	15.3	36.7	14.8	35.8
June	16.9	34.1	18.7	30.5	16.9	68.5	17.6	22.6	18.8	14.8

Additional File 2: *Exposed probability in a classic ZINB model. Histogram of probabilities of being exposed for the data (a) and zoom of only the zero FEC (b) using only FEC data in the ZINB model. Animals with non-zero FEC will always have an "infected" status in the model (= 1) while animals with zero FEC can be exposed or unexposed. If only the FEC data is used, each animal with zero FEC will have a probability of being infected similar to one minus the zero-inflation parameter (b).*

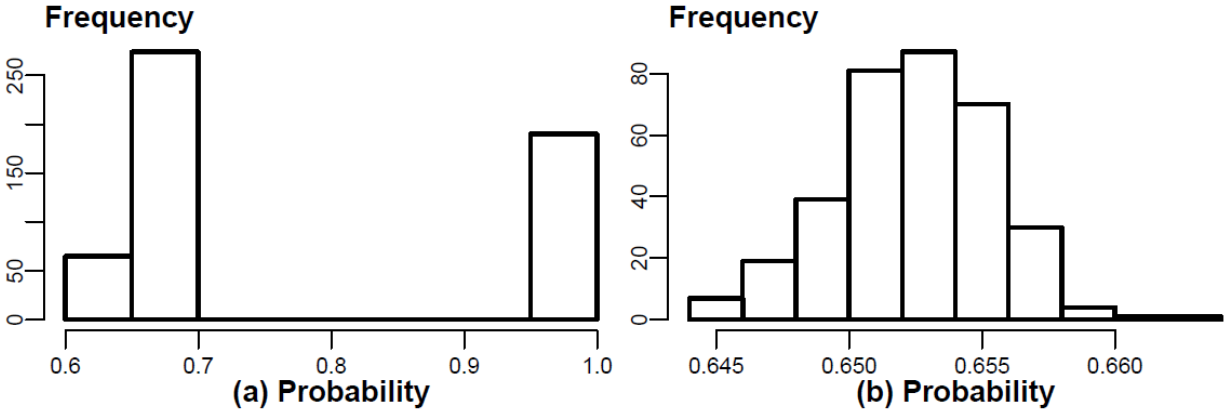

Additional File 3: *Annotated R code for the ZINB model.*

```
m <- “model {

for (i in 1 : nsheep) {

        Neggs[i] ~ dpois(lambda[i])

        lambda[i] <- lamb [i, status[i] + 1 ]

        status[i] ~ dbern(P) #animals status: 0 not recently infected, 1 infected

        lamb[i, 1] <- 0 #zero distribution for not recently infected

        lamb[i, 2]  dgamma(shape; rate) #gamma-poisson for infected


        IgA[i] ~ dgamma ( sh[i], rt[i] )  #IgA is gamma distributed

        #vector of means: position 2 exposed, 1 for non-exposed

        mn[i] <- vmn[ status[i] + 1]

        #vector of shapes: position 2 exposed, 1 for non-exposed

        sh[i] <- vsh[ status[i] + 1]

        rt[i] <- sh[i]/mn[i] #rate = shape / mean

}

# Prior zero-inflation

P ~ dbeta(1, 1)


#Priors Egg counts

shape ~ dgamma(0.001, 0.001)

p ~ dbeta(1, 1)

rate <- p/(1 – p)
```

```
# Priors IgA #
for(i in 1 : 2){
        unorderedmeans[i] ~ dgamma(0.001, 0.001) #uninformative means
}
vmn <- sort(unorderedmeans) #make sure uninfected mean is lower
vsh[1] ~ dgamma(0.001, 0.001)
vsh[2] ~ dgamma(0.001, 0.001)

#To avoid problems finding initial values
#inits# status, .RNG.seed, .RNG.name #initial values (animals status and RNG)
#data# FEC, IgA, nsheep #data used
#monitor# shape, rate, status, P, vmn, vsh # Outputs of the model
}"
```

Additional File 4: *Raw data used in this study.*

SheepID	IgA	FEC
1	13.38	0
2	13.38	30
3	2.39	0
4	3.74	0
5	2.39	120
6	10.14	0
7	4.44	0
8	2.2	0
9	2.48	0
10	3.3	240
11	2.38	45
12	2.49	30
13	3.59	30
14	5.37	195
15	4.43	0
16	6.19	0
17	4.64	0
18	4.74	30
19	2.14	0
20	1.69	0
21	3.41	0
22	0.86	15
23	2.02	0
24	2.76	0
25	2.6	0
26	2.16	0
27	3.47	15
28	5.31	0
29	1.39	0
30	3.27	0
31	3.49	0
32	3.38	0
33	2.33	45
34	2.82	0
35	4.33	0
36	5.73	0
37	3.08	0
38	4.34	120
39	3.43	0
40	5.22	0
41	1.24	15
42	2.6	0
43	3.37	0

44	2.66	0
45	4.9	0
46	2.28	15
47	3.44	0
48	4.89	0
49	6.37	0
50	6.24	0
51	5.35	45
52	6.03	45
53	3.36	0
54	4.49	0
55	0.74	45
56	3.86	0
57	2.34	15
58	4.91	15
59	4.63	45
60	3.41	15
61	12.56	0
62	2.8	45
63	9.43	15
64	2.92	0
65	1.55	45
66	7.79	0
67	28.98	15
68	1.29	0
69	9.29	75
70	6.69	0
71	9.79	274
72	16.81	0
73	6.51	390
74	6.51	135
75	12	15
76	29.95	30
77	10.37	0
78	4.61	15
79	13.87	0
80	7.31	0
81	7.31	135
82	6.79	105
83	6.03	150
84	32.87	45
85	2.54	15
86	10.95	45
87	10.76	0
88	1.35	30

89	6.36	0
90	8.34	0
91	2.41	165
92	3.54	195
93	3.04	15
94	2.06	225
95	1.93	135
96	1.49	90
97	1.67	120
98	3.22	105
99	4.51	0
100	3.16	15
101	2.63	195
102	5.84	0
103	1.82	0
104	3.48	75
105	7.45	165
106	1.78	165
107	1.99	270
108	6.34	75
109	2.22	0
110	0.56	0
111	3.2	0
112	3.17	0
113	0.17	0
114	3.05	0
115	1.68	0
116	3.02	0
117	0.45	0
118	0.84	0
119	0.44	0
120	0.75	0
121	4.31	0
122	1.33	0
123	1.92	0
124	1.66	0
125	0.68	0
126	2.2	0
127	5.41	0
128	2.75	0
129	0.99	0
130	2	0
131	0.65	0
132	3.33	0
133	2.27	0

134	2.72	0
135	1.21	0
136	2.81	0
137	1.36	0
138	1.06	0
139	3.64	0
140	3.83	0
141	1.25	0
142	1.55	0
143	2.94	0
144	0.39	0
145	2.77	0
146	2.11	0
147	1.08	0
148	2.09	15
149	6.79	0
150	2.97	0
151	4.28	0
152	1.2	0
153	2.08	0
154	1.54	0
155	3.36	0
156	0.89	0
157	1.46	0
158	1.3	0
159	4.44	0
160	1.52	0
161	0.76	0
162	0.98	0
163	0.94	0
164	1.7	0
165	1.51	0
166	2.39	0
167	0.86	0
168	2.44	0
169	1.36	0
170	4.53	0
171	3.53	0
172	2.3	135
173	6.93	0
174	5.76	0
175	4.26	0
176	5.25	30
177	9.03	135
178	1.75	0

179	3.17	135
180	3.19	0
181	5.71	0
182	6.89	0
183	2.39	0
184	3.23	15
185	5.32	0
186	2.05	30
187	2.43	180
188	1.18	135
189	2.97	135
190	4.33	30
191	3.12	255
192	3.99	0
193	4.77	30
194	3.34	0
195	2.25	150
196	1.36	0
197	3.02	45
198	1.71	60
199	1.08	15
200	1.06	0
201	0.65	0
202	5.23	0
203	0.84	0
204	2.92	0
205	2.65	0
206	3.45	0
207	1.42	0
208	1.04	0
209	1.28	0
210	12.63	0
211	2.11	0
212	1.97	0
213	9.3	0
214	8.72	0
215	0.83	0
216	0.81	0
217	5.15	0
218	0.5	0
219	1.09	0
220	1.41	0
221	0.67	0
222	3.21	0
223	4.82	15
224	3.1	0

225	3.82	0
226	1.27	0
227	4.41	0
228	3.03	0
229	8.57	0
230	0.22	0
231	0.55	0
232	0.55	0
233	2.89	0
234	5.74	15
235	3.16	0
236	4.14	0
237	0.67	0
238	1.08	0
239	4.74	0
240	1.2	0
241	8.46	15
242	2.81	0
243	1.13	0
244	4.07	15
245	8.21	0
246	2.83	0
247	7.43	15
248	2.34	0
249	1.01	0
250	4.94	0
251	0.64	0
252	2.46	15
253	3.1	0
254	1.59	15
255	3.56	0
256	2.27	0
257	1.71	15
258	0.73	15
259	1.15	0
260	2.21	15
261	0.51	0
262	0.09	0
263	2.97	0
264	4.26	0
265	3.61	0
266	4.67	0
267	4.34	210
268	5.17	255
269	4.79	0
270	5.36	0

271	1.92	255
272	3.41	15
273	2.95	90
274	2.9	120
275	3.33	0
276	3.13	120
277	1.94	15
278	7.22	0
279	5.02	0
280	1.97	15
281	1.94	0
282	3.42	90
283	3.47	0
284	3.22	60
285	3.87	0
286	5.54	45
287	5.48	0
288	6.39	0
289	2.13	105
290	2.48	0
291	21.6	165
292	6.8	30
293	4.37	255
294	3.66	45
295	4.05	0
296	11.69	0
297	21.1	15
298	10.37	0
299	6.58	0
300	8.6	15
301	2.81	0
302	20.87	0
303	17.73	150
304	14.6	60
305	7.55	90
306	2.32	45
307	5.94	0
308	13.52	0
309	9.61	0
310	4.52	60
311	0.77	0
312	3.57	210
313	1.34	240
314	7.84	30
315	7.61	60
316	8.66	0

317	1.32	210
318	9.74	15
319	1.45	120
320	3.47	0
321	1.16	0
322	1.01	0
323	2.56	0
324	1.19	0
325	3.03	0
326	2.19	0
327	6.43	0
328	7.01	0
329	0.76	0
330	2.49	0
331	3.09	0
332	10.71	0
333	0.67	0
334	4.34	0
335	2.83	0
336	0.48	0
337	1.13	0
338	1.59	0
339	3.25	0
340	2.03	0
341	1.66	0
342	6.94	0
343	1.78	0
344	0.27	0
345	3.08	0
346	3.61	0
347	3.26	0
348	3.77	0
349	5.33	0
350	4.83	0
351	3.29	0
352	0.23	0
353	1.13	0
354	2.73	0
355	1.32	0
356	1.51	30
357	2.05	30
358	0.54	0
359	2.27	0
360	0.88	0
361	1.74	0
362	1.21	0

363	1.97	0
364	1.88	0
365	2.39	0
366	1.88	0
367	2.92	0
368	5.61	0
369	1.11	0
370	2.77	15
371	0.79	15
372	2.82	0
373	1.14	15
374	1.25	0
375	2.25	15
376	1.65	0
377	1.14	0
378	0.87	0
379	1.51	0
380	1.68	0
381	1.07	0
382	0.89	0
383	4.92	0
384	6.54	0
385	2.53	0
386	3.42	0
387	1.12	0
388	1.77	0
389	4.09	0
390	4.81	0
391	10.29	0
392	4.31	0
393	2.27	0
394	4.4	0
395	2.42	0
396	1.84	0
397	5.82	0
398	1.05	0
399	2.97	0
400	5.55	0
401	2.97	0
402	1.07	0
403	0.95	0
404	7.29	0
405	4.06	0
406	3.49	0
407	6.58	0
408	2.54	0

409	1.86	0
410	3.09	0
411	12.31	0
412	3.01	0
413	2.95	0
414	7.04	0
415	2.01	0
416	2.05	0
417	4.39	120
418	2.76	30
419	4.88	15
420	1.18	225
421	5.82	45
422	9.58	90
423	1.84	220
424	3.56	60
425	1.62	165
426	2.18	90
427	3.56	90
428	3.44	360
429	2.42	105
430	1.44	0
431	0.59	90
432	8.48	45
433	6.93	120
434	2.48	180
435	0.93	0
436	4.98	105
437	2.27	90
438	1.36	15
439	5.38	0
440	2.88	45
441	5.22	60
442	4.08	0
443	9.98	0
444	1.06	15
445	1.17	15
446	4.67	45
447	3.23	0
448	0.74	0
449	5.62	0
450	5.83	0
451	5.83	0
452	4.75	0
453	4.7	0
454	3.86	45

455	10.04	0
456	1.83	0
457	5.6	0
458	2.78	15
459	3.26	0
460	2.72	0
461	1.38	30
462	4.38	0
463	3.6	0
464	0.52	0
465	1.77	0
466	4.48	15
467	4.65	15
468	0.49	0
469	3.74	18
470	2.3	300
471	0.87	0
472	1.41	15
473	4.85	0
474	7.32	45
475	7.94	0
476	3	15
477	1.12	30
478	10.04	0
479	3.27	0
480	6.12	0
481	1.67	15
482	3.82	0
483	3.71	45
484	0.59	0
485	2.76	0
486	2.74	0
487	3.03	0
488	2.61	135
489	4.06	0
490	1.34	0
491	3.11	270
492	6.55	15
493	2.09	0
494	2.16	0
495	3.65	15
496	19.11	1080
497	27.38	45
498	3.84	1290
499	15.37	120
500	5.22	180

501	4.04	15
502	7.4	0
503	3.63	210
504	3.94	30
505	6.12	0
506	21.62	645
507	3.84	30
508	11.08	30
509	4.27	165
510	8.78	248
511	4.29	240
512	14.11	0
513	6.32	30
514	9.94	300
515	2.41	210
516	6.18	195
517	5.95	60
518	2.75	15
519	14.95	180
520	7.43	60
521	32.24	165
522	3.71	120
523	6.02	45
524	22.27	30
525	7.08	0
526	0.32	180
527	6.87	165
528	5.54	45
529	9.89	255
530	0.67	600
531	4.23	30
532	4.24	15
533	13.28	705

Results, discussion and perspectives

Globally, gastrointestinal nematodes infections are one of the most important threats to the health, welfare and productivity of sheep populations (Morgan et al., 2013). Nowadays, the resistance to all families of anthelmintic is reported and this resulted in the current anthelmintic approach to GIN control being unsustainable for a long period of time. Therefore, several mechanisms of GIN control are proposed as alternative and sustainable strategies, where one of the most promising options is selective breeding of resistant animals. This strategy takes advantages of the host immune response that is a present as the host's ability to mount a protective adaptive immune response against the GINs.

Moreover, the rapid advances in the field of genomics have led to the development of SNP marker applications to plants and animals. The availability of the 50K-SNP chip for the sheep genome, which was introduced in 2009 by the International Sheep Genomics Consortium (ISGC), has been a significant milestone in sheep genomic research. In addition, a new array that enhances the marker density offered by the previous one is the Ovine Infinium High density (HD) SNP BeadChip, which was released in 2013 and allows the analysis of 600,000 markers. Apart from the ovine chip, in other animal species and in human research, the availability of high density SNP arrays has been present for a longer period of time with more than 600,000 (in cattle, chicken, horse and plants) and around 2.5 million (HumanOmni2.5-8) SNPs per chip, respectively (Illumina; Ha et al., 2014). As consequence of the higher marker density offered by these genomic tools, new gene mapping methods based on the exploitation of population information of LD, such as the GWAS (Aulchenko et al., 2007, 2010) or the mixed LDLA (Legarra and Fernando, 2009) approaches, or imputation methods (Browning and Browning, 2007) enhance the potential of the classical LA-based classical gene mapping studies. In parallel to the development of the new genomic tools, a large number of bioinformatic applications have been released with the aim solving the difficulties that appear when dealing with the large datasets of information generated by massive SNP-chip genotyping (Nicolazzi et al., 2015). All these elements increase our potential to obtain useful genetic information that can be directly applied to breeding programmes and that increases our knowledge on the underlying biology and genetic architecture of complex production traits.

The identification of the genes and mutations that influence traits of economic importance to directly use the molecular information as a complement of classical breeding programs

is of primary interest to livestock industries, especially for the traits with low heritability and those difficult or expensive to measure routinely. That is the case for the resistance to GINs, which, as we mentioned before, has a large economic impact on the sheep industry worldwide and is rather cumbersome and costly to measure. Therefore, the availability of the 50K-SNP chip and has encouraged us to carry out a new QTL mapping study designed as a follow up step of the microsatellite-based genome scan reported by Gutiérrez-Gil et al. (2009b) in order to refine, replicate and update the QTL results previously reported in Spanish Churra sheep. In addition, the international collaborations established in the framework of the European ITN NematodeSystemHealth have provided additional opportunities to better understand the genetic architecture of parasite resistance in Churra sheep. Hence, we report here a detailed study on the variability of two genes of the MHC class II genomic region in the Churra 15 sires included in the experimental design of the QTL mapping study of this PhD Thesis. Also, a mathematical model has been specifically developed to better explain the phenotypic measurements of the indicator traits analyzed in the mapping study, FEC and IgA, which correspond to animals showing very low infection levels. For that, a model assessing the extent of zero-inflation for the FEC trait and integrating the information provided by the IgA response has been implemented.

In this section, we present a brief summary of the results and discussion reported in relation to each of the three specific aims of this PhD memory (related to the main three research articles included herein), as well as a global discussion of the outcomes of this PhD memory.

1. ***Objective 1.*** *Detection and replication of QTL underlying resistance to gastrointestinal nematodes in adult sheep using the ovine 50K SNP array*

Nowadays, taking into account the failure of anthelmintic treatments as a sustainable method to control GIN infections in sheep, the detection of QTL influencing parasite resistance in sheep has an increasing economic and scientific interest for the sheep industry worldwide. Hence numerous QTL and SNP markers (379) related to indicator traits of parasite resistance in sheep have been published up to date (see SheepQTLdb at http://www.animalgenome.org/cgi-bin/QTLdb/OA/index; Kemper et al., 2011; Sallé et al., 2012; Riggio et al., 2013, 2014; McRae et al., 2014a; Benavides et al., 2015). Whereas most of these studies are focused on young animals, the research group where

this PhD research has been carried out, the ULE MEGA group, is interested in the study of parasite resistance in adult ewes. Generally, the adult ewes are resistant to GIN infections. However, the breakdown of the ewe's resistance to GINs is manifested as a rise in FEC - called the periparturient period. Therefore, reproductive ewes play a key role in the epidemiology of GIN infection because eggs deposited during the periparturient period influence the severity of the infection during the grazing season (Stear et al., 2007). Hence, this group previously performed a genome scan to detect QTL with influence to GIN infection traits in a commercial population of Spanish Churra sheep (Gutiérrez-Gil et al., 2009b). In this study, a total of 182 markers (181 microsatellites and 1 SNP) distributed along the 26 ovine autosomes were genotyped in a total of 322 animals distributed in eight half-sib families following a daughter design. By implementing a classical LA approach, this work identified five significant QTL associated to the FEC and IgA indicator traits on OAR1, 6, 10 and 14. Only the QTL located on OAR6 and with effects on the FEC trait reached 5% genome-wide significance level. This previous genome scan study provided a baseline on which the activities in the initial phase of this thesis were proposed with the aim of confirming some of its results, with a special interest focused on the most significant results identified on OAR6.

But, against the classical approaches to confirm and fine-map previously detected QTL by increasing microsatellite marker density and perform, performing comparative mapping and identify candidate genes by the gene cloning strategy (García-Gámez et al., 2012a; Grisart et al., 2004), the availability of the ovine 50K-SNP chip allowed the proposal of a medium-density SNP-chip based genome scan where different types of analysis methods could be implemented, LA, LDLA and GWAS. A medium-density SNP array offers a much higher resolution compared to the microsatellite-based scanning and using this chip is an opportunity to enrich genetic linkage information. It has been proven that the linkage results from SNP maps can result in narrower linkage regions with higher LOD scores when compared with microsatellite marker maps (Chen et al., 2005). In any case, considering the same analysed data, other factors, such as differences between microsatellite and SNP maps, and/or genotyping errors could also influence the replication of QTL detected by both type of markers (Chen et al., 2005).

Taking all this into account, the main objective of the new QTL mapping study reported here was the use of the 50K-SNP chip to replicate some of the QTL previously reported by Gutiérrez-Gil et al. (2009b), and also detect new QTL for parasite resistance traits in

Churra sheep that due to the limitations of the previous study (e.g. limited marker density, exclusive use of LA approach, limited statistical power, etc.) had not been identified. With this objective, a different subset of half-sib families of the commercial population of Spanish Churra sheep related to the ANCHE Selection Nucleus was genotyped and three different QTL mapping analyses, based on LA, LDLA and GWAS, were performed. In this case, the resource population under analysis included 518 ewes that were sampled for faeces and blood at the initial stages of this PhD Thesis project to obtain measurements of two indicator traits of parasite resistance, FEC and IgA. These animals, which belonged to different flocks of the ANCHE Selection Nucleus and were distributed in 14 half-sib families, were a subset from the larger population of 1,696 Churra animals (distributed in 16 half-sib families) genotyped with the 50K-SNP chip in a previous analysis for milk traits (García-Gámez et al., 2012c). Hence, genotypes and phenotypes were available for QTL map analyses based on the 50K-SNP chip genotypes.

The use of the QTLmap software (Filangi et al., 2010) gave us an opportunity to run and compare the results from the LA and LDLA approaches, whereas a GWAS was performed by using the DMU software, which was running through the R terminal using a package "Rdmu" (Madsen et al., 2014).

A total of three, 63 and 10 significant QTL identified were detected by LA, LDLA and GWAS, respectively. Half of the total of significant QTL/SNP associations identified overlapped with QTL effects described in other studies. Because classical LA will only detect QTL in our design if several sires are heterozygous at the same QTL (*Qq*), many marker-trait associations that do not satisfy this assumption but have a genuine association at the population level, will not be detected by LA. Because of that, and based on the higher marker density offered by the 50K-SNP chip, compared with microsatellite-based scans, we have performed the genome scan based on three different methodological approaches, trying to present a global picture of all kind of QTL that segregate in this commercial population. Hence the limitations of classical LA, which is exclusively built on pedigree information, have been compensated with the alternative approaches of LDLA and GWAS, which exploit population information. The classical LA method only identified three significant QTL at the 5% chromosome-wise significance level on OAR6, 8 and 22. This reduced number of identified QTL by LA fits with the limited power to detect QTL that, following Weller et al. (1990), was estimated for the experimental design of our analysis, which was approximately 11% (assuming a substitution effect of

0.2 phenotypic SD units, two alleles with frequencies of 0.25 and 0.75, respectively, a 0.2 of the trait heritability, a type I error rate of 0.05, a 1% recombination frequency between the QTL and marker and 37.5% of the analyzed sires are heterozygous at the QTL). Interestingly, according to the current sheep genome assembly (Oar_v3.1), the LFEC QTL detected on OAR6 by LA (80.8–91.4 Mb) overlaps with the genome-wise significant QTL reported by Gutiérrez-Gil et al. (2009b) for the same trait in a different subset of half-sib families of the Churra sheep commercial population (in the region corresponding to 68 and 85.1 Mb of OAR6). The fact that in the present work the significance level reached by this QTL is lower than in the microsatellite-based genome scan may be due to several factors such as the low infection level of the new analysed animals, the number of sampled animals which was not substantially large, and, as mentioned previously, the limited power of the global experimental design.

On the other hand, LDLA identified significant QTL overlapping with the LA-detected QTL and identified 60 additional significant haplotype associations. Furthermore, LDLA shows to be more accurate mapping method, as the significant LDLA intervals were much narrower and better defined than the confidence intervals estimated by LA. For example, whereas the LDLA also supports the OAR6 QTL for LFEC reported by Gutiérrez-Gil et al. (2009b), it identifies two clearly differentiated significant haplotype associations in that region, one in the 72.3–77.2 Mb interval, and the other one at 85–90.2 Mb.

The results have shown that the LDLA approach is able to identify more significant QTL than the two other methods. This is a similar outcome that that previously observed in the analysis of milk traits in the larger commercial population previously mentioned (García-Gámez et al., 2012c). As discussed by Legarra and Fernando (2009), the LDLA method implemented in QTLMap permits to map QTL more accurately than LA while retaining its robustness to spurious associations. Also the GWAS approach identified a substantial lower number of significant associations than LDLA. Among the different advantages highlighted for the use of LDLA versus GWAS in animal breeding populations with known family structure, Meuwissen et al. (2010) claimed that LDLA is expected to suffer less from the multiple testing than GWAS, and therefore offers more power to detect the existing QTL. Hence, our work adds support to the previous observations previously drawn by our group (García-Gámez et al., 2012c) and confirms that, by exploiting simultaneously the familiar structure of the pedigree and the linkage disequilibrium

information from the global population, LDLA offers the most efficient strategy to perform SNP-chip based QTL searches for traits of economic interest in Churra sheep.

Since the results of the GWAS-based genome scan did not show concordance with the three QTL identified by LA, the available LDA analysis option (*calcul = 26*) in the QTLMap software gave us the possibility to perform a different association analysis that is based on the "LDA decay" method described by Legarra and Fernando (2009). This alternative analysis is also based on LD but instead of testing one SNP per analysis it tests the effect of a 4-SNP haplotype in a way that the parental haplotypes are pooled in classes defined by the haplotype IBS status, with each different haplotype class having a specific effect on the quantitative trait (Legarra and Fernando, 2009). This LDA approach was only performed for those chromosomes with coincident significant results between LA and LDLA. Since the QTLMap software is dedicated to perform QTL mapping analyses in outbred half-sib families, the LDA offered by this software is particularly adapted to populations characterized by a family structure. In contrast to the GWAS results, this analysis supported mostly the LDLA's associations reported for three chromosomes, whereas only one of the significant LA QTL, that on OAR6 and also detected by LDLA, was also confirmed by LDA. This observation bolsters support for the FEC QTL identified by LA on OAR6, suggesting that in addition to a family-based linkage information signal, the effect is also due to a genuine association with the trait.

Apart from the methodological considerations, the most important result of this QTL mapping study is the replication of the most significant QTL identified through a microsatellite-based genome scan previously reported in a different population of Churra sheep half-sib families (Gutiérrez-Gil et al., 2009b). The higher marker density and the information provided by the complementary analyses reported for this region herein suggest that the OAR6 region spanning from of 68 to 91.4 Mb includes several different QTL that directly influence the FEC trait, and indicator traits of GIN resistance, in Churra sheep. Interestingly, a GWAS-based study of a Red Maasai x Dorper backcross population (Benavides et al., 2015) also suggests the presence of several QTL for the FEC trait in lambs within the 55.9–78.19 Mb region of OAR6. This finding was based on the fact that the most significant SNP association identified on that chromosome, located at 74.86 Mb, was proven not to be in LD with surrounding significant markers. With the exception of the study by Gutiérrez-Gil et al. (2009b), studies found in the literature refer to QTL detected in lambs; thus, the most distal region on OAR6 where the replicated

QTL from this study is positioned (related to the LA signal at 80.8-91.4 Mb, and the LDLA signal at 85-90.2 Mb) could be related to specific mechanisms of the immune response that is activated in adult animals. In relation to the differences in the host response depending on the age, it has been suggested that in lambs the genetic variation in fecal egg counts is a consequence of genetic variation in worm length and hence worm fecundity, whereas mature sheep may be able to regulate both fecundity and worm number (Stear et al., 1999). Moreover, it has been shown that young lambs at first exposure to GIN parasites fail to generate effective protective immunity in comparison to older sheep (Craig et al., 2014).

It has been shown that resistant animals mount faster the effective protective immunity to GIN parasites than susceptible or young animals (reviewed in Alba-Hurtado and Muñoz-Guzmán, 2013). Therefore, we considered a large list of 5029 genes known to be involved in the immune response (extracted from the IRIS and ImmPort databases available at http://www.innatedb.com/redirect.do?go=resourcesGeneLists) to filter the large number of genes (905) that we extracted from the defined significant LA, LDLA and GWAS regions. A total of 205 immune-related genes were identified in relation to the significant LA and LDLA intervals, whereas no functional candidates were extracted from the significant GWAS-defined intervals. Some of these immune-related genes are involved in the Th1 and Th2 cell responses, which are associated with progression to chronic infection and orchestrates the mechanisms of tissue repair as a primary host defense against helminthes, respectively. Our study presents a detailed discussion of the 20 functional candidate genes identified in relation to the QTL for LFEC identified by LA on OAR6 (TGI: 80.9–91.4 Mb), which include the genes extracted for the significant LDLA QTL located between 85 and 90.2 Mb Among them, we would like to highlight a group of genes coding for chemokines (*IL8, CXCL1, CXCL10, CXCL11, CXCL9, PF4, PPBP*), a family of small proteins that play important roles in the immune system through leukocyte recruitment, cell communication and cell activation during infection (Schumacher et al., 1992; Trotta et al., 2009). That genomic interval also includes three genes coding for members of the epidermal growth factor family, *AREG* (amphiregulin), *BTC* (betacellulin) and *EREG* (epiregulin), for which links with the immune response or GIN expulsion mechanisms have been identified. *AREG* is expressed by diverse cell types involved in the immune response, such as activated Th2 cells (Zaiss et al., 2013), and is a central mediator of epithelial repair (Monticelli et al., 2013).

In summary, this study reported a large number of QTL which supports the suggestion that disease resistance is a complex trait, which is controlled by many loci/genes. Despite of the low statistical power of this study and the low infection levels of the sampled animals, this study has replicated the most significant QTL previously detected on OAR6 in a previous genome scan, which supports for the design and planning of future fine-mapping studies for this chromosomal region. On this regard, our research group has already performed additional analyses for the FEC and IgA traits with the ovine high-density chip, which become commercially available in 2013 and allows the analysis of around 600,000 SNP markers (Chitneedi et al., 2015). Also, within the framework of the ITN project, and based on the within-family LA results reported here, I have performed the selection of a segregating sire (*Qq*) and two homozygous daughters for alternative haplotype alleles at the QTL region (*QQ* and *qq*) and showing extreme divergence for the resistance phenotype. Hence, future studies of this research group will focus on the bioinformatic analysis of this dataset and the filtering of allelic variants that show concordance with the predicted QTL genotypes, with the aim of deciphering the mutations that could be responsible of the replicated QTL effect.

Overall, the results identified through the research here reported are first steps towards the identification of allelic variants directly controlling the phenotypic variation observed for parasite resistance in adult Churra sheep, which could be implemented into the breeding scheme of the Churra sheep commercial population. Nevertheless, the complexity of the immune response against parasite infections may need more global approaches to produce practical results. Hence, future studies combining genomic variation analysis and functional genomic information may help to elucidate the biology of GIN disease resistance in sheep.

2. ***Objective 2.*** *The genomic variation of MHC class IIB candidate genes*

The second objective proposed for this PhD thesis arises as a scientific collaboration between the ULE Mega group and one other group involved in the NematodeSystemHealth ITN project, the group led by Dr. Johannes Buitkamp at the Institute for Animal Breeding in Germany, the Bayerische Landesanstalt für Landwirtschaft (LFL). Following the ITN project philosophy, where the different students have to spend part of the training period in a different institution included in the project, I performed a short stay at the laboratory of Dr. Johannes Buitkamp (LFL group), in

Munich for about 1,5 months from 11 November to 31 December 2013. At that time the LFL group was working on improving the system for genotyping genetic variation in the MHC genomic region. The MHC is gene rich and encodes proteins involved in the innate and adaptive immune system. An exhaustive study of the genetic variability of this region had never been performed in Churra sheep. Hence, as an extension of the initial objective of this PhD thesis and as part of the global objective proposed for this PhD memory, we planned and designed the study on the genetic variability of two genes of the MHC class IIB in Spanish Churra sheep DNA samples. For that, the 15 Spanish Churra rams that were pedigree heads of the resource population analysed in the QTL mapping study previously reported were analysed through sequencing analysis.

Specificity of the adapted immunity response is known to be under control of the MHC, where three classes of genes, I, II and III have been characterized, with the class II genes being the most extensively studied. Polymorphisms in the class IIB genes, *DRB* and *DQB*, have become a hot research topic in the past decades as these genes are among the most polymorphic in the mammalian genome. Because in many cases different numbers of class IIB genes per haplotype exist, the genotyping and sequencing of these genes is not straightforward. The MHC is located on OAR20 and has been regularly detected as a major region in resistance to helminthic infectious. Our analysis included the genotyping of a microsatellite located immediately downstream of the *DRB1* gene exon 2 and the sequencing analysis of *DRB1* gene exon 2, and *DQB* gene exon 2. For the latter four different downstream primers were used.

The results of this work showed, as expected when analyzing two MHC class II genes in a new population, previously unknown alleles. The *DRB1* microsatellite fragment length (from 200 to >450 pb) was within the full range of alleles reported in other breeds for the same polymorphism (Schwaiger et al., 1993). In addition, the exon 2 of the *DRB1* gene revealed nine known and three new DRB1 alleles in the 15 Churra rams analysed. Moreover, we have observed that five Churra rams were homozygous at the microsatellite marker and *DRB1* gene.

The used of four different downstream primers for the sequencing analysis of the *DQB* genes resulted in all the *DQB* alleles being unambiguously determined. Accordingly, a total of 25 *DQB* alleles were observed of which 15 had not been previously described. In contrast to the *DRB1* gene, none of the 15 rams was homozygous at the *DQB* locus.

In this study, a total of 14 MHC Class IIB haplotypes were identified in 15 Spanish Churra rams, where it was observed that the genotypes for the microsatellite and *DRB1* alleles are highly correlated, whereas recombination events between *DRB1* and *DQB* genes seem to occur. Also the occurrence of mutation and/or microconversion could explain some haplotypes carrying alleles that differ only by one base. In addition, we observed one or two DQB genes per haplotype which is supported by the findings from previous investigations (van Oorschot et al., 1994; Schwaiger et al., 1996; Feichtlbauer-Huber et al., 2000).

Even though a small number of Churra DNA samples were used in this study, the results indicate that an efficient genotyping system can be developed for the establishment of efficient genotypes of the MHC IIB genes in Churra sheep. The methods optimized in this work could be used in future studies aiming at the typing of MHC class IIB genes in Churra or other sheep breeds across the world, which would contribute to the better understanding of class IIB haplotype organization and evolution.

In terms of applying the results of this work to the study of the genetic control of parasite resistance in Churra sheep, future studies could consider performing additional typing of MHC class IIB genes in daughters of these rams and to perform association analyses between the class IIB alleles/haplotypes targeted herein and indicator traits of resistance to GIN infection in the Churra sheep commercial population.

3. ***Objective 3.*** *Implementation of an extended ZINB model in the study of low levels of natural gastrointestinal nematode infections in adult sheep*

The raw phenotypic data analysed in the QTL mapping study included in the first objective of this PhD Memory were initially processed at University of Leon (ULE) to obtain the Yield Deviations (YDs) that were later used as dependent variables for statistical analyses to identify genomic regions influencing resistance to GIN infection. However due to the high proportion of FEC measurements equal to zero in our phenotypic dataset, as result of the low infection levels of the animals related to the extremely dry meteorological conditions during the sampling period, and the difficulties to find an appropriate transformation method for the FEC data normalization data, we decided to apply additional statistical analyses. These additional analyses were implemented through a second scientific collaboration established through the ITN

NematodeSystemHealth project with the research group led by Professor Michael Stear at the University of Glasgow, United Kingdom (GLA group). This scientific collaboration was based on another short stay of six weeks (from 13 January to 28 February 2013) that I performed at the University of Glasgow, and where I worked in close collaboration with Joaquín Prada Jiménez de Cisneros, another PhD student of the ITN project specialized in mathematical and statistical modelling applied to parasite infection related datasets.

Adult female sheep play a key role in the epidemiology of GIN infections because eggs deposited during the peripartum period influence the severity of the infection during the grazing season. However, outside the peripartum period, in naturally infected adult sheep egg counts are typically low or overdispersed, which is also proven to occur in naturally infected lambs (Stear et al., 2007). Hence, it is difficult to determine the infective status of the animals using only the FEC count. Therefore, in addition to the egg counts, supplementary information is needed to more accurately estimate the prevalence of infection in naturally infected adult sheep flocks.

In this study, the prevalence of gastrointestinal nematode infections are very low compared with other studies carried out in the same area (NW of Spain) (Gutiérrez-Gil et al., 2010; Martínez-Valladares et al., 2013). In the present study, the low levels of infection are likely a consequence of the exceptional climatic conditions that took place during the sampling period of this study. On this regard, it has to be considered that the longevity and survival of infective Trichostrongylid L3 nematodes is related to the environmental temperature and humidity (O'Connor et al., 2006; Martínez-Valladares et al., 2013).

About the two phenotypic indicators for the diagnosis of GIN parasite infections that we measured in our resource population of Churra adult ewes, FEC and IgA, the FEC trait is the most commonly used indicator of parasite resistance because of its properties, such as inexpensive, easy to perform and lack of special equipment required for its determination. However, when the excretion of eggs in faeces is low as in this study, FEC should not be used by itself and it is necessary to use other, more sensitive, diagnostic method or methods that might provide efficient information to indicate the presence and level of infection. In the present study, in contrast to the FEC trait, IgA activities were moderately high, which may be explained by the fact that the antibodies persist for some time after GIN infection and might provide potential information for the detection of pre-patent

infections. Three experimental studies performed in different breeds of sheep infected with GINs showed that the IgA activity is detected for prolonged periods of time post infection (Henderson and Stear, 2006; Martínez-Valladares et al., 2005; MacKinnon et al., 2010).

Taking all this information into account we decided to use a zero-inflated negative binomial model (ZINB) model to analyse our FEC dataset and calculate the extent of zero-inflation. This methodological approach has been previously applied by several studies focused on parasitic infection datasets (Nødtvedt et al., 2002; Denwood et al., 2008; Walker et al., 2009). Since the initial ZINB model applied, which was only based on FEC data, could not distinguish among the animals with zero FEC those that were infected or uninfected, we implemented an extension of that model to identify the animals that were likely to be uninfected by adding the IgA information.

To our knowledge, the resulting model reported in this work provides the first description of a ZINB model for the analysis of multiple traits with the aim of discerning which animals are infected and which have not been recently exposed or which have been exposed at a very low infection level. This approach is relatively straightforward and allows the study of nematode infections in adult animals, in flocks with low prevalence of infection. This modelling methodology could also be applied to other hosts where parasite overdispersion has been reported such as cattle, free-range pigs, chickens, humans and wild animals (Boes et al., 1998; Vercruysse and Dorny, 1999; Weyher et al., 2006). In sheep, the proposed approach improves our ability to identify animals infected at low level, which is a key point to be considered when studying host resistance in naturally infected individuals and when trying to improve parasite resistance through breeding strategies.

4. Global discussion

Genetic variation of the host significantly contributes to striking difference in the outcomes of parasite infections, especially in natural infections where the host is infected with several parasitic genera. The genetic resistance of the host to parasites is a complex multifactorial genetic trait in which many genes contribute to the host phenotype. In addition, the different parasite species trigger different immune response (Anthony et al., 2007) and because the natural infections usually involve the action of different parasite species, the studied phenotype may be considered of especial complexity. This

complexity is confirmed by the results of many studies which bring a lot of difficulties to relive truthful genomic regions of interest that could be of use for breeding selection. So far numerous QTL have been identified on all ovine chromosomes. There are many QTL regions associated to parasite resistance in a specific study that have not been confirmed in other sheep populations, whereas there are some chromosomal regions that appear to be of particular interest in relation to the genetic architecture of parasite resistance because the high number of QTL identified within these regions by different studies. In addition, it has been shown that some QTL are species specific like the QTL identified on OAR14 for Nematodirus FEC (Riggio et al., 2014).

Here, in this PhD thesis, we have attempted to obtain more information about the genomic regions related to phenotypic indicator traits of parasitic infection in the commercial population of Spanish Churra sheep by using a substantially higher number of markers (43,613 SNPs) than the 182 markers analysed some years ago in a different subset of half-sib families of the same commercial population (Gutiérrez-Gil et al., 2009b). By using different and complementary analysis methods, LA, LDLA, LDA and GWAS we have identified a high number of QTL related to the two indicator traits of parasite resistance considered, LFEC and IgA_t in the studied population. Some of the QTL identified in our study are coincident with other QTL reported for parasite resistance in young animals, whereas some others could be related to the specific immune response activated in adult animals. The large number of QTL identified in this study supports the previously mentioned idea that disease susceptibility is determined by complex multi-gene interactions (Allen and Sutherland, 2014). However, the results of our gene mapping study should take into account that at the sampling time we confronted unpredictable environmental conditions that had a great impact on the development of infective larva stage on pasture, which was reflected on the low level of infection of the studied sheep population. Despite of this limitation, the infection conditions of our study may be more similar to the reality than the conditions of the majority of the studies in this field, which are based on controlled experimental exposures of the animals to parasites to avoid the effect of environmental factors that give additional complexity to the studied trait. Therefore, it could be assumed that the indicator traits measured under experimental infections are not truthful predictors of either disease patterns in the field or selection response in animals that are infected simultaneously by several genera. This could have an impact to detect genuine QTL.

The faecal egg count is one of the most used phenotypic traits to measure resistance to GINs. This trait, in naturally infected animals, has an extremely skewed, non-normal distribution, which is under the influence of the small percentage of animals that are responsible for the majority of parasite transmission. This pattern is also observed in natural infected populations of wild animals as well as humans (Guyatt et al., 1990; Weyher et al., 2006). In this PhD thesis, during the sampling period, the environment conditions were not suitable for the development of parasites in the field, which resulted in a remarkable low burden of parasites in the infected animals. Normally, the environmental conditions favorable for the development of parasitic infective larvae on the pasture where animals graze, will result in aggregation of animals' FEC. However, in the opposite situation, under a low burden of parasites, the animals that mount a fast immune response to parasites will effectively clear the infection, and the infection will not be detected. In this situation, the FEC trait is not a good indicator of a parasite infection and using additional indicators would increase accuracy to identify the infection levels. Among possible additional indicators of infection many authors have suggested immune markers, which are shown as a much improved measure of host resistance (de Cisneros et al., 2014). Based on this premises, and using the information of two indicators traits, FEC and IgA, we modified the initially implemented ZINB model to capture and identify animals that had not been exposed to infection at the day of sampling.

The results of the new extended ZINB model showed that the initial dataset of FEC phenotypes that had been used in the QTL analyses was including uninfected animals, and that this fact could have had an influence on the results of our QTL mapping study. Therefore, we acknowledge here the need of repeating the QTL mapping analyses by including in those analyses only the subset of animals from our resource population that, according our ZINB model, has been proven to be infected at the sampling time. The new analyses could be used to assess the impact of the inclusion of uninfected animals in the QTL mapping model and to confirm or reject the previously identified QTL genomic regions. That is especially important before planning additional research efforts towards the identification of the causal variant/s of the replicated OAR6 QTL. In addition, the implementation of our extended ZINB model should be performed as a previous step of additional genetic analysis of parasite resistance traits in adult Churra sheep, such as future genome scans (QTL mapping and/or GWAS) and candidate gene association study

In addition to the QTL mapping and the novel modelling implementation, this PhD thesis has also studied the genetic variability of the MHC class IIB genes in the 15 Churra rams siring to half-sib families of the resource population. The most common statement about the MHC genes is that heterozygous individuals for these genes can recognize a higher variety of pathogen antigens than individuals with two identical alleles. This implies that a population carrying more alleles for these genes is assumed to be fitter than the one with a lower number of alleles. In relation to this, at the University of Glasgow, the GLA group involved in the ITN, has proposed a new model for the maintenance of the MHC diversity at the population level, taking into account the allele fitness and allele distance between the studied populations. This study has shown that a population that has a large number of very similar alleles might be less fit than a population with a smaller number of very diverse alleles (Stefan, 2016). Based on this new information, measurements of the MHC genetic diversity could be considered in sheep selection programmes with the aim of improving the resistance of animals against GINs and avoiding adverse effects on susceptibility to other diseases. In this context, the information obtained in this PhD thesis in relation to the MHC could be a starting point for a future research line focused on the genotyping of these genes in a larger population and the identification of possible associations between MHC class IIB genes alleles/haplotypes and parasite indicator traits. This, together with following-up studies of QTL mapping and identification of causal genetic variants, would contribute to increase our knowledge about the genetic architecture of parasite resistance in Spanish Churra sheep and the possible improvement that could be reached for these traits through the use of genomic information.

Conclusions

First,

The results of a medium marker density scan of the sheep genome, based on the ovine *Illumina* OvineSNP50 BeadChip (50K-SNP chip), performed in a half-sib commercial population of Spanish Churra sheep with the aim of identifying and replicating QTL influencing two indicator traits of parasite resistance, the FEC and the serum levels of IgA, have shown that:

- By exploiting the high marker density offered by the 50K-SNP chip and applying different and complementary statistical analysis methodologies our study provides a global picture of the QTL that segregate in this ovine population (with a total of three 5% chromosome-wise significant QTL being identified by LA, 63 significant regions being detected by LDLA, of which 13 reached the 5% genome-wise significance level, and 10 significant SNPs being found to be associated with IgA_t by GWAS).
- By combining in a single analysis both the pedigree information and the linkage disequilibrium information obtained at the population level, the LDLA appears, among the three applied methods, as the most robust and efficient methodology to perform QTL searches for indicator traits of parasite resistance and other traits of economic interest in the family-structured analysed resource population.
- By identifying a FEC-related QTL located on OAR6 (within the interval 72.3-91.4 Mb of the Oar_v3.1 sheep genome assembly) the present study replicates a previously reported QTL in Churra sheep through a microsatellite-based genome scan. This finding provides support for the design and planning of future studies aiming to the identification of the causal allelic variant/s responsible of the replicated QTL effect.

Second,

The sequencing analysis that was performed in order to determine the genetic variability of the MHC class IIB genes in 15 Spanish Churra rams identified a total of 12 (nine known and

three new) alleles and 25 (from which 15 were new) alleles of exon 2 of *DRB1* and *DQB* genes, respectively. Considering the variations in these two gene fragments and the *DRB1* microsatellite analysed, a total of 14 haplotypes could be formally deduced. Based on these results, an efficient MHC IIB genotyping system can be developed for the Churra sheep population, which would contribute to a better understanding of the class IIB haplotype organization and evolution.

Third,

Based on the low level of infection shown by the adult ewes of the resource population analysed in this study, a ZINB model, initially used to assess the level of zero-inflation in the FEC dataset under analysis, has been extended to include information from the IgA levels. The new developed model allows discerning, among the animals with zero FEC values, which animals are infected and which have not been recently exposed to infection, or have been exposed to a very low infection level. By improving our ability to identify animals that have been infected with GINs, even at low FEC, the proposed approach will assist the study of natural nematode infections in flocks with low prevalence of infection and the breeding of GIN resistant sheep.

Conclusiones

Primera,

Los resultados de un barrido genómico de densidad media del genoma ovino, basado en el "*Illumina* OvineSNP50 BeadChip" (chip de 50K-SNP), realizado en una población comercial de familias de medio-hermanas de raza Churra con el objetivo de identificar y replicar QTL que influyen sobre dos caracteres indicadores de resistencia parasitaria, el recuento de huevos en heces (FEC) y los niveles séricos de inmunoglobulina A (IgA), han demostrado que:

• Aprovechando la alta densidad de marcadores que ofrece el chip de 50K-SNP y aplicando metodologías de análisis estadístico diferentes y complementarias, nuestro estudio proporciona una visión global de los QTL que segregan en esta población ovina (siendo identificados tres QTL significativos a nivel *chromosome-wise* por LA, 63 regiones significativas por LDLA, de las cuales 13 alcanzaron el nivel de significación *genome-wise;* además el análisis GWAS identificó 10 SNPs significativa asociados con IgA_t).

• Al combinar en un solo análisis tanto la información de pedigrí como la información de desequilibrio de ligamento obtenido a nivel de población, el LDLA aparece entre los tres métodos aplicados, como la metodología más robusta y eficiente para realizar búsquedas QTL de rasgos indicadores de la resistencia parasita, además de otros caracteres de interés económico en la población de familias de medio-hermanas analizada.

• Mediante la identificación de un QTL relacionado con el FEC, localizado en OAR6 (dentro del intervalo de 72,3 a 91,4 Mb de la versión Oar_v3.1 de la secuencia del genoma ovino), el presente estudio replica un QTL previamente descrito en oveja Churra en base a un barrido genómico basado en microsatélites. Este resultado apoya el diseño y planificación de futuros estudios dirigidos a la identificación de la o las variantes alélicas directamente responsables del efecto QTL replicado.

Segundo,

El análisis de secuenciación que se realizó con el fin de determinar la variabilidad genética de los genes de la clase IIB del MHC en 15 machos de la raza Churra identificó un total de

12 (nueve conocidos y tres nuevos) alelos y 25 (de los cuales 15 eran nuevos) alelos en los exones 2 de los genes *DRB1* y *DQB*, respectivamente. Teniendo en cuenta las variaciones en estos dos fragmentos de estos genes y el microsatélite del gen *DRB1* analizado, se podrían inferir formalmente un total de 14 haplotipos. En base a estos resultados, se puede desarrollar un eficiente sistema de genotipado de la región genómica MHC IIB para la población ovina de raza Churra, lo cual podría contribuir a una mejor comprensión de la organización y evolución de los haplotipos de clase IIB.

Tercero,

Debido al bajo nivel de infección que presentaban las ovejas adultas incluidas en la población analizada en el presente estudio, se ha extendido un modelo binomial negativo inflado de ceros (ZINB), utilizado inicialmente para evaluar el nivel de inflado de ceros de los datos del carácter FEC, para incluir información de los niveles de IgA. El nuevo modelo desarrollado permite discernir, entre los animales con valores cero de FEC, pudiendo ser animales que están infectados. o que no han sido expuestos recientemente a la infección, o han sido expuestos a un nivel de infección muy bajo. Al mejorar nuestra capacidad para identificar a los animales que han sido infectados con NGIs, incluso con bajos niveles de FEC, el enfoque propuesto ayudará al estudio de las infecciones naturales por nematodos en rebaños ovinos con baja prevalencia de infección así como para la selección de animales resistentes a las NIGs.

Summary

This PhD thesis was planned after SNP-chips were available for most of the domestic livestock species, including sheep. Hence, and considering the previous efforts of the research group involved in this work to identify QTL influencing resistance to gastrointestinal nematodes (GIN)s in Spanish Churra sheep through a microsatellite-based genome scan, the initial objective for this thesis project was to use the *Illumina* OvineSNP50K BeadChip (50K-SNP chip) to replicate some of the QTL previously reported in Churra sheep for traits of resistance to GINs, and, if possible, redefine their confidence interval, at the same time that identifying some new segregating QTL for this complex trait in this commercial dairy sheep population.

For that purpose, we used the 50K-SNP chip, developed by the International Sheep Genomics Consortium and commercialized by Illumina in 2009, to perform a genome scan of the sheep genome to identify QTL influencing parasite resistance in Churra sheep. This study involved 14 half-sib families of the Spanish Churra sheep population that were genotyped with the 50K-SNP chip and sampled for two indicator traits of resistance to GINs: the egg count in feces (FEC) and serum levels of IgA. The genotype and phenotype datasets were analysed using classical linkage analysis (LA), a combined linkage disequilibrium and linkage analysis (LDLA) and a whole genome association study (GWAS). By performing the three different analyses performed in this study, which can detect significant associations with different features, we have tried to present a global picture of the loci influencing resistance to GINs that segregate in this commercial sheep population by complementing the limits of classical LA with these alternative LDLA and GWAS approaches, which exploit population information.

Apart of some preliminary analyses presented in conference papers, initially considering the SNP order and positions of the Ovine Genome Assembly v2.0 (Oar_v2.0), or analyzing only one of the analysed traits, the final three genome scan analyses (LA, LDLA and GWAS) performed, based on the updated reference genome sequence Oar_v3.1, identified a total of 76 genomic regions significantly associated with the two phenotypes under study (FEC and IgA). For the FEC trait the LA revealed two previously detected genomic regions on OAR6 and 8, and for IgA only one significant region was detected on OAR22. A total of 63 significant regions were detected by LDLA (of which 30 showed effects on the FEC trait and

33 on the IgA trait), whereas 10 significant SNPs located on several different chromosomes were identified as significantly associated solely with the IgA trait by the GWAS carried out. Interestingly, according to the current sheep genome assembly (Oar_v3.1), the LFEC QTL detected on OAR6 by LA (80.8–91.4 Mb) overlaps with the most significant QTL previously reported in Churra sheep based on the mentioned microsatellite-based genome scan within the interval 68-85.1 Mb of OAR6. Further, on OAR6, the LDLA results for FEC revealed three significant genomic regions, one reaching the genome-wise significance level, at 72.5 cM, and two reaching the chromosome-wise significance threshold, at 36 and 89.9 cM. The latter of these LDLA significant associations is included within the CI of the FEC OAR6 QTL detected by LA and therefore the LDLA results also support the replication of the QTL previously reported in that region by our research group. At the methodological level, LDLA identified more significant results than LA and GWAS together. Hence, for the family structure of our resource population this approach appears to map QTL more accurately than LA while retaining its robustness to spurious associations whereas suffers less from multiple-testing than GWAS, providing a larger power to detect the existing QTL.

Based on the results obtained in our study, the comparison with QTL reported in other studies, mainly carried out in young animals, and the known differences of the immune mechanisms in adult and young animals, we have proposed that the replicated QTL on OAR6 could be related to specific immune mechanisms that are activated during the exposure of adult animals to parasites. However, due to the complexity of the immune response against helminths infections future studies are needed to reveal the causal mutation/s of the QTL replicated herein in Spanish Churra sheep.

As an extension of the initial objective of this thesis, the two other objectives of this PhD project arose as scientific collaborations with two other groups involved in the European funded NematodeSystemHealth ITN project related to this PhD thesis: i) the study of the genetic variability of two genes of the Major Histocompatibility Complex (MHC) class IIB in the Spanish Churra rams that were pedigree heads of the resource population studied in the QTL mapping study previously described, and ii) determination of the prevalence of GIN infections in naturally infected adult sheep showing low levels of infection by combining information from the two indicators traits used in this study; for that a zero-inflated negative

binomial model (ZINB) model was applied on the FEC data and this model was later extended to include data from the IgA responses with the aim of discriminating which animals were infected and which had not been recently exposed to the infection or had been exposed at a very low infection level.

In reference to the second proposed objective our diversity analysis identified nine known and three new DRB1 alleles as well as ten known and 15 new DQB alleles in the 15 Spanish Churra rams analysed. Based on the genetic variability of the MHC class IIB genes in the analysed samples, we were able to identify 14 different haplotypes. Even though a small number of animals were used in this study, the results have shown that an efficient genotyping system can be developed for this population, which could be of interest for future studies on this topic involving a larger number of Spanish Churra individuals.

Nowadays, the climate change is of increasing importance to determining the occurrence and impact of parasitic diseases. The prevalence of GIN infections in natural infected animals is affected by the environment conditions influencing directly on the number of viable free-living forms in the environment and, consequently, on the infective stages. In this PhD thesis it was observed that unfavorable climatic conditions had a remarkable impact on the development of free-living parasitic stages during pasture. In the sense, we observed a high number of grazing animals sampled for the QTL mapping study showing FEC values of zero (64%). The previous GIN-related studies that were conducted in the same geographical area of Castilla y León had shown a higher proportion of the GIN prevalence. Under these circumstances, the third objective of this thesis is planned with the aim of specifically deal with data of resistance indicator traits corresponding to very low infection levels. Therefore, for animals with FEC equal to zero we have developed a novel approach that distinguishes between not recently infected sheep and infected sheep at very low infection levels. For that purpose, a ZINB model was used to calculate the extent of zero-inflation by using the FEC trait and, following that ZINB model was extended to include information from the IgA responses. For our dataset, this extended ZINB model suggested that 38% of the sampled sheep were not exposed to GIN infection. Afterwards, the sub-dataset (a total of 328 animals) including the animals that were considered as exposed to GIN infections was used to calculate the correlations among the studied indicators. A correlation close to zero was

obtained between FEC and IgA, and a significant positive correlation was found between IgA and P_i^exp (estimated probability of being exposed to infection). These results indicate that in addition to FEC data, the evaluation of the level of IgA in the serum may be a useful method for the control of GIN infections in flocks of adult animals with low level of infection, which may be highly relevant when planning selective breeding aimed at improving the resistance of sheep populations to these infections.

Resumen

La presente tesis doctoral se planteó una vez de que los SNP-chips estuvieron disponibles para la mayoría de las especies domésticas, incluyendo la oveja. Así, teniendo en cuenta los esfuerzos previos del grupo de investigación en el que se ha desarrollado este trabajo para identificar QTL que influyen sobre la resistencia a los nematodos gastrointestinales (NGI)s en ovejas de raza Churra utilizando un barrido genómico con microsatélites, el objetivo inicial de este proyecto de tesis consistió en utilizar el *Illumina* OvineSNP50 BeadChip (el chip de 50K-SNP) para replicar algunos de los QTL anteriormente descritos en la raza Churra para caracteres indicadores de resistencia a NGIs, y si fuera posible, redefinir su intervalo de confianza e identificar nuevos QTL que influyen sobre este carácter complejo en esta población comercial de ovino lechero.

Con ese propósito, se utilizó el chip de 50K-SNP, desarrollado por el Consorcio Internacional para la Genómica de la Oveja, y comercializado por Illumina en 2009, con el fin de realizar una scaneo del genoma ovino para identificar QTL con influencia sobre la resistencia a los parásitos en la oveja Churra. Este estudio incluyó 14 familias de medio hermanas de una población comercial de raza Churra que fueron genotipadas con el chip de 50K-SNP y muestradas para dos caracteres indicadores de la resistencia a NGI: el recuento de huevos en heces (Faecal egg Count o FEC) y los niveles séricos de IgA. Los datos de los genotipos y fenotipos fueron analizados usando el clásico análisis de ligamiento (LA), un análisis de desequilibrio de ligamiento combinado con análisis de ligamiento (LDLA) y un estudio de asociación del genoma completo (GWAS). Utilizando estos tres tipos de análisis, que pueden detectar asociaciones significativas con diferentes características, hemos tratado de presentar una visión global de los loci que influyen sobre la resistencia a los NGI en esta población comercial de ovejas, complementando las limitaciones del clásico LA con las aproximaciones alternativas de LDLA y GWAS, que aprovechan información a nivel poblacional.

A parte de algunos análisis preliminares, presentados en diferentes conferencias, considerando inicialmente el orden y las posiciones de los marcadores SNPs analizados según la versión 2.0 del Genoma Ovino, o analizando solamente uno de los indicadores estudiados, los tres barridos genómicos realizados (LA, LDLA y GWAS), basados en la versión 3.1 del Genoma Ovino, identificaron un total de 76 regiones genómicas

significativamente asociadas con los dos fenotipos en este studio (FEC e IgA). Para el indicador FEC el análisis LA reveló dos regiones genómicas detectadas previamente en OAR6 y 8, y para IgA se detectó una sola región significativa en OAR22. El barrido genómico con LDLA identificó un total de 63 regiones significativas (de las cuales 30 mostraron efectos sobre FEC y 33 sobre IgA). Finalmente, el análisis GWAS detectó 10 SNPs significativos, distribuidos en varios cromosomas, significativamente asociados con el indicador IgA. Es de interés que, según la versión actual del genoma ovino (Oar_v3.1), el QTL para el carácter FEC detectado en OAR6 mediante LA (80,8-91,4 Mb) se solapa con el QTL más significativo descrito anteriormente por nuestro grupo en la población de Churra analizada en el barrido genómico basado en microsatélites, en la región 68-85,1 Mb de OAR6). Además, en OAR6, los resultados LDLA para FEC revelaron tres regiones genómicas significantivas, una alcanzó el nivel de significación *genome-wise* en la posicion 72,5 cM y las otras dos asociaciones significativas a nivel *chromosome-wise* en las posiciones 36 y 89,9 cM. La última de estas asociaciones significativas del scan LDLA está incluida dentro del intervalo de confianza (IC) del QTL detectado por LA en ese cromosoma; por tanto, los resultados del análisis LDLA también apoyan la replicación del QTL descrito anteriormente en esta región por nuestro grupo. A nivel metodológico, el barrido genómico LDLA identificó más resultados significativos que los análisis basados en LA y GWAS. Por lo tanto, considerando la estructura familiar de la población aquí estudiada, la aproximación LDLA presenta mayor precisión para mapear QTL que LA, conservando su robustez frente a la detección de asociaciones espurias. Además, el análisis LDLA parece sufrir menos los efectos de la corrección de múltiples test que el método GWAS, por lo que el LDLA proporcionaría una potencia mayor para detectar verdaderos QTL.

Basándonos en los resultados obtenidos en nuestro trabajo, la comparacion con QTL descritos por otros autores y las diferencias conocidas sobre los mecanismos inmunes en animales jóvenes y adultos, hemos propuesto que el QTL replicado en OAR6 podría estar relacionado con mecanismos inmunes específicamente activados en animales adultos durante la exposición al parásito. Sin embargo, dada la complejidad de la respuesta inmune contra las infecciones por helmintos, se necesitan futuros estudios para llegar a identificar la mutacion causal de este QTL replicado en oveja Churra.

Como extensión del objetivo inicial planteado en la presente tesis doctoral, surgen sendas colaboraciones científicas con otros dos grupos de trabajo que participan en el proyecto Europeo NTI del *NematodeSystemHealth* relacionado con esta tesis doctoral*:* i) el estudio de la variabilidad genética de dos genes de clase IIB del Complejo Mayor de Histocompatibilidad (MHC) en los machos de raza Churra cabeza de pedigrí de la población ovina estudiada en el estudio de mapeo de QTL descrito previamente, y ii) la determinación de la prevalencia de infecciones por NGI en ovejas adultas sometidas a una infección natural aunque con bajas cargas parasitarias, mediante la combinación de la información de los dos caracteres indicadores utilizados en este estudio; para esto último aplicamos un modelo binomial negativo de ceros inflados (ZINB) a los datos del carácter FEC y posteriormente, el modelo se extendió para incluir la información de los datos de la respuesta de IgA, a fin de discriminar qué animales estaban infectados y cuáles no habían sido expuestos o lo habían sido pero con un nivel muy bajo de infección.

Con relación al segundo objetivo propuesto, nuestro estudio de variabilidad ha identificado en el gen *DRB1* nueve alelos conocidos y tres nuevos, así como diez alelos conocidos y quince nuevos alelos en el gen *DQB* en los 15 machos de raza Churra analizados. En base a la variabilidad de los genes de clase IIB del MHC en las muestras analizadas fuimos capaces de identificar 14 haplotipos. A pesar del limitado número de animales analizado en este estudio, los resultados han demostrado que es posible desarrollar un sistema de genotipado de estos genes eficiente para esta población, lo cual podría ser de interés para futuros estudios en este tema que involucren un mayor número de individuos de la raza Churra española.

En la actualidad, el cambio climático está adquiriendo una creciente importancia en cuanto a la presencia y el impacto de las enfermedades parasitarias. La prevalencia de las infecciones por NGI en los animales infectados de forma natural se ve afectada por las condiciones ambientales que influyen directamente sobre la viabilidad de las fases de vida libre de los parásitos en el medio ambiente, y por lo tanto sobre la fase infectantes. En el desarrollo de la presente tesis doctoral se observó que las condiciones climáticas adversas tuvieron un importante efecto sobre el desarrollo de las fases parasitarias de vida libre en el pasto. En este sentido se observó que un elevado número de los animales en pastoreo muestreados para el estudio del QTL tuvieron cero como valor de FEC (64%). Los estudios anteriores sobre las

infecciones por NGI realizados en la misma zona geográfica de León mostraron una mayor prevalencia de la infección. Ante esta situación, el tercer objetivo de esta tesis doctoral se plantea con el fin de estudiar de una forma concreta los caracteres indicadores de resistencia bajo condiciones de niveles muy bajos de infección. Por lo tanto, para los animales con datos de FEC igual a cero, hemos desarrollado un nuevo método que discrimina entre ovejas que no habían sido infectadas y aquellas infectadas pero con cargas parasitarias muy bajas. A tal fin, se aplicó un modelo ZINB para calcular el grado de inflación de ceros del carácter indicador FEC; posteriormente este modelo ZINB se extendió para incluir la información de las respuestas del carácter IgA. En relación a nuestra base de datos, este modelo ZINB extendido sugirió que el 38% de las ovejas muestreadas no estuvo expuesto a la infección por NGI. Después, se utilizó el sub-conjunto de datos que incluía los animales que se consideraron como expuestos a la infección por nematodos, un total de 328, para calcular las correlaciones entre los caracteres estudiados. Encontramos una correlación cercana a cero entre FEC e IgA y una correlación positiva significativa entre la IgA y P_i^{exp} (probabilidad estimada de estar expuesto a la infección). Los resultados de este trabajo indican que además de los datos de FEC, la evaluación del nivel de IgA en el suero puede ser un método útil en el control de las infecciones por NGI en rebaños de animales adultos con bajo nivel de infección, lo que podría ser de gran importancia para la planificación de estrategias de selección encaminadas a mejorar la resistencia de las poblaciones ovinas a estas infecciones

References

Alba-Hurtado F., Muñoz-Guzmán M. A., 2013 Immune responses associated with resistance to haemonchosis in sheep. Biomed Res. Int. **2013**: 1-11.

Allen J. E., Sutherland T. E., 2014 Host protective roles of type 2 immunity: Parasite killing and tissue repair, flip sides of the same coin. Semin. Immunol. **26**: 329–340.

Altaif K. I., Dargie J. D., 1978 Genetic resistance to helminths. Comparison of the development of Ostertagia circumcincta infections in Scottish Blackface sheep of different haemoglobin type. Res. Vet. Sci. **24**: 391–393.

Anderson R. C., 2000 *Nematode Parasites of Vertebrates: Their Development and Transmission*. CABI Publishing: Wallingford. ISBN 085199-421-0.

Andronicos N., Hunt P., Windon R., 2010 Expression of genes in gastrointestinal and lymphatic tissues during parasite infection in sheep genetically resistant or susceptible to Trichostrongylus colubriformis and Haemonchus contortus. Int. J. Parasitol. **40**: 417–429.

Anthony R. M., Rutitzky L. I., Urban J. F., Stadecker M. J., Gause W. C., 2007 Protective immune mechanisms in helminth infection. Nat. Rev. Immunol. **7**: 975–987.

Aulchenko Y., Ripke S., Isaacs A., Duijn C. Van, 2007 GenABEL: an R library for genome-wide association analysis. Bioinformatics. **23**: 1294-1296.

Aulchenko Y. S., Struchalin M. V, Duijn C. M. van, 2010 ProbABEL package for genome-wide association analysis of imputed data. BMC Bioinformatics **11**(134):1-10.

Axford R. F. E., Bishop S. C., Nicholas F. W., Owen J. B., 1999 *Breeding for disease resistance in farm animals (2nd edition).* CABI Publishing. ISBN 085199-325-7.

Barger I. A., 1985 The statistical distribution of trichostrongylid nematodes in grazing lambs. Int. J. Parasitol. **15**: 645–649.

Barger I. A., 1993 Influence of sex and reproductive status on susceptibility of ruminants to nematode parasitism. Int. J. Parasitol. **23**: 463–469.

References

Baro J. A., Carriedo J. A., San Primitivo F., 1994 Genetic parameters of test day measures for somatic cell count, milk yield, and protein percentage of milking ewes. J. Dairy Sci. **77**: 2658–2662.

Becker D., Tetens J., Brunner A., Bürstel D., Ganter M., Kijas J., Drögemüller C., 2010 Microphthalmia in Texel sheep is associated with a missense mutation in the paired-like homeodomain 3 (PITX3) gene. PLoS One **5**: e8689.

Beh K. J., Hulme D. J., Callaghan M. J., Leish Z., Lenane I., Windon R. G., Maddox J. F., 2002 A genome scan for quantitative trait loci affecting resistance to Trichostrongylus colubriformis in sheep. Anim. Genet. **33**: 97–106.

Benavides M. V, Weimer T. A., Borba M. F. S., Berne M. E. A., Sacco A. M. S., 2002 Association between microsatellite markers of sheep chromosome 5 and faecal egg counts. Small Rumin. Res. **46**: 97–105.

Benavides M. V, Weimer T. A., Borba M. F. S., Berne M. E. A., Sacco A. M. S., 2009 Genetic analyses of polymorphisms on ovine chromosomes 5 and 20 and their effect on resistance to internal parasites. Small Rumin. Res. **83**: 67–73.

Benavides M. V., Sonstegard T. S., Kemp S., Mugambi J. M., Gibson J. P., Baker R. L., Hanotte O., Marshall K., Tassell C. Van, 2015 Identification of Novel Loci Associated with Gastrointestinal Parasite Resistance in a Red Maasai x Dorper Backcross Population. PLoS One **10**: e0122797.

Beraldi D., Mcrae A. F., Gratten J., Slate J., Visscher P. M., Pemberton J. M., 2007 Mapping quantitative trait loci underlying fitness-related traits in a free-living sheep population. Evolution (N. Y). **61**: 1403–1416.

Bishop S., Bairden K., McKellar Q., 1996 Genetic parameters for faecal egg count following mixed, natural, predominantly Ostertagia circumcincta infection and relationships with live weight in young lambs. Anim. Sci. **63**: 423–428.

Bishop S., Jackson F., Coop R., Stear M., 2004 Genetic parameters for resistance to nematode infections in Texel lambs and their utility in breeding programmes. Anim. Sci. **78**: 185–194.

Bishop S. C., Morris C. A., 2007 Genetics of disease resistance in sheep and goats. Small Rumin. Res. **70**: 48–59.

Bishop S. C., 2012 Possibilities to breed for resistance to nematode parasite infections in small ruminants in tropical production systems. Animal **6**: 741–747.

Bisset S. A., Vlassoff A., Morris C. A., Southey B. R., Baker R. L., Parker A. G. H., 1992 Heritability of and genetic correlations among faecal egg counts and productivity traits in Romney sheep. New Zeal. J. Agric. Res. **35**: 51–58.

Blitz N. M., Gibbs H. C., 1972 Studies on the arrested development of Haemonchus contortus in sheep. II. Termination of arrested development and the spring rise phenomenon. Int. J. Parasitol. **2**: 13–22.

Boes J., Medley G. F., Eriksen L., Roepstorff A., Nansen P., 1998 Distribution of Ascaris suum in experimentally and naturally infected pigs and comparison with Ascaris lumbricoides infections in humans. Parasitology **117**: 589–596.

Bradley R. E., Radhakrishnan C. V, Patil-Kulkarni C. G., Loggins P. E., 1973 Responses in Florida Native and Rambouillet lambs exposed to one and two oral doses of Haemonchus contortus. Am. J. Vet. Res. **34**: 729–735.

Broman K. W., Sen S., 2009 *A Guide to QTL Mapping with R/qtl*. Springer New York. ISBN: 978-0-387-92124-2.

Browning S., Browning B., 2007 Rapid and accurate haplotype phasing and missing-data inference for whole-genome association studies by use of localized haplotype clustering. Am. J. Hum. Genet. **81**(5):1084-1097.

Buitkamp J., Filmether P., Stear M. J., Epplen J. T., 1996 Class I and class II major histocompatibility complex alleles are associated with faecal egg counts following natural, predominantly Ostertagia circumcincta infection. Parasitol. Res. **82**: 693–696.

References

Chen G., Adeyemo A., Zhou J., Yuan A., Chen Y., Rotimi C., 2005 Genome scan linkage analysis comparing microsatellites and single-nucleotide polymorphisms markers for two measures of alcoholism in chromosomes 1, 4, and 7. BMC Genet. **6**(S4): 1-5.

Chitneedi P. K., Atlija M., Arranz J. J., Gutiérrez-Gil B., 2015 Análisis GWAS para resistencia a nematodos gastrointesitnales mediante la imputación de genotipos del chip de alta desidad en el ganado ovino. In: *AIDA, XVI Jornadas sobre Producción Animal*, pp. Tomo II, 471–473.

Clark C. H., Kiesel G. K., Goby C. H., 1962 Measurements of blood loss caused by Haemonchus contortus infection in sheep. Am. J. Vet. Res. **23**: 977–980.

Clarke R. A., Burn A. L., Lenane I., Windon R. G., Beh K. J., 2001 Molecular analysis and nematode resistance association of a polymorphism at the 5' end of the sheep IgE gene. Vet. Immunol. Immunopathol. **79**: 15–29.

Coltman D. W., Wilson K., Pilkington J. G., Stear M. J., Pemberton J. M., 2001 A microsatellite polymorphism in the gamma interferon gene is associated with resistance to gastrointestinal nematodes in a naturally-parasitized population of Soay sheep. Parasitology **122**: 571–582.

Coondoo A., 2011 Cytokines in dermatology - a basic overview. Indian J. Dermatol. **56**(4): 368–374.

Coop R., Sykes A., Freer M., Dove H., 2002 Interactions between gastrointestinal parasites and nutrients. In: *Sheep Nutrition*, 313–331.

Courtney C. H., Parker C. F., McClure K. E., Herd R. P., 1985 Resistance of exotic and domestic lambs to experimental infection with Haemonchus contortus. Int. J. Parasitol. **15**: 101–109.

Craig N. M., Smith D. W., Pate J. A., Morrison I. W., Knight P. A., 2014 Local cytokine transcription in naive and previously infected sheep and lambs following challenge with Teladorsagia circumcincta. BMC Vet. Res. **10**(87): 1-14.

Crawford A., McEwan J., 1998 Identification of animals resistant to nematode parasite infection. New Zeal. Provisional Pat.: 330201.

Crawford A. M., Paterson K. A., Dodds K. G., Diez Tascon C., Williamson P. A., Roberts Thomson M., Bisset S. A., Beattie A. E., Greer G. J., Green R. S., Wheeler R., Shaw R. J., Knowler K., McEwan J. C., 2006 Discovery of quantitative trait loci for resistance to parasitic nematode infection in sheep: I. Analysis of outcross pedigrees. BMC Genomics **7**(178): 1-10.

Cresswell P., 1994 Assembly, transport, and function of MHC class II molecules. Annu. Rev. Immunol. **12**: 259–291.

Cunningham F., Amode M. R., Barrell D., Beal K., Billis K., Brent S., Carvalho-Silva D., Clapham P., Coates G., Fitzgerald S., Gil L., Girón C. G., Gordon L., Hourlier T., Hunt S. E., Janacek S. H., Johnson N., Juettemann T., Kähäri A. K., Keenan S., Martin F. J., Maurel T., McLaren W., Murphy D. N., Nag R., Overduin B., Parker A., Patricio M., Perry E., Pignatelli M., Riat H. S., Sheppard D., Taylor K., Thormann A., Vullo A., Wilder S. P., Zadissa A., Aken B. L., Birney E., Harrow J., Kinsella R., Muffato M., Ruffier M., Searle S. M. J., Spudich G., Trevanion S. J., Yates A., Zerbino D. R., Flicek P., 2015 Ensembl 2015. Nucleic Acids Res. **43**: D662–D669.

Davies G., Stear M. J., Bishop S. C., 2005 Genetic relationships between indicator traits and nematode parasite infection levels in 6-month-old lambs. Anim. Sci. **80**: 143–150.

Davies G., Stear M. J., Benothman M., Abuagob O., Kerr A., Mitchell S., Bishop S. C., 2006 Quantitative trait loci associated with parasitic infection in Scottish blackface sheep. Heredity (Edinb). **96**: 252–258.

Day-Williams A. G., Zeggini E., 2011 The effect of next-generation sequencing technology on complex trait research. Eur. J. Clin. Invest. **41**: 561–567.

De Cisneros J. P. J., Matthews L., Mair C., Stefan T., Stear M. J., 2014 The transfer of IgA from mucus to plasma and the implications for diagnosis and control of nematode infections. Parasitology **141**: 875–879.

References

Denwood M. J., Stear M. J., Matthews L., Reid S. W. J., Toft N., Innocent G. T., 2008 The distribution of the pathogenic nematode Nematodirus battus in lambs is zero-inflated. Parasitology **135**: 1225–1235.

Denwood M. J., 2013 runjags: interface utilities for MCMC models in Just Another Gibbs Sampler (JAGS) using parallel and distributed computing methods. URL http//cran.r-project.org/web/packages/runjags.

Dervishi E., Uriarte J., 2011 Structural and functional characterisation of the ovine interferon gamma (IFNG) gene: its role in nematode resistance in Rasa Aragonesa ewes. Vet. Immunol. Immunopathol. **141**: 100–108.

Diez-Baños N., Cabaret J., Diez-Baños P., 1992 Interspecific interactions in naturally acquired nematode communities from sheep abomasum in relation to age of host and season in four areas of León (Spain). Int. J. Parasitol. **22**: 327–334.

Diez-Tascón C., Keane O. M., Wilson T., Zadissa A., Hyndman D. L., Baird D. B., McEwan J. C., Crawford A. M., 2005 Microarray analysis of selection lines from outbred populations to identify genes involved with nematode parasite resistance in sheep. Physiol. Genomics **21**: 59–69.

Dobson, R.J., Hosking B. C., Jacobson C. L., Cotter J. L., Besier R. B., Stein P. A., Reid S. A., 2014 Monepantel resistance reported on Dutch sheep farms. Vet. Rec. **175**: 418.

Doenhoff M. J., Chiodini P. L., Hamilton J. V., 2004 Specific and sensitive diagnosis of schistosome infection: can it be done with antibodies? Trends Parasitol. **20**: 35–39.

Dominik S., Hunt P. W., McNally J., Murrell A., Hall A., Purvis I. W., 2010 Detection of quantitative trait loci for internal parasite resistance in sheep. I. Linkage analysis in a Romney× Merino sheep backcross population. Parasitology **137**: 1275–1282.

Domke A. V. M., Chartier C., Gjerde B., Höglund J., Leine N., Vatn S., Stuen S., 2012 Prevalence of anthelmintic resistance in gastrointestinal nematodes of sheep and goats in Norway. Parasitol. Res. **111**: 185–193.

Douch P. G., Green R. S., Morris C. A., McEewan J. C., Windon R. G., 1996 Phenotypic markers for selection of nematode-resistant sheep. Int. J. Parasitol. **26**: 899–911.

Dunsmore J. D., 1962 Anthelmintic activity of thiabendazole against mature and immature Ostertagia spp. in sheep. Aust. Vet. J. **38**: 412–413.

Fariello M. I., Boitard S., Naya H., SanCristobal M., Servin B., 2013 Detecting Signatures of Selection Through Haplotype Differentiation Among Hierarchically Structured Populations. Genetics **193**: 929–941.

Feichtlbauer-Huber P., Stear M., Fries R., Buitkamp J., 2000 Reference-strand-mediated conformation analysis of MHC alleles: a new method for high-resolution typing of the Ovar-DQB genes. Immunogenetics **51**: 65–68.

Filangi O., Moreno C., Gilbert H., 2010 QTLMap, a software for QTL detection in outbred populations. In: *9th World Congress on Genetics Applied to Livestock Production (WCGALP).* Leipzig; 1–6 August.

Forrest R. H. J., Zhou H., Fang Q., Smyth A., Frampton C. M., Hickford J. G. H., 2010 No evidence for a universal association between variation in faecal egg count for a mixed field-challenge of gastrointestinal parasites and the presence of the Ovar-DQA1 null haplotype in sheep. Vet. Immunol. Immunopathol. **135**: 303–305.

Fox J., Weisberg S., Bates D., Fox M. J., 2012 Package "car." R Found. Stat. Comput. Vienna, Austria.

Fumagalli M., Pozzoli U., Cagliani R., Comi G. P., Riva S., Clerici M., Bresolin N., Sironi M., 2009 Parasites represent a major selective force for interleukin genes and shape the genetic predisposition to autoimmune conditions. J. Exp. Med. **206**: 1395–1408.

Gamble H. R., Zajac A. M., 1992 Resistance of St. Croix lambs to Haemonchus contortus in experimentally and naturally acquired infections. Vet. Parasitol. **41**: 211–225.

Gao X., Becker L. C., Becker D. M., Starmer J. D., Province M. A., 2010 Avoiding the high Bonferroni penalty in genome-wide association studies. Genet. Epidemiol. **34**: 100–105.

References

García-Gámez E., Gutiérrez-Gil B., Sánchez J. P., Arranz J. J., 2012a Replication and refinement of a quantitative trait locus influencing milk protein percentage on ovine chromosome 3. Anim. Genet. **43**: 636–641.

García-Gámez E., Sahana G., Gutiérrez-Gil B., Arranz J. J., 2012b Linkage disequilibrium and inbreeding estimation in Spanish Churra sheep. BMC Genet. **13**: 43.

García-Gámez E., Gutiérrez-Gil B., Sahana G., Sánchez J. P., Bayón Y., Arranz J. J., 2012c GWA analysis for milk production traits in dairy sheep and genetic support for a QTN influencing milk protein percentage in the LALBA gene. PLoS One **7**: e47782

Gause W. C., Wynn T. A., Allen J. E., 2013 Type 2 immunity and wound healing: evolutionary refinement of adaptive immunity by helminths. Nat. Rev. Immunol. **13**: 607–614.

Gibbs H. C., 1982 Mechanisms of survival of nematode parasites with emphasis on hypobiosis. Vet. Parasitol. **11**: 25–48.

Gibson T. E., Parfitt J. W., 1975 Egg output by Trichostrongylus axei in sheep given a single infection. J. Comp. Pathol. **85**: 335–339.

Gossner A., Wilkie H., Joshi A., Hopkins J., 2013 Exploring the abomasal lymph node transcriptome for genes associated with resistance to the sheep nematode Teladorsagia circumcincta. Vet. Res. **44**: 68.

Grisart B., Farnir F., Karim L., Cambisano N., Kim J. J., Kvasz A., Mni M., Simon P., Frère J. M., Coppieters W., Georges M., 2004 Genetic and functional confirmation of the causality of the DGAT1 K232A quantitative trait nucleotide in affecting milk yield and composition. Proc. Natl. Acad. Sci. U. S. A. **101**: 2398–2403.

Grosjean P., Ibanez F., 2014 pastecs: Package for analysis of space-time ecological series. R package version 1.3-18.

Gruner L., Bouix J., Brunel J. C., 2004 High genetic correlation between resistance to Haemonchus contortus and to Trichostrongylus colubriformis in INRA 401 sheep. Vet. Parasitol. **119**: 51–58.

Gunn A., Irvine R. J., 2003 Subclinical parasitism and ruminant foraging strategies: a review. Wildl. Soc. Bull. 117–126.

Gutiérrez-Gil B., El-Zarei M. F., Bayón Y., Alvarez L., la Fuente L. F. de, San Primitivo F., Arranz J. J., 2007 Short communication: detection of quantitative trait loci influencing somatic cell score in Spanish Churra sheep. J. Dairy Sci. **90**: 422–426.

Gutiérrez-Gil B., El-Zarei M. F., Alvarez L., Bayón Y., la Fuente L. F. de, San Primitivo F., Arranz J. J., 2008 Quantitative trait loci underlying udder morphology traits in dairy sheep. J. Dairy Sci. **91**: 3672–3681.

Gutiérrez-Gil B., Pérez J., Alvarez L., Martínez-Valladares M., la Fuente L.-F. de, Bayón Y., Meana A., San Primitivo F., Rojo-Vázquez F.-A., Arranz J.-J., 2009a Quantitative trait loci for resistance to trichostrongylid infection in Spanish Churra sheep. Genet. Sel. Evol. **41**: 46.

Gutiérrez-Gil B., El-Zarei M. F., Alvarez L., Bayón Y., la Fuente L. F. de, San Primitivo F., Arranz J.-J., 2009b Quantitative trait loci underlying milk production traits in sheep. Anim. Genet. **40**: 423–434.

Gutiérrez-Gil B., Pérez J., la Fuente L. F. de, Meana A., Martínez-Valladares M., San Primitivo F., Rojo-Vázquez F. a, Arranz J. J., 2010 Genetic parameters for resistance to trichostrongylid infection in dairy sheep. Animal **4**: 505–512.

Gutiérrez-Gil B., Alvarez L., la Fuente L. F. de, Sanchez J. P., San Primitivo F., Arranz J. J., 2011 A genome scan for quantitative trait loci affecting body conformation traits in Spanish Churra dairy sheep. J. Dairy Sci. **94**: 4119–4128.

Gutiérrez-Gil B., Arranz J. J., Pong-Wong R., García-Gámez E., Kijas J., Wiener P., 2014 Application of selection mapping to identify genomic regions associated with dairy production in sheep. PLoS One **9**: e94623.

Guyatt H. L., Bundy D. A., Medley G. F., Grenfell B. T., 1990 The relationship between the frequency distribution of Ascaris lumbricoides and the prevalence and intensity of infection in human communities. Parasitology **101 Pt 1**: 139–143.

References

Ha N.-T., Freytag S., Bickeboeller H., 2014 Coverage and efficiency in current SNP chips. Eur. J. Hum. Genet. **22**: 1124–1130.

Hall T., 1999 BioEdit: a user-friendly biological sequence alignment editor and analysis program for Windows 95/98/NT. Nucleic Acids Symp. Ser. **41**: 95–98.

Hassan M., Good B., Hanrahan J., 2011 The dynamic influence of the DRB1* 1101 allele on the resistance of sheep to experimental Teladorsagia circumcincta infection. Vet Res **42**: 46.

Henderson N. G., Stear M. J., 2006 Eosinophil and IgA responses in sheep infected with Teladorsagia circumcincta. Vet. Immunol. Immunopathol. **112**: 62–66.

Hickford J., Forrest R., Zhou H., 2011 Association between variation in faecal egg count for a mixed field-challenge of nematode parasites and ovine MHC-DQA2 polymorphism. Vet. Immunol. Immunopathol. **144**: 312–320.

Hu Z.-L., Park C. A., Wu X.-L., Reecy J. M., 2013 Animal QTLdb: an improved database tool for livestock animal QTL/association data dissemination in the post-genome era. Nucleic Acids Res. **41**: D871–879.

Hutchings M. R., Milner J. M., Gordon I. J., Kyriazakis I., Jackson F., 2002 Grazing decisions of Soay sheep, Ovis aries, on St Kilda: a consequence of parasite distribution? Oikos **96**: 235–244.

Hutchings M. R., Athanasiadou S., Kyriazakis I., J. Gordon I., 2003 Can animals use foraging behaviour to combat parasites? Proc. Nutr. Soc. **62**: 361–370.

Hutchings M. R., Knowler K. J., McAnulty R., McEwan J. C., 2007 Genetically resistant sheep avoid parasites to a greater extent than do susceptible sheep. Proc. R. Soc. London B Biol. Sci. **274**: 1839–1844.

Hutchinson G. W., 2009 Nematode parasites of small ruminants, camelids and cattle diagnosis with emphasis on anthelmintic efficacy and resistance testing. Aust. New Zeal. Stand. Diagnostic Proced. February: 1-61.

Idris A., Moors E., Sohnrey B., Gauly M., 2012 Gastrointestinal nematode infections in German sheep. Parasitol. Res. **110**: 1453–1459.

Janeway C., Travers P., Walport M., Shlomchik M., 2001 *Immunobiology: the immune system in health and disease*. Taylor & Francis, Inc. 5th edition. New York: Garland Science. ISBN-10: 0-8153-3642-X.

Jankovic D., Liu Z., Gause W. C., 2001 Th1- and Th2-cell commitment during infectious disease: asymmetry in divergent pathways. Trends Immunol. **22**: 450–457.

Jann O. C., King A., Corrales N. L., Anderson S. I., Jensen K., Ait-Ali T., Tang H., Wu C., Cockett N. E., Archibald A. L., Glass E. J., 2009 Comparative genomics of Toll-like receptor signalling in five species. BMC Genomics **10**: 216.

Kaminsky R., Bapst B., Stein P. A., Strehlau G. A., Allan B. A., Hosking B. C., Rolfe P. F., Sager H., 2011 Differences in efficacy of monepantel, derquantel and abamectin against multi-resistant nematodes of sheep. Parasitol. Res. **109**: 19–23.

Kaplan R. M., 2004 Drug resistance in nematodes of veterinary importance: a status report. Trends Parasitol. **20**: 477–481.

Karlsson L. J. E., Greeff J. C., 2005 Sustainable internal parasite control in Australian merino sheep. 56th Annu. EAAP Meet. Uppsala, Sweden: 5-8 June; 377.

Karlsson L. J. E., Greeff J. C., 2006 Selection response in fecal worm egg counts in the Rylington Merino parasite resistant flock. Aust. J. Exp. Agric. **46**: 809.

Karlsson L. J. E., Greeff J. C., 2012 Genetic aspects of sheep parasitic diseases. Vet. Parasitol. **189**: 104–112.

Keane O. M., Dodds K. G., Crawford A. M., McEwan J. C., 2007 Transcriptional profiling of Ovis aries identifies Ovar-DQA1 allele frequency differences between nematode-resistant and susceptible selection lines. Physiol. Genomics **30**: 253–261.

Kelley J., Bono B. de, Trowsdale J., 2005 IRIS: a database surveying known human immune system genes. Genomics **85**: 503–511.

References

Kemper K. E., Palmer D. G., Liu S. M., Greeff J. C., Bishop S. C., Karlsson L. J. E., 2010 Reduction of faecal worm egg count, worm numbers and worm fecundity in sheep selected for worm resistance following artificial infection with Teladorsagia circumcincta and Trichostrongylus colubriformis. Vet. Parasitol. **171**: 238–246.

Kemper K. E., Emery D. L., Bishop S. C., Oddy H., Hayes B. J., Dominik S., Henshall J. M., Goddard M. E., 2011 The distribution of SNP marker effects for faecal worm egg count in sheep, and the feasibility of using these markers to predict genetic merit for resistance to worm infections. Genet. Res. (Camb). **93**: 203–219.

Lander E. S., Botstein D., 1989 Mapping mendelian factors underlying quantitative traits using RFLP linkage maps. Genetics **121**: 185–199.

Lee C. Y., Munyard K. a, Gregg K., Wetherall J. D., Stear M. J., Groth D. M., 2011 The influence of MHC and immunoglobulins a and e on host resistance to gastrointestinal nematodes in sheep. J. Parasitol. Res. **2011**: 101848.

Legarra A., Fernando R., 2009 Linear models for joint association and linkage QTL mapping. Genet. Sel. Evol. **41**: 43.

Lenth R., 2013 lsmeans: least-squares means. R package version 1.06–05.

Levine N. D., 1968 *Nematode parasites of domestic animals and of man*. Burgess Publishing Company, Minneapolis. MN.

Little P. R., Hodges A., Watson T. G., Seed J. A., Maeder S. J., 2010 Field efficacy and safety of an oral formulation of the novel combination anthelmintic, derquantel-abamectin, in sheep in New Zealand. N. Z. Vet. J. **58**: 121–129.

MacKinnon K. M., Burton J. L., Zajac A. M., Notter D. R., 2009 Microarray analysis reveals difference in gene expression profiles of hair and wool sheep infected with Haemonchus contortus. Vet. Immunol. Immunopathol. **130**: 210–220.

MacKinnon K. M., Zajac A. M., Kooyman F. N. J., Notter D. R., 2010 Differences in immune parameters are associated with resistance to Haemonchus contortus in Caribbean hair sheep. Parasite Immunol. **32**: 484–493.

Maddox J. F., Cockett N. E., 2007 An update on sheep and goat linkage maps and other genomic resources. Small Rumin. Res. **70**: 4–20.

Madsen P., Sørensen P., Su G., Damgaard L. H., Thomsen H., Labouriau R., 2006 DMU – A package for analyzing multivairate mixed models. 8th World Congr. Genet. Appl. to Livest. Prod. Belo Horizonte, Brazil. **247**: 13–18.

Madsen P., Jensen J., Labouriau R., Christensen O. F., Sahana G., 2014 DMU - A Package for Analyzing Multivariate Mixed Models in quantitative Genetics and Genomics. In: *10th World Congress on Genetics Applied to Livestock Production (WCGALP)*, 17-22 August 2014.

MAFF, 1986 *Manual of Veterinary Parasitological Techniques* London, UK: Her Majesty's Stationary Office.

Marshall K., Maddox J. F., Lee S. H., Zhang Y., Kahn L., Graser H., Gondro C., Walkden-Brown S. W., Werf J. H. J. Van Der, 2009 Genetic mapping of quantitative trait loci for resistance to Haemonchus contortus in sheep. Anim. Genet. **40**: 262–272.

Marshall K., Mugambi J. M., Nagda S., Sonstegard T. S., Tassell C. P. Van, Baker R. L., Gibson J. P., 2013 Quantitative trait loci for resistance to *Haemonchus contortus* artificial challenge in Red Maasai and Dorper sheep of East Africa. Anim. Genet. **44**: 285–295.

Martínez-Valladares M., Vara-Del Río M., Cruz-Rojo M., Rojo-Vázquez F., 2005 Genetic resistance to Teladorsagia circumcincta: IgA and parameters at slaughter in Churra sheep. Parasite Immunol. **27**: 213–218.

Martínez-Valladares M., Robles-Pérez D., Martínez-Pérez J. M., Cordero-Pérez C., Famularo M. D. R., Fernández-Pato N., González-Lanza C., Castañón-Ordóñez L., Rojo-Vázquez F. A., 2013 Prevalence of gastrointestinal nematodes and Fasciola hepatica in sheep in the northwest of Spain: relation to climatic conditions and/or man-made environmental modifications. Parasit. Vectors **6**: 282.

References

Matika O., Pong-Wong R., Woolliams J. a., Bishop S. C., 2011 Confirmation of two quantitative trait loci regions for nematode resistance in commercial British terminal sire breeds. Animal **5**: 1149–1156.

McRae K. M., McEwan J. C., Dodds K. G., Gemmell N. J., 2014a Signatures of selection in sheep bred for resistance or susceptibility to gastrointestinal nematodes. BMC Genomics **15**: 637.

McRae K. M., Good B., Hanrahan J. P., Glynn A., O'Connell M. J., Keane O. M., 2014b Response to Teladorsagia circumcincta infection in Scottish Blackface lambs with divergent phenotypes for nematode resistance. Vet. Parasitol. **206**: 200–207.

Mederos A. E., Ramos Z., Banchero G. E., 2014 First report of monepantel Haemonchus contortus resistance on sheep farms in Uruguay. Parasit. Vectors **7**: 598.

Meuwissen T., 2010 Use of whole genome sequence data for QTL mapping and genomic selection. In: *9th World Congress on Genetics Applied to Livestock Production (WCGALP)*. Leipzig; 1–6 August.

Monticelli L., Sonnenberg G., Abt M., Osborne L., Wojno E. T., Alenghat T., Ziegler C., Wherry E., Artis D., 2013 Innate lymphoid cells promote airway epithelial repair through the amphiregulin-EGFR pathway (P3250). J. Immunol. **190**: 136–137.

Morgan E., Charlier J., Hendrickx G., Biggeri A., Catalan D., Samson-Himmelstjerna G. von, Demeler J., Müller E., Dijk J. van, Kenyon F., Skuce P., Höglund J., O'Kiely P., Ranst B. van, Waal T. de, Rinaldi L., Cringoli G., Hertzberg H., Torgerson P., Wolstenholme A., Vercruysse J., 2013 Global Change and Helminth Infections in Grazing Ruminants in Europe: Impacts, Trends and Sustainable Solutions. Agriculture **3**: 484–502.

Morris C. A., Watson T. G., Bisset S. A., Vlassoff A., Douch P. G. C., 1995 Breeding sheep in New Zealand for resistance or resilience to nematode parasites. In: *Breeding for Resistance to Infectious Diseases of Small Ruminants*, pp. 77–98.

Morris C. A., Bisset S. A., Vlassoff A., West C. J., Wheeler M., 2004 Genetic parameters for Nematodirus spp. egg counts in Romney lambs in New Zealand. Anim. Sci. **79**: 33–40.

Mosmann T., Coffman R., 1989 TH1 and TH2 cells: different patterns of lymphokine secretion lead to different functional properties. Annu. Rev. Immunol. **7**: 145–173.

Mugambi J. M., Bain R. K., Wanyangu S. W., Ihiga M. A., Duncan J. L., Murray M., Stear M. J., 1997 Resistance of four sheep breeds to natural and subsequent artificial Haemonchus contortus infection. Vet. Parasitol. **69**: 265–273.

Nicolazzi E. L., Picciolini M., Strozzi F., Schnabel R. D., Lawley C., Pirani A., Brew F., Stella A., 2014 SNPchiMp: a database to disentangle the SNPchip jungle in bovine livestock. BMC Genomics **15**: 123.

Nicolazzi E., Biffani S., 2015 Software solutions for the livestock genomics SNP array revolution. Anim. Genet. **46**: 343–353.

Nimbkar C., Ghalsasi P., Swan A., Walkden-Brown S., Khan L., 2003 Evaluation of growth rates and resistance to nematodes of Deccani and Bannur lambs and their crosses with Garole. Anim. Sci. **76**: 503–515.

Nødtvedt A., Dohoo I., Sanchez J., Conboy G., DesCjteaux L., Keefe G., Leslie K., Campbell J., 2002 The use of negative binomial modelling in a longitudinal study of gastrointestinal parasite burdens in Canadian dairy cows. Can. J. Vet. Res. **66**: 249–257.

O'Connor L. J., Walkden-Brown S. W., Kahn L. P., 2006 Ecology of the free-living stages of major trichostrongylid parasites of sheep. Vet. Parasitol. **142**: 1–15.

Oorschot R. van, Maddox J., Adams L., Fabb S., 1994 Characterization and evolution of ovine MHC class II DQB sequence polymorphism. Anim. Genet. **25**: 417–424.

Papadopoulos E., Gallidis E., Ptochos S., 2012 Anthelmintic resistance in sheep in Europe: a selected review. Vet. Parasitol. **189**: 85–88.

Paterson S., Wilson K., Pemberton J. M., 1998 Major histocompatibility complex variation associated with juvenile survival and parasite resistance in a large unmanaged ungulate population (Ovis aries L.). Proc. Natl. Acad. Sci. **95**: 3714–3719.

References

Pearson T. A., Manolio T., 2008 How to Interpret a Genome-wide Association Study. Jama **299**: 1335-1344.

Pedreira J., Paz-Silva A., Sánchez-Andrade R., Suárez J. L., Arias M., Lomba C., Díaz P., López C., Díez-Baños P., Morrondo P., 2006 Prevalences of gastrointestinal parasites in sheep and parasite-control practices in NW Spain. Prev. Vet. Med. **75**: 56–62.

Pernthaner A., Cole S. A., Morrison L., Hein W. R., 2005 Increased expression of interleukin-5 (IL-5), IL-13, and tumor necrosis factor alpha genes in intestinal lymph cells of sheep selected for enhanced resistance to nematodes during infection with Trichostrongylus colubriformis. Infect. Immun. **73**: 2175–2183.

Pernthaner A., Cole S.-A., Morrison L., Green R., Shaw R. J., Hein W. R., 2006 Cytokine and antibody subclass responses in the intestinal lymph of sheep during repeated experimental infections with the nematode parasite Trichostrongylus colubriformis. Vet. Immunol. Immunopathol. **114**: 135–148.

Plummer M., Best N., Cowles K., Vines K., 2006 CODA: Convergence diagnosis and output analysis for MCMC. R news **6**: 7–11.

Qamar M. F., Maqbool A., Ahmad N., 2011 Economic losses due to haemonchosis in sheep and goats. Sci. Int.: 321–324.

Raadsma H. W., Gray G. D., Woolaston R. R., Piper L., Ruvinsky A., 1997 Genetics of disease resistance and vaccine response. In: *The genetics of sheep.*, CAB INTERNATIONAL, pp. 199–224.

Radhakrishnan C. V, Bradley R. E., Loggins P. E., 1972 Host responses of worm-free Florida native and Rambouillet lambs experimentally infected with Haemonchus contortus. Am. J. Vet. Res. **33**: 817–823.

R Core Team, 2014 R: A language and environment for statistical computing. R Found. Stat. Comput. Vienna, Austria. 2013.

Richards D. T., Lewis J. W., 2001 Fecundity and egg output by Toxocara canis in the red fox, Vulpes vulpes. J. Helminthol. **75**: 157–164.

Riggio V., Matika O., Pong-Wong R., Stear M. J., Bishop S. C., 2013 Genome-wide association and regional heritability mapping to identify loci underlying variation in nematode resistance and body weight in Scottish Blackface lambs. Heredity (Edinb). **110**: 420–429.

Riggio V., Pong-Wong R., Sallé G., Usai M. G., Casu S., Moreno C. R., Matika O., Bishop S. C., 2014 A joint analysis to identify loci underlying variation in nematode resistance in three European sheep populations. J. Anim. Breed. Genet. **131**: 426–436.

Rizopoulos D., 2006 ltm : An R Package for Latent Variable Modeling and Item Response Theory Analyses. J. Stat. Softw. **17**: 1–25.

Roeber F., Jex A. R., Gasser R. B., 2013 Impact of gastrointestinal parasitic nematodes of sheep, and the role of advanced molecular tools for exploring epidemiology and drug resistance - an Australian perspective. Parasit. Vectors **6**: 153.

Ron M., Weller J. I., 2007 From QTL to QTN identification in livestock--winning by points rather than knock-out: a review. Anim. Genet. **38**: 429–439.

Roy E. A., Hoste H., Beveridge I., 2004 The effects of concurrent experimental infections of sheep with Trichostrongylus colubriformis and T. vitrinus on nematode distributions, numbers and on pathological changes. Parasite **11**: 293–300.

Sallé G., Jacquiet P., Gruner L., Cortet J., Sauvé C., Prévot F., Grisez C., Bergeaud J. P., Schibler L., Tircazes A., François D., Pery C., Bouvier F., Thouly J. C., Brunel J. C., Legarra A., Elsen J. M., Bouix J., Rupp R., Moreno C. R., 2012 A genome scan for QTL affecting resistance to Haemonchus contortus in sheep. J. Anim. Sci. **90**: 4690–4705.

Sallé G., Moreno C., Boitard S., Ruesche J., Tircazes-Secula A., Bouvier F., Aletru M., Weisbecker J. L., Prévot F., Bergeaud J. P., 2014 Functional investigation of a QTL affecting resistance to Haemonchus contortus in sheep. Vet Res **45**: 68.

Sambrook J., Fritch E. F., Maniatis T., 1989 *Molecular Cloning: A Laboratory Manua (2nd edition)*. Cold Spring Harbor Laboratory Press, Cold Spring Harbor, NY. ISBN 0879693096.

References

Sayers G., Good B., Hanrahan J. P., Ryan M., Sweeney T., 2005a Intron 1 of the interferon gamma gene: Its role in nematode resistance in Suffolk and Texel sheep breeds. Res. Vet. Sci. **79**: 191–196.

Sayers G., Good B., Hanrahan J. P., Ryan M., Angles J. M., Sweeney T., 2005b Major Histocompatibility Complex DRB1 gene: its role in nematode resistance in Suffolk and Textel sheep breeds. Parasitology **131**: 403–409.

Sayers G., Sweeney T., 2005 Gastrointestinal nematode infection in sheep – a review of the alternatives to anthelmintics in parasite control. Anim. Heal. Res. Rev. **6**: 159–171.

Schneider D. S., Ayres J. S., 2008 Two ways to survive infection: what resistance and tolerance can teach us about treating infectious diseases. Nat. Rev. Immunol. **8**: 889–895.

Schumacher C., Clark-Lewis I., Baggiolini M., Moser B., 1992 High- and low-affinity binding of GRO alpha and neutrophil-activating peptide 2 to interleukin 8 receptors on human neutrophils. Proc. Natl. Acad. Sci. U. S. A. **89**: 10542–10546.

Schwaiger F. W., Buitkamp J., Weyers E., Epplen J. T., 1993 Typing of artiodactyl MHC-DRB genes with the help of intronic simple repeated DNA sequences. Mol. Ecol. **2**: 55–59.

Schwaiger F. W., Gostomski D., Stear M. J., Duncan J. L., McKellar Q. A., Epplen J. T., Buitkamp J., 1995 An ovine Major histocompatibility complex DRB1 allele is associated with low faecal egg counts following natural, predominantly Ostertagia circumcincta infection. Int. J. Parasitol. **25**: 815–822.

Schwaiger F. W., Maddox J., Ballingall K., Buitkamp J., Crawford A. M., Dutia B. M., Epplen J. T., Ferguson E. D., Groth D., Hopkins J., Rhind S. M., 1996 The ovine major histocompatibility complex. In: *The major histocompatibility complex region of domestic animal species*, pp. 121–176.

Scott I., Pomroy W. E., Kenyon P. R., Smith G., Adlington B., Moss A., 2013 Lack of efficacy of monepantel against Teladorsagia circumcincta and Trichostrongylus colubriformis. Vet. Parasitol. **198**: 166–171.

Shakya K. P., Miller J. E., Horohov D. W., 2009 A Th2 type of immune response is associated with increased resistance to Haemonchus contortus in naturally infected Gulf Coast Native lambs. Vet. Parasitol. **163**: 57–66.

Shalaby H. A., 2013 Anthelmintics Resistance; How to Overcome it? Iran. J. Parasitol. **8**: 18–32.

Shaw R. J., Morris C. A., Wheeler M., Tate M., Sutherland I. A., 2012 Salivary IgA: a suitable measure of immunity to gastrointestinal nematodes in sheep. Vet. Parasitol. **186**: 109–117.

Silva M. V. B., Sonstegard T. S., Hanotte O., Mugambi J. M., Garcia J. F., Nagda S., Gibson J. P., Iraqi F. a., McClintock a. E., Kemp S. J., Boettcher P. J., Malek M., Tassell C. P. Van, Baker R. L., 2012 Identification of quantitative trait loci affecting resistance to gastrointestinal parasites in a double backcross population of Red Maasai and Dorper sheep. Anim. Genet. **43**: 63–71.

Silvestre A., Humbert J. F., 2002 Diversity of benzimidazole-resistance alleles in populations of small ruminant parasites. Int. J. Parasitol. **32**: 921–928.

Singleton D. R., Stear M. J., Matthews L., 2011 A mechanistic model of developing immunity to Teladorsagia circumcincta infection in lambs. Parasitology **138**: 322–332.

Skorping A., Read A., Keymer A., 1991 Life history covariation in intestinal nematodes of mammals. Oikos **60**: 365–372.

Slate J., Gratten J., Beraldi D., Stapley J., Hale M., Pemberton J. M., 2009 Gene mapping in the wild with SNPs: guidelines and future directions. Genetica **136**: 97–107.

Smith W. D., Jackson F., Jackson E., Williams J., Willadsen S. M., Fehilly C. B., 1984 Resistance to Haemonchus contortus transferred between genetically histocompatible sheep by immune lymphocytes. Res. Vet. Sci. **37**: 199–204.

Sréter T., Kassai T., Takács E., 1994 The heritability and specificity of responsiveness to infection with Haemonchus contortus in sheep. Int. J. Parasitol. **24**: 871–876.

References

Stear M. J., Bishop S. C., Duncan J. L., McKellar Q. A., Murray M., 1995a The repeatability of fecal egg counts, peripheral eosinophil counts, and plasma pepsinogen concentrations during deliberate infections with Ostertagia circumcincta. Int. J. Parasitol. 25: 375–380.

Stear M. J., Bishop S. C., Doligalska M., Duncan J. L., Holmes P. H., Irvine J., McCririe L., McKellar Q. a, Sinski E., Murray M., 1995b Regulation of egg production, worm burden, worm length and worm fecundity by host responses in sheep infected with Ostertagia circumcincta. Parasite Immunol. 17: 643–652.

Stear M. J., Bairden K., Bishop S. C., Buitkamp J., Epplen J. T., Gostomski D., McKellar Q. A., Schwaiger F. W., Wallace D. S., 1996 An ovine lymphocyte antigen is associated with reduced faecal egg counts in four-month-old lambs following natural, predominantly Ostertagia circumcincta infection. Int. J. Parasitol. **26**: 423–428.

Stear M. J., Bairden K., Bishop S. C., Buitkamp J., Duncan J. L., Gettinby G., McKellar Q. A., Park M., Parkins J. J., Reid S. W. J., Strain S., Murray M., 1997 The genetic basis of resistance to Ostertagia circumcincta in lambs. Vet. J. **154**: 111–119.

Stear M. J., Wakelin D., 1998 Genetic resistance to parasitic infection. Rev. Sci. Tech. **17**: 143–153.

Stear M. J., Bishop S. C., 1999 The curvilinear relationship between worm length and fecundity of Teladorsagia circumcincta. Int. J. Parasitol. **29**: 777–780.

Stear M. J., Strain S., Bishop S. C., 1999 Mechanisms underlying resistance to nematode infection. Int. J. Parasitol. **29**: 51–56.

Stear M. J., Bishop S. C., Mallard B. A., Raadsma H., 2001 The sustainability, feasibility and desirability of breeding livestock for disease resistance. Res. Vet. Sci. **71**: 1–7.

Stear M. J., Bishop S. C., Henderson N. G., Scott I., 2003 A key mechanism of pathogenesis in sheep infected with the nematode Teladorsagia circumcincta. Anim. Heal. Res. Rev. **4**: 45–52.

Stear M. J., Bairden K., Innocent G. T., Mitchell S., Strain S., Bishop S. C., 2004 The relationship between IgA activity against 4th-stage larvae and density-dependent effects on

the number of 4th-stage larvae of Teladorsagia circumcincta in naturally infected sheep. Parasitology **129**: 363–369.

Stear M. J., Fitton L., Innocent G. T., Murphy L., Rennie K., Matthews L., 2007 The dynamic influence of genetic variation on the susceptibility of sheep to gastrointestinal nematode infection. J. R. Soc. Interface **4**: 767–776.

Stear M. J., Boag B., Cattadori I., Murphy L., 2009 Genetic variation in resistance to mixed, predominantly Teladorsagia circumcincta nematode infections of sheep: from heritabilities to gene identification. Parasite Immunol. **31**: 274–282.

Stefan T., 2016 Mathematical modelling of the selective forces maintaining diversity at the Major Histocompatibility Complex, PhD thesis.

Strain S. A. J., Bishop S. C., Henderson N. G., Kerr A., McKellar Q. A., Mitchell S., Stear M. J., 2002 The genetic control of IgA activity against Teladorsagia circumcincta and its association with parasite resistance in naturally infected sheep. Parasitology **124**: 545–552.

Suarez V. H., Cristel S. L., Busetti M. R., 2009 Epidemiology and effects of gastrointestinal nematode infection on milk productions of dairy ewes. Parasite **16**: 141–147.

Suárez-Vega A., Gutiérrez-Gil B., Cuchillo-Ibáñez I., Sáez-Valero J., Pérez V., García-Gámez E., Benavides J., Arranz J. J., 2013 Identification of a 31-bp deletion in the RELN gene causing lissencephaly with cerebellar hypoplasia in sheep. PLoS One **8**: e81072.

Suárez-Vega A., Gutiérrez-Gil B., Benavides J., Perez V., Tosser-Klopp G., Klopp C., Keennel S. J., Arranz J. J., 2015 Combining GWAS and RNA-Seq Approaches for Detection of the Causal Mutation for Hereditary Junctional Epidermolysis Bullosa in Sheep. PLoS One **10**: e0126416.

Sutherland I., Scott I., 2010 *Gastrointestinal nematodes of sheep and cattle: biology and control.* Wiley-Blackwell. ISBN: 978-1-4051-8582-0.

Sykes A. R., 1987 *Endoparasites and herbivore nutrition. The Nutrition of Herbivores.* (JB Hacker and JH Ternouth, Eds.). Marrickvale, New South Wales: Academic Press.

References

Taylor M., 2009 Changing patterns of parasitism in sheep. In Pract. **31**: 474–483.

Terefe G., Lacroux C., Andreoletti O., Grisez C., Prevot F., Bergeaud J. P., Penicaud J., Rouillon V., Gruner L., Brunel J. C., Francois D., Bouix J., Dorchies P., Jacquiet P., 2007 Immune response to Haemonchus contortus infection in susceptible (INRA 401) and resistant (Barbados Black Belly) breeds of lambs. Parasite Immunol. **29**: 415–424.

Thaventhiran T., Sethu S., Yeang H. X. A., Al-Huseini L., Hamdam J., Sathish J. G., 2012 T Cell Co-inhibitory Receptors-Functions and Signalling Mechanisms. J. Clin. Cell. Immunol.**S4**: 1-12

Thompson J. D., Higgins D. G., Gibson T. J., 1994 CLUSTAL W: improving the sensitivity of progressive multiple sequence alignment through sequence weighting, position-specific gap penalties and weight matrix choice. Nucleic Acids Res. **22**: 4673–4680.

Trotta T., Costantini S., Colonna G., 2009 Modelling of the membrane receptor CXCR3 and its complexes with CXCL9, CXCL10 and CXCL11 chemokines: putative target for new drug design. Mol. Immunol. **47**: 332–339.

Turner J. D., Faulkner H., Kamgno J., Cormont F., Snick J. Van, Else K. J., Grencis R. K., Behnke J. M., Boussinesq M., Bradley J. E., 2003 Th2 cytokines are associated with reduced worm burdens in a human intestinal helminth infection. J. Infect. Dis. **188**: 1768–1775.

Valilou R. H., Rafat S. a., Notter D. R., Shojda D., Moghaddam G., Nematollahi A., 2015 Fecal egg counts for gastrointestinal nematodes are associated with a polymorphism in the MHC-DRB1 gene in the Iranian Ghezel sheep breed. Front. Genet. **6**: 1–11.

Vercruysse J., Dorny P., 1999 Integrated control of nematode infections in cattle: A reality? A need? A future? Int. J. Parasitol. **29**: 165–175.

van der Wal R., Irvine J., Stien A., Shepherd N., Albon S. D., 2000 Faecal avoidance and the risk of infection by nematodes in a natural population of reindeer. Oecologia **124**: 19–25.

Walker M., Hall A., Anderson R. M., Basáñez M. G., 2009 Density-dependent effects on the weight of female Ascaris lumbricoides infections of humans and its impact on patterns of egg production. Parasit Vectors **2**: 1–18.

Waller P. J., 1994 The development of anthelmintic resistance in ruminant livestock. Acta Trop. **56**: 233–243.

Weller J. I., Kashi Y., Soller M., 1990 Power of daughter and granddaughter designs for determining linkage between marker loci and quantitative trait loci in dairy cattle. J. Dairy Sci. **73**: 2525–2537.

Weyher A. H., Ross C., Semple S., 2006 Gastrointestinal Parasites in Crop Raiding and Wild Foraging Papio anubis in Nigeria. Int. J. Primatol. **27**: 1519–1534.

Wilkie H., Xu S., Gossner A., Hopkins J., 2015 Variable exon usage of differentially-expressed genes associated with resistance of sheep to Teladorsagia circumcincta. Vet. Parasitol. **212**: 206–213.

Van Wyk J. A., Bath G. F., 2002 The FAMACHA system for managing haemonchosis in sheep and goats by clinically identifying individual animals for treatment. Vet. Res. **33**: 509–529.

Zaiss D. M. W., Loosdregt J. van, Gorlani A., Bekker C. P. J., Gröne A., Sibilia M., Bergen en Henegouwen P. M. P. van, Roovers R. C., Coffer P. J., Sijts A. J. a M., 2013 Amphiregulin Enhances Regulatory T Cell-Suppressive Function via the Epidermal Growth Factor Receptor. Immunity **38**: 275–284.

Zajac A. M., 2006 Gastrointestinal nematodes of small ruminants: life cycle, anthelmintics, and diagnosis. Vet. Clin. North Am. Food Anim. Pract. **22**: 529–541.